



universität
wien

DISSERTATION

Titel der Dissertation

Simulation of Beyond Design Basis Accidents – a Contribution to Risk
Analysis of Nuclear Power Plants

angestrebter akademischer Grad

Doktor der Naturwissenschaften (Dr. rer.nat.)

Verfasserin / Verfasser:	Mag. Nikolaus Müllner
Matrikel-Nummer:	9209030
Dissertationsgebiet (lt. Studienblatt):	A 091 411
Betreuerin / Betreuer:	Ao. Univ.-Prof. Dr. Wolfgang Kromp

Wien, am 13. November 2010

Intentionally left blank

Zusammenfassung

“Accident Management” (AM) Programme werden gemeinhin als wichtiger Punkt des “Defence in Depths” Konzepts für Kernkraftwerke gesehen. Durch sorgfältige Analyse von auslegungsüberschreitenden Reaktorstörfällen ist es möglich, dem Reaktorfahrers eines Kernkraftwerks Richtlinien zu geben, die den Gebrauch von Systemen ausserhalb ihrer Auslegung zur Rückführung des Reaktors in ein sicheres Regime erlauben, oder zumindest mildernd auf den Unfallhergang einwirken. Accident Management Programme wurden erstmalig in den USA eingeführt, sind aber mittlerweile auch in Europa weit verbreitet. In den letzten Jahren entschlossen sich auch die Staaten, die ehemals der Sowjetunion angehörten, Accident Management Programme zu übernehmen.

Die vorliegende Arbeit ist im Rahmen eines Europaid-Projekts entstanden, welches zum Ziel hatte, die Entwicklung von AM für den VVER 1000 voranzutreiben. Der VVER 1000 ist ein Druckwasserreaktor russischen Designs der in Russland, der Ukraine, Bulgarien, Indien, Iran, China und Tschechien im Bau oder im Betrieb ist. Das Projekt wurde von Europaid, TACIS Programm der Europäischen Kommission zur Verbesserung der Sicherheit von russischen Kernkraftwerken finanziert. Das Projekt hatte mehrere Zielsetzungen. Eine wichtige Zielsetzung war die Ausführung von Experimenten mit komplexen Unfallhergang an der integralen Versuchsanlage PSB-VVER. Die Versuchsanlage bildet den Reaktor VVER 1000 mit einer Höhenskala von 1:1, einer Volumen- und Leistungsskalierung von 1:300 ab. Zwölf Versuche, und drei zusätzliche Einzelvariationen zu je einem der zwölf Versuche wurden durchgeführt. Als auslösender Unfall wurden Primärkühlmittelverlust durch kleine Lecks, Primär- zu Sekundärlecks, Speisewasserverlust und Netzverlust mit gleichzeitigem Versagen aller Dieselgeneratoren angenommen. Zusätzlich wurden Mehrfachversagen verschiedener Sicherheitssysteme angenommen. Als AM-Strategien wurden Primär- und Sekundärseitige Druckentlastung, und Einspeisung aus unkonventionellen Quellen getestet.

Die entstandene experimentelle Datenbank wurde verwendet, um die Codes Relap5 und Cathare2 für auslegungsüberschreitende Störfälle zu qualifizieren - eine weitere Zielsetzung des Projekts. Vorhersagen von Computerprogrammen und experimentelle Daten wurden verglichen. Es wurde versucht, den Störfallhergang aller Experimente vor und nach Durchführung des Experiments vorherzusagen. Obwohl die Versuchsanlage PSB-VVER gut skaliert wurde, ist anzunehmen, dass das Verhalten des Kraftwerks bei gleichen Rahmenbedingungen beträchtliche Unterschiede aufzeigen würde. Das Ziel der Experimente ist deshalb in erster Linie, qualitativ die gleichen physikalischen Phänomene nachzubilden. Es soll gezeigt werden, dass die Computercodes in der Lage sind, das Verhalten der Versuchsanlage hinreichend genau nachzubilden. Schlussfolgerungen für das Kernkraftwerk müssen dann auf Code Simulationen des Kernkraftwerks basieren.

Eine dritte Zielsetzung war es, die Wirksamkeit der untersuchten AM-Strategien zu testen. Die Simulationen, die während des Projekts mit dem Code Relap5 ausgeführt wurden, um Aussagen für das eigentliche Kraftwerk zu stützen, sind in dieser Arbeit präsentiert. Simulationen des Kraftwerks war zu mehreren Anlässen für das Projekt von Nöten. In der Planungsphase der Experimente wurden die experimentellen Rahmenbedingungen vorerst in der Kraftwerkssimulation getestet, um ihre Relevanz fuer AM sicherzustellen. Nach der Ausführung aller Experimente, und den Erkenntnissen aus den Post-Test Simulationen der Experimente, wurde die Simulation des eigentlichen Kraftwerks entsprechend adaptiert, und die Berechnungen wurden wiederholt, um Aussagen über die Effizienz der angewandten AM Strategien treffen zu können.

In enger Zusammenarbeit mit dem Referenzkraftwerk Balakovo, Block 3, wurde ein Störfall und eine AM Strategie zur detaillierten Analyse und Optimierung ausgewählt. Ein lang andauernder Verlust des Netzanschluss mit gleichzeitigem Versagen aller Dieselgeneratoren (Station Blackout) wurde als Störfall ausgewählt. Verlust des Netzanschluss über einen längeren Zeitraum als zwei Stunden ist unter normalen Bedingungen sehr unwahrscheinlich. Allerdings ist die Wahrscheinlichkeit eines solchen Störfalls schwer abzuschätzen, wenn man auch terroristische Anschläge als möglich erachtet. Leitungen und Dieselgeneratoren könnten weniger geschützt, oder schwerer zu schützen sein, als andere Sicherheitssysteme. Aber selbst wenn alle aktiven systeme in diesem Fall nicht verfügbar sind, die Speisewasserleitungen und die Deaeratoren bleiben für einige Zeit unter Druck und können als zusätzliches Speisewasser genutzt werden, wenn eine sekundärseitige Druckentlastung zeitgerecht durchgeführt wird. Ebenfalls primärseitig stehen die Druckspeicher zur Verfügung, bei entsprechender primärseitiger Druckentlastung. Die AM Strategie, die im Detail untersucht wurde, war eine Kombination von Sekundär- und/oder Primärseitiger Druckentlastung.

Um den Zeitpunkt der Intervention zu optimieren wurde eine Methode zur generellen Optimierung von accident management interventionen entwickelt. Die Methode umfasst vier Schritte. Die Parameter, die optimiert werden sollen, müssen festgelegt werden. Die Randbedingungen müssen festgelegt werden. Es muss definiert werden, welches Ziel die Optimierung erreichen will. Ein Algorithmus muss angewandt werden,

um schrittweise-iterativ den Zielparameter zu verbessern, und letztlich müssen die Resultate entsprechend dargestellt werden.

Das Ergebnis der Arbeit ist, dass die “Gnadenfrist”, d.h. die Zeit bis zum Eintritt der (teilweisen) Kernschmelze, mit der richtigen AM-Strategie bedeutend verlängert werden konnte. Während in einem Station Blackout ohne AM nach zwei- bis drei Stunden Schaden am Reaktorkern zu erwarten ist, kann sekundärseitige Druckentlastung und damit die passive Verfügbarkeit von zusätzlichem Speisewasser aus Speisewasserleitungen und Deaeratoren den Naturumlauf erneut in Gang setzen und die Gnadenzeit verlängern. Primärseitige Druckentlastung erlaubt die Intervention der Druckspeicher, und senkt den primärseitigen Druck. Sollte die Stromversorgung nicht wiederhergestellt werden können, verhindert Primärseitige Druckentlastung Versagen des Reaktordruckgefäßes bei hohem Druck.

Summary

Accident management (AM) programmes are considered to be an important step in the defense in depth concept for nuclear power plants. By carefully analyzing possible accident conditions in advance, a nuclear power plant operator may use plant equipment outside of its foreseen functions to cope with situations beyond the design of the plant. Accident management programmes have been first introduced in NPP in the USA, but are now also widely adopted in Europe. The introduction of AM in Republics of the former Soviet Union is a rather recent development.

The present work has been performed as part of a Europaid Project with the goal to support the development of AM for the VVER 1000, a pressurized water reactor used in Russia, Ukraine, Bulgaria, India, Iran, China, Czech Republic. The project was funded by Europaid, TACIS programme, with the aim to enhance the safety of Russian nuclear reactors. The project had several objectives. One of the main goals was to execute complex experiments on the PSB-VVER integral test facility. The facility is a full height, 1:300 volume and power scaled model of the VVER 1000. Twelve diverse and three additional single variant experiments have been executed. The initiating events for the experiments were small break loss of coolant accidents, primary to secondary side leaks, loss of feed water and station black out. In addition, multiple failures of the safety systems and accident management strategies like primary side and secondary side depressurization, and injection into primary and/or secondary side with non standard equipment have been assumed.

The experimental database has then been used for the next main goal of the project, to qualify the codes Relap5 and Cathare2 for simulation of beyond design basis accidents at the VVER 1000, by performing code - experiment comparisons. All experiments have been tried to predict at a pre- and post test level. Although the PSB-VVER facility is well scaled, the behavior of the real NPP will differ considerable. Therefore, the experiments serve to show qualitatively the phenomena that can be expected, and to confirm that the available thermal hydraulic system codes are capable of predicting these phenomena for the facility. Conclusions for the real plant have to be based on simulation with a plant nodalisation.

A third main goal of the project was to test the effectiveness of the adopted AM-Strategies. The simulations, that have been performed with the thermal hydraulic system code Relap5 for the actual NPP to support this part of the project are presented in the current work. Support was given on several occasions. In the planning phase of the experiments, all test designs have been simulated with a plant simulation to confirm their relevance for accident management. After the experimental campaign, the calculations have been repeated, taking into account the experience gained. All AM strategies have been evaluated for their effectiveness.

In close cooperation with the reference NPP, Balakovo Unit 3, one initiating event and AM strategy has been selected for detailed study and optimization. A long term station black out was the selected initiating event. While an SBO of more than 2 hours is extremely unlikely under normal conditions, it is still important if one considers terroristic attacks - the power lines and diesel generators might be less protected than other systems. Even if all active systems are unavailable in this case, the feed water in the feed water lines and deaerator tanks stays pressurized for some time and might be an additional source of water for the secondary side. Likewise, the hydro accumulators can be used as water source for the primary side. The strategy that has been investigated was based on depressurization of secondary and/or primary side, to be able to use the above mentioned sources of water.

To optimize the intervention of the operator, a method for optimization of accident management procedures has been worked out. The method is based on four steps. The parameters to be optimized have to be selected and the boundary conditions have to be fixed. The goal of the optimization (target parameter) has to be defined. An algorithm to iteratively improve the target parameter has to be applied, and finally, the results

have to be displayed.

The findings of the work are that the grace time, i.e. the time before core damage takes place, can be considerably extended by the right accident management strategy. While a in a station black out without accident management after two to three hours core damage can be expected to take place, depressurizing the secondary side and thereby furnishing additional feed water from feed water lines and deaerator tanks passively into the steam generators can restart natural circulation and gain additional grace time. Depressurizing the primary side allows the hydro accumulators to intervene, and to lower the primary side pressure. In case the connection to the grid or emergency power can not recovered, by depressurizing the primary side failure of the reactor pressure vessel at high pressure can be avoided.

Contents

1	Introduction	1
1.1	Scope	2
1.2	Objective	3
1.3	Achievement of the objective	3
2	Background	5
2.1	Accident Management	5
2.1.1	Three Mile Island	5
2.1.2	Safety barriers	6
2.1.3	Phases of AM	6
2.1.4	Preventive AM	7
2.2	Description of the VVER-1000	9
2.2.1	Reactor cooling system	9
2.2.2	Reactor core	11
2.2.3	Emergency core cooling system	13
2.2.4	Containment system	15
2.2.5	Operating conditions	15
2.2.6	Overview on the VVER1000 operation in the world	15
2.3	The PSB-VVER Test Facility	25
2.4	Methods and Tools	33
2.4.1	Relap5	33
2.4.2	Aspects of UMAE	50
2.4.3	FFTBM	55
3	VVER-1000 NPP calculations	63
3.1	Connection to PSB	63
3.1.1	Description of the PSB-VVER nodalisation	64
3.1.2	Post test analysis 12 - 0.7% CL break	69
3.1.3	Post test analysis 11 - 0.7% CL break	95
3.1.4	Post test analysis 7 - SBO with with operator actions	114
3.1.5	Post test analysis 1 - LOFW with operator actions	126
3.2	Nodalisation	150
3.2.1	Description of the nodalisation	150
3.2.2	Qualification of the nodalisation	158
3.2.3	Matrix of performed calculations	164
3.3	LOFW and SBO	165
3.3.1	Scenario 1	165
3.3.2	Scenario 2	166
3.3.3	Scenario 6	167
3.3.4	Scenario 7	169
3.4	SBLOCA	178
3.4.1	Scenario 3 - Zaphoroshye	178
3.4.2	Scenario 4	178
3.4.3	Scenario 8	180
3.4.4	Scenario 10	180

3.4.5	Scenario 11	181
3.4.6	Scenario 12	181
3.5	PRISE transients	188
3.5.1	Scenario 5	188
3.5.2	Scenario 9	189
4	EOP Optimization	193
4.1	Situation at Balakovo	194
4.1.1	Strategy	194
4.1.2	Signals	194
4.1.3	Equipment	195
4.2	Qualitative	199
4.3	Quantitative	211
4.3.1	Methodology	211
4.3.2	Application Of The Procedure	211
5	Conclusions	219
5.1	Code validation	219
5.2	AM strategy evaluation	220
5.3	EOP Optimization	221
5.4	Achievements and open issues	222
	Bibliography	226

List of Tables

2.1	Critical safety functions of Balakovo3	8
2.2	The VVER1000 NPP system elevations and main dimensions [Mikhailchuk, 1997]	10
2.3	The VVER1000 steam generator elevations and dimensions [Mikhailchuk, 1997]	11
2.4	The VVER1000 reactor pressure vessel [Mikhailchuk, 1997]	11
2.5	Feed water system main technical data [Groudev, 2002]	12
2.6	The VVER1000 reactor core and fuel assembly parameters [BNPP1-DB, 1996]	13
2.7	Evolution VVER1000 safety concept	15
2.8	The VVER1000 nominal operational parameters taken from Mikhailchuk [1997]	16
2.9	Overview of VVER1000 reactors in operation and under construction	17
2.10	PSB-VVER and VVER-1000 comparison	26
2.11	PSB selected measurements (nom. value) and associated errors	26
2.12	Quantities for general balance equation	34
2.13	Relap wall to fluid heat transfer correlations	39
2.14	Selected weighting factor components for typical thermal hydraulic parameters	61
3.1	Test facility configuration, taken from Elkin et al. [2004]	69
3.2	Imposed sequence of main events for PSB Test 12, CL-0.7-11, taken from Elkin et al. [2004]	71
3.3	Comparison experiment/ Relap5 calculation test 12, base and improved	75
3.4	Judgement of code calculation performance on the basis of phenomena included in the CSNI matrix, test 12	76
3.5	Relap5 - judgement of code calculations on the basis of RTA (part 1), test 12	77
3.6	Relap5 - judgement of code calculations on the basis of RTA (part 2), test 12	78
3.7	Post test 12 results, base, the accuracy evaluation following the FFTBM	79
3.8	Test 11 facility configuration, taken from Elkin [2004a]	95
3.9	Imposed sequence of main events for PSB Test 11, CL-0.7-12, taken from Elkin et al. [2004]	97
3.10	Sequence of the principal events in the experiment 11 [Elkin, 2004a]	98
3.11	Post test 11 results, accuracy evaluation following the FFTBM	100
3.12	Relap5 comparison experiment/calculation, test 11	101
3.13	Test 11 - judgement of code calculations on the basis of RTA (part 1)	112
3.14	Test 11 - judgement of code calculations on the basis of RTA (part 2)	113
3.15	Test facility configuration, taken from Elkin et al. [2005d]	114
3.16	Imposed sequence of main events for PSB Test 7	116
3.17	Sequence of the principal events in test 7 taken from Elkin et al. [2005c]	116
3.18	Post test 7 comparison experiment/calculation	117
3.19	Post test 7 results, the accuracy evaluation following the FFTBM	117
3.20	Test 1 facility configuration, taken from Elkin et al. [2005b]	126
3.21	Imposed sequence of main events for PSB Test 1	129
3.22	Sequence of the principal events in the experiment 1 taken from Elkin et al. [2005a]	129
3.23	Relap5 test1 comparison experiment/calculation	130
3.24	Relap results test 1, the accuracy evaluation following the FFTBM	130
3.25	Parameters of the steady state calculation	158
3.26	Relap5 nodalisation qualification - key parameters	160
3.27	Relevant thermalhydraulic aspects on-transient qualification	162
3.28	Overview on presented Relap5 calculations.	165
3.29	Resulting events, test 1	166

3.30	Resulting events, test 2	168
3.31	Resulting events, test 6	170
3.32	Resulting events, test 7	170
3.33	BC for analysis	171
3.34	Resulting events, test 3	178
3.35	Resulting events, test 4	179
3.36	Resulting events, test 8	181
3.37	Resulting events, test 5	188
3.38	Resulting events, test 9	191
4.1	Deaerator and FW lines, relevant parameters	198
4.2	SBO optimization - boundary conditions	199
4.3	Performed SBO sensitivity calculations	200
4.4	Chosen single parameters - results	201
4.5	Calculation REF1 - resulting events	202
4.6	Optimization of two parameters, the time of SDE and PDE	217
4.7	Optimization of three parameters, the time of PDE, normalized PORV area, normalized BRU-A area	217

List of Figures

2.1	Scope of accident management	6
2.2	The VVER1000 V320 main equipment primary side	18
2.3	The VVER1000 steam generator	19
2.4	The VVER1000 steam generator - cross section	19
2.5	The VVER1000 steam generator - top view	20
2.6	The VVER1000 reactor pressure vessel and core baffle	20
2.7	The VVER1000 scheme of deaerator - feed water lines	21
2.8	The VVER1000 steam lines	21
2.9	The VVER1000 assemblies with control rods (ten groups)	22
2.10	The VVER1000 pressure vs flow rate diagrams for the active ECCS injection systems	23
2.11	The VVER1000 containment	24
2.12	PSB-VVER NPP simulator	27
2.13	PSB - general scheme	28
2.14	PSB core simulator	29
2.15	PSB SG simulator	29
2.16	PSB - RPV model measurement points	30
2.17	PSB - core simulator measurement points (1/2)	31
2.18	PSB - core simulator measurement points (2/2)	31
2.19	PSB - instrumented fuel rod simulator	32
2.20	Upward co-current flow in a vertical pipe ([Roumy, 1969])	35
2.21	Convective boiling in a heated channel ([Hewitt and Hall-Taylor, 1970])	36
2.22	Flow regimes for horizontal flow	37
2.23	Flow regimes for vertical flow	38
2.24	Wall to fluid heat transfer mode	47
2.25	Relap5 vertical stratified flow (left), meaning of angle θ in (2.8) (right)	48
2.26	Two possible configurations for the horizontal stratification entrainment/pullthrough model	48
2.27	CCFL model used if (H_f, H_g) in accessible region (left), interface liquid/steam with/without mixture level tracking model (right)	49
2.28	Converging-diverging nozzle	49
2.29	Subcooled choking process	49
2.30	UMAE flowchart	50
2.31	Nodalisation qualification procedure	51
3.1	PSB test matrix and VVER calculations. Red - additional assumed failures, green - AM strategy.	64
3.2	Relap5 nodalization of the PSB-VVER facility, general scheme	67
3.3	Relap5 nodalization scheme of the PSB-VVER - RPV	68
3.4	Post test 12 results, base, primary side pressure, short and long term	80
3.5	Post test 12 results, base, secondary side pressure, short and long term	81
3.6	Post test 12 results, base, core inlet temperature, short and long term	82
3.7	Post test 12 results, base, core outlet temperature, short and long term	83
3.8	Post test 12 results, base, primary mass, short and long term	84
3.9	Post test 12 results, base, integral flow rate through the break, short and long term	85
3.10	Post test 12 results, base, heater rod cladding temperature top, short and long term	86
3.11	Post test 12 results, base, heater rod cladding temperature middle, short and long term	87

3.12	Post test 12 results, base, heater rod cladding temperature bottom, short and long term	88
3.13	Post test 12 results, base, integral eccs flow rate	89
3.14	Post test 12 results, base, pressure in accumulator 1	89
3.15	Post test 12 results, improved, primary side pressure, short and long term	90
3.16	Post test 12 results, improved, secondary side pressure, short and long term	91
3.17	Post test 12 results, improved, pressure in accumulator 1	92
3.18	Post test 12 results, improved, heater rod cladding temperature top, short and long term . . .	93
3.19	Post test 12 results, improved, heater rod cladding temperature bottom, short and long term .	94
3.20	Post test 11 results, primary side pressure, short and long term	102
3.21	Post test 11 results, secondary side pressure, short and long term	103
3.22	Post test 11 results, core inlet temperature, short and long term	104
3.23	Post test 11 results, core outlet temperature, short and long term	105
3.24	Post test 11 results, primary mass, short and long term	106
3.25	Post test 11 results, integral flow rate through the break, short and long term	107
3.26	Post test 11 results, heater rod cladding temperature top, short and long term	108
3.27	Post test 11 results, heater rod cladding temperature middle, short and long term	109
3.28	Post test 11 results, heater rod cladding temperature bottom, short and long term	110
3.29	Post test 11 results, integral eccs flow rate	111
3.30	Post test 11 results, pressure in accumulator 1	111
3.31	Post test 7 results, primary side pressure	118
3.32	Post test 7 results, SG1 pressure	119
3.33	Post test 7 results, SG2 pressure	120
3.34	Post test 7 results, core inlet temperature, short and long term	121
3.35	Post test 7 results, core outlet temperature, short and long term	122
3.36	Post test 7 results, level SG1, short and long term	123
3.37	Post test 7 results, loop 1 mass flow rate, short and long term	124
3.38	Post test 7 results, loop 2 mass flow rate, short and long term	125
3.39	Relap results test 1, primary side pressure, short and long term	132
3.40	Relap results test 1, SG1 secondary side pressure, short and long term	133
3.41	Relap results test 1, SG2 secondary side pressure, short and long term	134
3.42	Relap results test 1, SG4 secondary side pressure, short and long term	135
3.43	Relap results test 1, core inlet temperature, short and long term	136
3.44	Relap results test 1, core outlet temperature, short and long term	137
3.45	Relap results test 1, upper head temperature, short and long term	138
3.46	Relap results test 1, heater rod cladding temperature top, short and long term	139
3.47	Relap results test 1, heater rod cladding temperature middle, short and long term	140
3.48	Relap results test 1, heater rod cladding temperature bottom, short and long term	141
3.49	Relap results test 1, level SG1, short and long term	142
3.50	Relap results test 1, level SG2, short and long term	143
3.51	Relap results test 1, level SG4, short and long term	144
3.52	Relap results test 1, level PRZ, short and long term	145
3.53	Relap results test 1, loop 1 mass flow rate, short and long term	146
3.54	Relap results test 1, loop 2 mass flow rate, short and long term	147
3.55	Relap results test 1, loop 3 mass flow rate, short and long term	148
3.56	Relap results test 1, loop 4 mass flow rate, short and long term	149
3.57	Relap5 nodalisation scheme - core	151
3.58	Relap5 nodalisation scheme - loop	156
3.59	Relap5 nodalisation scheme - pressurizer	157
3.60	Relap5 nodalisation scheme - feed water line and deaerator tanks	157
3.61	KV scaled calculation, OECD test No3, primary pressure	163
3.62	KV scaled calculation, OECD test No3, hot rod temperature	163
3.63	Relap5 primary and secondary side pressure, temperature and mass inventory, calculation 1 .	167
3.64	Relap5 primary and secondary side pressure, temperature and mass inventory, calculation 2 .	169
3.65	Relap5 primary and secondary side pressure, temperature and mass inventory, calculation 6 .	171
3.66	Relap5 primary and secondary side pressure, temperature and mass inventory, calculation 7 .	172
3.67	SG heat transfer, heuristic	174
3.68	Level of the SG and heat transfer, heuristic evaluation	175

3.69	Sc 7 heat transfer across SG, six levels, nodalisation, exchanged power, level, void fraction (Relap)	175
3.70	Sc 7 heat transfer across SG, three levels, nodalisation, exchanged power, level, void fraction	176
3.71	Sc 7 heat transfer across SG, one level, nodalisation, exchanged power, level, void fraction	176
3.72	Sc 7 heat transfer across SG, SG levels	177
3.73	Relap5 primary and secondary side pressure, temperature and mass inventory, calculation 3	179
3.74	Relap5 primary and secondary side pressure, temperature and mass inventory, calculation 4	180
3.75	Relap5 primary and secondary side pressure, temperature and mass inventory, calculation 8	182
3.76	Relap5 primary and secondary side pressure, temperature and mass inventory, calculation 10	183
3.77	Relap5 primary and secondary side pressure, temperature and mass inventory, calculation 11	184
3.78	Relap5 primary and secondary side pressure, temperature and mass inventory, calculation 12	185
3.79	Relap5 calculation scenario 12 for PSB-VVER and VVER-1000, primary system mass	186
3.80	PSB-VVER test 12 RPV simulator levels	186
3.81	PSB-VVER post test calculation test 12 RPV liquid void fraction	187
3.82	PSB-VVER Relap5 test 12 void fraction and fluid velocities	187
3.83	Relap5 primary and secondary side pressure, temperature and mass inventory, calculation 5	189
3.84	Relap5 primary and secondary side pressure, temperature and mass inventory, calculation 9	190
4.1	Potential reservoir of water in feed water lines and deaerator tanks	197
4.2	Potential connection between SG and deaerator tanks	197
4.3	Calculation REF0, important parameters	202
4.4	Calculation REF1 - selected parameters	203
4.5	Calculation REF3 - main parameters	204
4.6	Calculation REF10 - main parameters	205
4.7	Calculation REF14 - main parameters	206
4.8	Calculation REF17 - main parameters	207
4.9	Calculation REF18 - main parameters	208
4.10	Calculation REF200 - main parameters, comparison to REF1	208
4.11	Calculation REF12 - main parameters (zoom on SDE)	209
4.12	Calculation REF5 - main parameters, comparison to REF1	210
4.13	Failure map of SBO AM calculations	210
4.14	Schematic overview on the method used	212
4.15	Function to normalize the extended grace time (equation 4.1)	214
4.16	Function to normalise the final primary pressure of the transient (equation 4.2).	215
4.17	The normalisation function (4.3) for the time interval in which the primary pressure stays below 2 MPa	216
4.18	Optimization of two parameters, the time of SDE and PDE	217
4.19	Optimization of three parameters, time of PDE, Area PORV and BRU-A	218

Abbreviations

AA	Average Amplitude
ACC	Accumulator
ADS	Automatic Depressurization System
AFW	Auxiliary Feed-Water
AM	Accident Management
AOO	Abnormal Operating Occurrence
ATG	Accident Termination Guideline
ATWS	Anticipated Transients Without Scram
BDBA	Beyond Design Basis Accident
BDBAMG	Beyond Design Basis Accident Management Guideline
BIC	Boundary Initial Conditions
BRU-A	(Russian) Steam Dump Valves to Atmosphere
BRU-K	(Russian) Steam Dump Valves to Condenser
CL	Cold Leg
CHF	Critical Heat Flux
CSF	Critical Safety Function
CSNI	Committee for the Safety of Nuclear Installations
DBA	Design Basis Accident
DCH	Direct Containment Heating
DG	Diesel Generator
DEWS	Depressurization and Wide Scope
DNB	Departure from Nucleate Boiling
ECCS	Emergency Core Cooling System
EGRS	Emergency Gas Removal System
EOP	Emergency Operating Procedure
EREC	Electrogorsk Research and Engineering Center
FFT	Fast Fourier Transform
FFTBM	Fast Fourier Transform Based Method
FTCS	Forward in Time Centered in Space
FW	Feed Water
GRNSPG	Gruppo di Ricerca San Piero a Grado
GRS	Gas Removal System
HA	Hydro Accumulator
HL	Hot Leg
HPIS	High Pressure Injection System
HHPIIS	High High Pressure Injection System
IAEA	International Atomic Energy Agency
ISP	International Standard Problem
LOCA	Loss Of Coolant Accident
LPIS	Low Pressure Injection System
LWR	Leight Water Reactor
MCP	Main Coolant Pump
MSIV	Main Steam line Isolation Valve
NPP	Nuclear Power Plant
ODE	Ordinary Differential Equation
ORG	Optimal Recovery Guidline
PDE	Primary side Depressurization
PDE	Partial Differential Equation
PORV	Power Operated Relief Valve

PRAMOPT	Procedure for Accident Management Optimization
PRISE	Primary to Secondary side leak
PRZ	Pressurizer
PS	Primary Side
PSA	Probabilistic Safety Assessment
PSB-VVER	Large Scale Integral Test Facility for VVER 1000 plant simulation
PTS	Pressurized Thermal Shock
PWR	Pressure Water Reactor
RTA	Relevant Thermal-hydraulic Aspect
RBMK	Reactor Bolsoi Mochnosti Kipyashiy (Large Power Boiling Reactor)
RCP	Reactor Coolant Pump
RHR	Residual Heat Removal
RPV	Reactor Pressure Vessel
SA	Severe Accident
SAMG	Severe Accident Management Guideline
SB	Small Break
SCRAM	Safety Cut Rope Axe Man
SDE	Secondary side Depressurization
SG	Steam Generator
SGTR	Steam Generator Tube Rupture
SIT	Safety Injection Tank
SL	Steam Line
SS	Secondary Side
TK	(Russian) Make up / Let down System
TQ	(Russian) Active Safety Injection System
TSC	Technical Support Center
TH-SYS	Thermal-Hydraulic-System
VVER	Russian Designed Pressurizer Water Reactor
WF	Weighted Frequency

Chapter 1

Introduction

In 2003 the University of Pisa, Department of Nuclear, Mechanical and Production Engineering was awarded a service contract by the European Union to support the development of Accident Management Programs for Russian Nuclear Power Plants. The work has been commissioned as part of the TACIS program of the EC. The nuclear part of the TACIS (Technical Assistance to the Commonwealth of Independent States) in the period from 1990-2006 aimed to upgrade the safety of Nuclear Power Plants in countries which have been part of the soviet union.

The project had two parts. The first part, part A, was dedicated to the VVER-1000 reactor, the Russian pendant of the western pressurized water reactor. The second part, part B, had the scope to contribute to safety analysis for RBMK reactors. Apart from the University of Pisa the research center EREC in Elektrogorsk, near Moscow, was involved to carry out the experimental campaign. Contributions came also from the research departments from Gidropress and Nikiet, as well as the Kurchatov Institute. To ensure that the results of the project will help the safety of current Russian NPP, the NPP Balakovo, unit 3, participated as reference NPP to the project. Final recipient of the action was the regulatory authority in Russia, GAN.

The present work has been performed in the frame of Part A of the project and deals exclusively with VVER-1000 reactors. Part A had several objectives:

- work out a database containing experimental results of an integral test facility for VVER-1000 reactor
- the experiments should be relevant for accident management to allow to
 - validate thermal hydraulic system computer codes, simulating the NPP behavior, for simulation of AM relevant transients for VVER 1000
 - verify, as far as possible on a test facility, the effectiveness of accident management strategies
- ensure that the design experiments are relevant for accident management by performing NPP analysis
- use the experience gained by the experiments to improve the NPP calculations performed before the experimental campaign
- investigate the effectiveness of selected AM strategies by the means of NPP calculations
- develop a “reference accident management strategy” and investigate its effectiveness

The current work has been performed in the frame of the project mentioned above.

The project was aimed to fill a hole in the development of accident management programmes for russian NPP, which was ongoing at the time of this work. To implement accident management programmes, analytic support is needed. Main tool for analysis and development of EOPs are thermal hydraulic system codes. Together with the analysis the analyst should be able to estimate to what extend his analysis reproduces the real situation at the plant. For this purpose, for validation of the tools, the computer codes should be tested by predicting scenarios, physical phenomena at the plant that can be compared against data coming from experiments. The experiments for the code - experiment comparison should come as close to the situation for which the code will be used, as possible. For the development of preventive accident management procedures this would be experiments at the plants, with a broad spectrum of initiating events and multiple failures of safety systems. Since such experiments cannot be conducted for obvious reasons, one has to

resort to integral test facilities. A large number of such experiments have been conducted for western type PWR. One goal of the project was to create an experimental database for validation of thermal hydraulic system codes for VVER reactors. The current work contributed to this goal.

A second goal of the current work (and the project) was to provide analytic support in the development of one specific accident management strategy - use of passive non safety equipment in case of a total station blackout, to extend the grace time (i.e. time before core damage) of the reactor as long as possible. In case of a station blackout the operator aims to maintain the heat sink until power can be restored. Mobile pumps, if available at the station, or fire brigade trucks could be used. A feed water flow of 90 tons/h is needed to keep the situation stable, 150 tons/h if cooldown should be achieved. While the analysis for use of mobile pumps in case of a station blackout for Balakovo3 NPP has already been performed, the possible use of water from deaerator tanks, and water still present in the feed water line was not yet fully investigated. The present work aimed to contribute to fill this gap.

1.1 Scope

The work is concerned with the simulation of beyond design basis accidents in nuclear power plants, and was embedded in the project mentioned above. Simulation of beyond design basis accidents for NPP in general is a huge field, so to be more precise, the analysis was restricted to accidents at the VVER-1000 reactor, and a certain type of beyond design basis accidents has been chosen:

The distinction between design basis and beyond design basis accidents is usually based upon a statistical criteria. Accidents, whose initiating event are more likely to occur than a certain figure per year (typical values range from 10^{-7} to 10^{-4}). The evaluation of the probability for each initiating event should derive from a probabilistic safety assessment of the NPP. Depending on the legislation in force, for the evaluation of each design basis accident the availability of the safety- and non-safety systems has to be considered. Most countries request that non-safety related systems should be considered to fail, unless their availability would worsen the accident, while for safety related systems the so called "single failure" criterion applies - which means, that the NPP must be able to fulfill given acceptance criteria (peak cladding temperature lower than a certain limit, energy release to the fuel lower than a certain limit, etc) without the most relevant safety system.

Everything beyond this set of accidents is called beyond design basis accident. Beyond design basis accidents are characterized by low probability and a large range of possible consequences. The cases that have been investigated in the current work fall in the category BDBA because multiple failures of safety equipment is assumed. In this case, even if the accidents are BDBA, the plant operator still has the possibility to prevent core damage by following accident management procedures. For example, the failure of all three independent trains of the high pressure safety injection system is a triple failure and therefore a beyond design basis accident. Nevertheless, the operator could eventually recover the make-up system, and still lead the reactor to safe conditions.

The analysis that has been performed, i.e. simulation of beyond design basis accidents, falls in the field of deterministic analysis. While as mentioned before, probabilistic safety assessment aims to calculate probabilities for initiating events, and tries to give a complete picture of the all over risk, deterministic analysis tries to simulate an accident and evaluate its consequences under given initial and boundary conditions. The present work falls into deterministic safety analysis. Twelve accidents with a set of initiating events, determined initial and boundary conditions have been chosen and analyzed.

Within the deterministic safety analysis one distinguishes conservative and best estimate analysis. Conservative analysis uses codes which try to worsen the situation by introducing a bias for certain parameters (e.g. core decay power for conservative analysis usually is assumed to be 20% higher than what would be realistically expected). The results of a conservative analysis typically give an upper bound for key parameters like peak cladding temperature. Application of conservative calculations typically can be found in licensing calculations. On the other hand best estimate calculations try to portrait the situation as realistically as possible. Since uncertainties are connected with the results in both directions, best estimate calculations on its own give an indication of the evolvement of a certain accident, but cannot assure with a certain probability that a certain parameter stays below or above a certain set point. Best estimate calculations are used in accident management, where the goal is to find an effective strategy for the plant operator. A new trend is to introduce best estimate calculations also for licensing applications, but here they have to be accompanied by uncertainty evaluation. The current work uses Relap5 mod 3.3 for the simulation, which is a one dimensional, best estimate, thermal hydraulic system code. The input parameters have not been penalized, so all

simulation results are best estimate calculations.

Beyond design basis accidents can evolve into accidents showing core damage. Upon impending core damage the operator switches priorities. Instead of preventing core damage, the operator now tries to prevent releases to the environment. He follows a different set of procedures. Up to impending core damage, the actions he should take are described in the emergency operating procedures. After core damage took place, he utilizes severe accident management guidelines. The present work focuses on the development of the accident up to impending core damage. If the cladding temperature shows values indicating core damage, the calculation is stopped and the accident management strategy is assumed to have failed.

Accident management procedures can be “symptom based” or “event based”. The former do not clearly identify the cause of the accident and are based on the plant stage. A huge amount of TH-SYS analysis has to ensure that the procedure is effective or at least not worsening the accident for all initiating events that might lead to the same plant state. The latter assume that the operator can clearly identify the initiating event. The current work focuses on event based accident management strategies.

Summarizing, the scope of the present work is in italic:

- Safety barriers - a series of consecutive barriers, to prevent the release of fission product to the environment
- Safety analysis - investigation on the effectiveness of the safety barriers
 - Probabilistic safety assessment Analysis with the aim to quantify the probability of core damage, releases to the environment, and off-site consequences.
 - Deterministic safety analysis Analysis with the aim to assess the plant response for a postulated initiating event with a given set of initial and boundary conditions
 - * Conservative safety analysis Biased analysis penalizing models and key plant parameters. The result should be an upper bound for the real plant behavior
 - * Best estimate safety analysis Analysis trying to predict the plant behavior as accurate as possible
 - Accident management A set of procedures to guide the plant operator during accident conditions
 - State or symptom based procedures - procedures applicable to a variety of accident conditions, stemming from different initiating events
 - *Event based procedures - procedures where the initiating event can be clearly identified, analysis up to impending core damage (EOP)*

1.2 Objective

The objective is to investigate the effectiveness of a number of accident management procedures for several postulated initiating events. The response of the plant in design basis conditions is well known and part of the final safety analysis report, upon which the operation of the plant will be licensed.

The goal of this work is to investigate the plant behavior in beyond design basis conditions. The method of investigation is numerical simulation.

The objective should not restrict itself in just analyzing the effectiveness. In addition, a selected strategy should be optimized. In order to do so, a method for optimization has to be elaborated, and applied.

1.3 Achievement of the objective

The present work is structured in three main sections. The next section 2 provides the information that has been used as basis for the present work. The terms and latest developments in the field of accident management is described. The basic concepts of AM (division in separate AM phases, the role of AM in the defense in depths concept, the difference between preventive and mitigative AM is explained).

The focus is on the VVER 1000, a Russian type pressurized water reactor. About 40 units of this type of reactor are under operation or construction, mainly in Russia, but also in countries associated previously with the soviet union. Key features of the reactor are described, as well as the status of AM programs for the VVER1000. All AM strategies that are described here have been tested on the integral test facility

PSB-VVER, to ensure that the codes used are capable of simulating the phenomena that can be expected. The PSB facility is shortly described. Finally, the main features of the computational tools that have been used, and their mathematical background, are shortly portrayed. The tools are mainly Relap5, the UMAE methodology which has been used to qualify the VVER 1000 nodalisation, and the FFTBM, which is a method to quantify the quality of code predictions.

Section 3 describes the simulations that have been performed to evaluate the main strategies primary side depressurization, secondary side depressurization and injection into primary and/or secondary side by non-standard equipment. The nodalisation that has been adopted and its qualification process are shown at the beginning of the section. The transients are numbered according to the number that they had in the project, and grouped after initiating events. For each transient, the results of key parameters are displayed. A large number of parameters for each transient can be found in an Appendix to the present work.

Section 4 describes the optimization process. A reference strategy has been selected and optimized for the project. The selection of the strategy, the general approach to optimize a AM strategy, and the application of the approach are described in this section.

The conclusions in Section 5 summarize the main findings from the previous two sections.

Chapter 2

Background

The work which is presented here was performed within the frame of the Project “Software Development for Accident Analysis of VVER and RBMK Reactors in Russia”, part A, dealing with VVER 1000 reactors D’Auria et al. [2006]. The University of Pisa implemented the project together with Elektrogorsk Research and Engineering Center (EREC), Kurchatov Institute and Gidropress.

The aim of the project was to confirm the availability of computational tools for accident management (AM) optimization studies in VVER 1000 reactor types.

To reach this goal an experimental campaign at Elektrogorsk was drawn up and executed in 2005. Fifteen experiments have been performed at the PSB-VVER integral test facility.

2.1 Accident Management

Accident Management Programmes are considered to be a key component in the “Defense in Depths” concept in NPP Safety [Misak, 2004a],[IAEA-INSAG-10, 1996]. The five levels commonly considered are

1. prevention of abnormal operation and failures,
2. control of abnormal operation and detection of failures,
3. control of accidents within the design basis.
4. The objective at the fourth level is to ensure that both the likelihood of an accident entailing significant core damage (severe accident) and the magnitude of radioactive releases following a severe accident are kept as low as reasonably achievable.
5. Off-site emergency response measures, with the objective of mitigating the radiological consequences of significant releases of radioactive material.

Level four is covered by accident management and complementary measures.

Figure 2.1 visualizes the scope of accident management.

Accident management takes over in case an accident leaves the design basis of a nuclear power plant. It means, that an organizational structure, provisions and procedures are in place, capable of coping with situations that haven’t been envisaged during the design phase of the plant.

2.1.1 Three Mile Island

Nuclear safety developed gradually. The trigger for the development of what is understood as accident management for NPP has been the TMI-2 accident. Various literature exists on the TMI-2 accident, e.g. [Petrangeli, 2005] or [Walker, 2004].

TMI-2 was the most serious accident of an commercial nuclear power plant in the USA. The initiating event was failure of the feed water pumps, causing the shut down of the reactor and turbine. As result, primary side pressure increased up to the set point of the pressurizer relief valve. The PORV, after opening as foreseen, did not close as expected. But the panel in the control room reported the valve as closed. Primary pressure started to drop (without any reason for the operators). Primary coolant inventory was leaking from

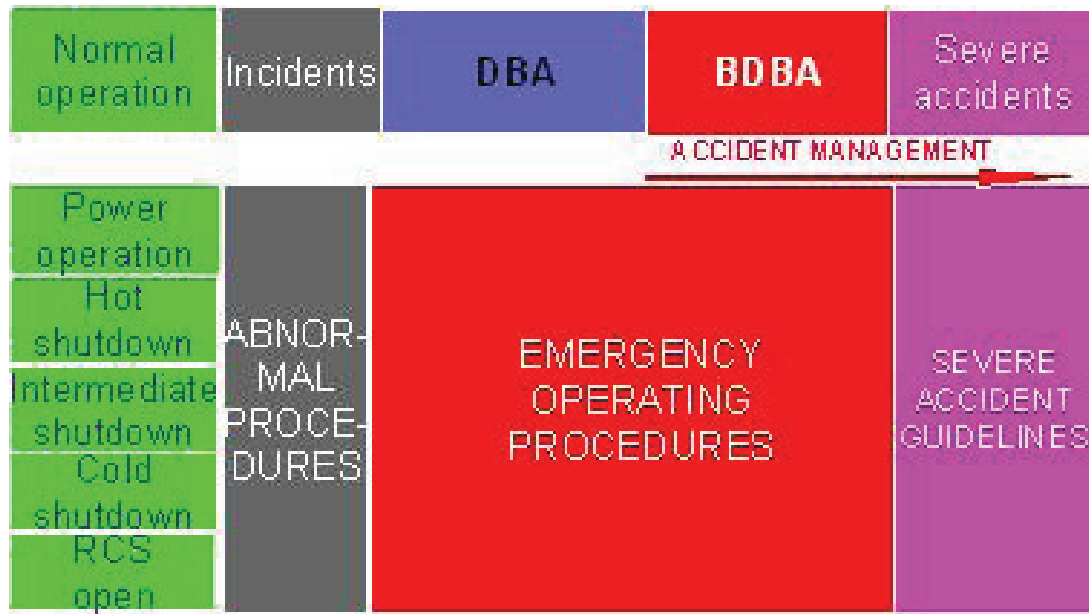


Figure 2.1: Scope of accident management

the system, without knowledge of the operators. The safety injection systems started to inject - but since the operators were not able to diagnose the situation correctly, they saw no reason for safety injection. In addition, the pressurizer level, that was taken as indication for the amount of coolant in the primary system, continued to rise (due to counter current flow). So also this reading led to a wrong conclusion - and the crew decided to shut down the safety injection system.

This led to core dry-out, heat up, start of the zirconium-water reaction and hydrogen generation. Sharp pressure spikes in the containment have been diagnosed later on as explosions of smaller hydrogen bubbles. Up to now there is a discussion ongoing whether or not releases of radioactive material did occur.

One lesson learned from TMI was that support for the crew of an NPP is needed in case of an accident. An operator might or might not diagnose the situation of the plant correctly. Therefore, a organizational structure, together with guidelines and procedure have been developed, aimed to relieve the operator from his responsibility to understand exactly whats going on in the plant. Leading in the development of emergency response guidelines was Westinghouse.

2.1.2 Safety barriers

The most widespread safety concept of NPP puts in place four different physical barriers against release of radioactive materials [IAEA-INSAG-10, 1996]. They are (for pressurized water reactors, like the VVER1000):

- the fuel matrix;
- the fuel cladding;
- the boundary of the reactor coolant system;
- the containment system.

Each level is different from the previous one, because one may assume that if one barrier of one type fails, a second barrier of the same type is also likely to fail.

2.1.3 Phases of AM

Accident management starts when an accident progresses beyond the design bases. This means, that the automatic systems and operational procedures are no longer the best course of action. At this point the operator can rely on a set of clear cut AM procedures, that permit to take a measure based on the plant symptoms, available to the operator.

2.1.4 Preventive AM

Generic

One signal is very important - the core exit temperature. A core exit temperature of more than 600 °C (value depending on country and NPP) is taken as indication that core damage is impending, or did already happen. This or an equivalent signal marks the transition from preventive measures to mitigative measures, with a quite significant change of priorities and way of working. The priorities of AM at various stages are [Misak, 2004a]

- Prevention of the accident from leading to core damage
- Termination of core damage
- Maintaining the integrity of the containment for as long as possible
- Minimizing on-site and off-site releases and their adverse consequences.

While the core exit temperature stays below this value, the decisions are taken in the control room by the operator, based on the emergency operating procedures (EOP). Aim is to prevent the accident from leading to core damage. If the initiating event could be clearly identified, i.e. the operator knows exactly what happens in the plant, the event-based EOP can be used as basis for the decision. Event based EOP are a collection of possible countermeasures for a clear known initial event. The initiating and the strategy has been investigated with best estimate thermal hydraulic system codes like Relap5, to make sure that the adopted strategy is capable of preventing further progression of the accident, and are capable of preventing core damage. The barrier in focus is the cladding of the reactor. If enough coolant can be provided, if it is possible to guarantee long term removal of the decay heat, core heat up will be prevented and the cladding will not fail.

If the operator cannot identify the initiating event, a second set of procedures should be at his disposition - symptom (or state) based procedures. The aim is still to prevent the accident to leading to core damage. The operator checks the state of the plant following a check-list, and tries to take action accordingly. The development of symptom based procedures needs a considerable amount of work, since a strategy has to be tested for all scenarios below a certain probabilistic cut-off criteria [IAEA, 1998], [Misak, 2004a].

Westinghouse approach

Russia decided in the late 1990 to change the Russian approach of accident management. The major part of the plants will take over the Westinghouse based approach. Balakovo3 will act as reference plant for VVER1000 in Russia, which means that after the Westinghouse procedures are implemented in Balakovo3, other VVER1000 units will follow. The section briefly reports the approach of Westinghouse to AM, following [Prior et al., 2000].

Scenario oriented in case the initial event can be clearly identified, the “Optimal Recovery Guidelines” ORG are applied. The OGR are typically applied after a reactor trip or occurrence of safety injection. If the operator successfully identifies the initial event, he applies the appropriate recovery procedure.

The list of initial events is chosen by a probabilistic cut-off criteria. Initial events occurring not less than $-8 \cdot 10^9$ per reactor year have been considered. For each scenario, different types of instructions have been developed, in case the main strategy fails. The accident has to be periodical re-diagnosed.

State based if identification of the initial event is not possible, or the accident was diagnosed but doesn't develop as foreseen, the operator switches to the state based approach. Westinghouse developed six so-called “critical safety functions” (CSF), which identify the state of the NPP. A table called status tree lists symptoms of the plant, and the corresponding state of each safety function.

The safety functions (in order of importance) are:

- Subcriticality
- Core cooling
- Heat sink

- Integrity of primary circuit
- Containment integrity
- Primary coolant inventory

Each function can have one of the following states:

- satisfied - (green)
- not satisfied - (yellow)
- severe challenge - (orange)
- extreme challenge - (red)

The operator should monitor the status tree, to see if one or more critical safety function is not satisfied. If so, he should take the “function restoration guidelines” (this are the state based procedures), and try to restore the safety functions. The operator should start with the function of the highest priority.

Balakovo3 adaptation

Balakovo3 is following the Westinghouse approach. Balakovo at the moment finished developing and implementing their EOP, and is currently working on the severe accident management guidance (SAMG). The following is taken from Sevastyanov et al. [2004].

Guidelines corresponding to the Westinghouse ORG are called in Balakovo terminology Accident Termination Guidance (ATG). The state based approach is called beyond design basis accident management guidance (BDBAMG). Balakovo added one safety function to the Westinghouse safety functions - equipment. The safety functions, and the symptoms indicating their state, is shown in Table 2.1.

	Critical Safety Function	Parameters/Symptoms		
		Extreme challenge	Severe challenge	Unsatisfactory
1	Equipment	All electricity is lost, rooms are flooded, the control room is lost		
2	Subcriticality	neutron power value above 5% after a reactor trip	positive velocity of the reactor run-away	neutron power and positive velocity of reactor runaway
3	Core cooling	Core outlet $> 400^{\circ}C$	Core outlet $> 350^{\circ}C$ or $T_{HL} - T_{CL} > 20^{\circ}C$	Subcooling less than $10^{\circ}C$ anywhere in the loops
4	Heat sink	$(l_{sg} < 150cm$ in 3 or 4 SGs) AND $(\dot{V}_{FW} < 90m^3/h(\approx 20kg/s))$		1.) $P_{SG} > 7.4MPa$ in one or more SGs, 2.) $l_{SG} > 3.9m$ in one or more SGs, 3.) $l_{SG} < 1.5m$ in one or more SGs
5	Primary circuit integrity	$\Delta T_{CL} > 60K$ within one hour in one or more of the cold legs AND PS pressure is high		
6	Containment integrity	$P_{containment} > 0.4MPa$		$P_{containment} > 0.13MPa$
7	Primary Coolant inventory	$l_{PRZ} < 3.5m$ AND $l_{sump} < 1.5m$ after reactor trip		$l_{PRZ} < 3.5m$ AND $l_{sump} > 1.5m$ after reactor trip

Table 2.1: Critical safety functions of Balakovo3

SAMG

Once the integrity of the core is lost, which is usually indicated by a high core outlet temperature, the technical support center (TSC) takes control. The priorities now are to maintain containment integrity. Severe accidents involve a large number of physical phenomena, and are therefore very difficult to predict. The analyst therefore can only provide very rough guidance, and one must be aware of the fact that huge uncertainties are connected to the analysis results.

The tools for preparing the EOP and the SAMGs are quite different. EOP are developed based on a PSA level 1, and investigation of the applicability of a certain procedure is done by TH-System codes. The SAMG sequences are chosen based on a PSA level 2, and integral codes like Melcor or MAAP are adopted, along with consideration of uncertainties.

The present work set its focus on the preventive part of accident management. Therefore, Relap5, a best estimate thermal hydraulic system code has been used.

2.2 Description of the VVER-1000

AM for the VVER-1000/V-320 is the main topic of the present work. The following section describes the VVER-1000. While some information on this NPP-design can be found in open literature, the present work provides in addition information from project reports, which cannot be obtained easily.

The VVER-1000/V-320 is a PWR with a thermal rating of 3000 MW and electrical output of 1000 MW. The unit under consideration in this analysis is a typical V-320 model with four circulation loops, each including a main circulation pump and a horizontal steam generator. The steam generators are fed by two different feed water systems. Each system consists of turbine-driven pumps and piping connecting the feed water line at four different locations in each steam generator. All elements of the primary side are situated in a steel-lined, cylindrical, concrete containment building. Configuration schemes with geometric dimensions and elevations (the value of zero is set to ground level) are shown in Figure 2.2.

In the VVER-1000 primary system, coolant enters into the reactor vessel through four inlet pipes (cold legs) associated with the four primary loops. The flow then passes into the downcomer between the reactor vessel and the inner vessel. The flow enters the lower plenum of the reactor vessel and passes through orifices in the inner vessel and then enters slots in the fuel support structures that lead directly to the fuel assemblies. The flow passes through the open bundles of the core. The fuel assemblies are in the configuration of a hexagon with each containing 312 fuel rods. There are 163 fuel assemblies of which 61 have control rods. After exiting the reactor core the coolant flows into the upper plenum, which contains the shielding block, and then out to the hot legs of each of the four primary loops in the system.

Hot and cold leg of one loop are attached to the RPV at the same angular position (i.e. on top of each other), with a distance between inlet and outlet nozzle central axis of 1.8 m. The loops one and four (two and three) are attached with an azimuthal angle of 55° between each other (i.e. not fully symmetric with 90° angles).

The following description is mainly taken from Groudev [2002].

2.2.1 Reactor cooling system

The reactor cooling system can be divided in primary and secondary system. The primary system comprises the reactor, pressurizer, four loops with steam generators, reactor coolant pump, the secondary system consists of steam generator, turbine, condenser, deaerator and feed water pumps.

Primary system components

Each loop has a horizontal SG and a shaft-sealed reactor coolant pump. A pressurizer is attached to loop 4. A spray line is attached to the cold leg of loop 2. Nominal primary system pressure is 15.7 MPa. The hot leg nozzles are located above the cold leg nozzles on the reactor vessel. There is a water seal in the pressurizer surge line. Low pressurizer level is about at the elevation of the hot legs, and the surge line nozzle into the pressurizer is at about the elevation of the top of the core. The total primary side water volume is 337 m^3 (including the water in the pressurizer). The entire primary geometric volume is 361 m^3 . There is a loop seal in the cold leg at the suction of the RCP.

The reactor coolant pumps are controlled leakage pumps with a four-stage seal. Seal injection is provided between seal number one and seal number two of each pump by the charging system (TK). One part of the

seal injection flow enters the primary system and the rest returns to the TK system through a seal return line. Table 2.2 reports key dimension and elevations of several parts of the primary system.

No	Parameter	Value	No	Parameter	Value
1	CL axis	23.9 m	12	Steam header axis	34.7 m
2	SG tubes top	30.1 m	13	SIT 1 top	29.4 m
3	Loop seal Axis	20.64 m	14	SIT 1 bottom	21.3 m
4	HL axis	25.7 m	15	SIT 3 top	35.7 m
5	RPV bottom	16.9 m	16	SIT 3 bottom	27.6 m
6	RPV top	28.7 m	17	HL length	9.83 m
7	PRZ bottom	22.3 m	18	CL length	28.0 m
8	PRZ top	34.6 m	19	CL internal diameter	0.85 m
9	PRZ Volume	79 m ³	20	HL internal diameter	0.85 m
10	SG top	31.9 m	21	PRZ diameter	3 m
11	SG bottom	27.9 m			

Table 2.2: The VVER1000 NPP system elevations and main dimensions [Mikhailchuk, 1997]

The pressurizer is the only location within a pressurized water reactor vessel that has a steam/liquid interface during normal operation. The interface reduces the risk from water hammer and provides a compressible steam (gas) space, which is used to set the absolute pressure of the reactor vessel. The bottom of the volume is connected hot leg No 4 by the surge line, while the top of the pressurizer has sprays with piping connected to cold leg No 2 and the charging (makeup) system. This configuration for the spray injection inherently allows the high pressure in the cold leg to inject into the pressurizer, but the make-up system is also available to inject water to condense and reduce the steam in the system.

The VVER-1000 typical main coolant pumps are run by electrical motors 6kV AC. The GCN-195M pump is a vertical, single stage, centrifugal pump. The nominal flow of the MCP at 50 HZ is 5.88 m³/s. The nominal head is 0.66 MPa. The actual pump capacity for 3 pumps in operation is 3x6.76 m³/s, for 2 pumps in operation 2x7.33 m³/s, for 1 pump 7.50 m³/s. The pump coast down time in case of loss of power supply is 232 s.

The steam generators of VVER-1000 type reactors are of horizontal, U-tube, natural circulation type. The horizontal steam generator represents an important difference between VVER designs and Western reactor designs. The response of horizontal steam generators can be very different than that of Western type vertical steam generators due to the larger water mass in horizontal steam generators. This larger water mass can affect the reactor transient response particularly during secondary side occurrences. The steam generators include horizontal U-shaped heat exchanger tubes and provide natural separation on the secondary side without the use of coarse separators

The main components of the steam generators are:

- steam generator vessel;
- heat transfer tubes (horizontal U-tubes) and primary coolant heads;
- feed water nozzle facility;
- emergency feed water nozzle facility;
- a perforated plate;
- moisture separator;

Feed water flows into the steam generator through a pipe 426x24 mm, then through 16 collectors of 80 mm inside diameter which couple to the distribution pipes, see Figures . Each of these distribution pipes have 38 perforated pipes. Some are at the upper steam tubing elevation while another portion is over the perforated sheet in order to balance the nonuniform steam generation. This is achieved by partial condensation of the voids in high steam areas. Table 2.3 presents an overview on key figures of the steam generator.

The reactor pressure vessel is the pressure boundary of the reactor core and high-pressure coolant. The detailed geometry of the vessel is presented in Figure 2.6. The total height of the RPV is 19.1 m, the internal height of from the lowest point of the lower plenum to the highest point of the upper head is 13.2 m. The

No	Parameter	Value	No	Parameter	Value
1	Average tube length	11.1 m	5	SG collector volume	2.4 m ³
2	Number of tubes	11000	6	SG collector height	5 m
3	Tube ID	13 mm	7	PS total volume	23.4 m ³
4	Tube OD	16 mm	8	PS tubes volume	16.2 m ³

Table 2.3: The VVER1000 steam generator elevations and dimensions [Mikhailchuk, 1997]

free volume of the RPV is 110 m³. The coolant enters from the cold legs into the RPV, and passes through the downcomer into the lower plenum. From there through the reactor core to the upper plenum. The temperature increase of the fluid core-inlet to core-outlet is equal to 30°C during nominal operation (core flow rate 84800 m³/h). The mass of the RPV, core baffle, spacing plate, support plate, the RPV structures except the active core sums up to 250 tons. In addition, there are 80 tons of fuel and about 25 tons of cladding material in the active core (source [Mikhailchuk, 1997]). Table 2.4 shows key figures on RPV dimensions.

No	Parameter	Value	No	Parameter	Value
1	Total internal height	11.76 m	7	Top of hydraulic core	22.36 m
2	RPV top	28.71 m	8	CL axis	23.9 m
3	RPV bottom	16.85 m	9	Top of DC	24.95 m
4	Bottom of hydraulic core	18.29 m	10	HL axis	25.7 m
5	Bottom of active core	18.48 m	11	UP top	26.75 m
6	Top of active core	22.03 m	12	UH top	28.71 m

Table 2.4: The VVER1000 reactor pressure vessel [Mikhailchuk, 1997]

Secondary system

The feed water system (Figure 2.7) supplies water from the condensate storage tank back into the steam generators through the high pressure heaters (or bypassing them) which controls the steam generator water level during plant operation. The system consists of two turbine driven feed water pumps (FWP) two auxiliary electrically driven feed water pumps (AFWP) and ten control valves.

The steam produced in the steam generators is transported to the turbine by the main steam lines (Figure 2.8). It is also used for in-house supply of steam to the turbo-pumps. The main steam lines system includes the following components:

- 8 SG relief valves;
- 4 steam dump valves to atmosphere BRU-A;
- 4 steam dump valves to the condenser BRU-K
- 4 main steam isolation valves (MSIV);

Key figures regarding the balance of plant are shown in Table 2.5.

2.2.2 Reactor core

The following is taken from Ivanov et al. [2002]. The reactor core of VVER-1000/V320 consists of 163 fuel assemblies, 61 fuel assemblies have control rods. Figure 2.9 shows the location of assemblies with control rods. The fuel assemblies of the VVER-1000 are hexagonal in shape and without a shroud. The fuel pins are arranged on a triangular pitch. Within the control assemblies, there are 18 positions occupied with stainless steel control rod guide tubes to control the movement of the cluster of control rods that move within them.

The VVER-1000 fuel cycle can be three, four, or even five years. Once in a year the reactor is shut down for maintenance and a according portion of the core is replaced. The enrichment ranges from 3.3% of U-235 up to 4.4%. Zones of highest enrichment are the outer portions of the core, Table 2.6 shows key figures of the VVER-1000 reactor core.

No	Description	Value	Unit
Pressure drops along FW line			
1	Hydrostatic pressure head between deaerator and FWP	0.229	MPa
2	Hydrostatic pressure head between FWP and HP Heater	0.126	MPa
3	Hydrostatic pressure head between HP Heater and SG	0.0536	MPa
4	Nominal pressure drop over HPH	0.98	MPa
5	Nominal pressure drop over the HPH bypass	1.1	MPa
6	Nominal pressure drop over the FW line and nozzle facility	0.981	MPa
Deaerator properties			
7	Nominal pressure	0.58	MPa
8	Nominal level	2.52	m
9	Nominal temperature	437.15	K
10	Feedwater flow rate	1944.44	kg/s
10	Inner diameter	3.41	m
11	Deaerator wall thickness	0.16	m
12	Total FW volume	210	m ³
13	Nominal volume	185	m ³
14	Deaerator elevation (axis)	31.07	m
15	Deaerator vessel length	23.4	m

Table 2.5: Feed water system main technical data [Groudev, 2002]

No	Parameter	Unit	
Core			
1	Equivalent diameter of the core	m	3.16
2	Flow area of the core	m ²	4.14
3	Core height in the working state	m	3.55
4	Fuel height in cold state	m	3.53
Fuel Assembly			
5	Geometry		Hex.
6	Number of FA in the core	#	163
7	FA height	m	4.57
8	Maximum width across flats of FA	m	0.2351
9	Pitch between fuel assemblies	m	0.236
Fuel Rod			
10	Number of fuel rods in each FA	#	311
11	Fuel rods cladding outer diameter	mm	9.1
12	Fuel rods cladding inner diameter	mm	7.73
13	Outside diameter of pellet	mm	7.57
14	Diameter of central hole in pellet	mm	1.5
15	Pitch between fuel rods in FA	mm	12.75
16	Helium pressure under fuel rod cladding	MPa	2
Spacing grid			
17	Number of spacing grid in FA		15
Lower grid			
18	Number of circle holes in the grids	#	350
19	20 holes with diameter	m	0.0063
20	40 holes with diameter (one half should be considered)	m	0.0063
21	290 holes with equivalent diameter	m	0.300144
Reactivity coefficients, hot conditions, BOC			
22	Fuel temperature feedback coefficient	pcm / K	-1.9

continued on next page

No	Parameter	Unit	
23	Coolant density feedback coefficient	pcm / (kg/ m ³)	5.02
24	Coolant temperature feedback coefficient	pcm / K	-12.8
25	Boron reactivity coefficient	pcm / ppm	-9.4
26	Boron concentration	g/kg	1.12
27	Total reactivity of all rods inserted (maximum worth cluster stuck)	%	-6.49
28	Delayed neutron fraction worth (β)	%	0.664
	Reactivity coefficients EOC		
29	Fuel temperature feedback coefficient	pcm / K	-2.1
30	Coolant density feedback coefficient	pcm / (kg/ m ³)	31.30
31	Coolant temperature feedback coefficient	pcm / K	-65.9
32	Boron reactivity coefficient	pcm / ppm	-9.5
33	Boron concentration	g/kg	0.0
34	Total reactivity of all rods inserted (maximum worth cluster stuck)	%	-6.41
35	Delayed neutron fraction worth (β)	%	0.585

Table 2.6: The VVER1000 reactor core and fuel assembly parameters
[BNPP1-DB, 1996]

2.2.3 Emergency core cooling system

The following paragraph is taken from Sholly [2001]. The plant safety system concept is, with some exceptions, a 3x100% redundancy design with three nominally identical trains of equipment for each system. The high pressure injection (TQ3), low pressure injection (TQ2), and containment spray (TQ1) systems take suction from a common containment sump, which is contained in an extension of the containment below the cavity basement. The high high pressure injection system or high pressure boron injection system (TQ4) takes suction from three tanks of highly borated water (three times 15 m³40g/kg of boric acid concentration). Figure 2.10 shows the pressure vs flow rate curve for the TQ2, TQ3 and TQ4 system.

The HPI system (TQ3) is designed to supply up to 255 m³/h (70 kg/s, at 1.67 MPa) and up to a pressure of 10.88 MPa (at a flow rate of 25 m³/h, 7 kg/s) The HPI pumps are also used in what is termed "feed and bleed" cooling, in which the operators depressurize the primary system to a pressure below the HPI injection capability by opening the PORV (flow rate through the PORV at 18.21 MPa is 50 kg/s), and injecting coolant with the HPI pumps. The fluid discharged from the PORV results in the barbotage tank including a rupture disk discharging the coolant into the containment sump. As the coolant is drawn from the sump by the HPI pumps, it is cooled by the residual heat removal (RHR) heat exchangers before being injected back into the primary coolant system. Feed and bleed cooling is used upon loss of secondary heat removal capability (loss of all feed water).

TQ4 and TQ3 are independent systems, but share the same injection points. Both systems inject in the cold legs of three of the loops, downstream the MCP. In Balakovo3 (the reference plant for this work) the loops are 1,3 and 4, however, in VVER1000 plants different loops have been chosen.

The low pressure injection system (TQ2) provide emergency coolant makeup in the event of a large pipe break. The system also can be operated in the RHR mode to remove decay heat from the reactor coolant system after shutdown. The LPIS can inject up to a PS pressure of 2.5 MPa, and the maximum flow rate amounts to 763 m³/h (at atmospheric pressure). Residual heat removal is a mode of operating the LPI system to take the primary system to, and maintain it in, cold shutdown. Initiation of RHR cooling is a series of operator manual actions taken from the main or emergency control room.

There are four accumulators (YT) pressurized by nitrogen which automatically inject borated water into the reactor coolant system at a pressure of 5.9 MPa. Three accumulators are needed to reach the intended safety goal in case of a large LOCA (4x33%). Two accumulators inject into the upper plenum and two into the down comer of the reactor pressure vessel. Each accumulator has a capacity of 50 m³ of water. Following injection, fast acting electric powered isolation valves close on low level in the accumulators to

prevent injection of nitrogen gas into the primary system. The accumulators are located in two pairs on elevation level 27.0m and 36.0m in the containment.

Two accumulators inject into upper plenum, two accumulators into the downcomer. They share the last part of the lines with two trains of the TQ2 system - train one injects into downcomer and upper plenum, train two injects into downcomer and upper plenum, while train three injects into hot- and cold leg of loop one (cold leg injection point between MCP and RPV, hot leg injection point close to the RPV).

The makeup system is part of the chemical and volume control system, which performs a variety of functions supportive of normal operation. From the standpoint of accident analysis the makeup pumps are important as regards steam generator tube rupture (SGTR) sequences and also in their role in providing reactor coolant pump (RCP) seal support functions to maintain RCP seal integrity. The system can be connected to the TB10 system which is made up of 2 tanks of 200 m³, each containing 40 g/kg (4 wt% or 7000 ppm) boric acid. With all three TB10 system pumps operating, the system can achieve a maximum flow of 100 m³/h. The high pressure boron injection system or high high pressure injection system (HHPIS) is capable of injecting up to 19.6 MPa at a flow rate of 6.2 m³/h. It takes suction from three tanks with highly borated water, with a volume of 15 m³ each.

SYSTEM	DESIGN					
	V-187	V-302	V-338	V-320	V-392	V-412
Start up of the 1st unit	1980	1983	1984	1984	Design stage	Design stage
PRIMARY CIRCUIT						
HPIS	3x100%	3x100%	3x100%	3x100%	-	4x100%
LPIS	3x100%	3x100%	3x100%	3x100%	-	4x100%
Combined HPIS-LPIS	-	-	-	-	4x100%	-
Emergency boron injection	+	+	+	+	-	+
Emergency gas removal	+	+	+	+	+	+
Number of pressurizer safety valves (G= 50 kg/s)	3	3	3	3	3	3
Fast boron injection system	-	-	-	-	4x25%	4x25%
1st step hydroaccumulators	4x33%	4x33%	4x33%	4x33%	4x33%	4x33%
2nd step hydroaccumulators	-	-	-	-	4x25%	4x25%
ECCS tanks with high boron concentration (40 kg/s)	1x150m3	3x150m3	3x150m3	3x150m3	-	-
ECCS tanks with low boron concentration (16 kg/s)	3x585m3	3x585m3	3x750m3	1x630m3	1x500m3	1x500m3
SECONDARY CIRCUIT						
Emergency feedwater system	3x100%	3x100%	3x100%	3x100%	-	-
Emergency cool-down system of steam generators	-	-	-	-	4x100%	4x100%
Passive residual heat removal	-	-	-	-	4x33%	4x33%
Number of SG safety valves	2	2	2	2	2	2

continued on next page

SYSTEM	DESIGN					
	V-187	V-302	V-338	V-320	V-392	V-412
Start up of the 1st unit	1980	1983	1984	1984	Design stage	Design stage
Fast acting safety valves on main steam lines	+	+	+	+	+	+
Check valves on main steam lines	+	+	+	+	-	-
Motor operated valves on main steam lines	+	+	+	+	+	+
Fast acting reduction station for steam release into the atmosphere (BRU-A)	1 on each main steam line	1 on each main steam line	1 on each main steam line	1 on each main steam line	4 on main steam header	4 on main steam header

Table 2.7: Evolution VVER1000 safety concept

2.2.4 Containment system

The following paragraph is mainly taken from Groudev [2002]. The main element of the VVER-1000/V320 containment (see Figure 2.11 containing the reactor pressure vessel and the primary side consist of a cylinder (height 38 m, diameter 45 m) with a dome on top. The building material is pre-stressed concrete with a thin steel liner (8 mm) on the inside. The concrete wall thickness is about 1.2 m for the cylinder and 1.1 m for the dome. The containment design overpressure is 0.41 MPa, covering the pressure peak after double-ended guillotine rupture of the main primary loop of 0.85 m diameter.

The bottom of the containment is at +13.7 m above the ground, the bottom of the ECC sump at +7.4 m. The ECC pumps and different supporting equipment are located in the lower part of the reactor building. The square building extends also above the containment shell base plate, up to about +40 m protecting large part of the containment shell with the reactor against external impact and improving the primary system shielding. There is a narrow gap between the cylindrical shell and the cylindrical inner shaft in the square building.

The containment is equipped with 3 (200 % backup) active spray systems to reduce pressure after steam leak from the primary or secondary circuit. Their distributors are rings with spray jets at the top of the dome. They are connected by vertical lines with the pumps and containment heat removal exchangers located below the containment which take water from the main recirculation sump. The sump is common for all three systems and is shared together with the heat exchangers of the containment heat removal system with the active ECC systems.

2.2.5 Operating conditions

The VVER-1000 nominal operating conditions are 3000 (± 60) MW, the nominal flow rate is 84800 (+4000 /-4800) m³/h, the primary side pressure is 15.7 MPa, the temperature at the reactor inlet 289 °C, the temperature at the reactor outlet is 320°C

2.2.6 Overview on the VVER1000 operation in the world

The following description can be found in Misak [2004b]. The VVER-1000 reactors constitute the latest generation of soviet-designed pressurized water reactors (PWRs). NPP with VVER-1000 reactors, which are in operation at present, have been developed in four different models. Main characteristics of different models are described based mainly on the book Denisov and Dragunov [2002].

The designs of earlier models 187, 302 and 338 were started in 1972 and were completed in 1979. The standard used for their design was the Russian regulatory document OPB-73. These early models have historically been called the small series because only five units of these models have been constructed. Originally the design of VVER-1000 small series differs significantly between each other and VVER-1000

No	Parameter	Unit		Comment
1	Power	[Mw]	3000	
2	Core inlet temperature	[deg C]	290	
3	Core Dtemperature	[deg C]	30	
4	Core outlet temperature	[deg C]	320	
5	Coolant pressure outlet core	[Mpa]	15.7	upper plenum
6	One loop flow rate	[m3/h]	21200	Core flowrate/4
7	Core flow rate	[m3/h]	84800	lower plenum
8	Pump rotation speed	[rev/min]	995	
9	PRZ pressure	[Mpa]	15.7	
10	PRZ temperature	[deg C]	346	
11	Pump flow rate	[m3/h]	20000	pump capacity
12	SG exchanged power	[Mw]	750	
13	SG steam production	[kg/s]	408	
14	SG pressure	[Mpa]	6.27	
15	SG steam temperature	[deg C]	279	
16	FW temperature	[deg C]	220	

Table 2.8: The VVER1000 nominal operational parameters taken from Mikhaltchuk [1997]

V-320 design. The design of VVER-1000 small series model 187 was developed in the early seventies in accordance with standards of that time, including such issues as insufficient environmental qualification of equipment belonging to instrumentation and control and electric power supply, as well as separation between control and safety functions. In addition, the overall system layout provided sometimes an insufficiency in protection against environmental impact. For example, all emergency feed water pumps were installed in the turbine hall without real separation. V320 model has been designed and built according to the requirements set out in the new OPB-82 safety regulations, which attempted at complying with international practices and safety standards. The concept of defense in depth was realized by general design criteria including the use of redundancy, diversity, independence and single failure criterion for safety systems. For standard VVER-1000/V320 units the design differences are not so significant, with exception for Temelin NPP at which a lot of upgrading measures have been implemented during the construction phase. Several generic design features for all VVER-1000 reactors remained unchanged for all models, and they are very similar to Western PWR with few exceptions as follows:

- Reactor pressure vessel has relatively small diameter, with inlet and outlet nozzles located at different elevations
- Hexagonal fuel assemblies, with triangular fuel rods array
- Fuel rods with relatively small diameter, with Zr+Nb used as a cladding material
- Four loops in the primary circuit, with the horizontal steam generators as a characteristic design feature
- As compared with initial (small series) VVER 1000 designs, evolutionary steps toward V-320 model in addition to already mentioned improved safety features included mainly:
 - Reduced number of control rods
 - Utilization of the 3-year fuel campaign
 - Fuel assemblies without shroud tubes
 - Main circulation loops without isolation valves
 - Improved seismic resistance
 - Possibility for residual heat removal during maintenance of a circulation loop
 - Possibility for operation of the reactor at reduced power.

There is a number of new designs derived from the basic V320 model, mainly upgraded toward better resistance to severe accidents; these are however not considered further in the present project.

No	COUNTRY	PLANT	UNIT/MODEL	START OF OPERATION (grid connection)
1	Bulgaria	Kozloduy	5/320	1987
2			6/320	1991
3	India	Kudankulam	1/412	Under construction
4			2/412	Under construction
5	Iran	Bushehr	1/446	Under construction
6	China	Tianwan	1/428	Under construction
7			2/428	Under construction
8	Czech Republic	Temelin	1/320	2000
9			2/320	2002
10	Russia	Balakovo	1/320	1985
11			2/320	1987
12			3/320	1988
13			4/320	1993
14			5/392	Under construction
15				
16		Kalinin	1/338	1984
17			2/338	1986
18			3/320	2004 (expected)
19			4/xxxx	xxxxx
20				
21		Novovoronezh	5/187	1980
22			6/392	Construction licensed
23				
24		Volgodonsk	1/320	2001
25			2/320	2004 (expected)
26	Ukraine	Khmelnitsky	1/320	1987
27			2/320	2004 (expected)
28		Rovno	3/320	1986
29			4/320	2004 (expected)
30				
31		South Ukraine	1/302	1982
32			2/338	1985
33			3/320	1989
34		Zaporozhe		
35			1/320	1984
36			2/320	1985
37			3/320	1986
38			4/320	1987
39			5/320	1989
40			6/320	1995

Table 2.9: Overview of VVER1000 reactors in operation and under construction

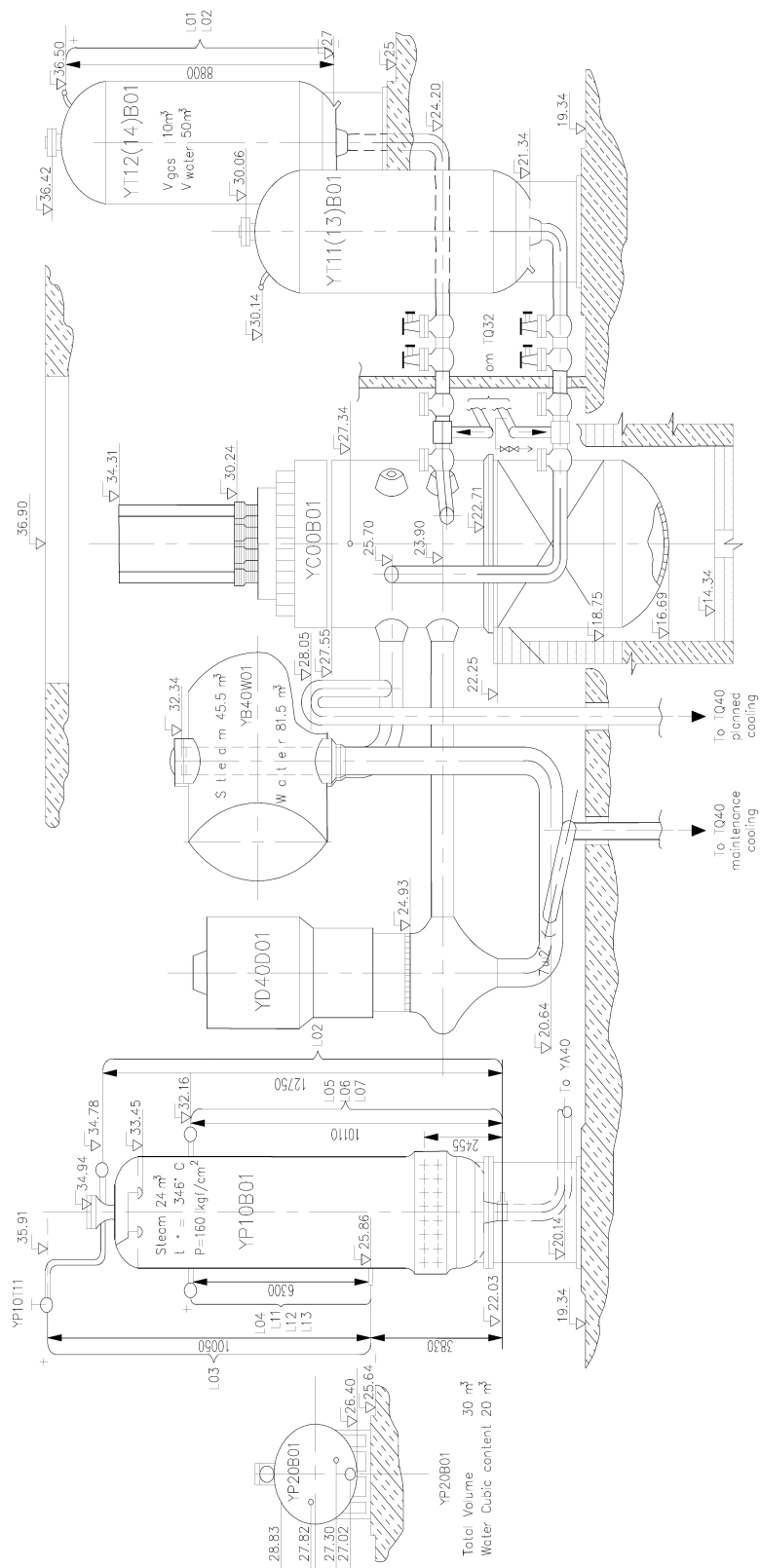


Figure 2.2: The VVER1000 V320 main equipment primary side

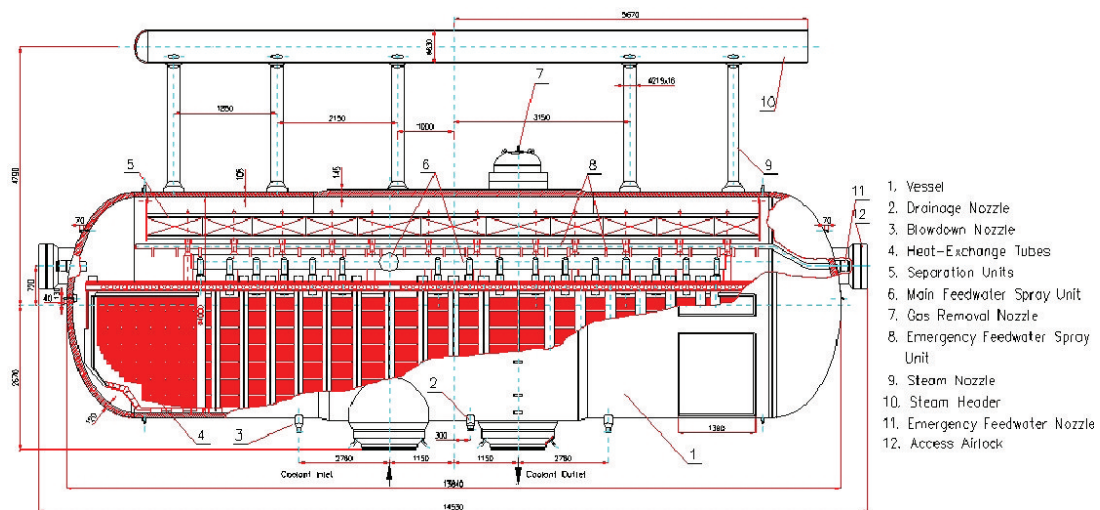


Figure 2.3: The VVER1000 steam generator

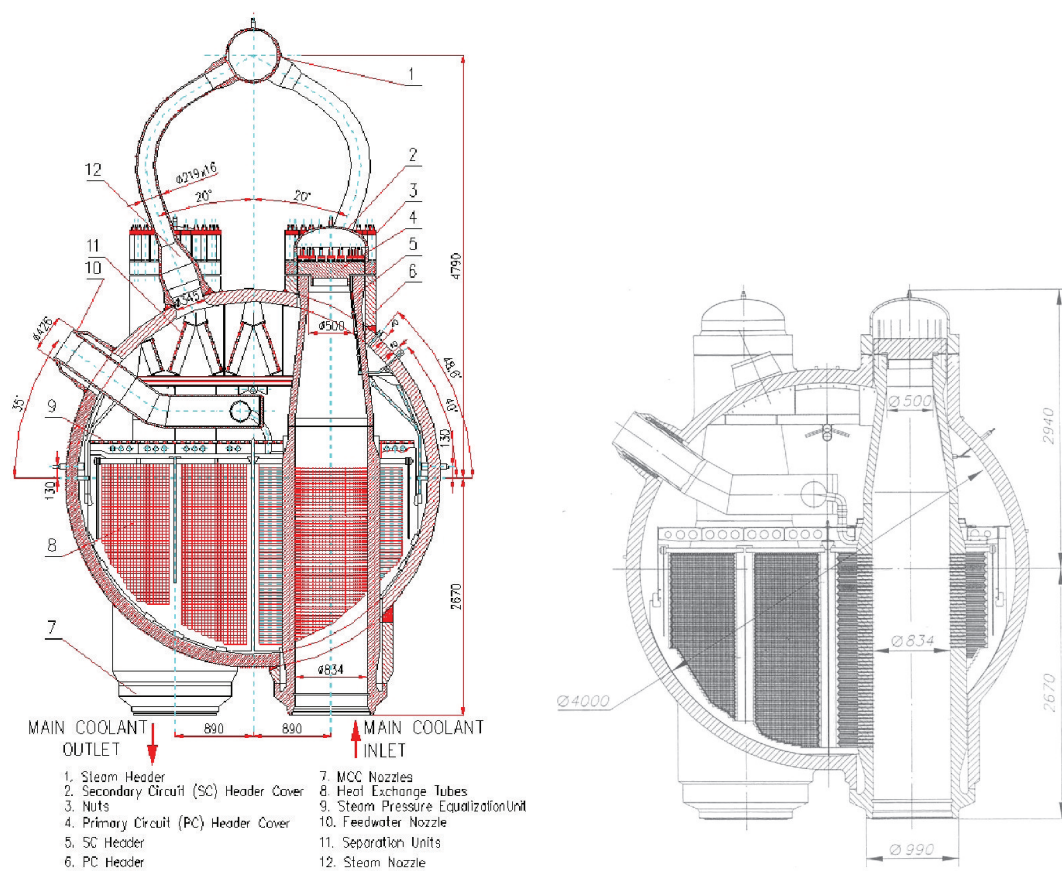


Figure 2.4: The VVER1000 steam generator - cross section

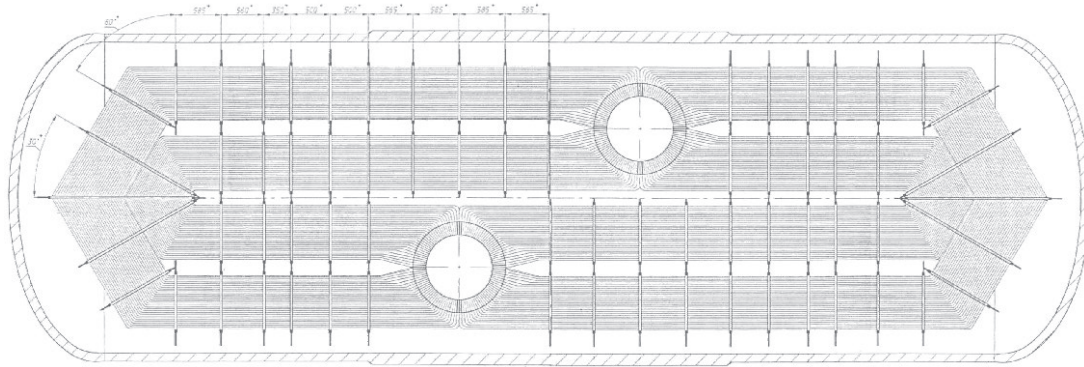


Figure 2.5: The VVER1000 steam generator - top view

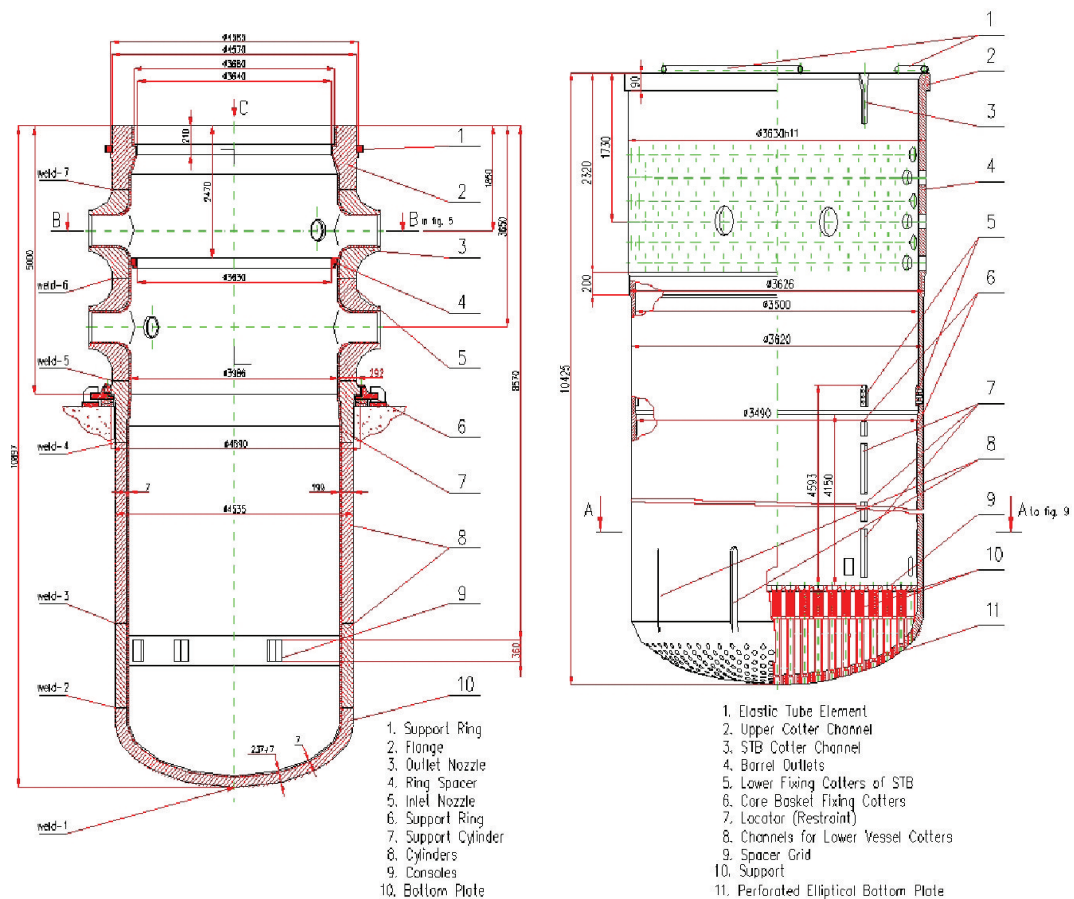


Figure 2.6: The VVER1000 reactor pressure vessel and core baffle

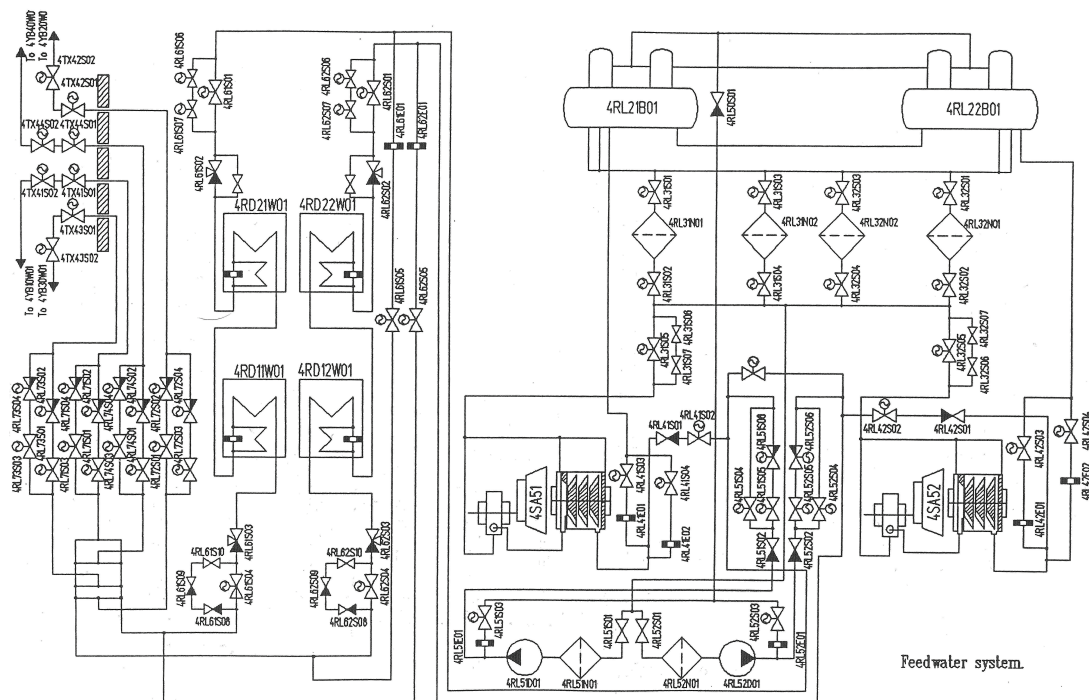


Figure 2.7: The VVER1000 scheme of deaerator - feed water lines

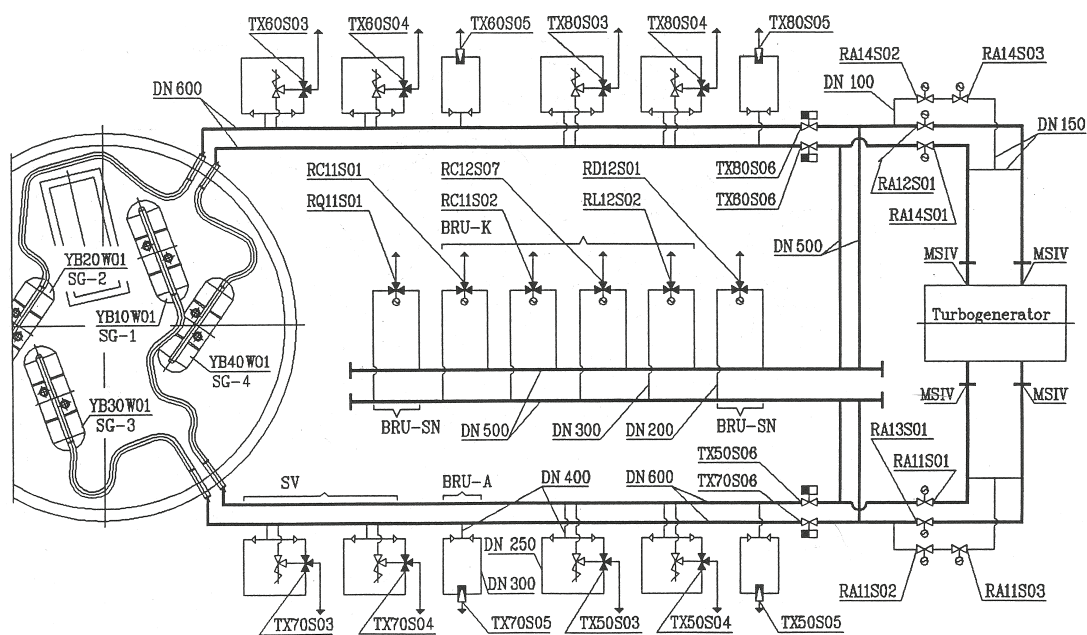


Figure 2.8: The VVER1000 steam lines

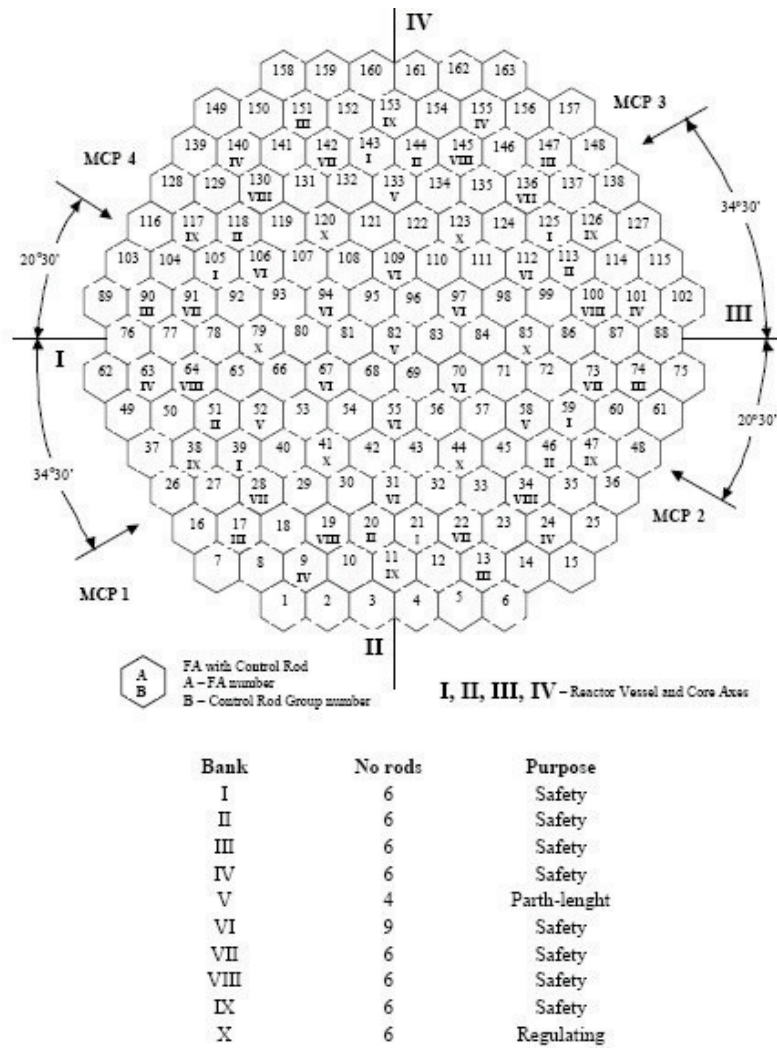


Figure 2.9: The VVER1000 assemblies with control rods (ten groups)

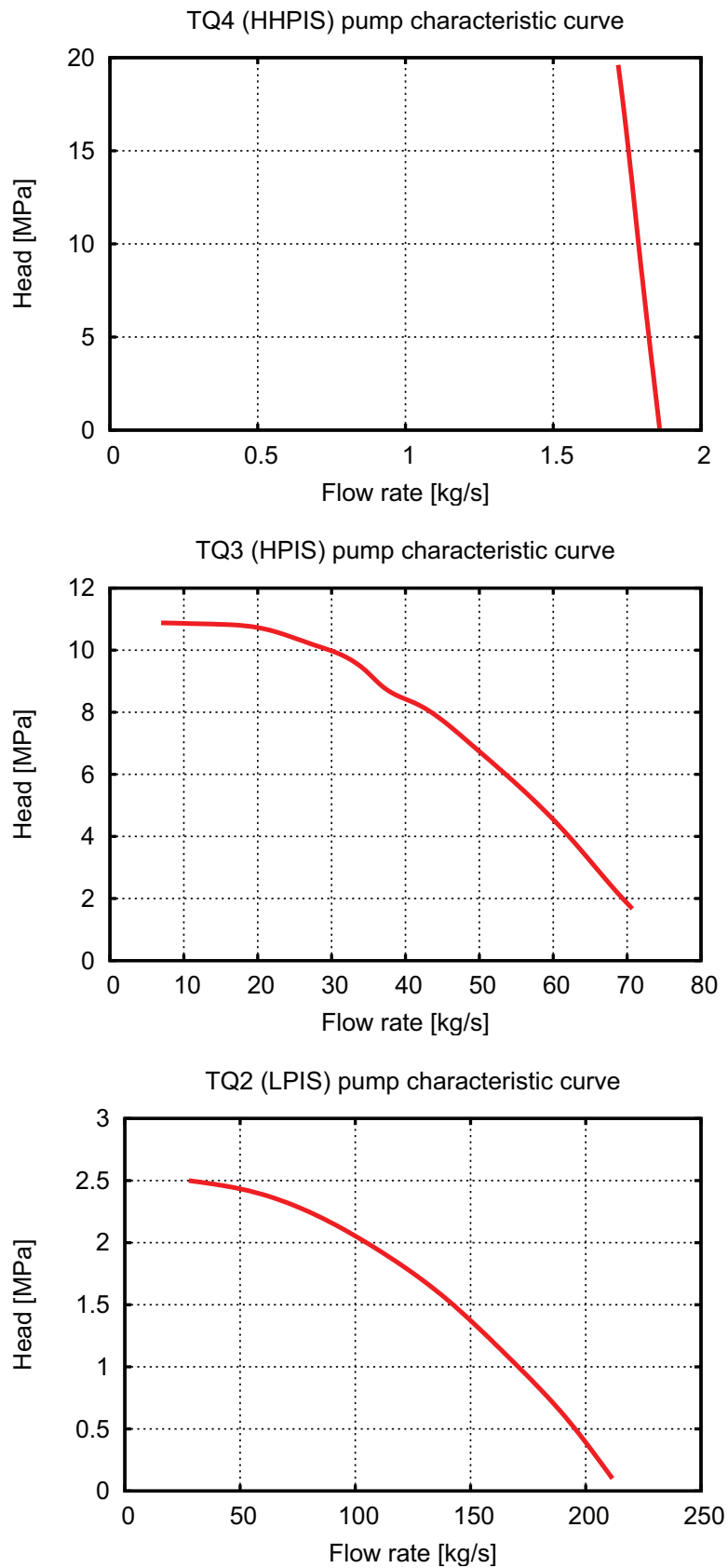


Figure 2.10: The VVER1000 pressure vs flow rate diagrams for the active ECCS injection systems

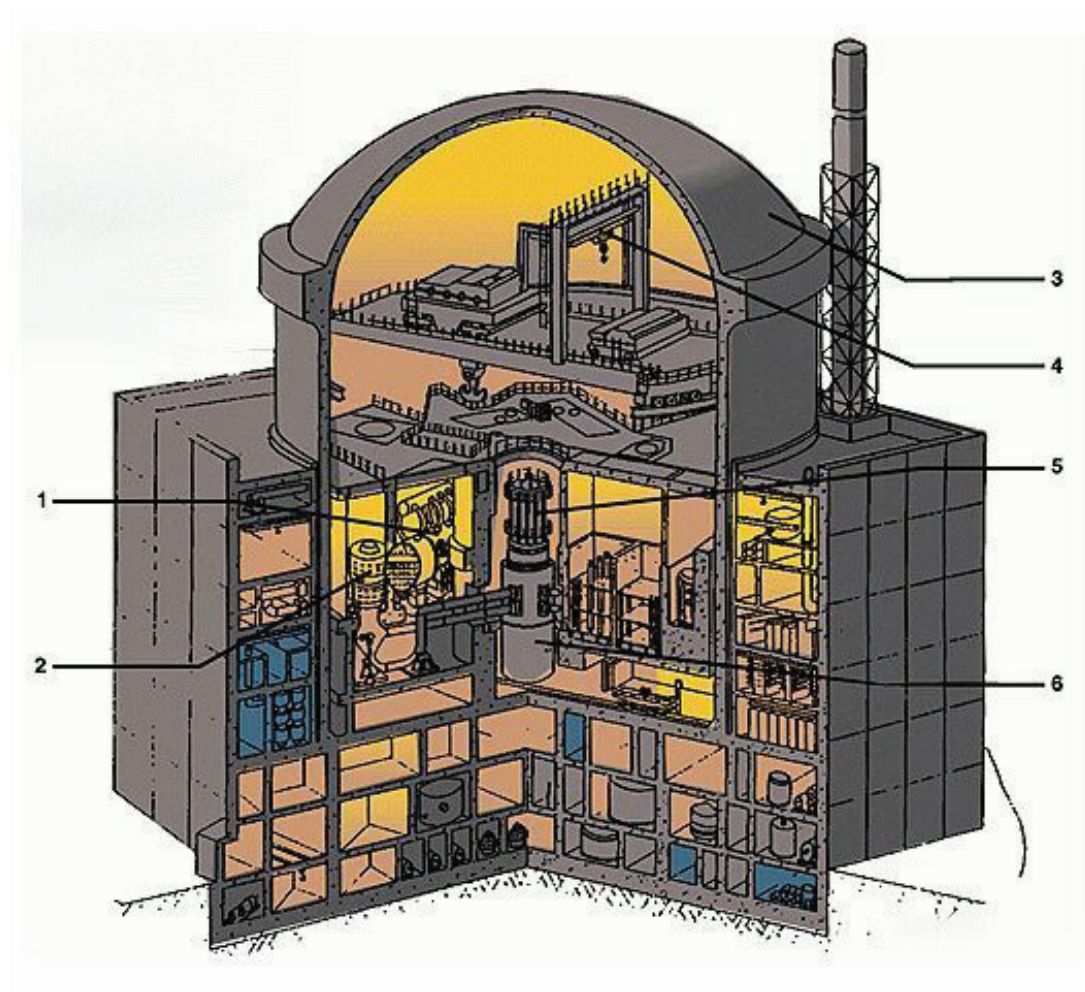


Figure 2.11: The VVER1000 containment

2.3 The PSB-VVER Test Facility

An experiment for each of the calculations presented in chapter 3 has been performed at the PSB-VVER test facility. An extensive description of the facility can be found in [Melikhov et al., 2003a]. The following description is taken from [D'Auria et al., 2005]. This section presents selected aspects of the PSB facility. For a comprehensive description of the considerations for the facility design (scaling issue), please refer to [D'Auria et al., 2005], and [D'Auria et al., 2006].

The PSB-VVER is a full height integral test facility (see Figure 2.12), power and volume are scaled 1:300. The facility has four loops (each one is constituted by a hot leg, a steam generator, a loop seal, a main circulation pump and a cold leg); a pressurizer, connected via the surge line to the hot leg of loop 4; the ECCS is provided by an active pump, that simulates high and low pressure injection systems, and four hydro-accumulators. All system components are insulated from the environment with glass wool to limit the heat losses. Figure 2.13 reports the scheme of the PSB facility.

The main parts of the VVER vessel are reproduced in the facility by separate pipes: one for the downcomer, one for the core model and upper plenum, and one for the core bypass. A horizontal pipe connects the downcomer to the lower plenum. Another bypass links the downcomer to the upper plenum (Figure 2.14).

The core model contains 168 Fuel Rod Simulators with an uniform power profile and a central unheated rod. The active bundle is of electrical type and has a hexagonal cross section. For the project, the maximum core power was limited to 1.5 MW (the right value would be 10 MW). This led to a distortion during the steady state operation. To account for the lower power, the pump speed was reduced. Following a scram, the power has been kept at a higher level to supply the right (scaled) amount of energy to the primary side fluid. Also the bypass section is heated over the same elevation range of the core, to simulate the heating that water receives in the channels, within the reactor core, in which the coolant flows from the lower plenum to the upper plenum, bypassing the assemblies. Figure 2.14 shows the PSB core simulator.

The primary side of the steam generator consists of a hot and a cold collector and of 34 tubes coiled in 10 complete turns with 51 mm difference from inlet and outlet height. The length of one tube is the same like the one of the reference plant (Figure 2.15 shows the simulation of the SG). The distributor of feed water is a ring with several holes placed above the steam generator tubes. Separators are completely absent. The four steam generators are connected to a common steam header via a “small power” steam line. A “full power” steam line was in place, but not used, since the full (scaled) power core was not available for the project.

A comparison between VVER1000 NPP and PSB-VVER test facility main data is presented in Table 2.10.

Measurement points: Figure 2.16 show measurement points of temperatures and differential pressures on the RPV simulator. Mass flow measurements are also provided, based on pressure differences (therefore only valid during single phase, or mainly single phase regimes). The core simulator is instrumented with a large number of thermocouples (see Figure 2.17 and 2.18). Thermocouples and connected wires are led within the electrical heated rods, as can be seen in Figure 2.19, so that they do not constitute any distortion to the flow. An additional parameter that is provided to the analyst is the mass inventory of the facility, and the break flow rate. Both are based on the measurement of the discharge flow, which is collected in a tank. Table 2.11 gives the typical measurement range of selected parameters, and the associated measurement error.

Selected PSB issues - MCP: The PSB facility has four scaled pumps. Several separate effect characterization tests have been performed to provide the pump characteristics to the analysts. Coast down times of the NPP pumps (232 s) are simulated by the pump control program. The pumps have two separate cooling cycles, one forced, and one natural circulation cycle. This poses a problem for

Selected PSB issues - heat losses: the heat losses of the PSB facility constitute one of the main distortions to the real plant. The overall surface to volume ratio is orders of magnitude higher at the facility than at the plant. While heat losses at the plant are neglectable (in fact, for the NPP simulations the boundary conditions of the containment surfaces of heat structures have been set to isolated), at the PSB facility they cannot be neglected. The heat losses along the loops are balanced by higher core power (compared to the known decay heat power curve of the plant). Pressurizer heaters are kept in operation to balance pressurizer heat losses, while the water level in the pressurizer is sufficiently high.

The main uncertainty regarding the heat losses comes from the PSB main coolant pump. The pumps are cooled also when they are not in operation. While the heat losses from the forced circulation cycle

eventually is known (even if the measurement errors are huge), nothing is recorded about the heat losses from the natural circulation cooling cycle. EREC experience is that the heat losses range between 2 kW and 15 kW for each pump, depending on the flow regime in the corresponding loop (so in the worst case 60 kW in total, compared to a core power of typically in the range of 300-500 kW after the scram). This was one of the main difficulties during the post-test analysis.

Name	VVER-1000	PSB-VVER	Scale Factor
Number of loops	4	4	-
Heat losses, [%]	0.063	1.8	-
Heating power, [MW]	3000	10	1:300
Primary circuit volume, [m ³]	370	1.23	1:300
Primary circuit pressure, [MPa]	15.7	15.7	1:1
Secondary circuit pressure, [MPa]	6.3	6.3	1:1
Coolant temperature, [°C]	290/320	290/320	1:1
Core length, [m]	3.53	3.53	1:1
Number of fuel rods	50856	169	1:300
Core volume, [m ³]	14.8	$4.9 \cdot 10^{-2}$	1:302
Upper plenum volume, [m ³]	61.2	$20.0 \cdot 10^{-2}$	1:306
Down-comer volume, [m ³]	34.0	$11.0 \cdot 10^{-2}$	1:309
Hot legs volume, [m ³]	22.8	$8.0 \cdot 10^{-2}$	1:285
Cold legs volume, [m ³]	60.0	$24.0 \cdot 10^{-2}$	1:250
Number of steam generators	4	4	-
Heat exchanging surface, [m ²]	6115	18.2	1:336
Water volume in SG primary circuit, [m ³]	21.0	$6.8 \cdot 10^{-2}$	1:309
PRZ volume, [m ³]	79	$26.3 \cdot 10^{-2}$	1:300
Number of hydro accumulators	4	4	-
Number of pumps	4	4	-
Volume of hydro accumulators, [m ³]	240	$80 \cdot 10^{-2}$	1:300
Water volume in ACCU, [m ³]	200	$66.6 \cdot 10^{-2}$	1:300

Table 2.10: PSB-VVER and VVER-1000 comparison

Parameter	Unit	Value	Error
UP pressure	MPa	15.8	± 0.05
UP outlet fluid temp	°C	310	± 3.0
DC inlet fluid temp	°C	277	± 3.0
Core power	kW	1520	± 15
Core bypass power	kW	15.1	± 0.4
PRZ lvl	m	6.67	± 0.3
Acc pressure	MPa	5.9	± 0.03
Acc lvl	m	4.88	± 0.07
SG pressure	MPa	6.29	± 0.05
SG lvl	m	1.70	± 0.08
SG FW	°C	216	± 3.0
SG AFW	°C	20	± 3.0

Table 2.11: PSB selected measurements (nom. value) and associated errors

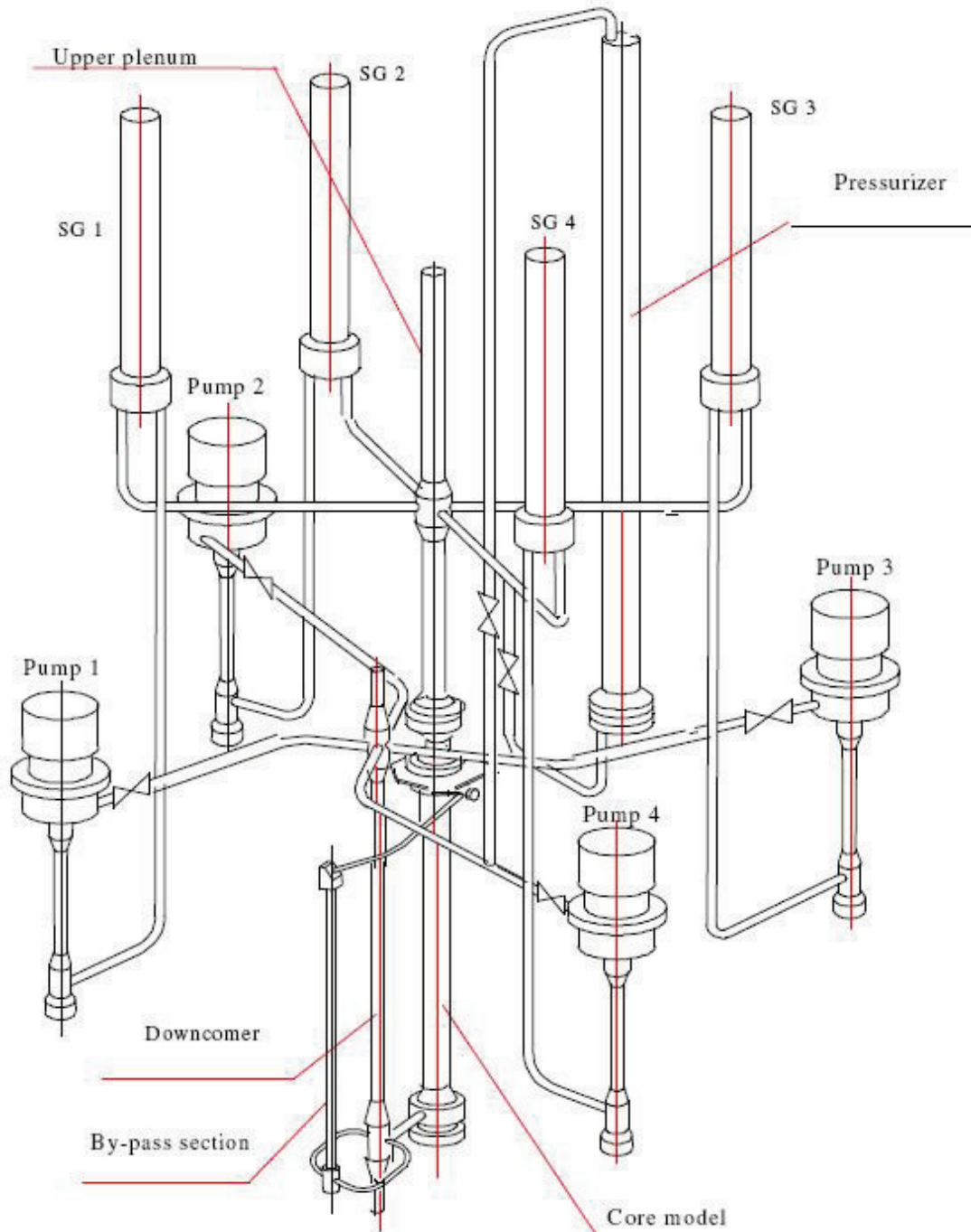


Figure 2.12: PSB-VVER NPP simulator

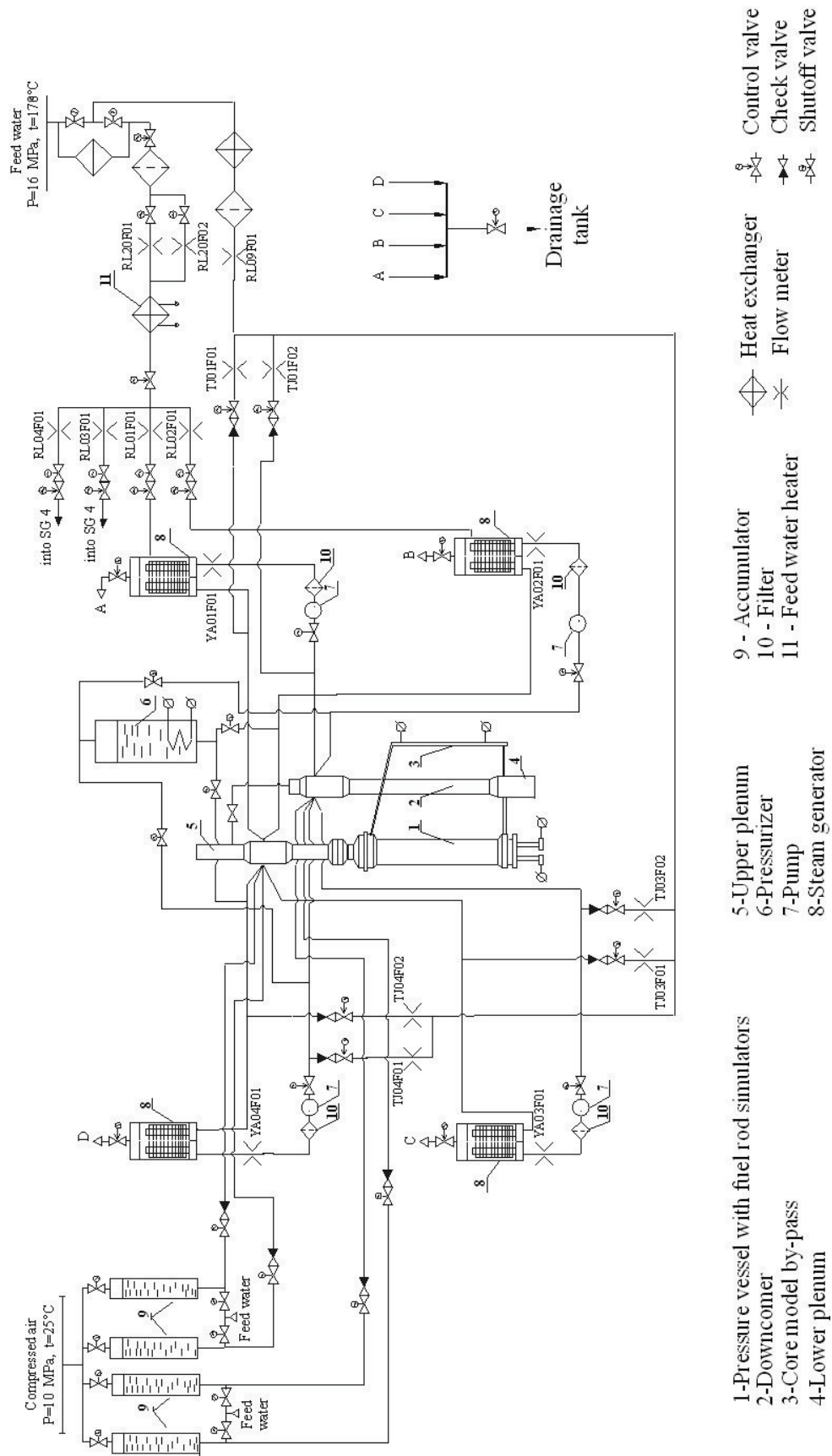


Figure 2.13: PSB - general scheme

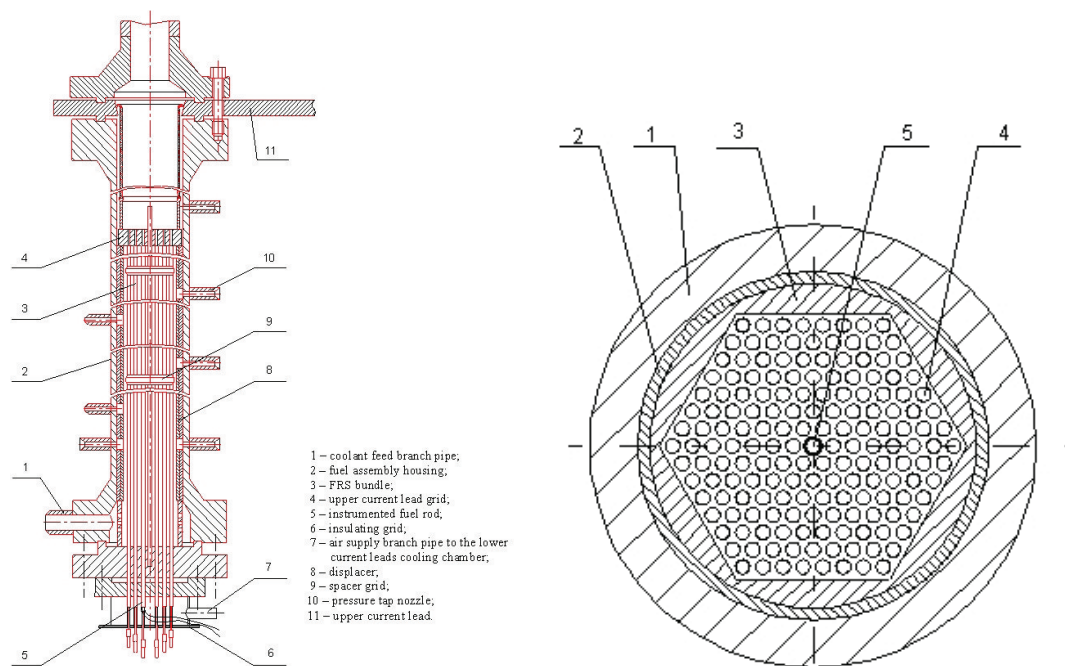


Figure 2.14: PSB core simulator

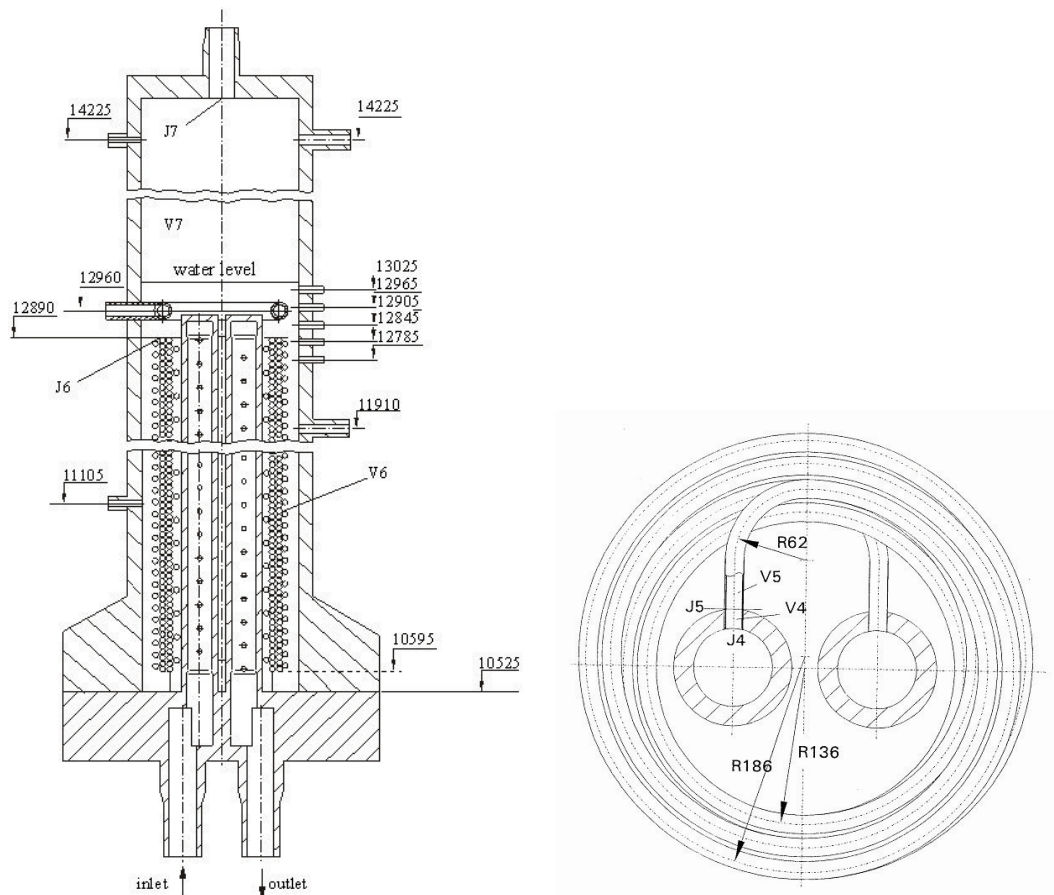


Figure 2.15: PSB SG simulator

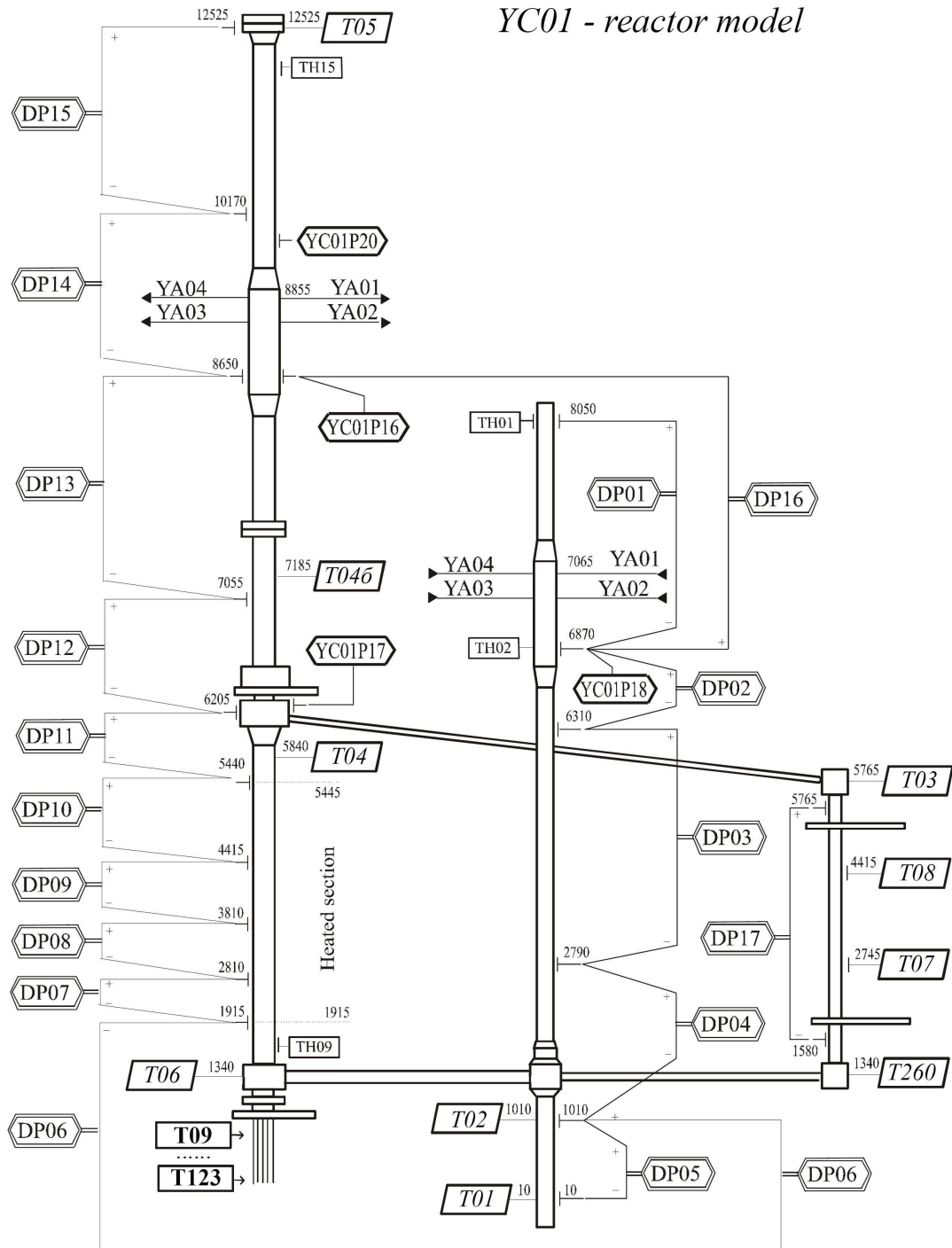


Figure 2.16: PSB - RPV model measurement points

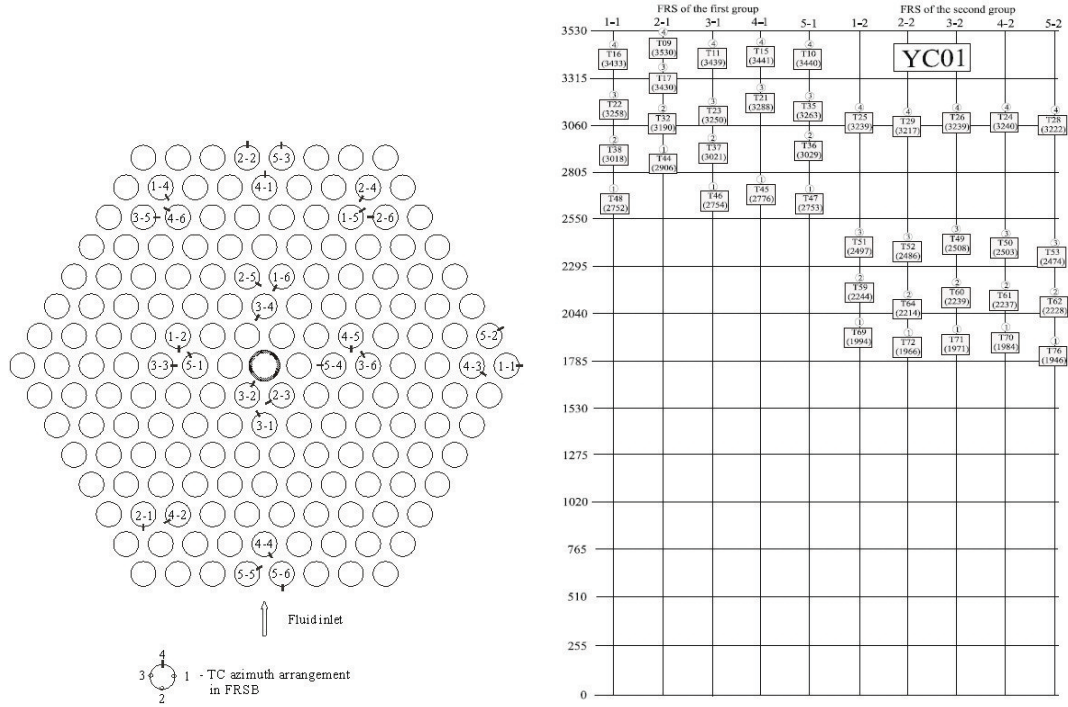


Figure 2.17: PSB - core simulator measurement points (1/2)

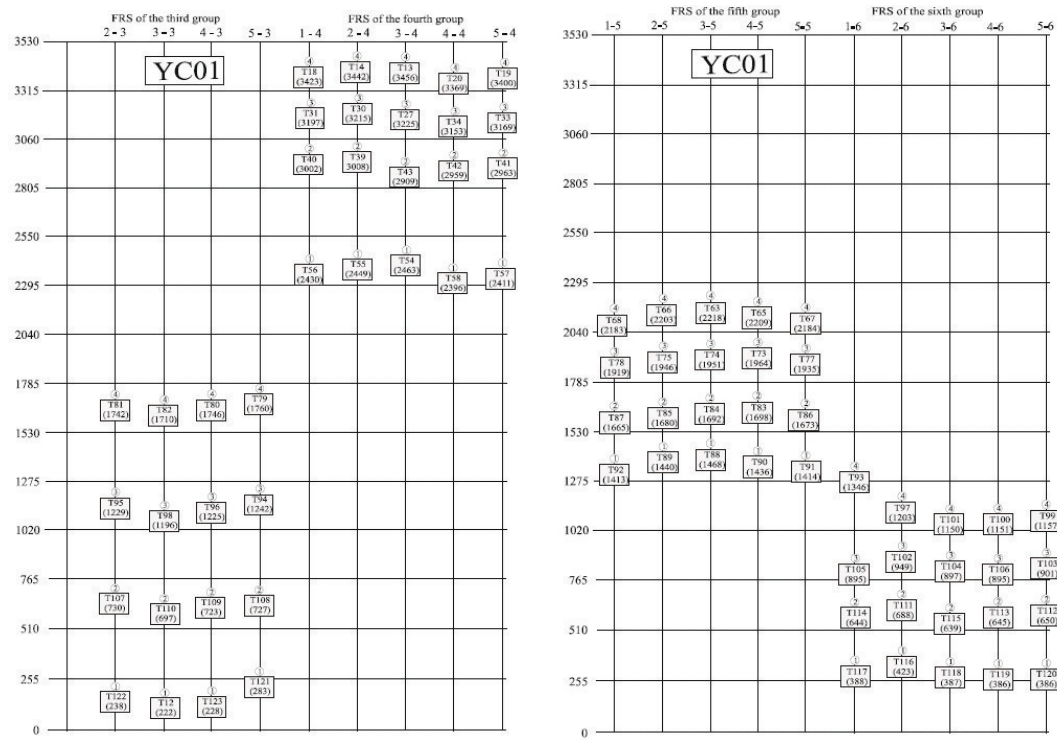


Figure 2.18: PSB - core simulator measurement points (2/2)

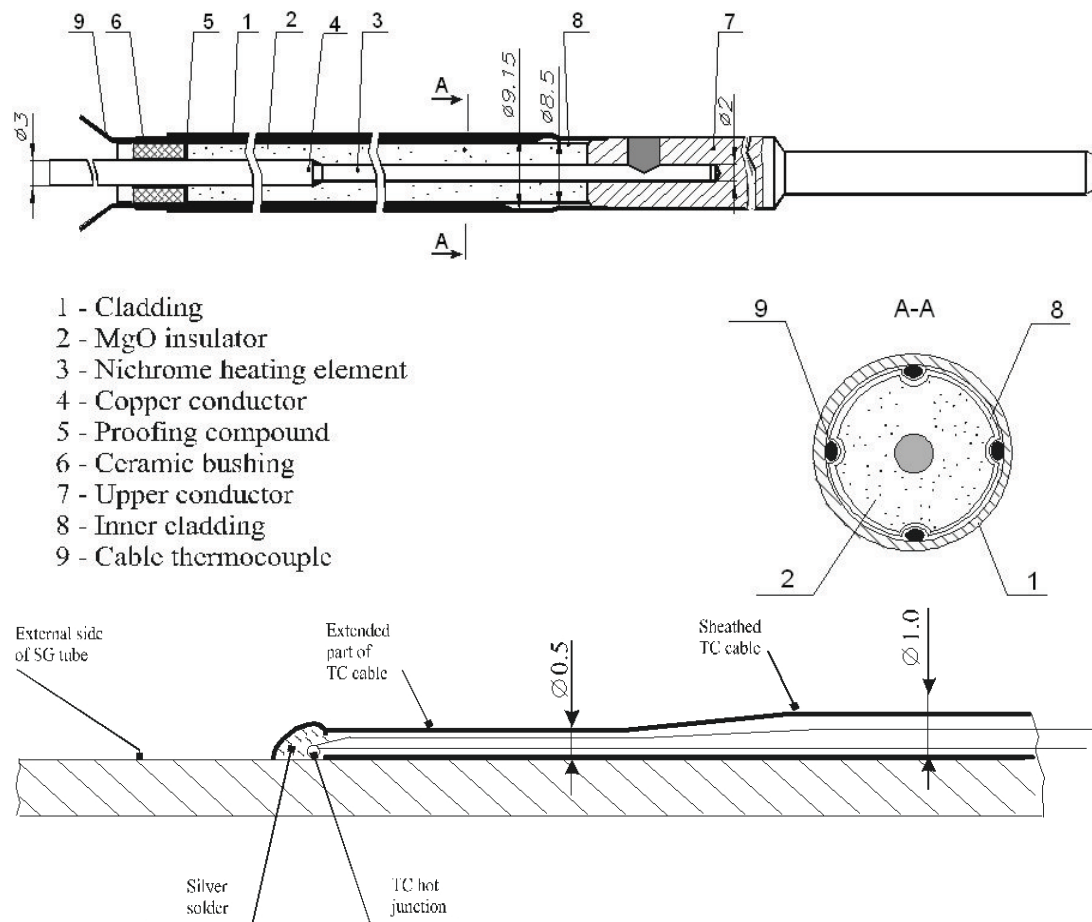


Figure 2.19: PSB - instrumented fuel rod simulator

2.4 Methods and Tools

2.4.1 Relap5

Introduction

The main tool that was used for NPP analysis was Relap5. The code version was Relap5 mod 3.3ef. The following section provides an overview on the capabilities and models used in Relap5. The code comes with extensive documentation - eight volumes and one annex. The first volume [ISL, 2003] gives an overview on models and structure of the code. The Relap5 computer code is a light water reactor transient analysis code developed for the U.S. Nuclear Regulatory Commission (NRC) for use in rule making, licensing audit calculations, evaluation of operator guidelines, and as a basis for a nuclear plant analyzer. Specific applications of this capability have included simulations of transients in LWR systems, such as loss of coolant, anticipated transients without scram (ATWS), and operational transients such as loss of feed water, loss of off site power, station blackout, and turbine trip. RELAP5 is a highly generic code that, in addition to calculating the behavior of a reactor coolant system during a transient, can be used for simulation of a wide variety of hydraulic and thermal transients in both nuclear and nonnuclear systems involving mixtures of steam, water, noncondensable, and solute. Relap5 is structured in components. A driver component has the task of calling the sub-components accordingly. There are three physical sub-components, the Hydro-dynamic component, the component on heat-structures, and the neutron (point) kinetics model. One component determines the state of the boundary volumes and the imposed conditions, one component determines the time step, and two components work on the logics, to model the control system of the NPP, called trips and control.

The RELAP code series started in 1966 with the release of the code RELAPSE (Reactor Leak and Power Safety Excursion). Several versions of RELAP have been released. In 1985 the first release of the Relap5 code series was available. Now the latest code version is Relap5 mod 3.3. Several other projects branched off the Relap5 project - Relap5-3D, a commercial closed-source code, providing the possibility of 3 dimensional arrangement of the control volumes, Relap5/SCDAP, another commercial, closed source project which, apart from a complete rewriting of the code adds the possibility to simulate core melt phenomena within Relap5, or trace, which provides a graphical user interface for the input preparation. The code Relap5 is no longer under active development, only code fixes are released from time to time.

Notwithstanding the fact that Relap5 is no longer actively developed, it is widely used and well tested. Relap5 has been customized for a large number of computer hardware architectures and different FORTRAN compilers (FORTRAN 77), and its applicability has been extended from light water reactors to CANDU and VVER as well. The following sections provides just a very brief summary of the Relap5 manuals, for more details please refer to [ISL, 2003], [ISL, 2006a], [ISL, 2006b], [ISL, 2006c], [ISL, 2006d], [ISL et al., 2006], [ISL, 2006e], [ISL, 2006f].

Physics in Relap5

Relap5, as thermal hydraulic system code, is based on the equation for mass, momentum and energy conservation of fluids to calculate the flow in the piping system. Eight dependent variables are evaluated for each time step, using eight **field equations**. The other quantities of interest are expressed as functions of this eight variables using **equations of state**. The field equations cannot cover the general situation. To calculate the energy and momentum transfer between the phases, the fluid and the wall, the friction between the phases, the friction between fluid and wall so called **constitutive models** are used. This means that criteria are defined to determine flow and heat transfer conditions, and to use for the above mentioned phenomena a correlation which suits the actual conditions.

Several additional models are used, like a simple model to calculate the reactor power. The section provides a brief overview on each of the three types of equations, i.e. hydrodynamic model or field equations, which are on the basis of the numerical scheme. The model is followed by the state equations, which are used to derive all other quantities of interest based on the outcome of the field equations, and, only as overview, the most relevant constitutive equations.

Hydrodynamic model - field equations

The relations for mass, momentum and energy conservation and the jump conditions be found in text books on fluid mechanics like [Truckenbrodt, 1968] or targeted to two phase flow, [Bergles et al., 1981]. The latter

one derives a general balance equation from the theorem of Gauss, which may be specialized for mass, momentum and energy conservation.

The generalized balance equation can be written in integral form as

$$\sum_{k=1}^2 \frac{d}{dt} \int_{V_k(t)} \rho_k \psi_k dV = \sum_{k=1}^2 \left(- \int_{S_k(t)} \rho_k \psi_k \mathbf{v}_k \cdot \mathbf{n}_k dS - \int_{S(t)_k} \mathbf{J}_\psi \cdot \mathbf{n} dS + \int_{V_k(t)} \rho_k \phi_k dV \right) \quad (2.1)$$

the general balance equation can be transformed from integral to differential form

$$\sum_{k=1}^2 \left(\frac{\partial}{\partial t} (\rho \psi) + \nabla \cdot (\rho \psi \mathbf{v}) + \nabla \cdot \mathbf{J}_k - \rho_k \phi_k \right) \quad (2.2)$$

The generalized balance equation basically states that the total change in an arbitrary volume V is equal to the integral of in- and out flow of a quantity through the surface S of the volume, the “diffusion” on the surface, and the integral of contribution of sources and sinks within the volume. The index $k = 1, 2$ specifies different phases. With different values for ψ , \mathbf{J} and ϕ one can derive mass, momentum, angular momentum and energy balance equation (see Table 2.12).

Balance	ψ_k	\mathbf{J}_k	ϕ_k
Mass	1	0	0
Momentum	\mathbf{v}_k	$-\mathbf{T}_k$	F
Energy	$u_k + (1/2)v_k^2$	$\mathbf{q}_k - \mathbf{T}_k \cdot \mathbf{v}_k$	$\mathbf{F} \cdot \mathbf{v}_k$

Table 2.12: Quantities for general balance equation

Each of the equation is associated with one “jump-condition”, which describes the transfer of the associated quantity between the phases.

The Relap5 hydrodynamic model resolves eight field equations for eight dependent variables (listed below, (2.3)).

$$\begin{aligned} &P(x, t), \\ &U_g(x, t), U_f(x, t), \\ &\alpha_g(x, t), \\ &v_g(x, t), v_f(x, t), \\ &X_n(x, t), \\ &\rho_b(x, t) \end{aligned} \quad (2.3)$$

Basic field equations Basic field equations are mass, momentum and energy conservation equation. They alone are not sufficient to find a unique solution to the problem. In addition, information which describes the change between the phases is needed. These equations are termed “closure equations” or “jump conditions”.

- Mass continuity (three equations, since the mass of fluid, non-condensibles and boron is conserved separately).
- Momentum conservation equation (one equation)
- Energy conservation equation (one equation)
- Closure equations - phase change conditions (3 equations - exchange of mass, momentum and energy)

Sums up to eight equations for eight variables. The field equations as used in Relap5 and their discretization are not presented here, but can be found in [ISL, 2003].

State equations

Five of the eight variables of the section “field equation” are used as independent state variables, the pressure P , the void fraction α_g , vapor and liquid specific internal energy U_g and U_f , and the fraction of non-condensable gases X_n .

The pressure, the specific internal energies and the void fraction allows to derive the major part of the quantities of interest from steam tables. Other quantities, like the sound speed, are calculated using standard formula. For more details please refer to [ISL, 2003] and [ISL, 2006c].

Relap5 supports a certain number of different fluids (e.g. among others H_2 , He , freon, blood) although as default h2o and d2o is supported.

Constitutive models - closure equations

Energy and momentum transfer between the phases and between fluid and wall is an input which is still missing in the field equations. Relap uses a number of correlations for this calculation, depending on the flow regime. For different flow regime maps are used, one for horizontal flow, one for vertical, one for high mixing and one for ECC mixer.

The most common flow patterns for horizontal and vertical two phase flow, and their description, can be found in [Bergles et al., 1981]. The most common flow patterns for a vertical pipe with upward co-current flow, are shown in figure 2.20. The shown flow patterns are air-water (1) independent bubbles, (2) packed bubbles, (3) slug flow, (4) churn flow, (5) annular flow. Diameter of the pipe shown in the Figure is 32 mm.

The most common flow is the bubbly flow. Bubbles keep their spherical shape up to a size of 1 mm, beyond 1 mm they are of variable shape. Roumy divides bubbly flow is divided in two flow patterns, independent bubbles (1) and packed bubbles (2). With increasing void fraction slug flow (3) is formed. Slug flow is composed of a series of gas plugs. Usually, the head of a gas plug is blunt, while the end is flat. The liquid film surrounding the gas plug moves downward in respect to the tube wall. With further increasing void fraction the gas plugs grow longer and longer, and a void center starts to form chaotically. This transition flow regime is called churn flow (4). If a central gas core is developed, the flow is called annular flow (5).

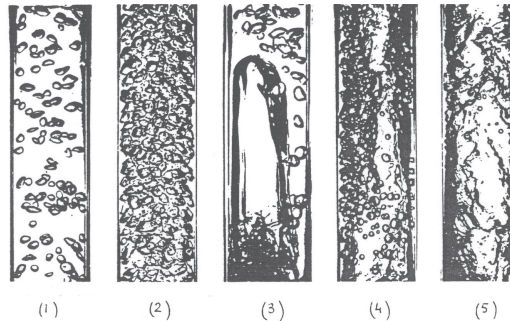


Figure 2.20: Upward co-current flow in a vertical pipe ([Roumy, 1969])

A similar situation is observed when a pipe is heated, see Figure 2.21. Only that the flow patterns evolve further from dispersed annular flow, where a central gas core loaded with liquid droplets moves faster than the film on the wall, to wispy annular flow, where the liquid droplets gather into clouds within the central gas core. If the wall temperature is high enough to evaporate also the liquid film, the droplets constitute a mist flow.

Figure 2.21 shows the a liquid-vapor flow through a heated pipe. Liquid enters the pipe at constant flow rate and temperature, while the wall heat flux is increasing from left to right. With increasing heat flux the appearance of vapor comes closer and closer to the entrance of the channel. The local boiling length is the length of the pipe where bubbles are generated at the wall, and condensed in the liquid core. Vapor is produced by two mechanism - nucleate boiling on the wall, and direct vaporization on the interfaces in the flow.

The wall heat flux can be high enough to transgress beyond annular flow, to evaporate completely the liquid mist on the wall. If this happens and the heat flux stays constant, the wall temperature rises very quickly and can exceed the melting temperature of the wall. This phenomenon is called dry-out, burnout, boiling crisis or critical heat flux.

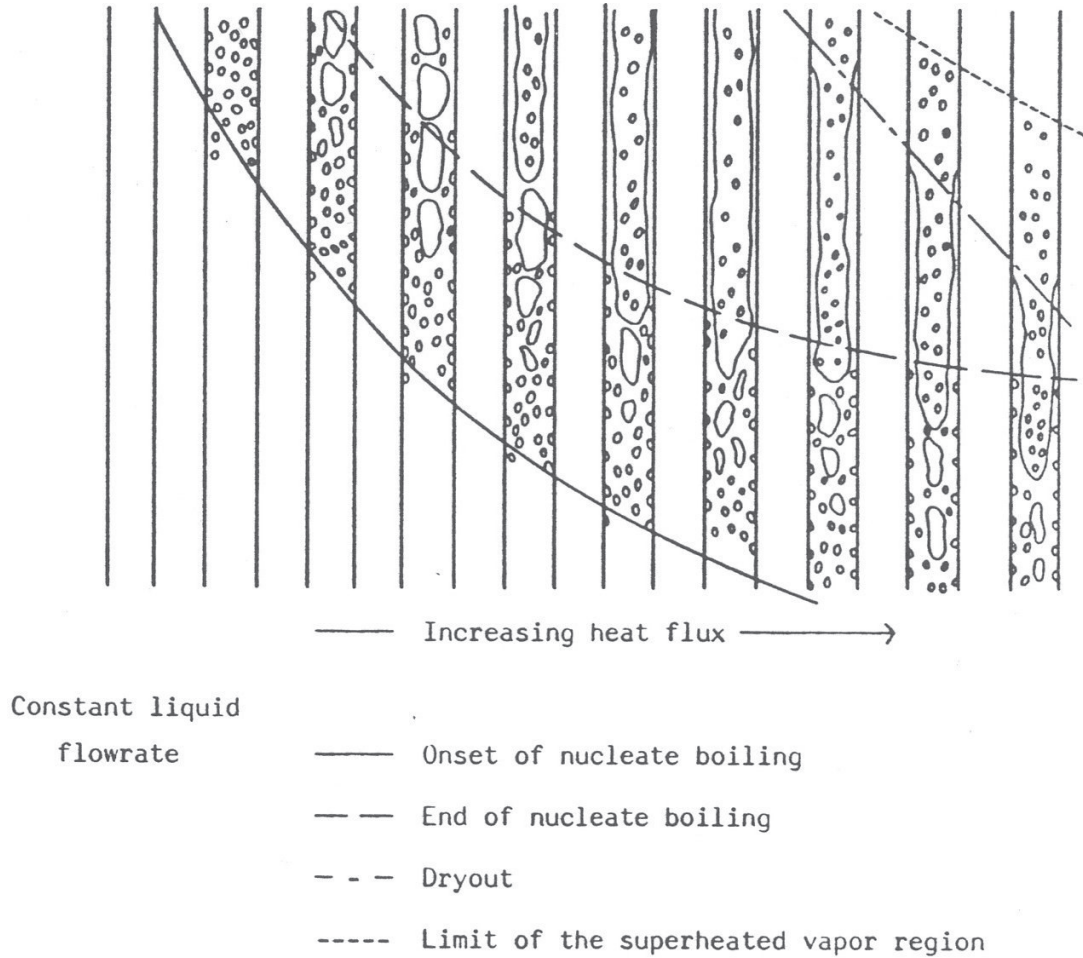


Figure 2.21: Convective boiling in a heated channel ([Hewitt and Hall-Taylor, 1970])

horizontal flow regimes can be found in more detail in [Bergles et al., 1981]. Flow regimes are usually used together with flow maps, i.e. conditions which determine which flow regime can be found depending on certain parameters. Relap uses four flow-regime maps: one for horizontal flow, one for vertical flow, one for high mixing volumes (e.g. pumps) and one for the ECC - Mixer component. The last component has not been used throughout this work, but the other flow regime maps are presented. The flow regime map for horizontal flow consists of bubbly, slug, annular mist, dispersed and horizontal stratified flow (see Figure 2.22). The parameters which determines the flow regime are based on the relative velocity between the two phases and the void fraction. The horizontal flow regime map is used for volumes with an inclination between 0 and 45 degrees. For volumes with an inclination between 45 and 90 degrees the vertical flow regime map (see Figure 2.23) is used. The map consists of bubbly, slug, annular-mist, and dispersed (droplet or mist) flows in the pre-CHF regime; inverted annular, inverted slug and dispersed (droplet or mist) flows in post-dryout; and vertically stratified for sufficiently low-mixture velocity ([ISL, 2006c]). A third The flow regime map for high mixing volumes is used, but not shown here since the corresponding Relap5 components have not been used.

similar to the flow regime maps Relap5 determines a heat transfer mode for the wall to fluid heat transfer. Figure 2.24 displays the logical flow chart, based on which the correlation for the heat transfer mode is chosen. P_{crit} in the diagram denotes the critical pressure, X_n the mass quality of non condensable gases, X_e the equilibrium quality, α_g the (gas) void fraction, T_w the wall temperature, T_{spt} the steam saturation pressure based on total pressure, T_{spp} the steam saturation pressure based on steam partial pressure, T_f the liquid temperature, CHF the critical heat flux, q'' the heat flux, q''_{FB} the film boiling heat flux, q''_{TB} transition boiling heat flux, Geom - type of hydraulic cell, 1Φ single phase.

The modes are

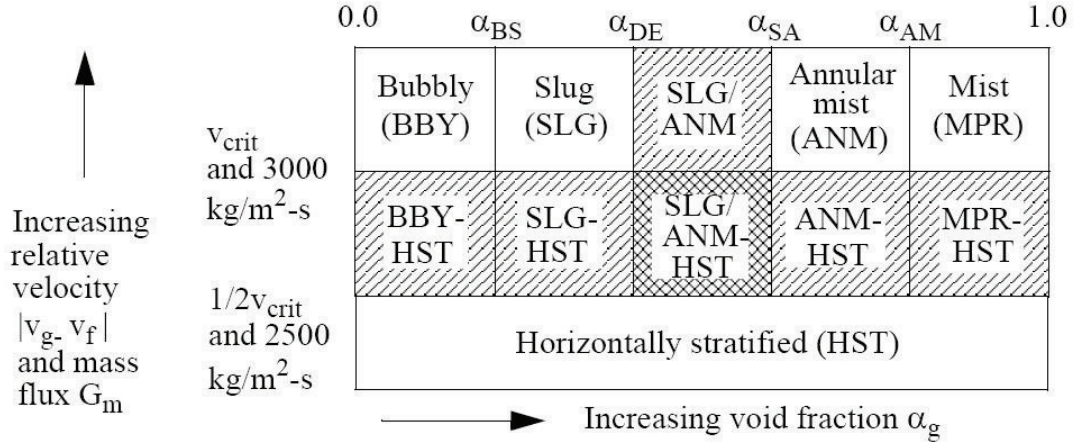


Figure 2.22: Flow regimes for horizontal flow

- Mode 0 Convection to noncondensable-steam-water mixture or superheated liquid
- Mode 1 Convection at supercritical pressure or superheat wall with negative heat flux due to superheated gas
- Mode 2 Single-phase liquid convection at subcritical pressure, subcooled wall and low void fraction
- Mode 3 Subcooled nucleate boiling
- Mode 4 Saturated nucleate boiling
- Mode 5 Subcooled transition boiling
- Mode 6 Saturated transition boiling
- Mode 7 Subcooled film boiling
- Mode 8 Saturated film boiling
- Mode 9 Single-phase vapor or supercritical two-phase convection
- Mode 10 Condensation when void is less than one
- Mode 11 Condensation when void is one
- Mode 12 Single-phase liquid convection at subcritical pressure, subcooled wall and low void fraction, uses Petukhov-Gnielinski and Swanson-Catton correlations.

Based on the flow map and heat transfer mode a (empirical) correlation is selected calculate the energy and momentum transfer between the phases. Based on the large number of flow regimes and, as result, the large quantity of possibilities for energy and momentum transfer, a vast number of correlations has been implemented in Relap5. All of them are described in the first and forth volume of the Relap5 manual, [ISL, 2003] and [ISL, 2006c]. Only to give an idea, a table providing an overview on the used correlations is presented in Table 2.13.

Structure heat transfer model

Apart from the hydraulic system Relap5 calculates also the heat transfer in metal structures or in the fuel rods. The model is based on the heat conduction equation (2.4) and (2.5) in differential form. In both equations, k denotes the thermal conductivity, s the surface, S an internal heat source, t the time, T the temperature, V the volume, x the space coordinates, and ρ^* the volumetric heat capacity ($\rho \cdot c$).

$$\int_V \rho^*(T, \mathbf{x}) \frac{d}{dt} T(\mathbf{x}, t) dV = \int_S k(T, \mathbf{x}) \nabla T(\mathbf{x}, t) \cdot d\mathbf{s} + \int_V S dV \quad (2.4)$$

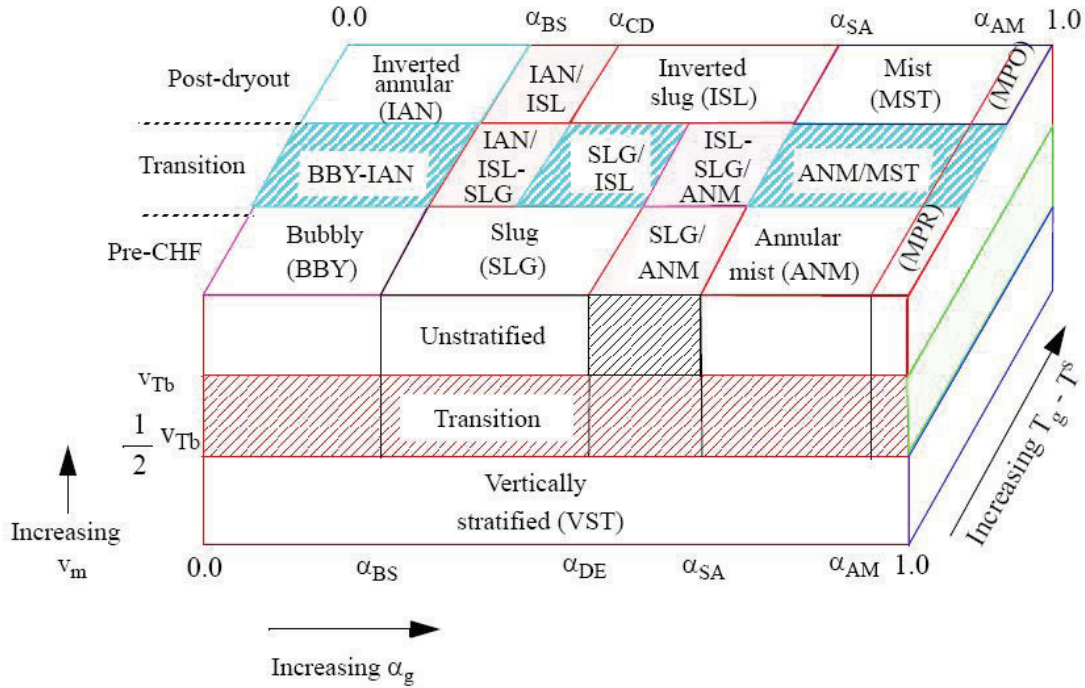


Figure 2.23: Flow regimes for vertical flow

$$\rho^* \frac{d}{dt} T = k \cdot \Delta T + S \quad (2.5)$$

The equations are integrated using a finite difference scheme. Material properties are stored in tabular form in the code for standard materials (carbon steel, stainless steel, UO_2 , zirconium etc), but can also be defined by the user.

One substantial simplification is that the heat transfer in structures is only considered to happen in the radial direction, not along the axis. Only the one-dimensional heat transfer equation is considered.

Since this assumption inserts a significant distortion in case of large break loss of coolant accidents, where in the real plant the colder part of the reactor might provide a heat sink for the hotter part and thereby mitigate the accident, for this specific boundary conditions the Relap5 user may enable a 2-D heat transfer calculation.

Phase separation and related process models

Relap5 field equations allow for unequal temperatures and unequal velocities of the two phases (UTUV). Nevertheless, for most circumstances Relap5 assumes that the two phases are homogeneously mixed in each control volume, which means that usually there is no notion of a level in a control volume. But during stagnant or low flow conditions gravity can cause a separation of the two phases, in these situations a clear interface between the phases is present, and the lumped parameter approach can introduce significant errors. Such situations are called stratified flow in Relap5. The following paragraph describes the handling of stratified flow in horizontal and vertical pipes, which is coded as one of the possible flow regimes in the horizontal (see Figure 2.22) and vertical (see Figure 2.23) flow map. Then the special process that handle counter current flow limitation (steam on top of water, inhibiting flow, typically at the upper tie plate), entrainment/pullthrough of steam during small break LOCA under stratified conditions, and level tracking for a slow moving water front in vertical pipes.

Stratified flow in vertical pipes The vertical stratified flow models are used if two requirements are met. The first requirement is that the average mixture velocity v_m (2.6) is below $\frac{1}{2}$ of the Taylor bubble rise velocity v_{TB} (2.7):

Mode	Heat transfer phenomena	Correlations
0	Noncondensable steam-water or superheated water	Kays, Dittus-Boelter, ESDU, Shah, Churchill-Chu, McAdams, Elenbaas, Petukhov-Kirillov, Swanson-Catton
1	Supercritical or single-phase liquid	Same as mode 0
2	Single-phase liquid or subcooled wall with $voidg < 0.1$	Same as mode 0
3	Subcooled nucleate boiling	Chen
4	Saturated nucleate boiling	Same as mode 3
5	Subcooled transition boiling	Chen-Sundaram-Ozkaynak
6	Saturated transition boiling	same as 5
7	Subcooled film boiling	Bromley, Sun-Gonzales-Ten, and mode 0 Correlations
8	Saturated film boiling	Same as mode 7
9	Supercritical two-phase or single phase gas	Same as mode 0
10	Filmwise condensation	Nusselt, Shah, Colburn-Hougen
11	Condensation in steam	Same as mode 10
12	Single-phase liquid or subcooled wall with $voidg < 0.1$	Same as mode 0
3,4 (hor.bund.)	Nucleate boiling	Forster-Zuber, Polley-Ralston-Grant, ESDU

Table 2.13: Relap wall to fluid heat transfer correlations

$$\begin{aligned}
v_m &= \frac{G_m}{\rho_m} \\
G_m &= \alpha_g \rho_g |v_g| + \alpha_f \rho_f |v_f| \\
\rho_m &= \alpha_g \rho_g + \alpha_f \rho_f
\end{aligned} \tag{2.6}$$

and

$$v_{TB} = 0.35 \sqrt{\frac{gD(\rho_f - \rho_g)}{\rho_f}} \tag{2.7}$$

with

ρ_f, ρ_g	density of liquid and steam phase
v_f, v_g	velocity of liquid and steam
α_g, α_f	void fraction and one minus void fraction
g	acceleration of gravity
D	pipe diameter

The second requirement regards the axial void fraction distribution. Each triple of vertical volumes (see Figure 2.25) is checked. The void fractions of the volumes are compared against each other, and, simplified, it is ensured that there is a sufficiently large change in void fraction from top to bottom.

Should both requirements be met, the correlations for vertically stratified flow are chosen for the closure equations, like the heat transfer coefficients between the phases, the wall and interfacial drag, interfacial friction etc. However, still no level inside volume K of Figure 2.25 is calculated. If a level of a slowly moving water front should be calculated, the mixture level tracking model has to be activated (described later in this section). The vertical stratified flow model is turned on by default (i.e. will be used if the requirements are fulfilled), but can be turned off by the user for each control volume.

Stratified flow in horizontal pipes Relap5 uses its models for horizontal stratified flow based on the relative velocity of the phases, and the mixture mass flux, see Figure 2.22. The mixture mass flux G_m has to

be below $2500 \frac{kg}{sm^2}$, while the relative phase velocity $|v_g - v_f|$ has to be below $\frac{1}{2}$ of the critical velocity, the velocity above which waves on the horizontal interface will begin to grow:

$$v_{crit} = \frac{1}{2} \sqrt{\frac{(\rho_f - \rho_g) g \alpha_g A}{g_g D \sin \theta}} (1 - \cos \theta) \quad (2.8)$$

with

A the area of the pipe

θ angle as shown in Figure 2.25

Should the requirements for stratified horizontal flow be met, the corresponding correlations to calculate the interfacial heat transfer coefficients and interfacial drag are used for the closure equations.

Horizontal stratification entrainment/pullthrough model The assumption that the two phases are homogeneously mixed can introduce errors in situations as shown in Figure 2.26. Consider the lower example of Figure 2.26 - Relap5 standard model would assume mixture of the phases, so disregardless of the level in the volume always steam and liquid would be discharged. To have a more realistic modelling of e.g. a small break, Relap5 offers the possibility to enable the horizontal stratification entrainment/pullthrough model in each junction connected to a horizontal pipe. The user has to specify the orientation of the junction (upwards, downwards, horizontal). The model is only applied if enabled by the user, and if the flow conditions in the control volume corresponds to horizontally stratified flow. The model considers the presence of a level, compares the position of the level to the position of the break (i.e. steam flow if the junction is connected to the steam volume of the pipe, water flow if the junction is connected to the water volume). For example, if the junction is connected on the bottom of the pipe and the model is enabled, liquid will be drained by the junction until the level approaches the junction position and vapor will be pulled through with liquid. Likewise, if the junction is connected to the top, vapor would be drained from the pipe, and eventually liquid would be entrained, provided the level is high enough. Without the model, a mixture of liquid and vapor would be drained regardless of the position of the level.

However, no use of the model has been made in the present work. A more detailed explanation of the model can be found in [ISL, 2003].

Counter current flow limitation model Mainly during small break loss of coolant accident in a PWR or VVER a special case of phase separation, which seems paradox at first, can occur. It may happen at a certain point (depending on the boundary conditions like availability of safety systems) that steam is produced in the reactor and the level in the reactor pressure vessel decreases. Safety injection systems injecting into the upper plenum, or condensation of steam in the steam generators and backflow in the core could eventually occur (reflux condensation). However, there is the possibility that the water will not reach the core, but will be kept at the upper tie plate by the outgoing steam. So in fact, a “opposite” separation of steam and water, water on top of steam, could exist. This phenomenon, water on top of steam, occurred during the Three Mile Island accident, where a pressurizer full of liquid led the plant operator to conclude that the core is covered with liquid and to switch of the emergency injection.

Relap5, by default, does not consider counter current flow limitation (CCFL). If the user expects CCFL to happen, he may switch on the CCFL model in the appropriate junction.

If CCFL occurs or not is depending on the ratio between upward flowing steam and downward flowing water. If the model has been enabled by the user, Relap5 uses equation (2.14) to detect if the model should be applied or not:

$$H_f = j_f \sqrt{\frac{\rho_f}{g w (\rho_f - \rho_g)}} \quad (2.9)$$

$$H_g = j_g \sqrt{\frac{\rho_g}{g w (\rho_f - \rho_g)}} \quad (2.10)$$

$$j_f = \alpha_f v_f, j_g = \alpha_g v_g \quad (2.11)$$

$$w = D_j^{1-\beta} L^\beta \quad (2.12)$$

$$L = \sqrt{\frac{\sigma}{g(\rho_f - \rho_g)}} \quad (2.13)$$

$$\sqrt{H_g} + m\sqrt{H_f} = c \quad (2.14)$$

with

H_f, H_g	dimensionless liquid and steam flux
j_f, j_g	liquid/vapor superficial velocity
L	Laplace capillary constant
σ	surface tension
ρ_f, ρ_g	density of liquid and steam phase
v_f, v_g	velocity of liquid and steam
α_g, α_f	void fraction and one minus void fraction
g	acceleration of gravity
D_j	pipe hydraulic diameter
c, m	user input parameters, default 1,1
β	model parameter, see text

The form for the CCFL check (2.9 - 2.14) has been proposed by Bankoff. Depending on the parameter β , which can be input by the user, (2.14) takes on Wallis form ($\beta = 0$) or Kutatetadze ($\beta = 1$), or any form in between. The user should choose depending on the geometry. Equation (2.14) describes the border between occurrence and non-occurrence of CCFL (see Figure 2.27). If CCFL is detected in a junction, and the model is enabled, a modified momentum equation is used to account for the reduced flow. For details more please refer to [ISL, 2003].

Mixture level tracking model If the analyst expects that in a vertical pipe a liquid level will be formed (steam on top of liquid, clearly separated) which he would like to model accurately, a coarse nodalisation of the problem will introduce errors (see e.g. [Muellner et al., 2008]). Relap5 default model works with average void fractions, so, assuming a stack of volumes, control volumes below the volume containing the interface will be treated correctly (mainly liquid), volumes above will be treated correctly (mainly vapor), but the volume which contains the interface will assume a mixture of the two phases and work with an average void fraction - see Figure 2.27. The user has two possibilities - one, to refine the nodalisation such that the error introduced by averaging will be small, second, switch on the Relap5 mixture level tracking model.

The model has to be turned on in the vertical control volumes where it should be used. During input processing the code recognizes connected vertical control volumes which have the model enabled as “stacks”. Several stacks can be formed of one vertical structure to model the occurrence of multiple levels.

The model consists of five parts:

1. Detection of the mixture level appearance
2. Calculation of mixture level parameters (such as position and velocity of the level, void fraction above and below the level)
3. Movement of the mixture level from volume to volume
4. Modification of the mass and energy equations of Relap5 according to the position of the mixture level
5. Modification of the heat transfer calculation according to the position of the mixture level

For a more detailed description of the model please refer to [ISL, 2006c].

Neutron kinetics

Relap5 uses a comparably simply model to calculate the reactor power. Spacial effects are not considered, homogeneous conditions over the reactor core are assumed (point kinetics or 0D kinetics model). The only independent variable is time. This assumption indicates also the limits of the model. Transients, which lead to a different conditions in different parts of the core cannot be modeled adequately. The model considers both, power from immediate fission, and power from decay of fission products. Several options are provided to evaluate the decay power (ANS Standard 5.1-1973, ANS Standard 5.1-1979).

The point kinetics equations that are used are presented below (2.15). t denotes the time, ϕ the neutron flux, C_i the number of delayed neutron precursors of group i , β the effective delayed neutron fraction, Λ the prompt neutron generation time, ρ the reactivity, f_i the fraction of delayed neutrons of group i , λ_i the decay constant of group i , S the source, ψ the fission rate, Σ_f the macroscopic fission cross-section, P_f the immediate fission power and Q_f the immediate fission energy per fission. A Runge-Kutta method is used to integrate the set of ODE (2.15).

$$\begin{aligned} \frac{d}{dt}\phi(t) &= \frac{(\rho(t) - \beta)\phi(t)}{\Lambda} + \sum_{i=1}^{N_d} \lambda_i C_i(t) + S \\ \frac{d}{dt}C_i(t) &= \frac{\beta f_i}{\Lambda} \phi(t) - \lambda_i C_i(t) \quad i = 1, \dots, N_d \\ \psi(t) &= \Sigma_f \phi(t) \\ P_f(t) &= Q_f \psi(t) \end{aligned} \tag{2.15}$$

Relap5 considers the reactivity feedback from the fuel temperature (doppler effect), the moderator temperature and density, and the boron concentration. The user can assume that the total feed back can calculated as sum of separate feed back contributions of each of the above mentioned variables (separable feed back model), or can enter a multi dimensional look up table. The separable feed back model is a good approximation if criticality of the reactor is to be expected at only one point of state (e.g. full power). If one expects recriticality (e.g. at a lower temperature), the tabular feed back model should be used.

Critical flow

Models for special processes are implemented in Relap5, e.g. a special model for horizontal stratification, entrainment and pull-through, a model to calculate the k-loss coefficients assuming abrupt area changes, a model to mitigate a numerical error that can cause pressure spikes when a water front passes a node boundary - the water packing model, a model for counter current flow limiting (e.g. to model steam flow from the reactor preventing water flow from entering the core region), and other models. For the scope of this work only the correlations modeling critical flow will be described in more detail.

One speaks of critical (or choked) flow if the conditions downstream of the pipe do not affect the flow velocity. Figures 2.28 and 2.29 from [ISL, 2006c] show the situation for subcooled critical flow. Consider a converging-diverging nozzle as shown in Figure 2.28. Flow will happen if the downstream pressure is lower than the upstream pressure. The pressure at the throat P_t will with decrease with decreasing downstream pressure until it reaches saturation pressure. At this point evaporation will happen at the throat, and the flow will pass from one phase to two phase flow. The presence also of only a small fraction of steam in the fluid will decrease the speed of sound dramatically, while the velocity of the fluid cannot change due to conservation of mass. The velocity of the fluid upstream of the throat will be below the sound speed, but the velocity downstream, in the two-phase region, will be above sound speed (supersonic flow). If this happens, signals may not propagate upstream to the throat, and the flow is choked (see (a) in Figure 2.29). Figures (b) and (c) in 2.29 show the situation when the upstream pressure decreases.

Choked or critical flow is very important in the context of the present work, since all discharge of valves and break flows from primary or secondary circuit, as well as primary to secondary leaks in the initial phase of the transient are choked flows.

Relap5 offers two models to choose from. The “original” Relap5 model has been developed by Ransom and Trapp, see [Trapp and Ransom, 1982]. Lately a decision has been taken to change the default model, which is now the Henry-Fauske critical flow model (see [Henry and Fauske, 1971]). The user has the possibility to force the use of the “original” Relap5 model, Ransom-Trapp.

A detailed explanation of both models can be found in [ISL, 2006c]. A short overview on both models follows shortly.

Ransom and Trapp model Ransom and Trapp [Trapp and Ransom, 1982] are using mass, momentum and energy conservation equation for a two phase fluid to develop a choking criteria. Independent variables are space and time (t, x) , dependent variables are the void fraction α_g , the density ρ , and vapor- and liquid velocities v_g and v_f .

The energy conservation equation is written in terms of entropy. Ransom and Trapp first developed a non-homogeneous, non-equilibrium model. Comparison with experiments suggested that the model might be simplified by assuming thermal equilibrium, which has been done for the implementation of the model in the code Relap5.

$$\begin{aligned}
& \text{Mass conservation} \\
& \frac{\partial}{\partial t} (\alpha_g \rho_g + \alpha_f \rho_f) + \frac{\partial}{\partial x} (\alpha_g \rho_g v_g + \alpha_f \rho_f v_f) = 0 \\
& \text{Momentum conservation} \\
& \alpha_g \rho_g \left(\frac{\partial}{\partial t} v_g + v_g \frac{\partial}{\partial x} v_g \right) + \alpha_g \frac{\partial}{\partial x} P + \\
& C \alpha_g \alpha_f \rho \left(\frac{\partial}{\partial t} v_g + v_f d n d x v_g - \frac{\partial}{\partial t} v_f - v_g \frac{\partial}{\partial x} v_f \right) = 0 \\
& \alpha_f \rho_f \left(\frac{\partial}{\partial t} v_f + v_f \frac{\partial}{\partial x} v_f \right) + \alpha_f \frac{\partial}{\partial x} P + \\
& C \alpha_f \alpha_g \rho \left(\frac{\partial}{\partial t} v_f + v_g d n d x v_f - \frac{\partial}{\partial t} v_g - v_f \frac{\partial}{\partial x} v_g \right) = 0 \\
& \text{Energy conservation} \\
& \frac{\partial}{\partial t} (\alpha_g \rho_g S_g + \alpha_f \rho_f S_f) + \frac{\partial}{\partial x} (\alpha_g \rho_g S_g v_g + \alpha_f \rho_f S_f v_f) = 0
\end{aligned} \tag{2.16}$$

with

- α_g vapor fraction
- α_f liquid fraction
- ρ_g vapor density
- ρ_f liquid density
- v_g vapor velocity
- v_f liquid velocity
- C virtual mass coefficient
- ρ mixture density
- S_g specific energy of vapor
- S_f specific energy of liquid

The equations can be cast in the form of (2.17) which is similar to the whitham equation $U = (\alpha_g, \rho, v_g, v_f)$, A , B and C four by four matrices:

$$\mathbf{A}(U) \frac{\partial}{\partial t} U + \mathbf{B}(U) \frac{\partial}{\partial x} U + \mathbf{C}(U) = 0 \tag{2.17}$$

According to [Whitham, 1974] one can derive the propagation velocities of the system (2.17) by solving the “characteristic polynomial” (2.18):

$$\mathbf{A} \lambda - \mathbf{B} = 0 \tag{2.18}$$

The polynomial (2.18) is of forth order. The real part of the roots give the velocity of signal propagation. From this, one can derive a criteria for the case that no signal can propagate upstream to the throat (see [ISL, 2006c] for details):

$$M_v + D \cdot M_r = \pm 1 \tag{2.19}$$

with

$$\begin{aligned}
M_v &= \frac{v}{a} \\
M_r &= \frac{v_g - v_f}{a} \\
v &= \text{frac} \alpha_g \rho_g v_g + \alpha_f \rho_f v_f \rho \\
a &= a_{HE} \sqrt{\left(\frac{C \rho^2 + \rho (\alpha_g \rho_f + \alpha_f \rho_g)}{C \rho^2 + \rho_g \rho_f} \right)} \\
a_{HE} &= \text{homogeneous equilibrium sound speed}
\end{aligned} \tag{2.20}$$

$$\begin{aligned}
a_{HE} &= \frac{V \frac{dP^s}{dT}}{\sqrt{X \cdot TERM_g + (1 - X) \cdot TERM_l}} \\
TERM_g &= \left(\frac{C_{pg}}{T_g} + V_g \frac{dP^s}{dT} \left(\kappa_g \frac{dP^s}{dT} - 2\beta_g \right) \right) \\
TERM_f &= \left(\frac{C_{pf}}{T_f} + V_f \frac{dP^s}{dT} \left(\kappa_f \frac{dP^s}{dT} - 2\beta_f \right) \right) \\
\frac{dP^s}{dT} &= \frac{h_g - h_f}{T^s (V_g - V_f) \text{ Clausius-Clapeyron-Equation}}
\end{aligned} \tag{2.21}$$

with

- V specific volume
- P^s saturation pressure
- X mass quality of steam
- C_{pg} saturated vapor specific heat
- C_{pf} saturate liquid specific heat
- κ_g isothermal compressibility for vapor
- κ_f isothermal compressibility for liquid
- β_g isopiestic coefficient for thermal expansion for vapor
- β_f isopiestic coefficient for thermal expansion for liquid

E.g. [Brennen, 2005] shows how to derive the homogeneous equilibrium sound speed (2.21).

One can see that (2.19) the flow is choked, if the Mach number is equal to unity. This is consistent with the considerations at the beginning of the section. The Ransom Trapp model offers the user the possibility to insert discharge coefficients, which are multiplied in the implementation of the model with the area of the junction, where the model is applied. Three different discharge coefficients may be entered, they may range from 0.0 to 2.0, one for subcooled, one for two-phase, and one for superheated critical flow.

Henry Fauske model The so called “Henry-Fauske” model was proposed first by R. E. Henry and H. K. Fauske in 1971, [Henry and Fauske, 1971]. The approach is different from the one of Ransom and Trapp shown above. Although the Ransom Trapp model is newer than Henry Fauske, Relap5 switched the default model from Ransom Trapp to a slightly modified Henry Fauske model starting from version mod 3.3 . The reason is that the modified Henry Fauske model handles the presence of non-condensable gases and shows in general better agreement with experimental data.

The approach to the Henry-Fauske model is different from the Ransom-Trapp approach and shortly outlined below.

Consider the same configuration as in Figure 2.28. Considering one-component, two-phase flow, and neglecting wall shear forces, the momentum equation and mass flow rate at the throat respectively can be approximated by

$$\begin{aligned}
-AdP &= d(\dot{m}_v + u_v + \dot{m}_l + u_l) \\
G &= \frac{dP}{du} \\
G_t^{-1} &= -\frac{du}{dP} = \frac{d(xu_v + (1-x)u_l)}{dP}
\end{aligned} \tag{2.22}$$

with

A	area of the nozzle [L^2]
\dot{m}	mass flow [$M T^{-1}$]
u	mixture velocity [$L T^{-1}$]
u_l	liquid velocity
u_v	vapor velocity
x	quality [-]
P	pressure [$MLT^{-2}L^{-2}$]
G	mass flux [$MT^{-1}L^{-2}$]
G_t	mass flux at the throat

the critical flow is the maximum flow in respect to the throat pressure, so that the condition for critical flow is

$$\left. \frac{dG_c}{dP} \right|_t = 0 \quad (2.23)$$

From equations (2.22) and (2.23) the following critical mass flux for an isentropic homogeneous mixture can be derived:

$$G_c^2 = \left(x \frac{\partial}{\partial P} v_v + (1-x) \frac{\partial}{\partial P} v_l + (v_v + v_l) \frac{\partial}{\partial P} x \right)^{-1} \quad (2.24)$$

with

v	specific volume [$L^3 M^{-1}$]
v_l	specific volume liquid
v_v	specific volume vapor

In a certain sense this corresponds to mass flux at sound speed

$$\begin{aligned} c^2 &= \frac{dP}{d\rho} = \frac{\partial P}{\partial v} \frac{dv}{d\rho} = \frac{dP}{dv} \frac{1}{\rho^2} \text{ with } v = \frac{1}{\rho} \\ G_{sound}^2 &= \frac{\partial P}{\partial v} \text{ and with } v = xv_v + (1-x)v_l \\ G^{-2} &= \frac{\partial}{\partial P} (xv_v + (1-x)v_l) \end{aligned} \quad (2.25)$$

To evaluate (2.24) one has to find an estimate of v_v , v_l , x , $\frac{\partial v_v}{\partial P}$, $\frac{\partial v_l}{\partial P}$, and $\frac{\partial x}{\partial P}$. The Henry-Fauske model assumes that the velocity of the phases are equal, that little or no mass transfer occurs between the phases, and the no heat is transferred between the phases. Calculation of the components (see [ISL, 2006c] for details) yields:

$$G_c^2 = \left(\frac{x_0 v_v}{\eta P} + (v_v - v_{l,0}) \left(\frac{(1-x_0)N}{s_{v,eq} - s_{l,eq}} \frac{ds_{l,eq}}{dP} - \frac{x_0 C_{p,v} \left(\frac{1}{\eta} - \frac{1}{\gamma} \right)}{P_t (s_{v,0} - s_{l,0})} \right) \right)^{-1}_t \quad (2.26)$$

The critical flow from (2.26) has similarities to the homogeneous equilibrium model flow rate (2.21). The major difference is the presence of a non-equilibrium factor N which stems from the contribution of $\left. \frac{dx}{dP} \right|_t$. It basically determines the amount of flashing at the throat. Henry and Fauske compared their model with experiments, and set the N to be

$$N = \frac{x_{eq,t}}{C_{ne}} \text{ with } C_{ne} = 0.14 \text{ being the non-equilibrium constant} \quad (2.27)$$

However, setting the non-equilibrium constant to 0.14 gives only for certain L/D ratios good results. In the Relap5 implementation of the model the user has the possibility to supply this parameter. While the influence for subcooled blow down is minimal, for qualities in the stagnation volume above 20% the contribution becomes visible. The original plan, to implement a correlation which would set the non-equilibrium

constant according to the geometry of the break, has not been put into effect. Instead, the user has to choose the constant, best by comparing the simulation of a certain break geometry against separate effect tests. The constant C_{ne} can take on every positive value. A value near to zero causes the model to be close to the homogeneous equilibrium model, while a large value corresponds to the homogeneous frozen model.

In the frame of the present work the Henry Fauske model with the default parameter of 0.14 has been adopted, since separate effect tests have not been available.

A second constant can be input by the user, an overall discharge coefficient. The discharge coefficient is effective during all phases of the blow down. For the present work, the default value of 1.0 has been adopted.

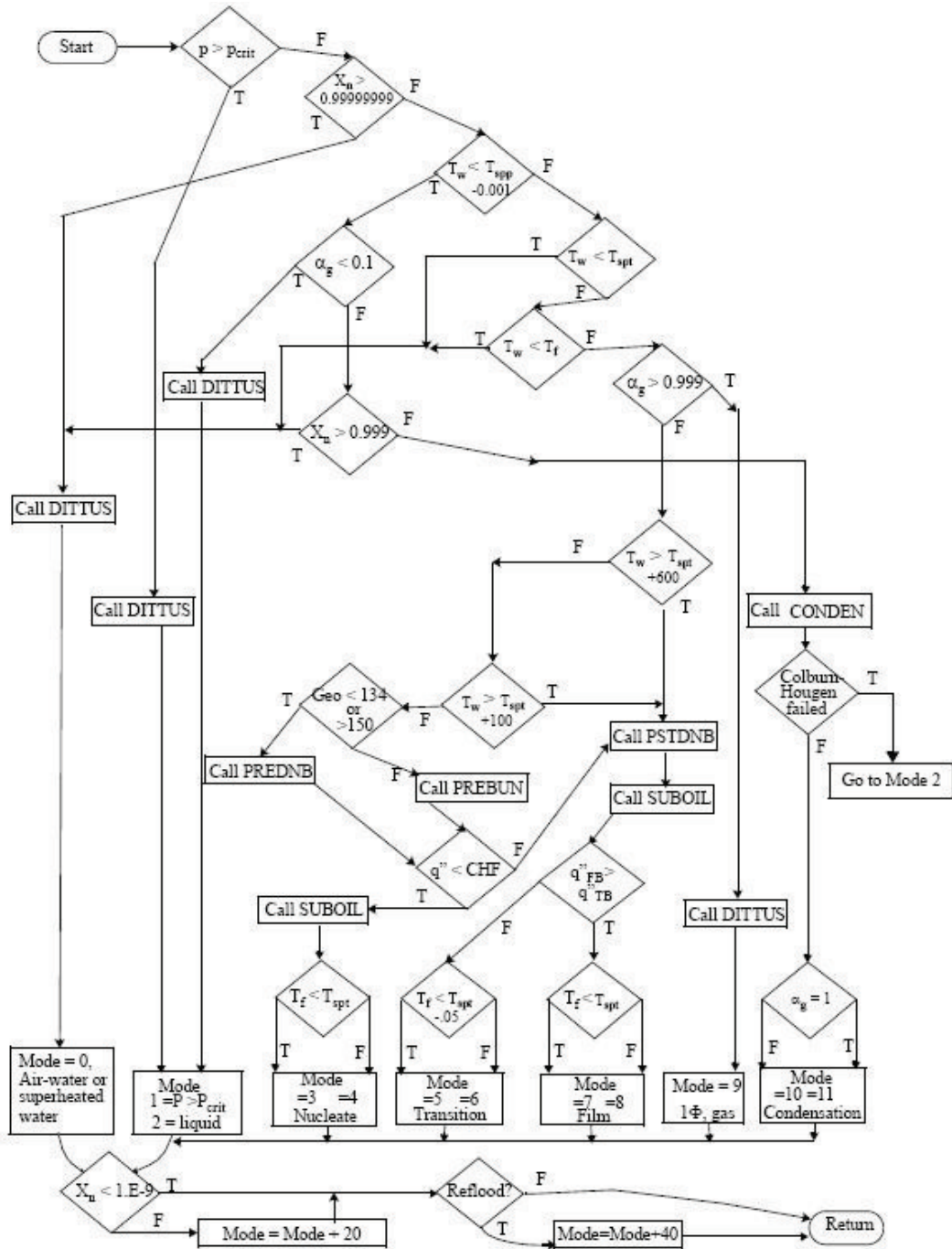


Figure 2.24: Wall to fluid heat transfer mode

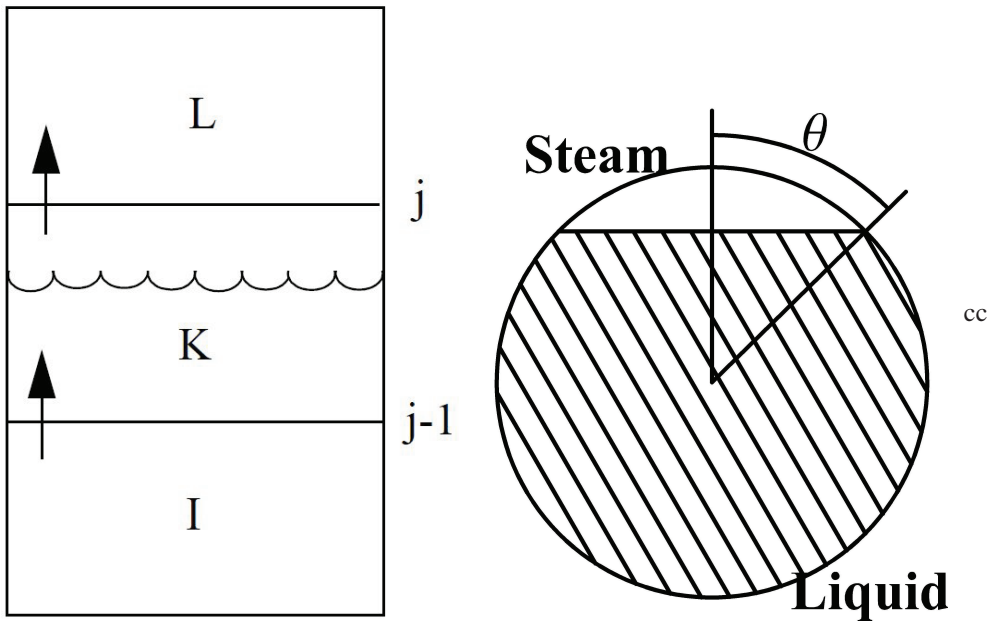


Figure 2.25: Relap5 vertical stratified flow (left), meaning of angle θ in (2.8) (right)

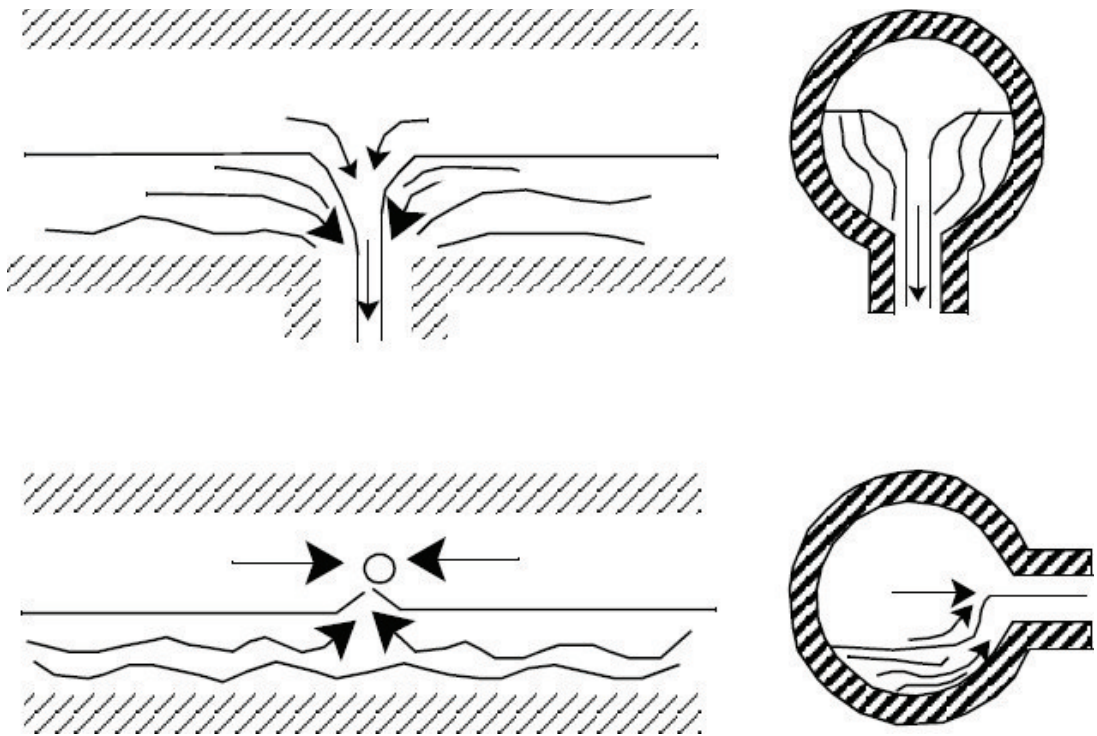


Figure 2.26: Two possible configurations for the horizontal stratification entrainment/pullthrough model

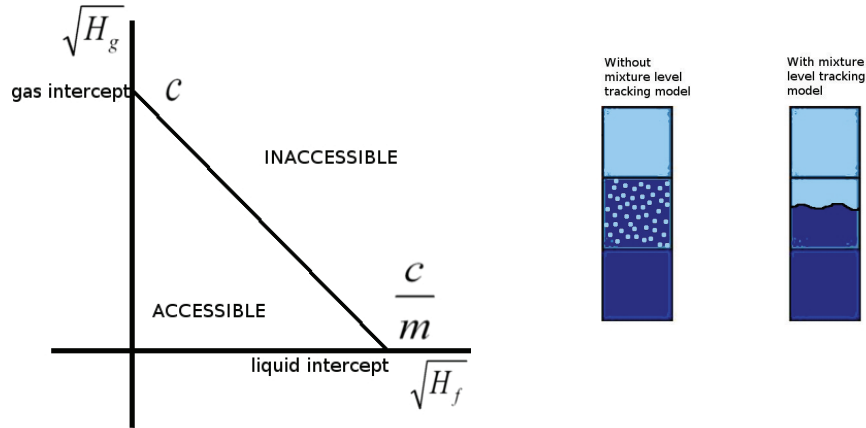


Figure 2.27: CCFL model used if (H_f, H_g) in accessible region (left), interface liquid/steam with/without mixture level tracking model (right)

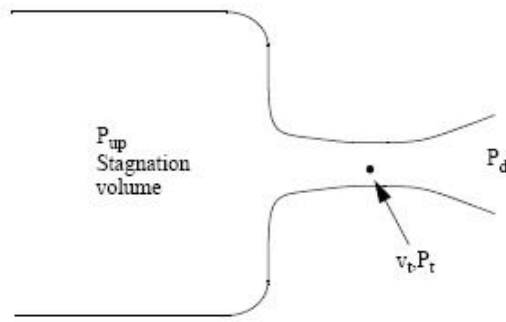


Figure 2.28: Converging-diverging nozzle

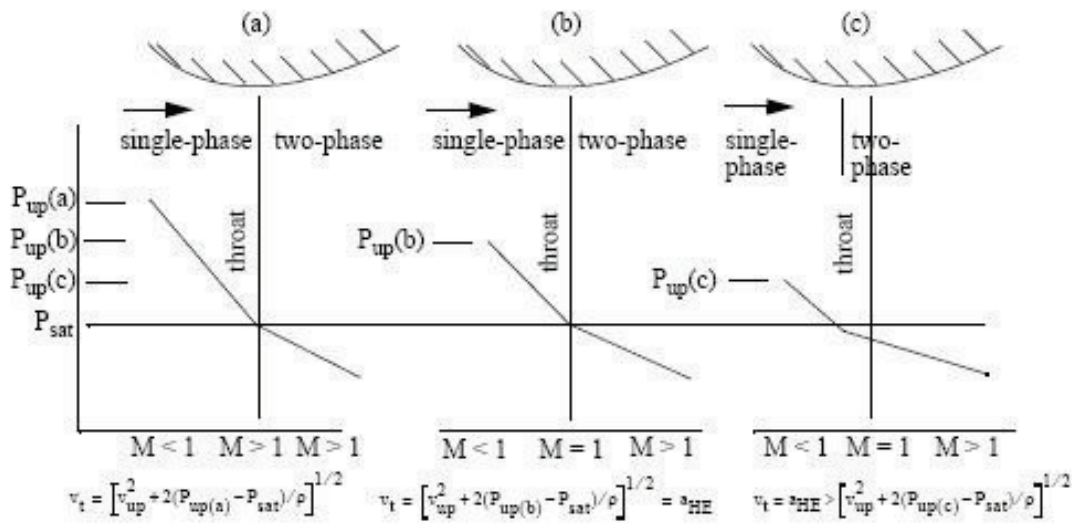


Figure 2.29: Subcooled choking process

2.4.2 Aspects of UMAE

Only a short overview, taken from [NEA/CSNI, 2005], on the uncertainty method based on accuracy extrapolation (UMAE), can be presented here. The method has been developed at the University of Pisa. It was first published [D'Auria et al., 1995] in 1995.

Calculating uncertainty bands to thermal hydraulic is an topic which is under active development in the nuclear field. One IAEA Tecdoc [IAEA, 2007] is in preparation on the topic. The basic idea of the UMAE method (see Figure 2.30) is that the uncertainty of a thermal hydraulic system code calculation is composed of

- Uncertainties due to the modeling of physical phenomena in the code
- Statistical uncertainty, depending on the complexity of the problem
- Uncertainty due to different level of skills and experience of the code user
- Uncertainty due to different approaches in developing a nodalisation

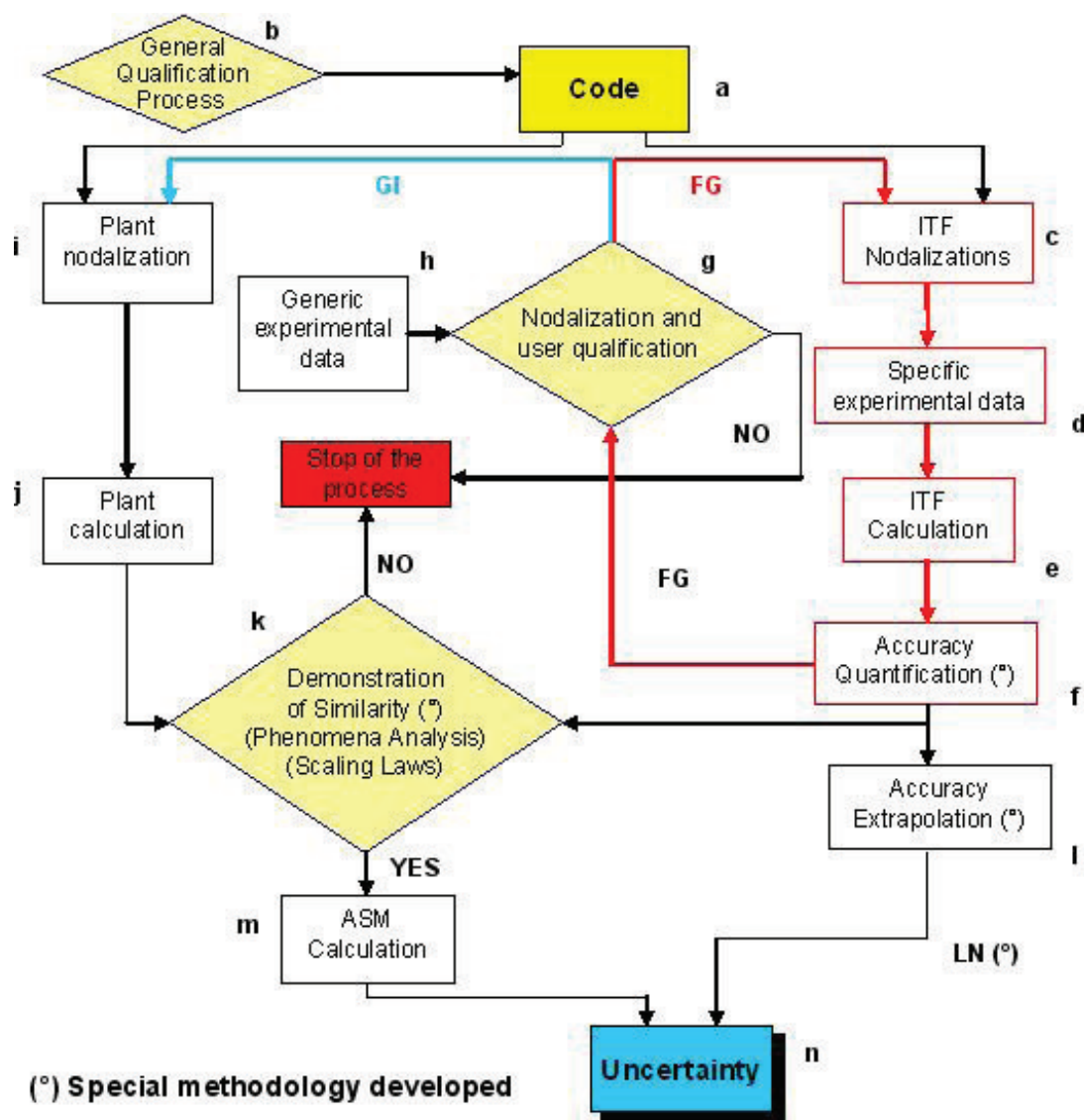


Figure 2.30: UMAE flowchart

basically, the uncertainty can be splitted in two parts: user dependent, and model-dependent. To control the user dependent contribution to the uncertainty, the UMAE requires that the user fulfills certain minimum

standards, and follows a strict nodalisation qualification procedure. The model-dependent part is derived by accuracy extrapolation, but for the purpose of the work presented here the “nodalisation qualification procedure” is of main interest.

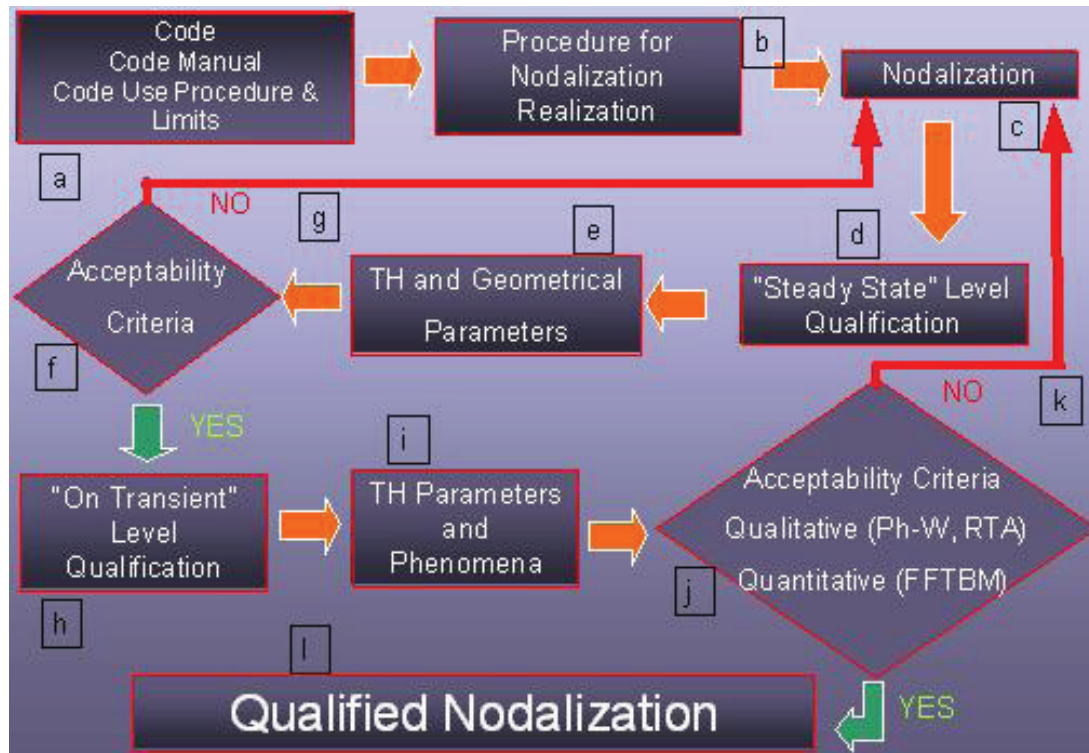


Figure 2.31: Nodalisation qualification procedure

Figure 2.31 shows the flow chart for the nodalisation qualification process. The following description is taken from Appendix B from [NEA/CSNI, 2005];

The first requirement is that the user of a TH-SYS code works with a “frozen” version of the code, and that he does not change any models or parameters other than the parameters foreseen by the developers.

The goal of the procedure is to qualify the code-nodalisation-user combination, to guarantee a pre set degree of quality of the calculation results.

A major issue in the use of mathematical model is constituted by the model capability to reproduce the plant or facility behavior under steady state and transient conditions. These aspects constitute two main checks that must be passed in the qualification process. The first of them is related to the realization of a schematization of the reference plant; the second one is related to the capability to reproduce the transient analysis to derive the needed information.

The check about the nodalisation is necessary to take into account the effect of many different sources of approximations:

- Data of the reference plant available to the user are typically non exhaustive to reproduce a perfect schematization of the reference plant;
- The user derives, from the available data, an approximated schematization of the plant reducing the detail level of the plant representation;
- The code capability for reproducing the hardware, the plant systems and actuation logic of the systems again reduces the schematization detail level.

The reasons for the checks about the capability to perform the transient analysis derive from the following statements:

- The code options must be adequate;
- The schematization solutions must be adequate;

- Some systems simulations can be tested only in the simulation of the transient (e.g. ECCS that is not involved in the normal plant operation);
- The “code-nodalisation” system capability to reproduce relevant TH phenomena expected in the transient must be tested.

A procedure has been set-up including the necessary checks for these different aspects and the criteria adopted to produce a judgment about acceptability of the code analysis results.

The goal of the procedure is to develop and obtain a qualified nodalisation considering the comparison with hardware data, BIC and time trends of relevant quantities. A procedure has been developed and applied in which a “steady state” and a “transient” level of qualification are distinguished. Criteria for selecting relevant quantities are mentioned in the following discussion. A scheme of the procedure can be seen in Figure 2.31. The two checks are represented by the two steps “f” and “j”. If the two checks are not fulfilled (paths “g” and “k”) the nodalisation must be improved (step “c”).

Step “a” An internationally recognized code version (“frozen” code) must be available. The consistency of the installation of the code on the computer must be checked. No special deficiencies should have been detected in predicting the phenomena to be considered.

The step is also related to the information that is available by the user manual and by the guidelines for the use of the code. This type of information takes into account the specific limits and assumptions of the code (specific of the code adopted for the analysis) and some directives about the way to realize best nodalisations.

From a generic point of view the following statements should be considered:

- Homogeneous nodalisation;
- Strict observation of the user guidelines;
- Standard use of the code options.

Step “b” User experience and developers recommendations are useful to set up procedures to be applied for a better nodalisation. These special procedures are related to the specific code adopted for the analysis. An example is constituted by the “slice” nodalisation adopted with the Relap5 code to improve the capability of the code in the simulation of the phase of transient involving the natural circulation phenomena.

Step “c” The nodalisation realization depends on several aspects: available data, user capability and experience and code capability. Data must be qualified and this implies data should derive from:

- Qualified facility (if the analysis is performed for a facility);
- Qualified test design;
- Qualified test data.

The data base for the realization of the nodalisation should be derived from official document and traceability of each reference should be maintained. However three different types of data sources can be identified:

- Qualified data from official sources;
- Data deriving from non-official sources. This type of data can be derived from similar plant data or other qualified nodalisation for the same type of plant. The use of these data can introduce potential errors and the effect on the calculation results must be carefully evaluated;
- Data assumed by the user. These types of data constitute assumptions of the user (based on of the experience or on similitude with other similar plants) and their use should be avoided. Any special assumptions adopted by the user or special solutions in the nodalisation must be recorded and documented.

The nodalisation must reproduce all the relevant parts of the reference plant including geometrical and materials fidelity and reproduction of systems and related logics.

Step “d” The ‘steady state’ qualification level step includes different checks: one is related to the evaluation of the geometrical data and of numerical values implemented in the nodalisation; the other one is related to the capability of the nodalisation to reproduce the steady state qualified conditions. The first check should be performed by a user different from the user has carried out the nodalisation. In the second check a ‘steady state’ calculation is performed. This activity depends on the different code peculiarities. As an example, for the RELAP, the steady state calculation is constituted by a ‘null transient’ calculation (‘null transient’ means that the ‘transient’ option is selected in a calculation with any variations of the relevant parameters).

Step “e” The relevant geometrical values and the relevant thermal-hydraulic parameters of the steady state conditions are identified. The selected geometrical values and the selected relevant parameters are derived from the nodalisation and from the steady state calculation for a comparison with the hardware values and the experimental parameters, respectively.

Step “f” Experimental and calculated geometrical values and steady state parameters are compared in order to satisfy acceptability criteria. The following considerations apply:

- Experimental data are typically available with an error band that must be considered in the comparison with the calculated values and parameters. No error is made if the calculated value is inside the experimental uncertainty bands;
- The convergence of the steady state calculation must be checked.

Step “g” If one or more than one of the checks in step “f” is not fulfilled a review of the nodalisation (step “c”) must be performed. This process can request more detailed data, improvement in the solution of the schematization, different user choices.

Step “h” This step constitutes the “On Transient” level qualification. This activity is necessary to demonstrate the capability of the nodalisation to reproduce the relevant thermal-hydraulic phenomena expected in the transient. This step also makes possible to verify the correctness of some systems operating only during transient events. Two different situations may be identified:

- The nodalisation is constituted by the schematization of a facility (in this case the code calculation is used for Code Assessment). It is necessary to prove the capability of the code and of the nodalisation scheme during the transient analysis: the code options selected by the user, the schematization solutions and the logic of some systems (i.e. ECCS) are involved during this check. Typically many experimental results are available from the facility and, at least, one similar test can be adopted for the ‘On Transient’ level qualification.
- The object of the code calculation is constituted by the analysis of a transient in a NPP. In this case it is necessary to check the nodalisation capability to reproduce the expected thermal-hydraulic phenomena occurring in the transient, the selected code options, the solutions adopted by the user for the plant schematization and the logic of the system not involved in the steady state calculation and called into operation during the transient.

As in general no data exist for transients or tests performed in the NPP, the qualification of the nodalisation is obtained through the use of the experimental tests performed in facilities and through the so-called “Kv-scaled” calculation. The “Kv-scaled” calculation consists in using the realized NPP nodalisation for the calculation of the same type of transient performed in a facility. The NPP nodalisation is prepared for a “Kv-scaled” calculation by properly scaling the boundary and initial conditions adopted in the facility. It generally means that power, mass flow rates and ECCS capacity are scaled adopting as scaling factor the ratio between the volumes of the facility and the volume of the schematized NPP. The capability of the nodalisation to reproduce the same transient evolution and the relevant thermal-hydraulic phenomena is the needed request for the ‘On Transient’ qualification level.

Step “i” In this step the relevant thermal hydraulic phenomena and parameters are selected to perform the comparison between calculated and experimental results. The selection of the phenomena derives from the following sources:

- Experimental data analysis;
- CSNI phenomena identification;
- Use of RTA (relevant thermal aspects).

Step “j” Checks from the qualitative and quantitative point of view are performed to evaluate the acceptability of the calculation on the “transient level”. For the qualitative evaluation the following aspects are involved:

- Visual observation: visual comparisons are performed between experimental and calculated relevant parameters time trends;
- Resulting Time Sequence of Events: it means that the list of the calculated significant events and the calculated timing of the events is compared with the experimental events
- Use of the phenomena specified in the CSNI validation matrix that are valid for any kind of transients (see Table B-2). The relevant phenomena suitable for code assessment, the relevance in the selected facility and the phenomena that are well defined in the selected test can be derived. A judgment can be expressed taking into account the characteristics of the facility, the test peculiarities, and the code results;

Use of the Phenomenological Windows (PhW), Key Phenomena and Relevant Thermal-hydraulic Aspects (RTA). Each test scenario (measured or calculated) should be divided into phenomenological windows (i.e., time spans in which a unique relevant physical process mainly occurs and a limited set of parameters controls the scenario). In each PhW, key phenomena and RTA must be identified. Key phenomena are attributed to a class of experiments. The lists prepared and agreed to by the Organization for Economic Cooperation and Development (OECD)/CSNI are used in the process (Refs. B6 and B7). RTAs are defined for a single transient and are characterized by numerical values of significant parameters:

- Single Valued Parameters, SVP (e.g., minimum level in the core);
- Nondimensional Parameters, NDP (e.g., Froude numbering the hot leg at the beginning of reflux condensation);
- Time Sequence of Events, TSE (e.g., time when dryout occurs);
- Integral Parameters, IPA (e.g., integral or average value of break flow rate during subcooled blow-down).

Around 20 RTAs, characterized by more than 40 values of significant parameters, must be selected for the qualitative evaluation of a database. Key phenomena and RTAs are used for the following purposes:

- to judge the relevance to scaling and the quality of a test facility (key phenomena);
- to judge the relevance to scaling and the quality of a test design (key phenomena);
- to judge the relevance of an experimental data- base (key phenomena and RTAs);
- to judge the calculation performance (RTAs);
- to assess the success of a similarity study and of the nodalisation qualification process (RTAs);
- to assess the similarity of different experimental databases (RTAs).

The qualitative analysis is based on five subjective judgment marks, which are applied both to the matrix of phenomena and to the list of RTAs: It essentially derives from a visual observation of the experimental and the predicted trends.

- The code predicts qualitatively and quantitatively the parameter (Excellent - the calculation falls within the experimental data uncertainty band).
- The code predicts qualitatively, but not quantitatively the parameter (Reasonable - the calculation shows only correct behavior and trends).

- The code does not predict the parameter, but the reason is understood and predictable (Minimal - the calculation does not lie within the experimental data uncertainty band and at times does not have correct trends).
- The code does not predict the parameter and the reason is not understood (Unqualified - calculations do not show the correct trend and behavior, and reasons are unknown and unpredictable).
- Not applicable (-).

A first classification about the calculation quality results from this analysis. A successful application of the qualitative process constitutes a prerequisite to the application of the quantitative analysis.

If the aforementioned steps are acceptable, the accuracy of code calculations can be quantified utilizing the Fast Fourier Transform Based Method (FFTBM). This tool produces a couple of values in the frequency domain from each comparison between calculated and measured time trends: 1) the so-called “average accuracy” and 2) the “weighted frequency”. The transformation from time to the frequency domain avoids the dependence of the error from the transient duration. Weight factors are attributed to each time trend to make possible the summing up of the error and the achievement of a unique threshold for accepting a calculation. A quantitative accuracy evaluation must be carried out following demonstration that the calculation is qualitatively acceptable. The same time trends selected for the qualitative analysis are utilized as input to the FFTBM. Acceptability criteria have been set-up and a full description of the FFTBM is given in the next section.

Step “k” This path is actuated if one or more than one check (qualitative and/or quantitative) is not fulfilled. The nodalisation is improved by changing some schematization solutions, some code options or increasing the level of detail eventually using new data. Every time the nodalisation is modified, a new process shall be performed through the loop “c-d-e-f-h-i-j”.

Step “I” This is the last step of the procedure. The obtained nodalisation is called, in the UMAE (Uncertainty Methodology based on Accuracy Extrapolation) nomenclature, Analytical Simulation Model (ASM). This consists of a qualified plant (or facility) nodalisation running on a qualified code by a qualified user. The ASM can be used to predict plant scenario characterized by the same Phenomenological Windows and Key Phenomena of the assigned transient. It should be noted that a modification of the nodalisation (i.e. necessary to better reproduce the experimental results) requests a new qualification process both “at steady state” and “on transient” level.

2.4.3 FFTBM

Several approaches have been proposed to quantify the accuracy of a given code calculation Ambrosini et al. [1990], Riebold [1987], Pochard and Porracchia [1986]. Even though these methods were able to give some information about the accuracy, they were not considered satisfactory because they involved some empiricism and were lacking of a precise mathematical meaning. Besides, engineering subjective judgment at various levels is deeply inside proposed methods.

Generally, the starting point of each method is an error function, by means of which the accuracy is evaluated. Some requirements were fixed which an objective error function should satisfy:

1. at any time of the transient this function should remember the previous history;
2. engineering judgment should be avoided or reduced;
3. the mathematical formulation should be simple;
4. the function should be non-dimensional;
5. it should be independent upon the transient duration;
6. compensating errors should be taken into account (or pointed out);
7. its values should be normalized.

The simplest formulation about the accuracy of a given code calculation, with reference to the experimental measured trend, is obtained by the difference function

$$DF(t) = F_{calc}(t) - F_{exp}(t) \quad (2.28)$$

The information contained in this time dependent function, continuously varying, should be condensed to give a limited number of values which could be taken as indexes for quantifying accuracy. This is allowed because the complete set of instantaneous values of $DF(t)$ is not necessary to draw an overall judgment about accuracy.

Integral approaches satisfy this requirement, since they produce a single value on the basis of the instantaneous trend of a given function of time. On the other hand, searching for functions expressing all the information through a single value, some interesting details could be lost. Therefore, it would be preferable to define methodologies leading to more than one value in order to characterize the code calculation accuracy.

Information that comes from the time trend of a certain parameter, be it a physical or a derivated one, may be not sufficient for a deep comprehension of the concerned phenomenon; in such a case, it may be useful to study the same phenomenon from other points of view, free of its time dependence. In this context, the complete behavior of a system in periodic regime conditions (periodic conditions due to instability phenomena are explicitly excluded) can be shown by the harmonic response function that describes it in the frequency domain.

Furthermore, the harmonic analysis of a phenomenon can point out the presence of perturbations otherwise hidden in the time domain.

Algorithm development

It is well known that the Fourier transform is essentially a powerful problem solving technique. Its importance is based on the fundamental property that one can analyze any relationship from completely different viewpoints, with no lack of information with respect to the original one. The Fourier transform can translate a given time function $g(t)$, in a corresponding complex function defined, in the frequency domain, by the relationship:

$$\tilde{g}(\omega) = \int_{-\infty}^{\infty} g(t) \exp(2\pi i \omega t) dt \quad (2.29)$$

Afterward, it is assumed that the experimental and calculated trends to which the Fourier transform is applied verify the analytical conditions required by its application theory; i.e., it is assumed that they are continuous (or generally continuous)¹ in the considered time intervals with their first derivatives, and absolutely integrable in the interval $(-\infty, \infty)$ ² Brigham [1974]. This last requirement can be easily satisfied in our case, since the addressed functions assume values different from zero only in the interval $(0, T)$.

Therefore:

$$\tilde{g}(\omega) = \int_0^T g(t) \exp(2\pi i \omega t) dt \quad (2.30)$$

The Fourier integral (2.30) is not suitable for machine computation, because an infinity of samples of $g(t)$ is required. Thus, it is necessary to truncate the sampled function $g(t)$ so that only a finite number of points are considered, or in other words, the discrete Fourier transform is evaluated. Truncation introduces a modification of the original Fourier transform (the Fourier transform of the truncated $g(t)$ has a rippling); this effect can be reduced choosing the length of the truncation function as long as possible.

When using functions sampled in digital form, the FFT can be used. The FFT is an algorithm that can compute more rapidly the discrete Fourier transform. To apply the FFT algorithm, functions must be identified in digital form by a number of values which is a power of 2. Thus, if the number of points defining the function in the time domain is:

$$N = 2m + 1 \quad (2.31)$$

¹i.e. discontinuous only in a finite number of points. The existence of the Fourier Transform is guaranteed if $g(t)$ is summable according to Lebesgue on the real axis

²i.e. $\int_{-\infty}^{\infty} |g(t)| dt < \infty$

the algorithm gives the transformed function defined in the frequency domain by $2m + 1$ values corresponding to the frequencies

$$f_n = \frac{n}{T}, (n = 0, 1, \dots, 2m) \quad (2.32)$$

in which T is the time duration of the sampled signal.

Taking into account the fact that the adopted subroutine packages evaluate the FFT normalized to the time duration T , from (2.30) and (2.31) it can be seen that $|\tilde{g}(0)|$ represents the mean value of the function $g(t)$ in the interval $(0, T)$, while $|\tilde{g}(f_i)|$ represents the amplitude of the i -th term of the Fourier polynomial expansion for the function $g(t)$.

Generally, the Fourier transform is a complex quantity described by the following relationship:

$$\tilde{g}(f) = \Re(f) + i\Im(f) = |\tilde{g}(f)| \exp(iq(f)) \quad (2.33)$$

where: $\Re(f)$ is the real component of the Fourier transform; $\Im(f)$ is the imaginary component of the Fourier transform $|\tilde{g}(f)|$ is the amplitude or Fourier spectrum of $g(t)$. $q(f)$ is the phase angle or phase spectrum of Fourier transform.

It is well known that:

$$|\tilde{g}(f)| = \sqrt{2\Re(f)^2 + 2\Im(f)^2} \quad (2.34)$$

$$\Theta(f) = \tan^{-1} \frac{\Im(f)}{\Re(f)} \quad (2.35)$$

The method developed to quantify the accuracy of code calculations is based on the amplitude of the FFT of the experimental signal and of the difference between this one and the calculated trend. In particular, with reference to the error function $DF(t)$, defined by the (2.28) method defines two values characterizing each calculation:

a dimensionless average amplitude

$$AA = \frac{\sum_{n=0}^2 |\Delta \tilde{F}(f_n)|}{\sum_{n=0}^2 |\tilde{F}_{exp}(f_n)|} \quad (2.36)$$

a weighted frequency

$$WF = \frac{\sum_{n=0}^{2\infty} |\Delta \tilde{F}(f_n)| \cdot f_n}{\sum_{n=0}^{2\infty} |\Delta \tilde{F}(f_n)|} \quad (2.37)$$

The AA factor can be considered a sort of "average fractional error" of the addressed calculation; the weighted frequency WF gives an idea of the frequencies related with the inaccuracy³.

The accuracy of a code calculation can be evaluated through these values, by representing the discrepancies of the addressed calculation with respect to the experimental data with a point in the WF - AA plane. The most significant information is given by AA , which represents the relative magnitude of these discrepancies; WF supplies a different information allowing to better identify the character of accuracy. In fact, depending on the transient and on the parameter considered, low frequency errors can be more important than high frequency ones, or vice versa.

Trying to give an overall picture of the accuracy of a given calculation, it is required to combine the information obtained for the single parameters into average indexes of performance.

This is obtained by defining the following quantities:

$$(AA)_{tot} = \sum_{n=0}^{N_{Par}} (AA)_i(w_f)_i, (WF)_{tot} = \sum_{n=0}^{N_{Par}} (WF)_i(w_f)_i \quad (2.38)$$

with

$$\sum_{n=0}^{N_{Par}} (w_f)_i = 1 \quad (2.39)$$

³In fact, it really represents the barycentre of the amplitude spectrum of Fourier transform of the difference function $DF(t)$; therefore, it evaluates the kind of error of the addressed calculation (which can be more or less relevant depending on the characteristics of the analyzed transient)

where: N_{var} is the number of parameters selected (to which the method has been applied) $(wf)_i$ are weighting factors introduced for each parameter, to take into account their importance from the viewpoint of safety analyses.

This introduces some degree of engineering judgment that has been fixed by a proper and unique definition of the weighting factors, necessary to account for the different relevance, from the point of view of safety and reliability of the measurement, of the various addressed quantities.

implementation

In the following, the FFT method application will be dealt with from an operative point of view. To apply the methodology described in the previous section, after selecting the parameters to be analyzed, it is necessary to choose the following parameters:

- number of points
- sampling frequency
- cut frequency.

All these items are related each other, nevertheless they will be treated in separate sub-sections, in order to allow a better comprehension of their requirements.

Sampling frequency In order to evaluate the discrete Fourier transform, it is necessary, first of all, the sampling of signals to be analyzed. The choice of the sampling frequency depends on transient, kind of parameter trend to be investigated (i.e. pressure, flow rate, clad temperature, etc.); obviously, the fulfillment of the sampling theorem⁴ is required to avoid distortion of sampled signals due to aliasing occurrence⁵ occurs until the frequency sampling is increased to

$$T = \frac{1}{2f_c} \quad (2.40)$$

where f_c is the highest frequency component of Fourier transform characterizing the spectrum of the continuous function $g(t)$.

Therefore, experimental data acquisition should be characterized by sampling frequency greater than $2f_c$ ⁶; similar frequencies of acquisition should have the corresponding calculated trends. Of course, compared analysis of these data requires that the lowest value of f_c (between the experimental and calculated one) should be taken as limiting value. A typical value of f_c related to parameters of interest in thermal hydraulic transients is 1 Hz; specifically, break flow rates or pressure drops measurements can include higher values.

Number of points Since the FFT algorithm requires that functions are identified by a number of values, equally spaced, which is a power of 2, an interpolation is necessary to satisfy this requirement. On the other hand, the comparison of experimental and calculated signals, and the evaluation of their difference function $DF(t)$, imposes that they have the same time scale.

Furthermore, after selecting the number of points N (see (2.31)), the maximum frequency of transformed functions by the FFT, is given by

$$f_{max} = \frac{2^m}{T_d} = \frac{f_c}{2} \quad (2.41)$$

where T_d is the transient time duration, f_c is the sampling frequency.

Then, the number of points is strictly associated with the adopted sampling frequencies; it is meaningless to choose a number of points corresponding to a frequency⁷ greater than the f_{max} achievable using a certain

⁴Sampling Theorem: if the Fourier transform of a continuous function $g(t)$ is zero for all frequencies greater than a certain frequency f_c , then $g(t)$ can be uniquely determined from the knowledge of its sampled values

⁵If the sample interval T is too large, the equidistant impulses of $\tilde{\delta}(f)$ (i.e. the Fourier transform of the sampling function $\delta(t)$) become more closely spaced, and their convolution with the frequency function of continuous signals $\tilde{g}(f)$ results in an overlapping waveform

⁶Normally 3-5 times f_c is used

⁷Beyond $f_c/2$ the sampling theorem doesn't hold, and we have no further information about these frequencies

fc. On the other hand, during the interpolation step, some information could be lost choosing a too low number of points. Last, it is worthwhile to remember that the increase of the number of points involves the growth of the array dimensions utilized by the program package set up for the full method application.

Besides, the interpolation introduces an additional effect on signals, i.e. each interpolation, using a linear method, adds a slope. It has been verified that this effect is negligible, because it causes the addition of some spurious frequencies in the original signal spectrum, having values greater than the typical frequencies of thermal hydraulic parameters. On the other hand, most thermal hydraulic quantities are characterized by low frequencies, then high frequency errors (therefore, these spurious contributions too) can be totally avoided considering proper filtering techniques.

Cut frequency To filter any spurious contribution, a cut frequency has been introduced. This cut frequency characterizes the frequency upper value which has to be considered in evaluating the AA and WF factors, as defined by (2.36) and (2.37).

Typical thermal hydraulic parameter trends (for different kinds of transients) have been analyzed Bovalini et al. [1992], aiming at defining an unique suitable value of cut frequency, in such a way to avoid partial loss of information.

A cut frequency value of 1 Hz is generally suitable to analyze trends of thermal hydraulics parameters; only flow rates and densities require cut frequency values up to 2 Hz, as a consequence of their higher frequencies, to avoid loss of information in accuracy evaluation.

Choice of the weights In order to give an overall picture of the accuracy of the addressed calculation, the FFT method accounts for the accuracy evaluated for each parameter, and defining some weighting factors $(w_f)_i$, global indexes of code performance are evaluated (see (2.38) and (2.44)). The need of $(w_f)_i$ definition derives from the fact that the addressed parameters are characterized among other things by different importance and reliability of measurement. Thus, each $(w_f)_i$ takes into account of:

"experimental accuracy": experimental measures of thermal hydraulic parameters are characterized by a more or less sensible uncertainty due to:

- intrinsic characteristics of the instrumentation
- assumptions formulated in getting the measurement
- unavoidable discrepancies existing between experimental measures and the code calculated ones (mean values evaluated in cross-sections, volume centers, or across junctions, etc.);

"safety relevance": particular importance is given to the accuracy quantification of calculations concerned with those parameters (e.g. clad temperature, from which PCT values are derived) which are relevant for safety and design.

Last, a further contribution is included in the weighting factors definition; this is a component aiming at accounting for the physical correlations governing most of the thermal hydraulic quantities. Taking as reference parameter the primary pressure (its measurement can be considered highly reliable), a normalization of the AA values calculated for other parameters with respect to the AA value calculated for the primary side pressure is carried out. In other words, the following factor has been defined (for the generic j-th parameter):

$$(W_{norm}) = \frac{AA_{pr}}{AA_j} \quad (2.42)$$

where $(AA)_{pr}$ is the average amplitude calculated for the primary side pressure $(AA)_j$ is the average amplitude calculated for the j-th parameter. So doing, the weighting factor for the generic j-th parameter, is defined as:

$$(w_f)_j = \frac{(W_{exp})_j \cdot (W_{saf})_j \cdot (W_{norm})_j}{\sum_{j=1}^{N_{var}} (W_{exp})_j \cdot (W_{saf})_j \cdot (W_{norm})_j} \quad (2.43)$$

$$\sum_{j=1}^{N_{var}} (w_f)_j = 1 \quad (2.44)$$

where N_{var} is the number of parameters to which the method is applied $(W_{exp})_j$ is the contribution related to the experimental accuracy $(W_{saf})_j$ is the contribution expressing the safety relevance of the parameter.

$(W_{exp})_j$ and $(W_{saf})_j$ values have to be assigned using engineering judgment, starting from measuring and safety related considerations. Such an evaluation of a suitable set of weights (see Tab. 1) to be utilized for typical thermalhydraulic quantities has been performed Bovalini et al. [1992]. Some criticism could be raised because engineering judgment is required in weights assignment, but actually, this appears the only practicable way to define the relative importance of the parameters selected to evaluate the accuracy of a code calculation. These weights must remain the same for any comparison between code results and experimental data concerning a same class of transient. Recently, an application of the FFT method to the quantification of the accuracy for containment system codes (based on ISP 35, NUPEC) has been carried out Leonardi et al. [1994]. For this application, different considerations were necessary in setting up a suitable set of weights, taking into account design features and safety concerns related to the containment. On the other hand, once chosen a set of weights with the above described criteria, any variation of some weight involves a homogeneous change of all the calculations analyzed, above all if a sufficiently high number of parameters has been selected for the accuracy evaluation. Obviously, this affects only global accuracy evaluation of a code calculation; no concern is related to the single parameters accuracy.

FFT package

In the first phase of the activities concerned with the definition of the method, some FORTRAN programs were written in order to perform in an independent way the basic steps of the method. This allowed to better focus the attention on the consistency of the obtained results, further adjusting and improving of the utilized algorithm, and obviously, the validation of each module. On the other hand, during this developmental phase, limited applications (in terms of number of code calculations and parameters analyzed) of the method were carried out, not making necessary the availability of an automatic tool.

Encouraging results achieved by various analysis, related to a wide application range of the FFT based method Leonardi et al. [1994], and the occurrence of the large application related to ISP 27 code calculations promoted something like an "assembling" of these programs. This activity was completed during the visiting period at the CEN-FAR, whenever it resulted in the complete development of new modules, allowing a complete use of the method and the execution of various kinds of analysis in a totally automatic way. In practice, an unique source program has been built, managing in the mean time experimental and several calculated data files for the extraction of the variables to be analyzed, application of the FFT method up to getting the evaluation of AA and WF quantities (see (2.36) and (2.37)). The results obtained for the single parameters are then processed by another small program in order to get global code accuracy (see (2.38)).

The program has a modular structure, consisting of a main program supervising the execution of the different tasks, performed by single subroutines, thus allowing the implementation of further modules without main changes in the program. In fact, being available such an automatic tool and from the experience gathered by previous applications, further options were included in the FFT package, increasing its versatility and applicability.

The source program has been coded in FORTRAN 77 standard. Up to date, it has been utilized on IBM 3090 (VM/CMS) mainframe and on CRAY (UNICOS) supercomputer; the advantage of such machines is associated with the huge amount of data to be processed for each analysis, especially in the case of many code calculations (normally many variables are included in a same data file).

Recently, considering the memory and computing speed performances of current personal computers, a version of the FFT package suitable for such microcomputers has been set up; moreover, running the program on a personal computer implies relatively (a little) slower performances, surely acceptable, taking into account that no data transfer is necessary and that all the results can be immediately processed by means of standard available software. This version has been built compiling the source program utilizing the Microsoft FORTRAN Compiler 5.1. Furthermore, obviously, this allowed a significant reduction of the fees related to the program running, being also optional the use of a workstation to perform these analysis.

As above mentioned, some new features have been introduced in the program, increasing its flexibility and applicability. The program capabilities can be summarized as follows:

- research and extraction of the addressed variable from data files, allowing various data format (ISP 27, X-Y blocks, X-Y generic from digitizer devices, see App. B);
- conversion of current data units in SI units, or more generally possibility of manipulate data (optional);
- analysis of several time windows in a same execution, where each time window can identify whatever phase in the transient;

- time shifting of data trends to analyze separately the effects of delayed or anticipated code predictions concerning some particular phenomena or systems interventions (optional);
- interpolation of data points to a power of 2 number of points, coherent with sampling frequency and minimum analysis frequency
- FFT evaluation of the signals to be processed;
- evaluation of the AA and WF quantities (see (2.36) and (2.37));
- output files generation, including information to be processed by standard software in order to trace any desired graphic concerning data curves, error curves, interpolated curves, FFT signals transforms, FFT data spectra, AA-WF data (optional).

After the application of the method to the selected variables, global code accuracy for the analyzed code calculations is carried out by a second program, also running in Windows environment, automatically determining AAtot and WFtot values in all the previously considered time windows. Obviously, this last step must be performed after the analysis of all the variables, then it is not automatically executed after the FFT analysis. Nevertheless, it is easy to build a shell of commands automatically launching the program for the selected variables and finally calculating the global values.

Applications of the FFTBM can be found e.g. in [Muellner et al., 2005b].

Parameter	Exp	Wsaf	Wnorm
Primary pressure	1.0	1.0	1.0
Secondary pressure	1.0	0.6	1.1
Pressure drops	0.7	0.7	0.5
Mass inventories	0.8	0.9	0.9
Flow rates	0.5	0.8	0.5
Fluid temperatures	0.8	0.8	2.4
Clad temperatures	0.9	1.0	1.2
Collapsed levels	0.8	0.9	0.6
Core power	0.8	0.8	0.5

Table 2.14: Selected weighting factor components for typical thermal hydraulic parameters

Chapter 3

VVER-1000 NPP calculations

This chapter describes the behavior of a VVER 1000 following a SBLOCA, a SBO or a PRISE transient. Each of the calculations corresponds to a PSB-VVER test - more precisely they should be called VVER 1000 NPP calculation corresponding to test one, two, etc. Correspondance between test and calculation means that the initial and boundary conditions adopted at the facility are also assumed for the NPP calculation (in the right scale).

Generally for each of the tests multiple failures of safety systems are assumed (Table 3.28 shows an overview of the assumed boundary- and initial conditions for each of the calculations, which are the also the BIC for the PSB experiments). Figure 3.1 shows a graphical representation on the different classes of experiments and their connection. Test 3, PORV stuck open, is categorized in the Figure as SB-LOCA, because the stuck open pressurizer relief valve constitutes a small break, and also as characterization test because this accident happened at the NPP Zaporoshye, and therefore gave the possibility to compare the experimental and calculated data with the data from the plant (different set of plant data are available, which show differences between each other - so just the qualitative behavior was recognized as reliable). The qualitative comparison was satisfactory.

In general all boundary- and initial conditions assume an initiating event, multiple failure of safety systems, and an AM-Strategy. Goal of the calculations is to affirm the effectiveness of the adopted AM-Strategy - which means, that the reactor can be lead to a long term coolable configuration.

Two cases are different: test three (and NPP calculation three) models an actual accident that took place at Zaporoshye NPP - the PORV was tested during hot shut-down conditions, and failed to close. Test ten (and NPP calculation ten) aims to characterize the natural circulation behavior of the VVER 1000. Boundary conditions for natural circulation regime are imposed initially. Then the primary side mass is drained in steps, until dryout in the core is detected. Following dryout, the primary side is refilled in steps.

The sections of this chapter describe the connection of NPP calculations and PSB experiments, the nodalisation that has been adopted for the VVER calculations, and then the results of the calculations grouped by initiating events.

3.1 Connection to PSB

This section describes how the NPP calculations are tied to the PSB-VVER experiments.

The NPP calculations presented in this work have been utilized as last step in a chain of calculations and experiments in the EC funded project "Accident Management in VVER 1000", see D'Auria et al. [2006]. Among the goals of the project was to a) verify that the TH-SYS codes Relap5 and Cathare2 are suitable for simulation of accident management strategies in VVER1000, and b) test the effectiveness of the strategies (keeping in mind that the experimental facility PSB will not show the same response as the plant, although well scaled).

The steps that have been performed in the project are:

1. Drawing up of the preliminary PSB-Test matrix
2. Confirmation of the relevance of the planned tests for accident management by pre-test plant calculations with Relap5 and Cathare2

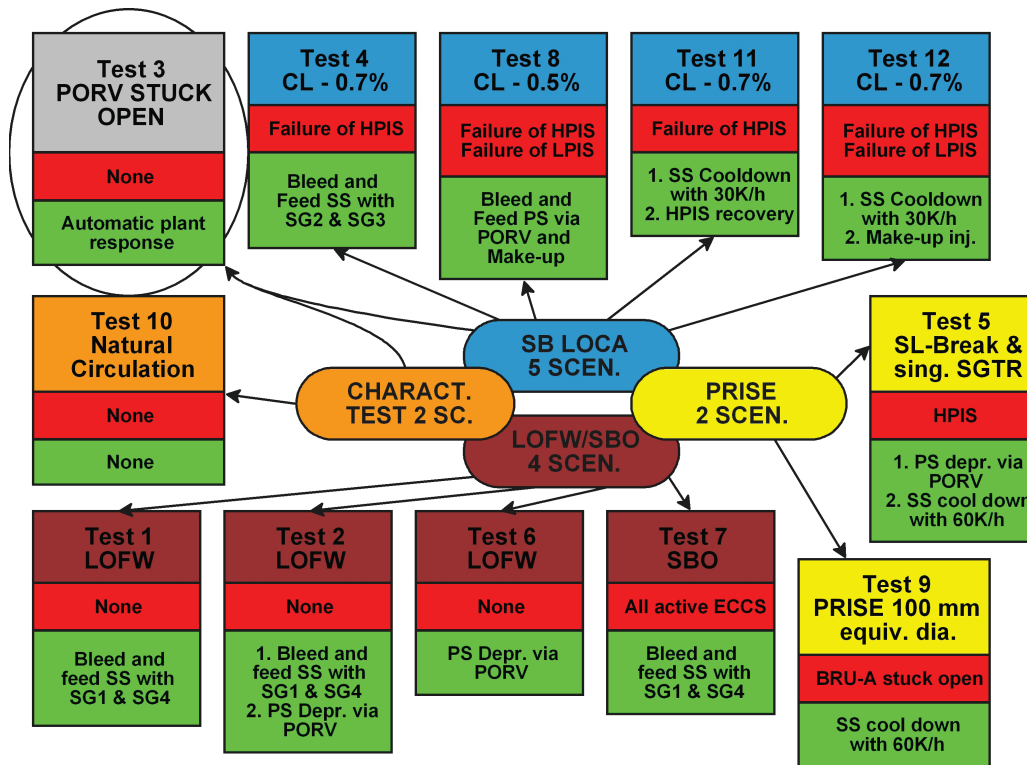


Figure 3.1: PSB test matrix and VVER calculations. Red - additional assumed failures, green - AM strategy.

3. Confirmation of the relevance of the planned tests for code validation (challenging to the codes) by preliminary pre-test facility calculations
4. Drawing up of the final PSB-Test matrix
5. Execution of final pre-test facility calculations with Relap5 and Cathare2
6. Execution of the experiments at the PSB facility
7. Execution of post-test facility calculations with Relap5 and Cathare2
8. Execution of post-test NPP calculation with Relap5 and Cathare2

The main focus of the present work are the calculations of step eight of the project, i.e. they reflect the lessons learned from code-experiment comparisons. Nevertheless, four examples for post-test analyses are presented here. The author performed in total 5 post-test analysis with Relap5, and two with Cathare2 in the frame of the project out of the 12 experiments plus 3 single variant tests. The Cathare2 calculation are not presented here, because Cathare2 is outside the scope of the present work. One Relap5 calculation is also not presented, because errors in the analysis, that have been discovered after the performed work, cast doubts on the results. For more information, please refer to the final project report D'Auria et al. [2006].

3.1.1 Description of the PSB-VVER nodalisation

The Relap5 input deck adopted for simulating the PSB-VVER facility behaviour is a detailed nodalization carried out with a "sliced" approach. This nodalization scheme is suitable for a better code response, especially in natural circulation and/or during low flow rate regimes. The data used in order to realize the nodalization are taken from [Melikhov et al., 2003a], [Elkin, 2003], [Melikhov, 2003], [Melikhov et al., 2003b], [Melikhov et al., 2003c], [Melikhov et al., 2003d]. The general noding scheme can be seen in Figure 3.2, the PRZ nodalization is shown in Figure 3.3.

All four loops are modeled separately; each loop includes a hot leg, a steam generator, a pump, a loop seal and a cold leg. The pressurizer is connected to the hot leg of loop No.4 via the surge line; the relief

valve (PORV) is modeled on top of the PRZ and at the bottom PRZ heaters are simulated. The RPV flow paths have been modeled separately, as they are in the facility, by three pipes: one for the down-comer, one for the core region, and one for the core bypass. The lower part of the downcomer is duplicated to simulate as well as possible the inner and the outer part of the element. To avoid stagnation flow in the upper part of the downcomer and of the upper plenum, small volumes are added in parallel of the main parts. The active core is represented by a single active structure with uniform power distribution subdivided in ten parts. The heated zone of the core bypass is simulated by imposed heat flux. The Emergency Core Cooling System is simulated by time dependent volumes and time dependent junctions. The four SIT are simulated by four accumulator components and are connected in pairs to the down-comer and to the upper plenum via their discharge line. In this line the orifice, installed in the facility to regulate the amount of water delivered to the RPV, is simulated. To take into account the heat losses in the facility, a Heat Transfer Coefficient based on EREC data [Elkin, 2003] has been inserted in the Relap5 nodalization using a general table (HTC vs. Temperature). The external temperature has been assumed to be 25 °C constant.

The SG primary side is schematized with 17 horizontal tubes that simulate the 34 tubes of the facility (these data are referred to a single SG). The SG secondary side has four different zones that are identified and simulated by four vertical pipes, representing the down-comer, the hot and cold collector and the tube region. The four pipes are connected to each other by cross flow junctions, to permit horizontal flow through the four regions. The feed water in the facility has one injection point, represented by a time dependent volume and a time dependent junction; the time dependent junction ensures the prescribed mass flow rate. All the FW passes through a branch that has flow area equal to the area of all the holes and simulates the ring distributor. A branch and a pipe represent the free space over the feed water ring and are connected to the so-called “small steam line”. In the upper part of each SG; a motor valve represents the BRU-A valve and in each steam line the main steam isolation valve is simulated by a trip valve. The four steam lines of the four SG are connected to the common steam header, that finally discharges to another time dependent volume, which stands for the steam condenser. An other trip valve placed at the end of the common steam header simulates the turbine stop valve.

Comment on code models The primary and secondary system of the facility has been mainly modeled with Relap5 pipe and branch components. The pump component has been used for main coolant pumps, ECCS flow rate is an imposed boundary condition (depending on the pressure). For the accumulators, the Relap5 accumulator component has been used. The pressurizer component has not been used. Pressurizer relief and safety valves have been modeled using the Relap5 motorvalve component.

Structures have been modeled using the Relap5 heat structure component.

The general policy for user dependend modeling choices has been to use default values, wherever possible. This means for volumes that

- the thermal front tracking model is disabled;
- the mixture level model (as mentioned in section 2.4.1) is disabled;
- the water packing scheme is used for the model (to soften unphysical pressure spikes, which may be caused by the numerics when the water-steam interphase passes a control volume boundary);
- the vertical stratification model is used (also dependent on parameters of the flow like void fraction and flow velocity, see section 2.4.1.;
- the pipe interface friction model will be used (other possibility the bundle interface friction model will be used);
- wall friction effects are to be calculated;
- the nonequilibrium model and not the equilibrium model is used.

For junctions, this means that

- the jet junction model is disabled;
- the CCFL model, as described in section 2.4.1, will not be applied;
- the horizontal stratification entrainment/pullthrough model, as described in section 2.4.1, will not be applied;

- the choked flow model will be applied (general policy is to use Henry-Fauske choked flow model);¹
- abrupt area change model is switched off by default, which means that energy loss coefficients as supplied in the input are used by the code;
- homogenous or non-homogeneous model (different velocities for liquid and steam), where the default is non-homogeneous;
- possibility to specify weather momentum flux between volumes should be calculated, default is yes.

The following exceptions from the general rule have been made and the following modelling decisions should be mentioned separately:

Momentum flux in hot- and cold collector To model the abrupt change in flow direction when the fluid passes from hot- or cold collector to the U-tubes, momentum flux in hot- and cold collector is not considered in the calculation (the option is set to 2, which means momentum flux is considered in the “to” volume, but not in the “from” volume, in the junctions which are connecting the SG hot- and cold header volumes with the SG U-tubes.

Horizontal stratified flow model disabled in SG U-tube coils The U-tube-coil of the PSB-VVER facility, which should model the SG U-tubes of the VVER 1000, has an elevation change of roughly 30 cm. In total, 36 coils are installed, and two coils are represented by one Relap5 pipe component (which has an elevation change). To avoid that Relap5 is calculating vertically stratified flow in this component (which would not represent the actual situation) the vertically stratified flow models have been switched off.

Calculation of critical heat flux Relap5 offers several possibilities to calculate the critical heat flux. The Groenveld lookup-table based method has been chosen.

Reflood model Relap5 models heat transfer in heat structures one dimensional. This might be adequate in most cases, but gives too conservative results for fuel and cladding temperatures in case of dryout and reflood. The user has therefore the possibility to activate in selected structures the “reflood model”, which re-meshes the heat structure (refines the mesh) and considers two dimensional heat transfer (radially and axially). The downside is that the model has been developed and qualified for a narrow range of parameters only (pressure less than 1 MPa and mass fluxes less than 200 kg/(s m²)). The use of the reflood model for the core simulator has been set to “automatic”, which means that it is used for pressures less than 1.2 MPa and void fractions of more than 0.9. In the calculations presented in this work these conditions have never been met.

Heat losses of the pump The modeling of the heat losses of the facility do not really constitute a choice on the code models, but are important for the simulation and therefore mentioned at this place. One important contribution to the facility heat losses comes from the heat losses along the loops, which are simulated by supplying a Table of heat transfer coefficients vs temperature as input (on the boundary to the environment of outer simulated heat structures of the facility). The second important contribution comes from the heat losses of the main circulation pumps. The pumps of the facility must be cooled, have two cooling circuits (one driven by forced circulation, another one by natural circulation). The heat losses by the pumps depend on one hand on the flow regime in the main coolant loops, on the other hand on the operation of the cooling system of the pumps. In practice, the heat losses of the pumps have been supplied together with the experimental results (mass flow through the cooling system, inlet and outlet temperature), and have been applied as boundary conditions in the Relap5 calculation. Heat losses range from 2 kW to 18 kW per pump (which is large compared to the core power).

Further options and code results will be discussed at the appropriate place.

¹See section 2.4.1). Henry Fauske is the default model in Relap5 mod 3.3. Relap5 mod 3.2 was using Ransom Trapp critical flow model, in this case the critical flow model in all junctions could be changed to Henry Fauske by activating a switch in card one. Henry Fauske requires a discharge coefficient and a thermal equilibrium coefficient. Those two numbers should be determined by experiments for a given break geometry. Since separate effect tests on the break geometry used for this work were absent, the default values (1.0 for the discharge coefficient, and 0.14 for the thermal equilibrium coefficient).

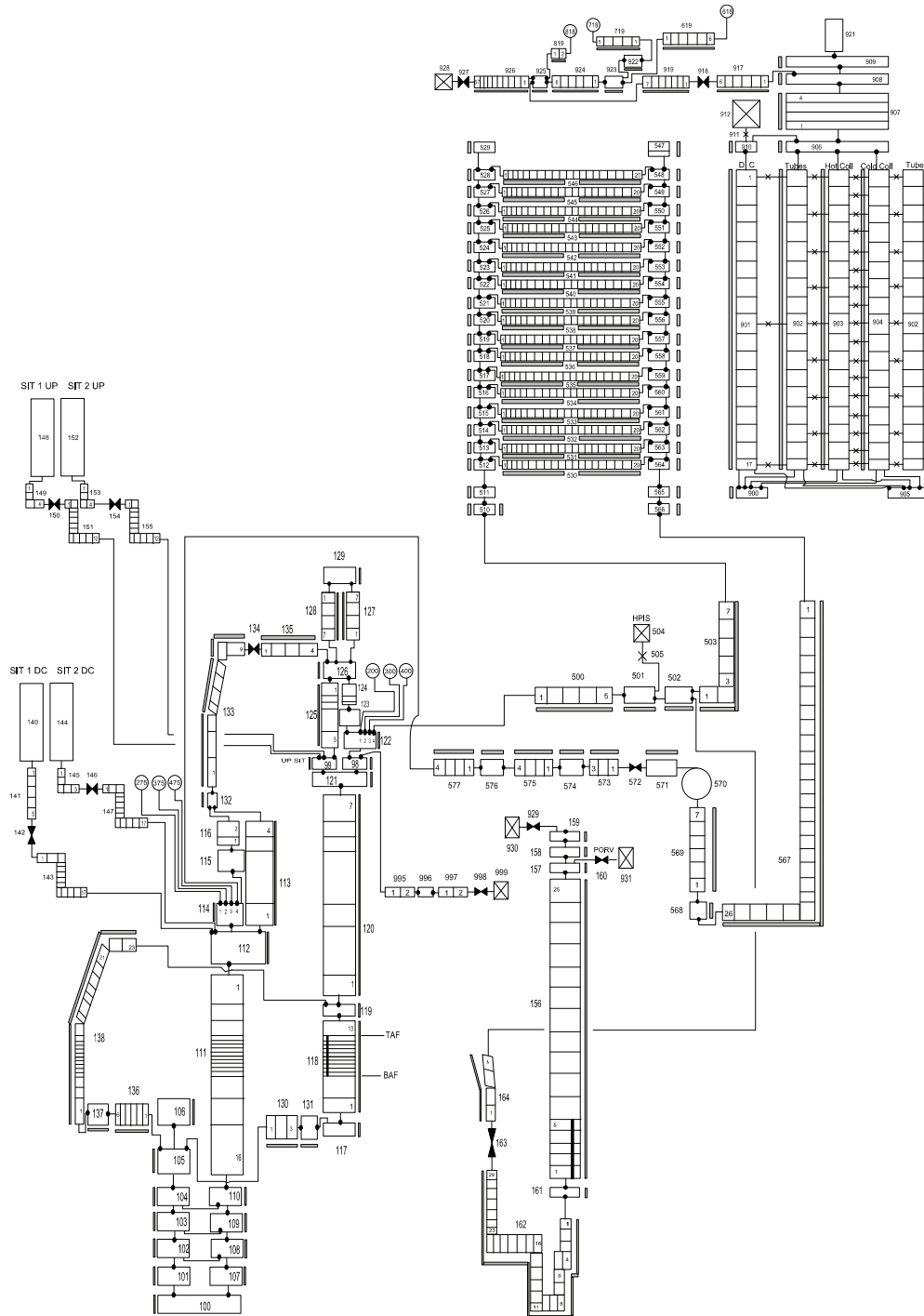


Figure 3.2: Relap5 nodalization of the PSB-VVER facility, general scheme

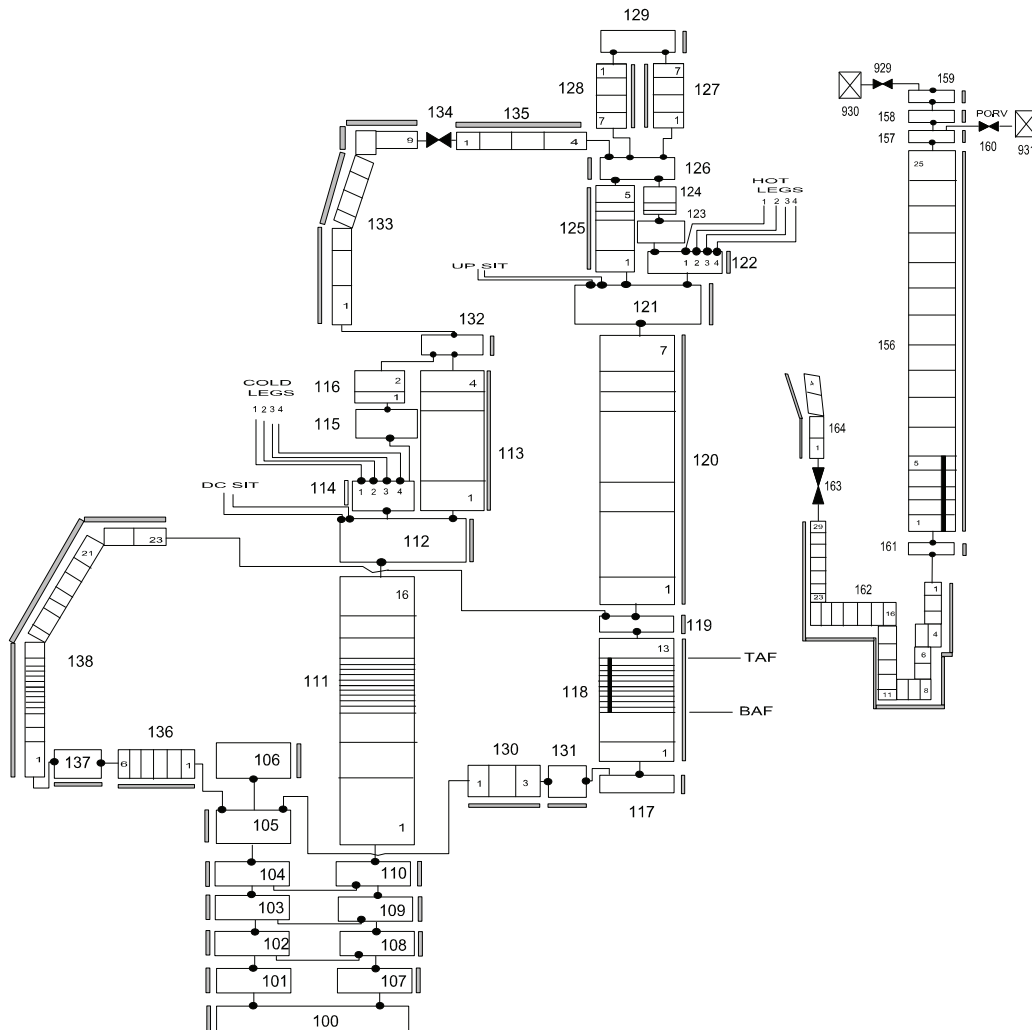


Figure 3.3: Relap5 nodalization scheme of the PSB-VVER - RPV

3.1.2 Post test analysis 12 - 0.7% CL break

The test 12 specifications and scenario can be found in detail in Andrioutschenko [2004] and Elkin et al. [2004]. Initial event is a break of the cold leg (break size 0.7% of CL). All HPIS are assumed to fail. As accident management measure the operator initiates cooldown of the primary side via secondary with a cooldown rate of 30K/h, and after the cladding temperature reaches more than 300°C, but not earlier than 1800s into the transient, the operator uses makeup and HHPIS TQ(123)4 to supply coolant to the primary side.

The experiment aims to achieve the following objectives:

- obtaining experimental data for validation of thermal-hydraulic system codes which are used for VVER NPP safety analyses;
- providing support for the verification of the accident management strategies in Balakovo Unit 3 NPP;
- identification and/or verification of the thermal-hydraulic phenomena included in validation matrix for SB-LOCA; Liesh and Reocreux [1995]

Configuration of the PSB-VVER facility

Please refer to table 3.1 for the configuration of the facility. A more detailed description on the configuration of the facility and the initial and boundary conditions can be found in Elkin et al. [2004] and Elkin [2004b].

Equipment	Connection status
Pressurizer	Connected to loop #2
Core by-pass	2 diaphragms with 2 orifices of diameter 7 mm are installed at inlet and outlet of core by-pass
ECCS hydroaccumulators	ACC #1 and #3 are connected to the outlet plenum, ACC #2 and #4 are connected to the inlet chamber
Make-up system of primary side and system TQ14	Both systems are modeled by one make-up system of a primary side.
Work of a make-up system is not modeled in a steady state	The system is connected to cold leg of all loops on an output from steam generators
Steam generators	Under steady state all SGs are connected to each other by steam header. The pressure is adjusted by one steam dumping valve RA06S01
Feed water heater	On. SG level under steady-state conditions is maintained by supply of feed water with a temperature of ≈ 218 °C
ADS simulation system	ADS are connected to each SG. In each ADS line, throttle channel - diameter 12.1 mm and L=50 mm is installed. Actuation set points are 7.16/6.28 MPa
Leak simulation system	Break is located in the cold leg in loop #4 between MCP and DC entrance and oriented upward. Leak channel: $\varnothing 4$ mm, L = 40 mm.
Simulation system of primary side cooldown by mean of ADS	For simulation of primary side cooldown by means of ADS with a rate 30°C/h a throttle with a diameter 2 mm and a length 20 mm is installed in the common ADS line.
UP warming-up line	Under steady state the line is open. The warming-up of the UP top part is stopped about 2 min before opening break line.
Warming-up line of break line	Under steady state the line is open. The warming-up of the break line is stopped about 1 min before opening break line.

Table 3.1: Test facility configuration, taken from Elkin et al. [2004]

Description of the experiment

Please refer to table 3.2 for an overview of the imposed events. A more detailed description of the initial and boundary conditions, as well as the experimental results can be found in Elkin et al. [2004] and Elkin [2004b]. The following description of the experiment is taken mainly from Elkin et al. [2004].

The transient as a whole may be divided into four main stages:

Ph1 blow down of sub-cooled coolant (0-300 s);

Ph2 primary side pressure stabilization at the secondary circuit rate and the first initial heating of the core model (300-717 s);

Ph3 decreasing the primary coolant mass under saturated coolant discharge and second core heat up (717-2914 s);

Ph4 primary side refilling after the primary side make up system actuation and primary side cooldown under the alternation of saturated and subcooled coolant discharge (2914-10014 s).

Phase 1 The Experiment was started by opening the break valve. A sharp decrease in PS pressure was observed. The PRZ level started to decrease. At 45 s PRZ level was lower than 2.32 m (according to the transducer YP01L02) and the PRZ heaters were turned off.

At 41 s the primary side pressure was lower than 13.7 MPa and the scram was simulated. Ten seconds after the scram the turbine shut valve simulator was closed, and the feed water temperature was changed from 220 °C to 150 °C. After the start of the turbine stop valve simulator closure the pressure in the secondary side increased. The SGs pressure increase stopped at 130 s, and the set values for the BRU-A valves simulation were not reached.

At 52 s the saturation margin became less than 10 °C. With a delay of 15s the coast-down of the MCPs started and continued up to 299 s.

After the coolant reached the saturation point and began to boil the stage of phase separation in the primary side started. At 111s a level was formed in UP, at 124s the levels started forming in hot legs and SG collectors.

Phase 2 At 300s the primary side pressure decreased to the secondary side pressure. The primary circuit pressure decrease stopped at this point. Between 300s and 717s the primary side pressure stabilized at the secondary side pressure level. At 561s the SGs hot collector voided (cold collectors voided by 370s), which led to the break down of the natural circulation in the primary side. Following hot collectors the hot legs of all four loops voided completely at 582s and a rapid decrease of the UP level could be seen a second time. At 700s the level decreased to the upper part of the core and at 710 s the cladding heat-up in the upper plenum of the test facility began.

Phase 3 At 729s the core simulator heat-up stopped due to the loop seals clearance in loop-2 and partially in loop-1. The loop seal of the loop-2 was cleared completely at 777s. From 729s the break flow changed from liquid to two phase. This can be seen from the pressure change in the primary side. From this moment on energy was no longer removed by the secondary side - at 731s the primary side pressure dropped beneath the secondary side pressure and the heat transfer was reversed (SS supplied heat to the PS). At 755s the DC level decreased to the cold legs and continued decreasing slowly up to 900s. Thus from 760s on saturated coolant was flowing out of the leakage. At 1187s the primary circuit pressure decreased to 5.9 MPa and starting at 1193s the water from ECCS accumulators was fed to the primary circuit. Between 990s and 2742s the coolant mass decreased in DC and UP. The level was constant in the core model and in the circulating loops until 2742 s.

At 1800 s the simulation of the operator action “cool down of the PS via SS with a cool down rate of 30K/h” was simulated by opening the isolation valve of the new installed cool down system. The complete opening of isolation valve was at 1811s. The primary and secondary side was not affected by this measure. At 1928 s primary side make-up system actuated spuriously for 43 s and water from this system was entered in the primary side.

Phase 4 The upper plenum was completely voided at 2741s. Immediately after the core level began to drop. At 2816s the upper part of the fuel rod simulator uncovered and a second heat up began. At 2914s the set point for the second operator action was reached (the cladding temperature reached 302 °C), and the make up and TQ(1,2,3)4 system was taken into operation. The make-up system cold water supply into the primary side led to acceleration of the primary pressure decrease rate and resulted in water flow rate increase from ACCs. The total water flow rate coming from the passive ECCS and make-up system exceeded the coolant flow rate discharged from the leakage and therefore at 2922s the refilling of the downcomer and core regions began. At 3456s it reached the cold legs.

Between 3456s and 10014s there was a slow pressure and primary side temperature decrease. The coolant flow rate discharged from the break was comparable to the coolant flow rate coming from ACCs and make up system which led to the level stabilization in the reactor model and circulating loops. This state was kept until 10014s.

EVENT	pre-set	actual
Leak opening	0 s	0 s
SCRAM signal	UP pressure < 13.7 MPa + 1 s	UP pressure < 13.7 MPa + 1.4 s
PRZ heaters switched off	PRZ level = 4.21 m	PRZ level = 4.18 m
Turbine valve simulation closure begins	UP pressure < 13.7 MPa + 11 s	UP pressure < 13.7 MPa + 11 s
SG SS isolated - Turbine valve simulation closure ends		69.6 s
Transition to the AFW	UP pressure < 13.7 MPa + 10 s	UP pressure < 13.7 MPa + 15 s
MCP coast-down on-set	Difference between saturation temperature (UP pressure) and HL temperature < 10°C + 15 s	Difference between saturation temperature (UP pressure) and HL temperature < 10 °C + 15.1 s
Start of ACC 1 operation	UP pressure < 5.9 MPa	UP pressure < 5.9 MPa + 11 s
Start of ACC 2 operation	UP pressure < 5.9 MPa	UP pressure < 5.9 MPa + 6 s
Start of ACC 3 operation	UP pressure < 5.9 MPa	UP pressure < 5.9 MPa + 13 s
Start of ACC 4 operation	UP pressure < 5.9 MPa	UP pressure < 5.9 MPa + 8 s
Primary side cool-down procedure	1800 s	1801 s
Make up systems injection start	Core cladding temperature = 300°C and $\tau > 1800$ s	Core cladding temperature = 302°C and =2914 s

Table 3.2: Imposed sequence of main events for PSB Test 12, CL-0.7-11, taken from Elkin et al. [2004]

Calculation - Primary Pressure

The primary pressure generally is well predicted. A comparison between the experimental and calculated pressure trend can be found in Figure 3.4

First phase, 0 s-300 s: in the first phase the calculated results stay within a band of 5% of the experimental data. In the

second phase (300 s - 717 s), the pressure seems to be slightly overpredicted by the calculation. In both, the calculation and the experiment the primary side pressure rests on the secondary side pressure. While the difference between primary and secondary side is about 1 bar in the experiment, the calculation predicts about 2 bars. In addition, the secondary side pressure is overpredicted by about one bar. So this sums up to a difference in primary pressure of about 3 bar for the second phase. The

third phase 717 s - 2914 s shows a difference in the time, when the break flow changes from liquid to two phase flow. In the experiment, this happens at 727 s, while the calculation predicts 840 s. From this time on, the depressurization rate changes - the primary pressure drops again. Since this happens about 100 s earlier in the experiment than in the calculation, the calculated trend is shifted, compared to the experimental one. From 800 s up to about 2000 s the primary pressure shows some steps, or oscillations. The reason for this steps is the use of the Relap5 reflood model outside its recommended pressure boundaries ISL [2006a] in combination with water injection in the core from the loop seals or the accumulators. The second AM measure (injection with make-up and TQ(123)4) is calculated to start at 2020s, while in fact it started at about 2920 s. This also gives rise to some distortions in the PS pressure during the third phase. In the

fourth phase (2914 s - 10014 s) calculated and experimental pressure trends converge, but for different reason. while in the experiment the reduction in pressure is governed by the fact that the cold water from the make-up systems cools the primary fluid, in the calculation the secondary pressure decrease reaches the primary pressure, and from there on the secondary side reduces the primary side pressure.

Calculation - Secondary Pressure

The secondary side pressure generally is rather well predicted up to the point when the cool down system is opened (to simulate the 30K/h primary via secondary side cool down). Although a number of attempts had been made, it was not possible to reproduce the secondary side pressure accurately after 1800s. The secondary side pressure trend, both the calculated and the experimental, is reported in Figure 3.5.

The first phase 0 s - 300 s is very well predicted (the calculated trend lies within a band of $\pm 2\%$ of the experimental results. In the

second phase, 300 s - 717 s calculated secondary side pressure stays with about one bar difference on top of the experimental results. Taking into account that the absolute value of the SS pressure at this phase is about 70 bars, one can say that the result is rather accurate. In the

third phase, 717 s - 2914 s the experimental curve shows a continuous descent with a small jump at 1800 s of about 0.5 bars, when the new installed cool down system is taken into operation. The Relap5 calculation predicts a slower depressurisation rate from 727 s to 1800 s, a faster depressurization rate later on, so that overall the calculated secondary side pressure trend stays reasonably close to the experimental results. The calculated results of the

fourth phase 2914 s - 10014 s continue to predict a faster depressurization rate up to about 6000 s, than the experimental curve catches up. At the end of the experiment the calculated results are about 5 bars below the experimental ones.

Calculation - Temperatures

The fluid temperatures are reasonably well predicted, refer to Figures 3.6 and 3.7. The comparison between calculated results and experimental ones for the cladding temperatures shows good agreement for the bottom (Figure 3.12) and middle level (Figure 3.11) of the core (because the temperature at these levels actually follows the fluid temperature). The upper level of the core, which two times is in dry-out conditions in this experiment, shows a difference (Figure 3.10): the first dry-out in the experiment starts at about 710 s and is quenched by the loop seal clearing. The calculation predicts a dry-out and loop seal clearing at about 810 s, so reasonably close. The second dry out however, is predicted for 2040 s, while the experiment shows the second dryout at 2810 s. Two reasons could be identified:

- this calculation doesn't consider the spurious injection of the make-up system, at about 1800 s for about one minute.
- the heat losses for the pumps in this calculation are set, after their coast down, to 6 kW each. This value might not be accurate.

Calculation - Break mass flow rate and primary side mass

The experimental and calculated mass flow through the break show an excellent agreement (Figure 3.9). Nevertheless, the total primary side mass shows some disagreement after the subcooled blow down phase (Figure 3.8). The experimental loss of primary side mass seems to be smaller than the calculated one, and this despite the fact that the calculated results for the break flow as well as the accumulator levels are in good agreement with the experimental data. The faster decrease of primary side mass could be one reason why the code predicts the second dryout earlier than it is seen in the experiment. It should also be mentioned that the experimental value has about $\pm 30\%$ error for this quantity.

Calculation - Pressure drops

All pressure drops between different points of the primary circuit are compared in figures. All of the comparisons, with different extent, suffer of the limitation connected to the fact that the pressure taps are not coincident with the center of the volumes of the nodalization. Pressure drops in the loops are reasonably well predicted by the code: notwithstanding the code predicts the occurrence of loop seal clearing in one loop, as in the experiment, this loop is not the correct one. This confirms the difficulty, already emphasized in previous analyses, see D'Auria et al. [1999] and D'Auria et al. [2003], in correctly predicting a critical phenomenon like loop seal clearing. The distribution of pressure drops in the initial steady state, both direct and reverse (in this last case calculated data can not be qualified), are responsible for the misprediction of loop seal clearing phenomena. This is a well known limitation, resulting from several code applications to SBLOCA analyses, that does not affect the code capability in predicting the overall transient scenario D'Auria et al. [1999] and D'Auria et al. [2003].

Possible improvements

After an extensive analysis it was possible to pin-point three key-issues. By changing the primary side heat-losses, simulating the spurious injection of feed water and removing the option "reflood" a number of aspects could be caught more precisely.

- Reflood option and related trips removed
- Heat losses of the pumps increased from 6kW to 15kW each after coast-down (18kW each before).
- Spurious activation of make-up for 43 s after 1928 s

Primary Pressure

Please compare the to figures, Figure 3.4 and Figure 3.15. While in the "base" calculation (Figure 3.4) the primary pressure shows almost a step like behavior from 700 s-2100 s, the "improved" calculation (Figure 3.15) shows a smooth decrease in the PS pressure, like in the experiment - only shifted, because the uncovering of the break and the connected decrease in pressure occurs about 100 s later in the calculation. In the long term the prediction for the primary side pressure is worse than in the base calculation. This fact must be

attributed to the heat losses of the pumps. To increase the heat losses after coast down was a decision based on experience when participating at experiments at EREC. For the initial phase of the experiment it is a valid assumption. For the later phase, obviously, 15kW overestimate the real heat losses, and so the primary side calculated pressure for the “improved” calculation drops below the experimental one, while the “base” calculation prediction is rather accurate. This discussion emphasizes the importance of the heat losses of the pumps. The heat losses of the pumps cannot be derived, because they depend on the way how the cooling systems of the pumps are operated. They must be a boundary condition, and precise knowledge of this quantity could help to improve the analysis.

Secondary Pressure

The secondary side pressure prediction for the first 1800 s is very accurate (Please compare the “improved” calculation, Figure 3.16 with the “base” calculation, Figure 3.5). The increased heat losses for the pumps are responsible for this result (as was verified in a independent sensitivity analysis, were only one parameter was modified). The “base” as well as the “improved” calculation fail to predict accurately the behavior of SG-pressure once the 30K/h cool down system is actuated. Several attempts were made to improve the results, including a sensitivity analysis on the break diameter, a sensitivity analysis on the loss coefficients of the break line, a sensitivity analysis on the secondary side heat losses, but without any real improvement.

Temperatures

The temperature trends of the cladding temperature are now without oscillations beginning from 700 s up to 2000 s, please compare e.g. the cladding temperature at the bottom of the heater rod bundle, Figure 3.12 for the base calculation and Figure 3.19 for the improved one. A sensitivity study could show that the Relap5 “reflood” option is responsible for the oscillations.

The second interesting observation can be seen at the top level clad temperatures, Figure 3.10 (the base calculation) and 3.18 (the improved calculation). The first dry out is smaller, which is well in the uncertainty connected with calculations of that kind, but still occurs at the same time, about 800 s into the transient. The second dry out now occurs about 300 s later. Separate sensitivity analyses (changing only one parameter at the time) demonstrated that about 100 s can be attributed to the spurious feed water injection, 200 s can be attributed to the increased heat losses of the pumps.

With now a difference of 500 s between calculation and experiment the calculation shows an accuracy which can be expected for phenomena hard to predict like small dry-outs.

Qualitative accuracy

The qualitative accuracy evaluation here discussed is based upon a systematic procedure consisting in the identification of phenomena (CSNI list) and of RTA. It essentially derives from a visual observation of the experimental and predicted trends.

The related results are reported in Table 3.4, Table 3.5 and Table 3.6, where the information are related to the reference calculations performed using Relap5 codes.

A positive overall qualitative judgment is achieved if ‘U’ is not present; in addition, the parameters characterizing the RTA (i.e., SVP = Single Valued Parameter, TSE = parameter belonging to the Time Sequence of Events, IPA= Integral Parameter and NDP = Non Dimensional Parameter) give an idea of the amount of the discrepancy.

In the present case the following conclusions can be reached:

1. no ‘U’ mark is present;
2. all RTA of the experiment are present in the calculated data
3. the accuracy evaluation by adopting RTA and Key Phenomena, supports the conclusion that the calculation is qualitatively correct.

Quantitative accuracy

The positive conclusion of the qualitative accuracy evaluation, makes it possible addressing the quantitative accuracy evaluation. To this aim a special methodology, developed at University of Pisa, has been adopted. The methodology is based upon the use of the Fast Fourier Transform (see Bovalini et al. [1992] and D’Auria

et al. [1996]). The results of the application of the method are given in 3.7, where again the information are related to Relap5 reference calculation. The conclusions from the quantitative accuracy evaluation analysis are as follows:

1. the achieved results are well below the acceptability threshold, particularly in relation to the overall accuracy (AA = 0.23 compared with the acceptability limit of 0.4), while the primary system pressure accuracy is just in the limit (AA = 0.10 compared with the acceptability limit of 0.1);
2. the achieved results appear comparable in both code calculations. Definitely, the documented reference calculation is acceptable from the code assessment point of view; i.e. the code is positively assessed in relation to its capabilities to predict this kind of transient.

EVENT	EXP (s)	R5 base (s)	
			R5 improved
Leakage opening	0	0	0
YC01P17=13.7 MPa	42.2	37	37
Start closing of steam discharge valve RA06S01	53	47	47
Start of MCPs coast-down (YD01-04R11)	68.5	60	60
Stopping of SGs steam discharge (full closing of RA06S01 valve)	70.6	67	67
Complete switching off of MCP	299	300	300
Start of the first bundle heat up	710	780	800
Pressure in the primary side is lower than in the secondary one:	731	850	830
Pressure in the primary side 5.9 MPa	1187	1160	1360
Coolant reached saturation at the core inlet	1283	1000	1200
Start of cooldown procedure (opening of RA15S01)	1801	1800	1800
Start of the second bundle heat up	2816	1950	2280
Start of operation of primary side make-up system	2914	1960	2300
Stop of experiment/calculation	10014	10000	10000

Table 3.3: Comparison experiment/ Relap5 calculation test 12, base and improved

Phenomena	Psb Facility		
		Experiment CL-0.7-12	Relap5
Natural circulation in one-phase flow	o	+	R
Natural circulation in two-phase flow	o	+	R
Reflux condenser mode and CCFL	-	-	-
Asymmetric loop behavior	o	+	R
Leak flow	o	o	E
Phase separation without mixture level formation	+	-	-
Mixture level and entrainment in SG secondary side	+	+	R
Mixture level and entrainment in the core	+	+	R
Stratification in horizontal pipes	-	-	-
Emergency core cooling mixing and condensation	-	-	-
Loop seal clearing	o	o	R
Pool formation in upper plenum - CCFL	o	o	R
Core wide void and flow distribution	+	+	R
Heat transfer in covered core	o	o	E
Heat transfer in partially uncovered core	o	o	R
Heat transfer in SG primary side	-	-	-
Heat transfer in SG secondary side	-	-	-
Pressurizer thermal hydraulics	o	o	E
Surge line hydraulics (CCFL choking)	o	-	-
One and two phase pump behavior	-	-	-
Structural heat and heat losses	+	+	R
Non condensable gas effect on leak flow	-	-	-
Phase separation in T-junctions	-	-	-
Separator behavior	-	-	-
Thermalhydraulic nuclear feedback	-	-	-
Boron mixing and transport	-	-	-

Facility vs. phenomenon	phe-phenomenon	Phenomenon vs. test	Phenomenon vs calculation
o suitable for code assessment	o	experimentally well defined	E Excellent
+ limited suitability	+	occurring but not well char.	R Reasonable
- not suitable	-	not occurring or not measured	M Minimal
			U Unqualified
			- Not applicable

Table 3.4: Judgement of code calculation performance on the basis of phenomena included in the CSNI matrix, test 12

		UNIT	EXP	CALC R5	Judg. R5
RTA: Pressurizer emptying					
TSE	emptying time*	s	65	70	E
	scram time	s	44	37	E
RTA: Steam generators secondary side behavior					
TSE	main steam line valve closure	s	51	48	E
	difference between PS and SS	MPa	6.71	6.68	E
SVP	SG level	m			
	· at the end of subcooled blow-down		2.3,2.25	2.4,2.25	E,E
			2.35, 2.35	2.4,2.45	E,E
	· when PS pressure equals SS pressure		2.3,2.25	2.4,2.45	E,E
			2.35,2.35	2.4,2.25	E,E
	· when MAKEUP starts		2.25,2.25	2.25,2.25	E,E
			2.25,2.25	2.25,2.25	E,E
SVP	SG pressure	MPa			
	· at the end of subcooled blowdown		7.1	7.0	E
	· when PS pressure equals SS pressure		7.1	7.0	E
	· when MAKEUP starts		5.22	5.33	E
RTA: Subcooled blowdown					
TSE	upper plenum in sat. conditions	s	110	130	E
	break two phase flow	s	720	820	R
IPA	break flow up to 30 s	kg	42	39	E
RTA: First dryout occurrence					
TSE	time of dry out	s	710	800	E
	range of dry out occurrence at various core levels	s	709-738	800 - 810	E
	peak cladding temperature	K	310	295	E
	average linear power	kW/m	0.38	0.34	E
	maximum linear power	kW/m	0.38	0.34	E
	core power / primary mass	kW/kg	0.65	0.7	E
NDP	primary mass / initial mass	%	41	34	R
RTA: Rewet by loop seal clearing					
	time of loop seal clearing	s	710	810	R
			Loop #1	Loop #1 & #2	R
TSE	range of rewet occurrence	s	728	803	E
	time when rewet is completed	s	733	810	E

Table 3.5: Relap5 - judgement of code calculations on the basis of RTA (part 1), test 12

		UNIT	EXP	CALC R5	Judg. R5
RTA: Saturated blowdown					
TSE	PS pressure equal to SS pressure	s	720	830	E
IPA	integrated flow from 400 to 1000 s	kg	350	370	E
RTA: Mass distribution in primary side					
TSE	time of minimum mass occurrence	s	3000	2350	M
SVP	minimum primary side mass	kg	241	204	R
	av. linear power at min. mass	kW/m	0.33	0.28	R
	minimum mass/ITF volume	kg/m ³	109	92	R
RTA: Accumulators behavior					
TSE	accumulators injection starts	s	1200	1370	E
IPA	total mass delivered by accumulators	kg	49	60	R
NDP	minimum primary mass/initial primary mass	%	22	27	R
	primary mass/initial accumulator mass	%	133	128	R
RTA: Final dryout occurrence					
TSE	time of dry out	s	2820	2270	M
	range of dry out occurrence at various core levels	s	2820-2960	2270-2330	M
	peak cladding temperature	°C	320	308	R
SVP	average linear power	kW/m	0.33	0.28	R
	rate of rod temperature increase	K/s	0.55	1.033	M
	core power / primary mass	kW/kg	0.94	0.83	R
NDP	primary mass / initial mass	%	22	27	E
RTA: Make-up intervention					
TSE	Make-up start	s	2910	2300	M
	range of rewet occurrence	s	2910 - 3030	2300 - 2380	M
	final rewetting	s	3030	2380	M
IPA	integrated flow from start to end of rewet	kg	11	7	R
NDP	primary mass/initial mass	%	22	27	R

Table 3.6: Relap5 - judgement of code calculations on the basis of RTA (part 2), test 12

	Parameter	AA	WF
0	PRZ pressure	0.0827	0.012
1	SG1 pressure	0.1692	0.020
2	SG4 pressure	0.1709	0.021
3	ACC1 pressure	0.1039	0.007
4	ACC4 pressure	0.1149	0.008
5	Core inlet temperature	0.1393	0.019
6	Core outlet temperature	0.0612	0.013
7	Upper head fluid temperature	0.0977	0.014
8	Integral break flow	0.1842	0.070
9	Active eccs integral flow rate	0.1478	0.021
10	ACC1 level	0.1341	0.015
11	ACC4 level	0.1134	0.015
12	Heater rod bottom	0.0977	0.030
13	Heater rod middle	0.0897	0.030
14	Heater rod top	0.2991	0.025
15	Primary side mass	0.2982	0.040
16	Core power	0.3570	0.053
17	DP core	1.2876	0.042
18	DP loop seal	0.7147	0.015
19	DP across DC and UH bypass	0.8604	0.042
20	DP sg1 inlet and top	0.9682	0.053
21	DP SG4 inlet and top	1.1984	0.048
	TOTAL	0.2041	0.023

Table 3.7: Post test 12 results, base, the accuracy evaluation following the FFTBM

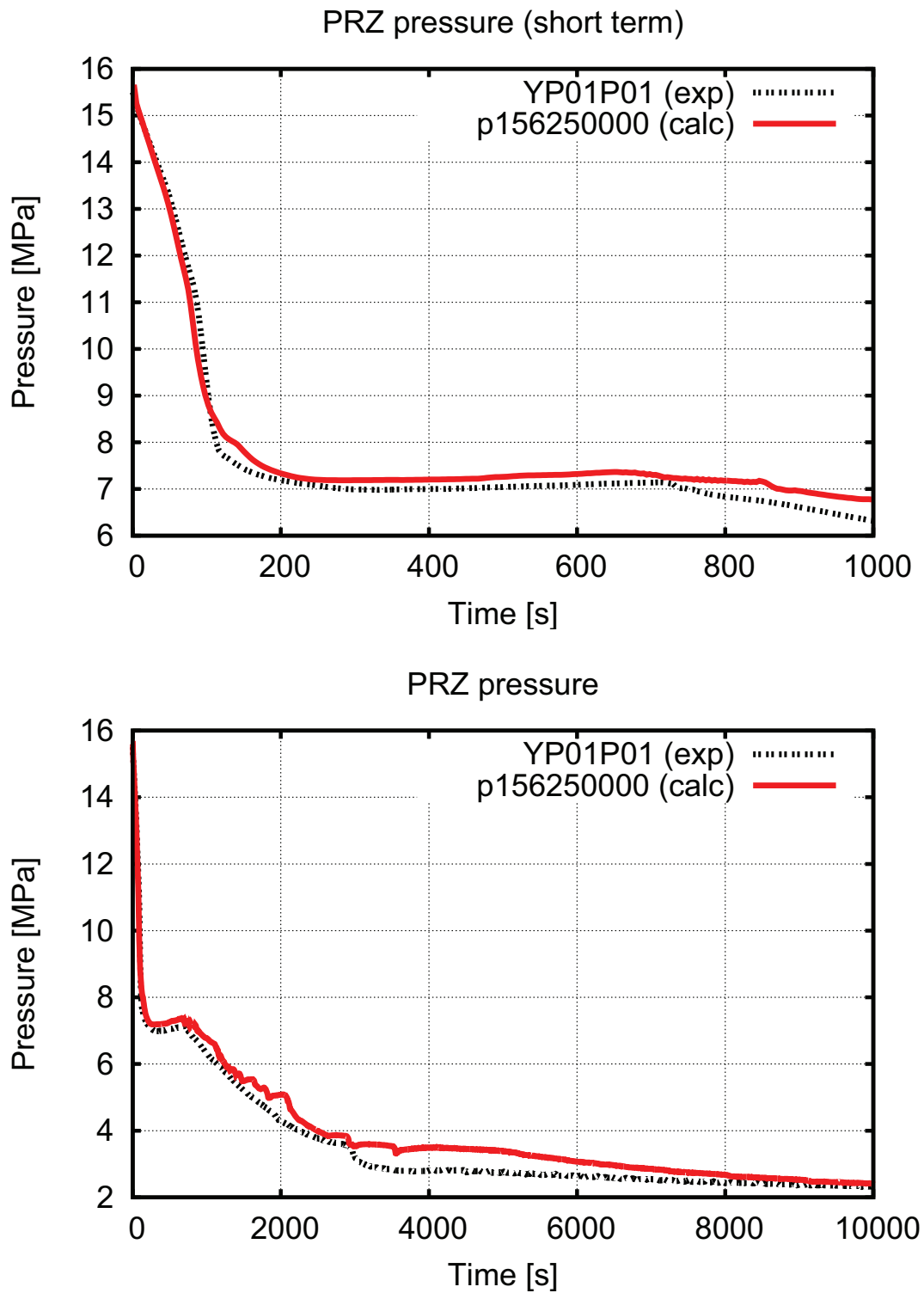


Figure 3.4: Post test 12 results, base, primary side pressure, short and long term

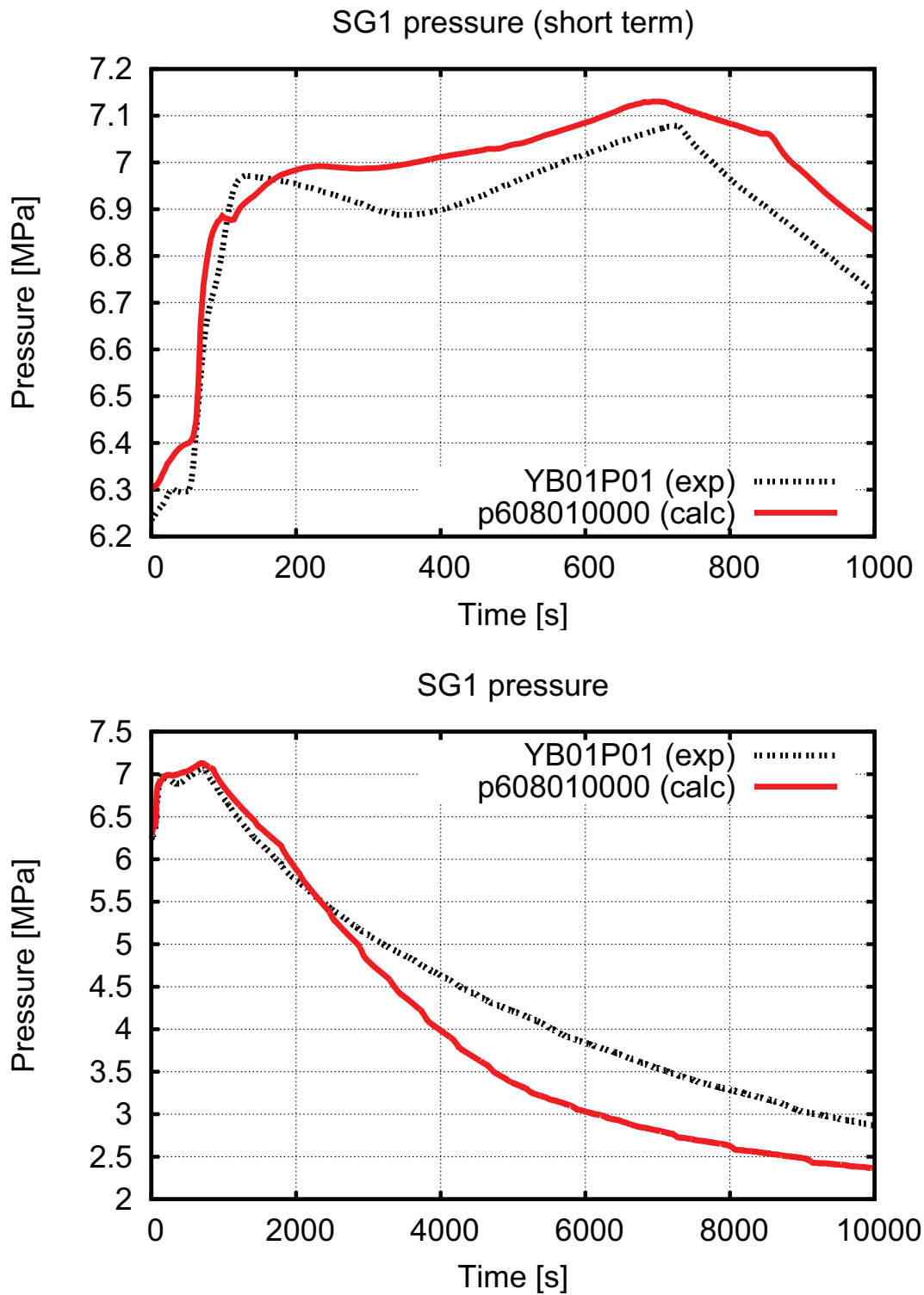


Figure 3.5: Post test 12 results, base, secondary side pressure, short and long term

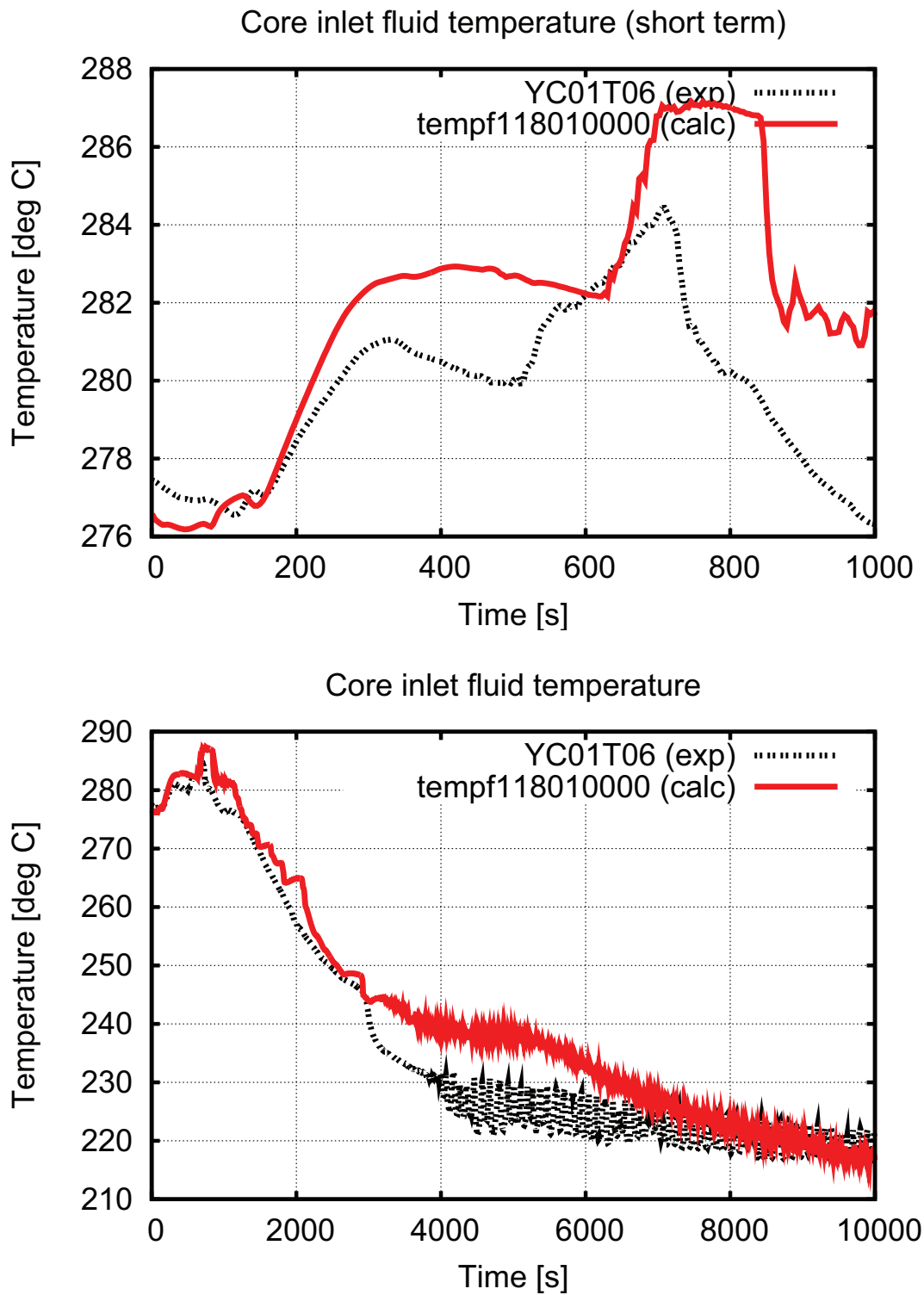


Figure 3.6: Post test 12 results, base, core inlet temperature, short and long term

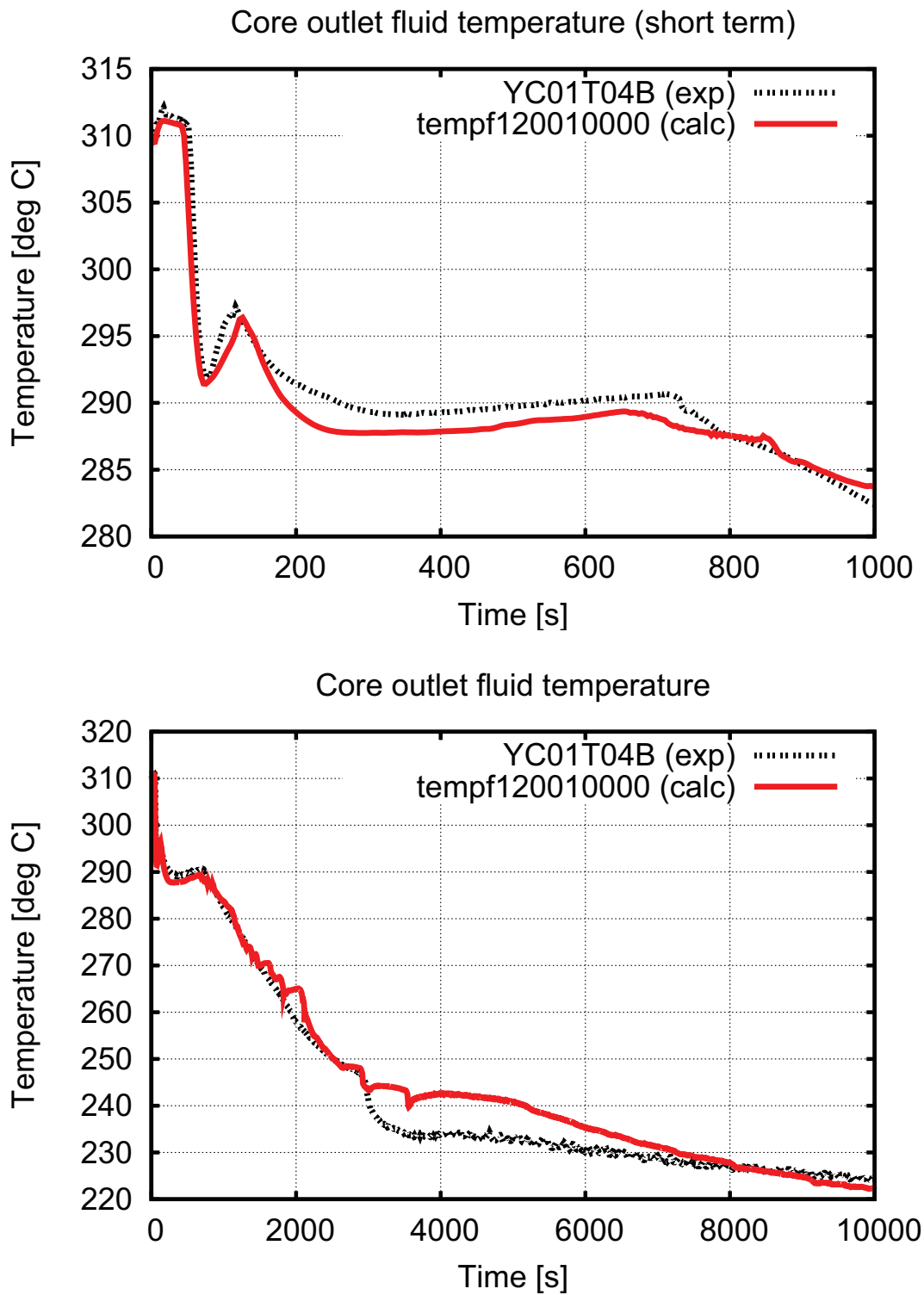


Figure 3.7: Post test 12 results, base, core outlet temperature, short and long term

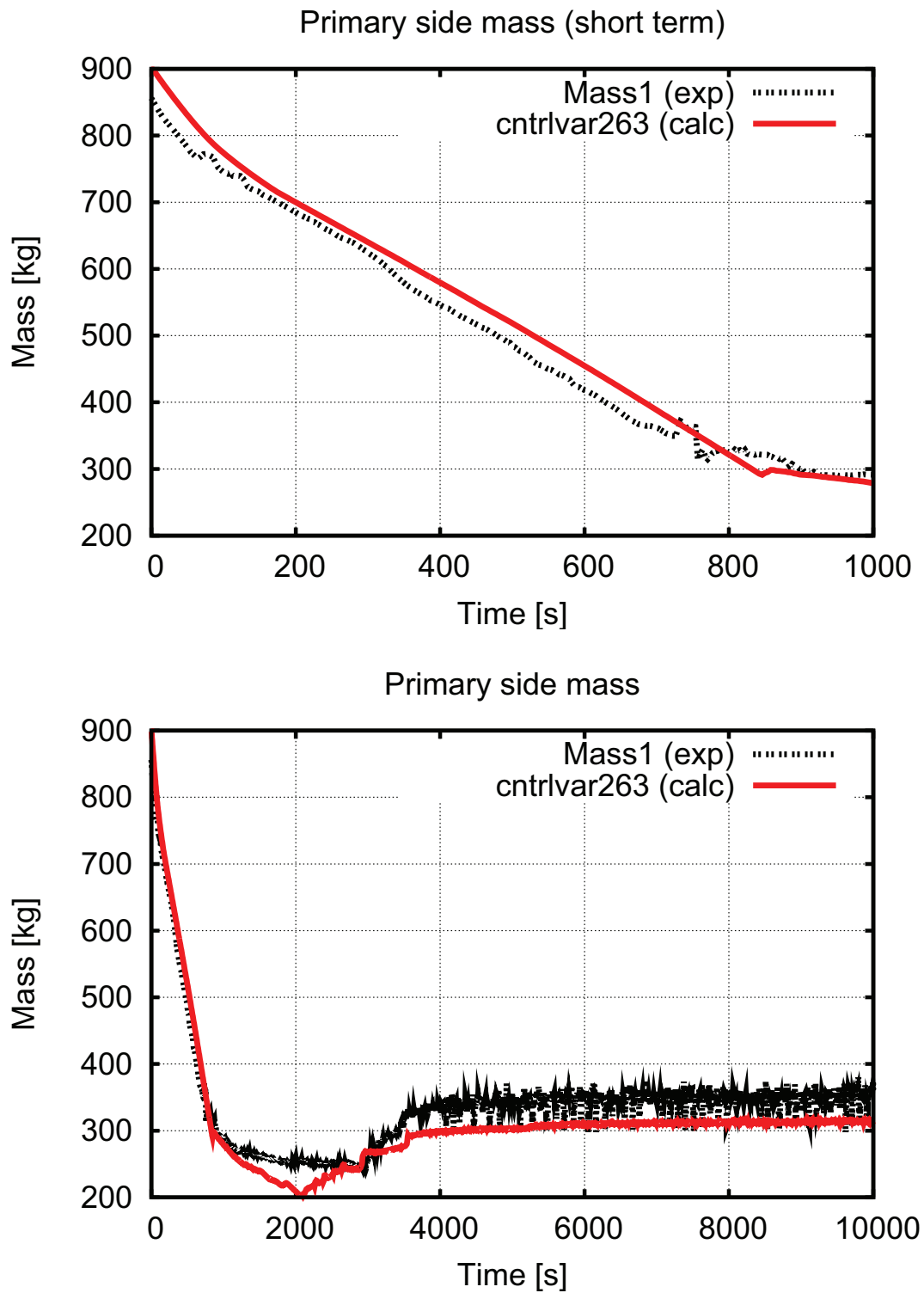


Figure 3.8: Post test 12 results, base, primary mass, short and long term

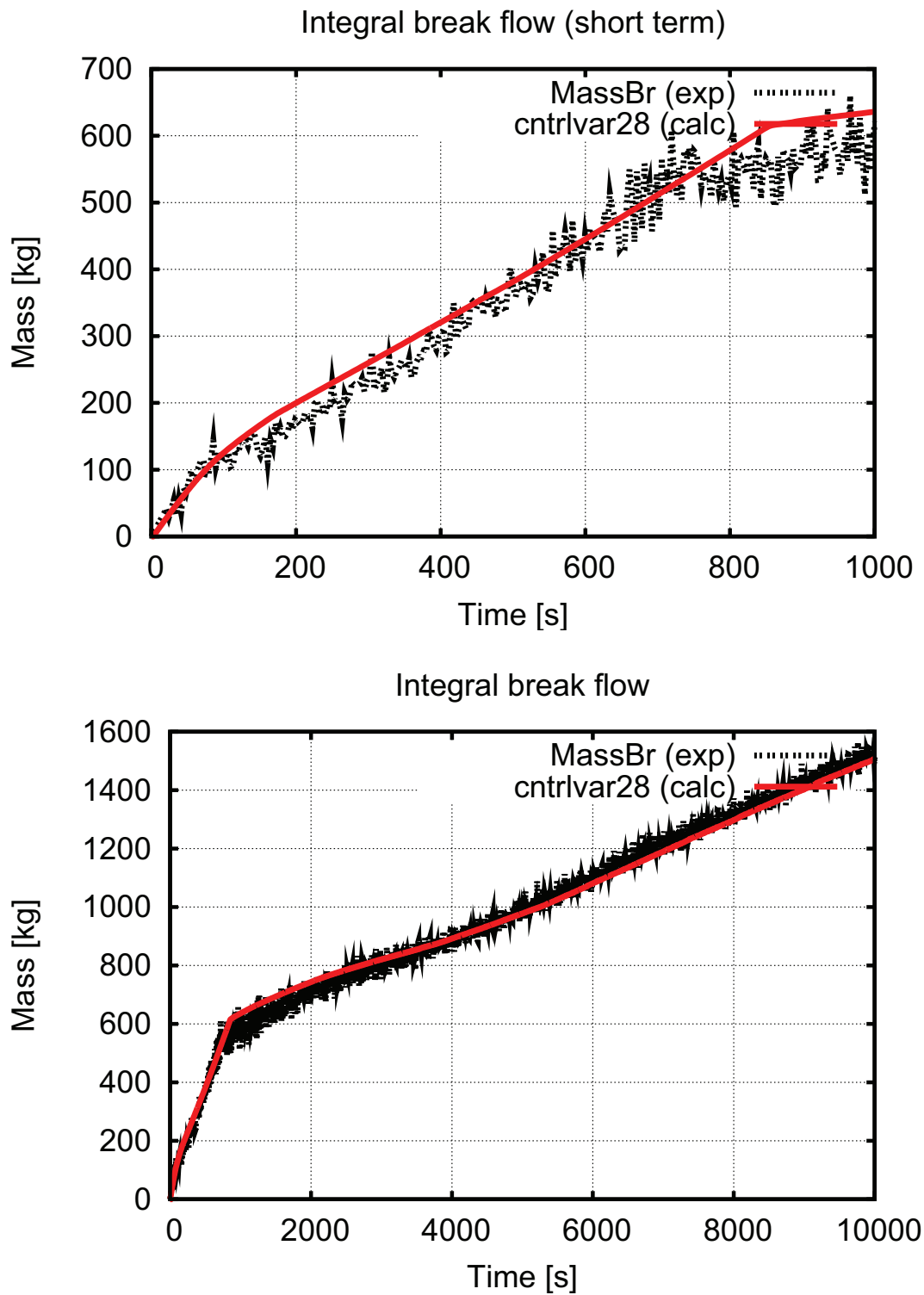


Figure 3.9: Post test 12 results, base, integral flow rate through the break, short and long term

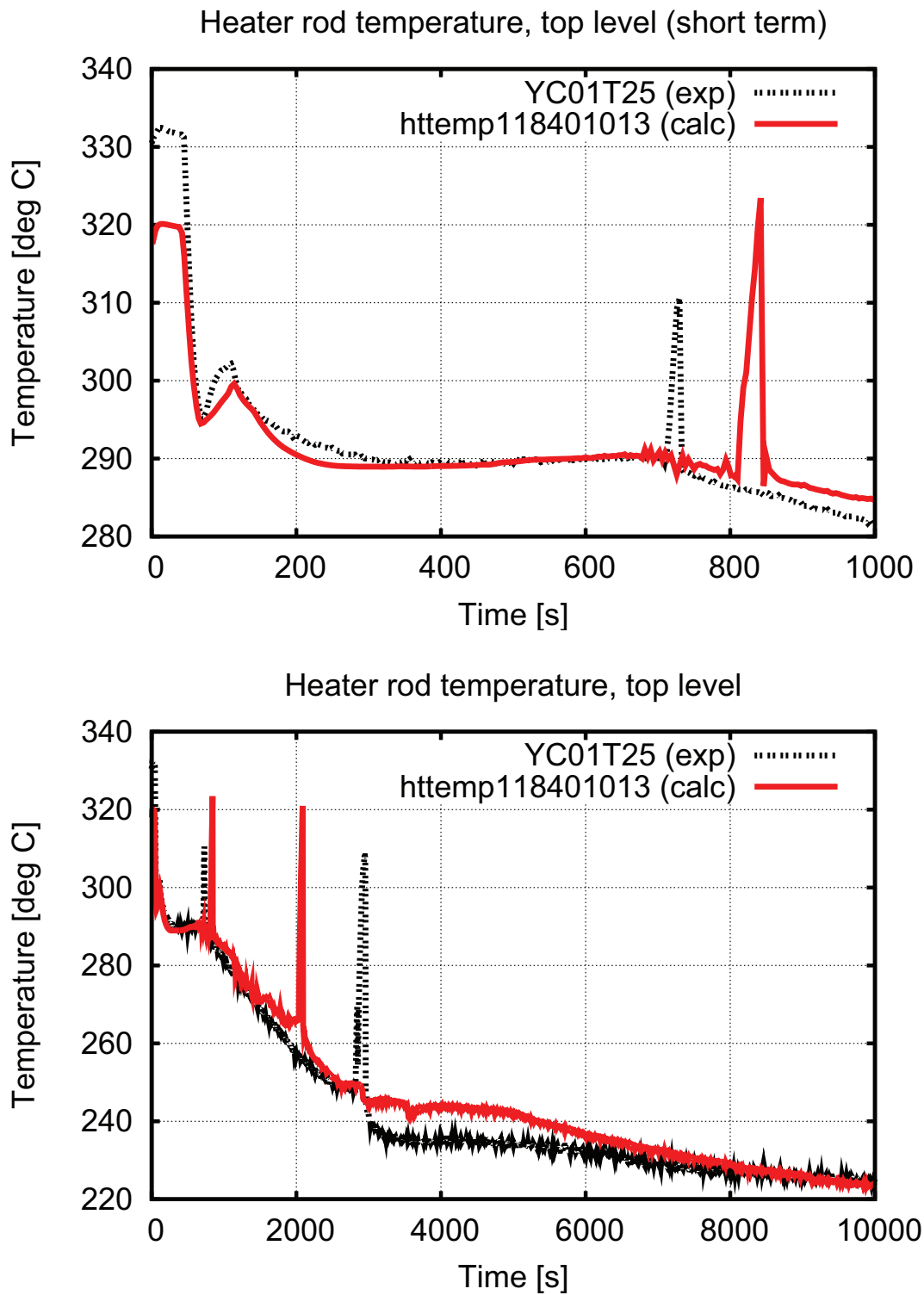


Figure 3.10: Post test 12 results, base, heater rod cladding temperature top, short and long term

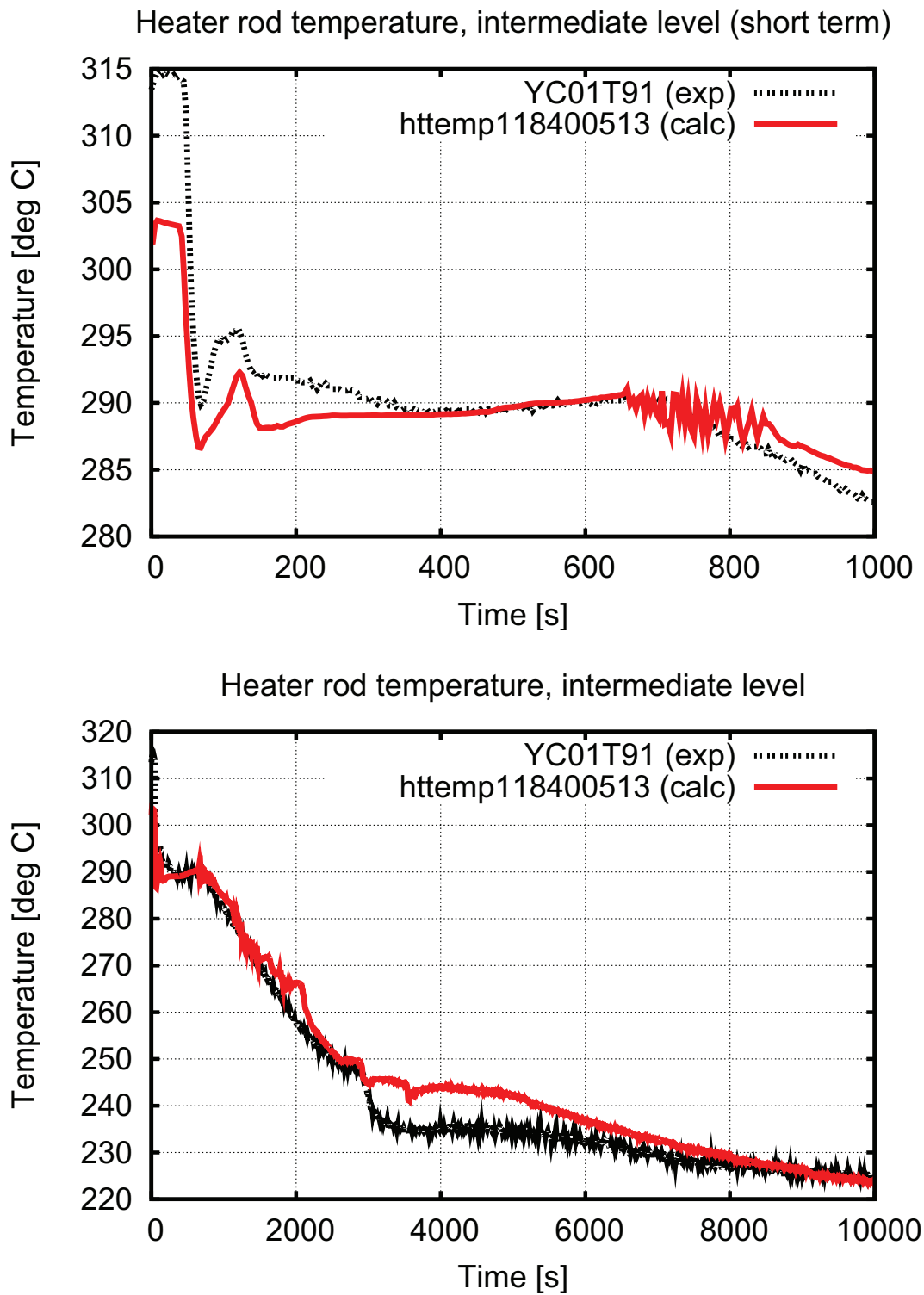


Figure 3.11: Post test 12 results, base, heater rod cladding temperature middle, short and long term

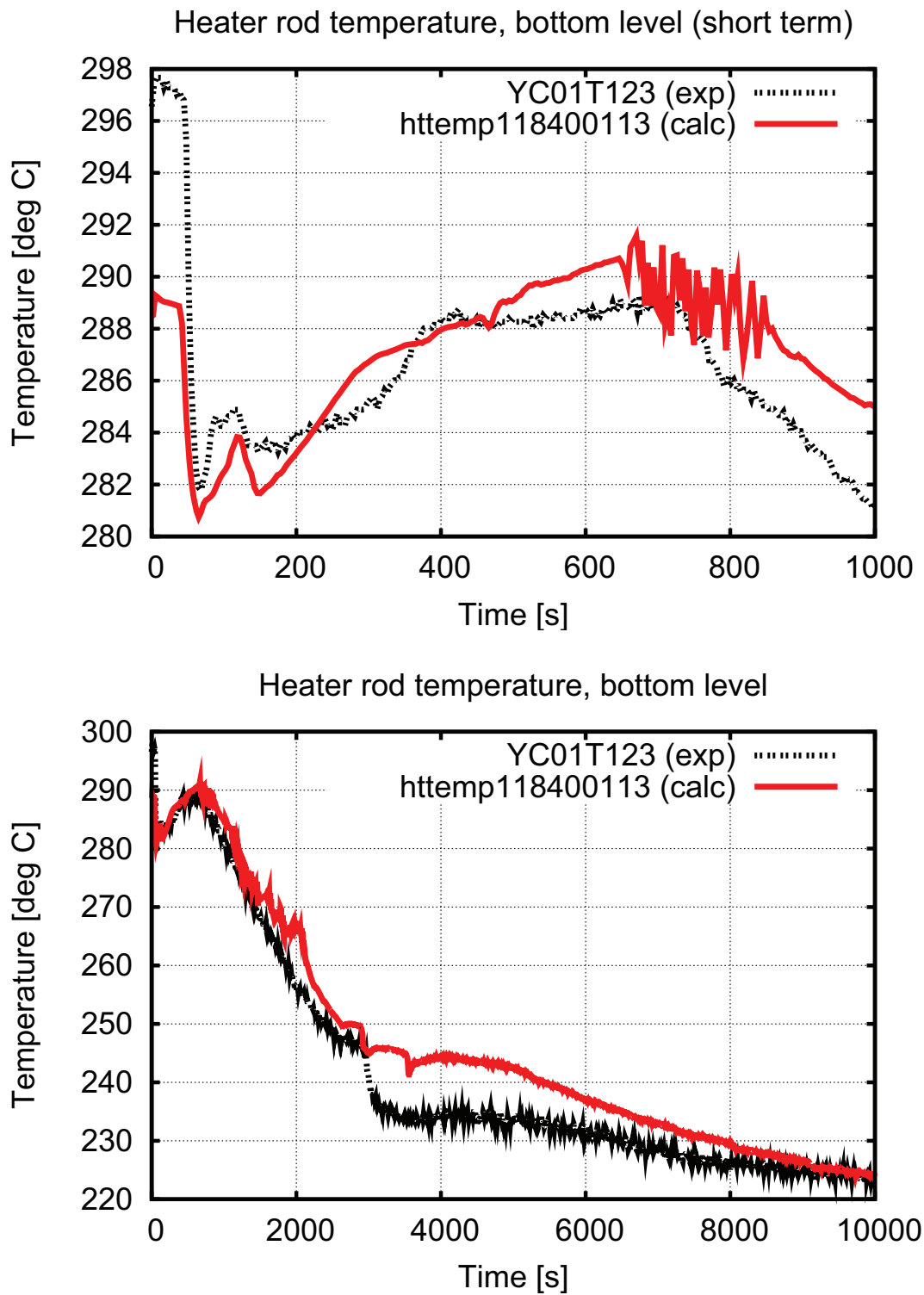


Figure 3.12: Post test 12 results, base, heater rod cladding temperature bottom, short and long term

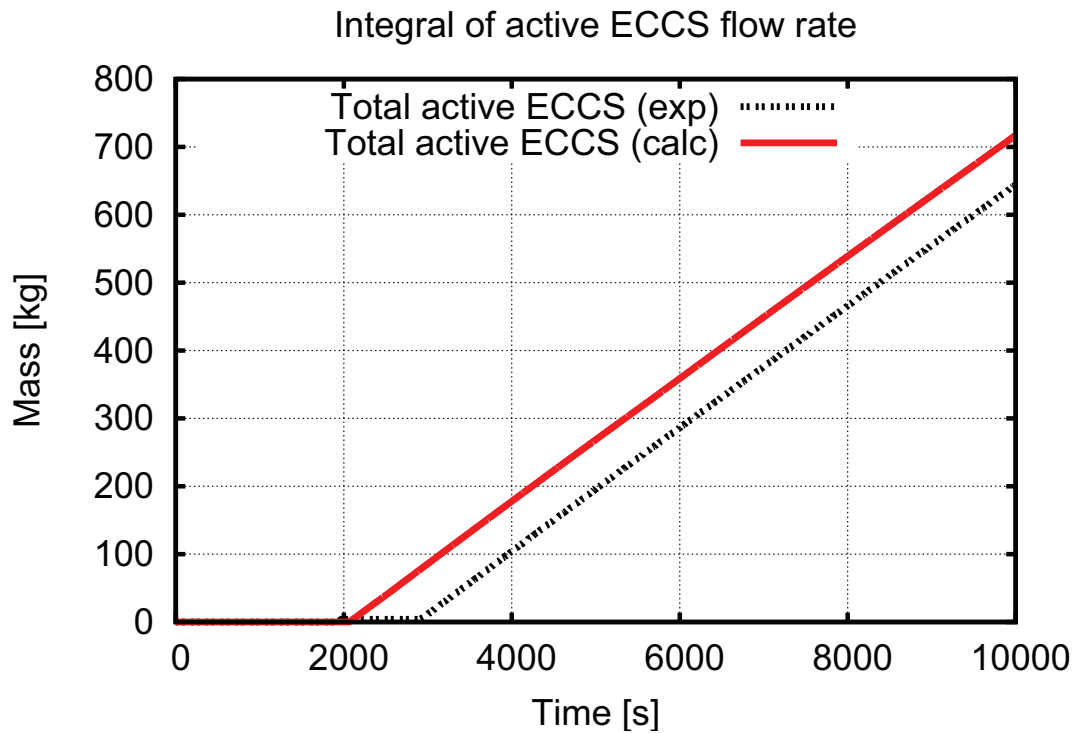


Figure 3.13: Post test 12 results, base, integral eccs flow rate

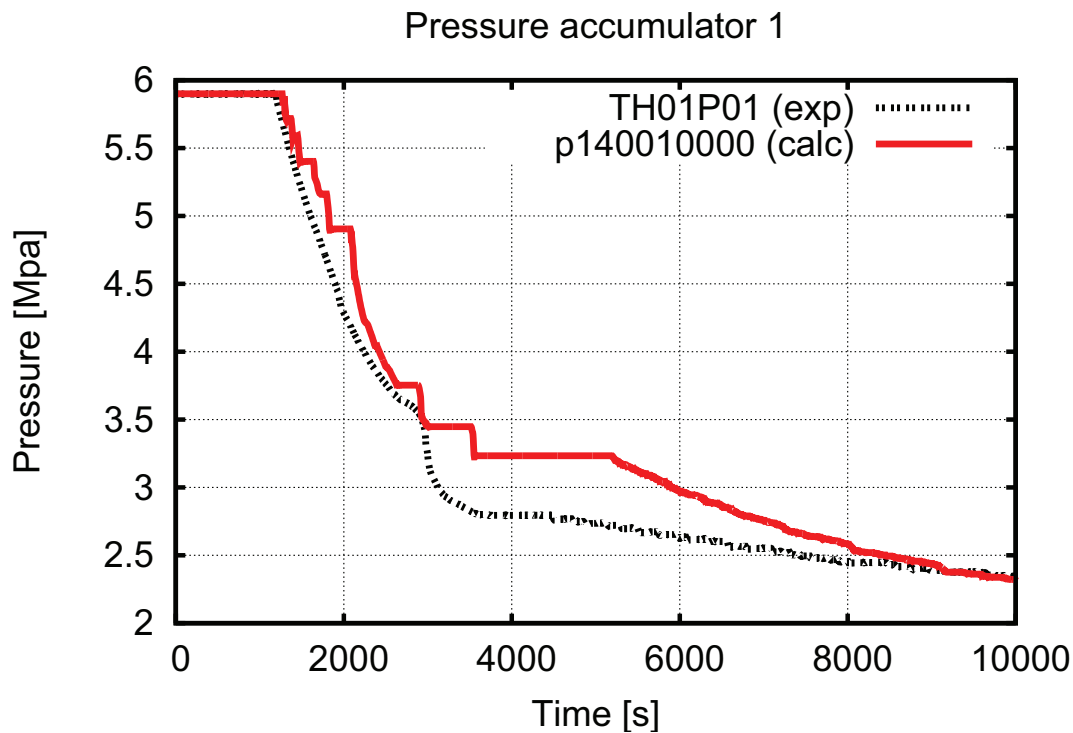


Figure 3.14: Post test 12 results, base, pressure in accumulator 1

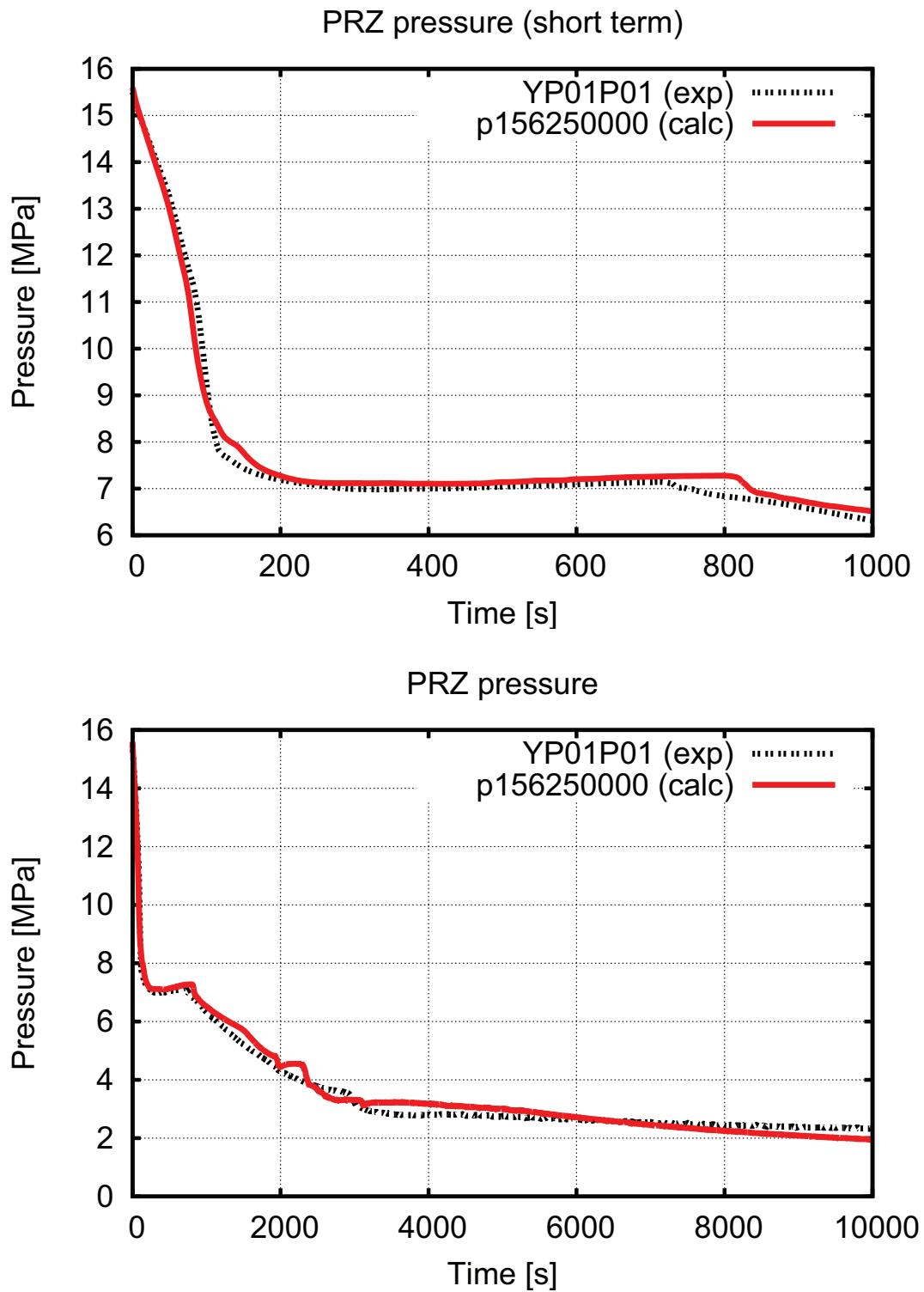


Figure 3.15: Post test 12 results, improved, primary side pressure, short and long term

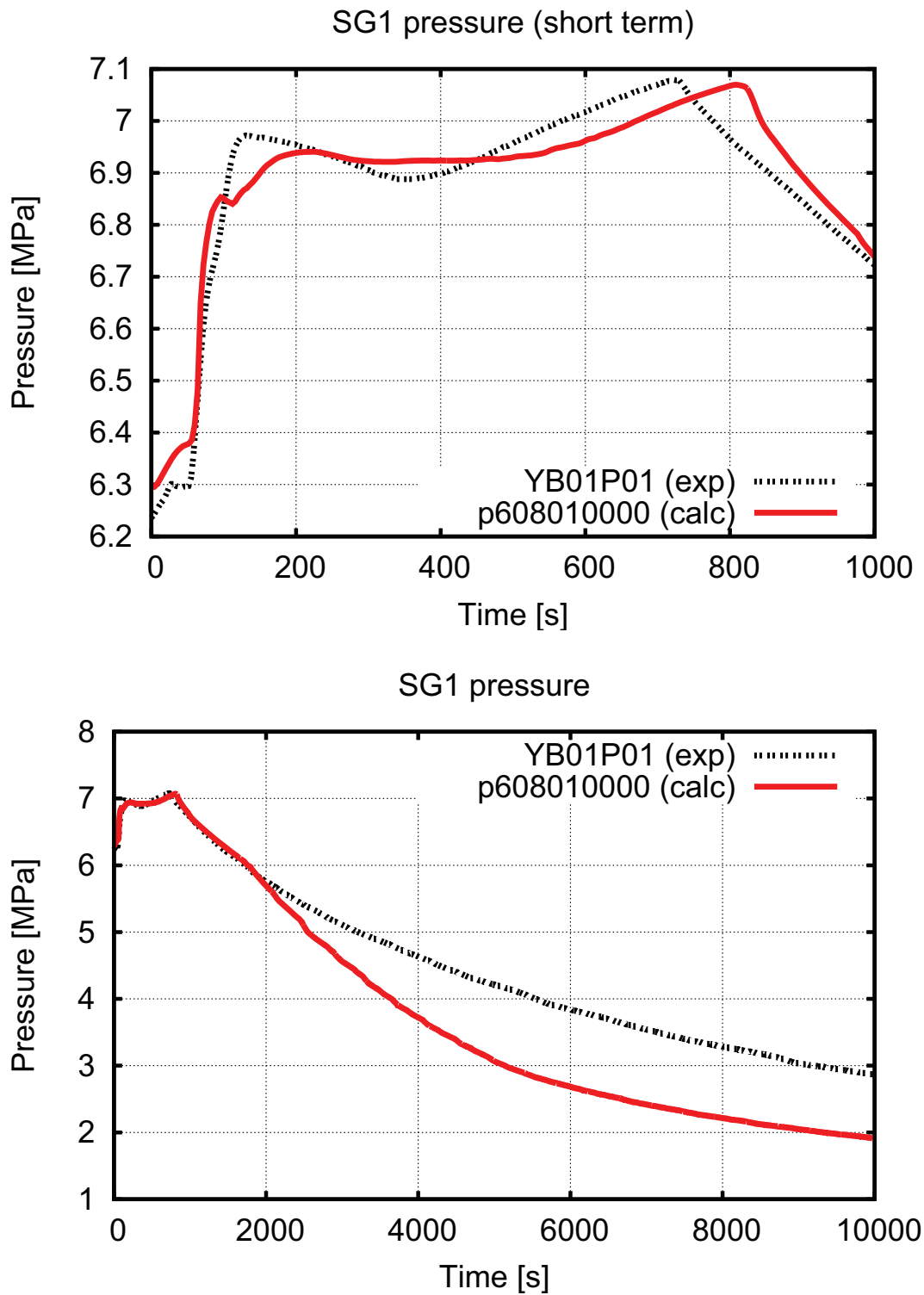


Figure 3.16: Post test 12 results, improved, secondary side pressure, short and long term

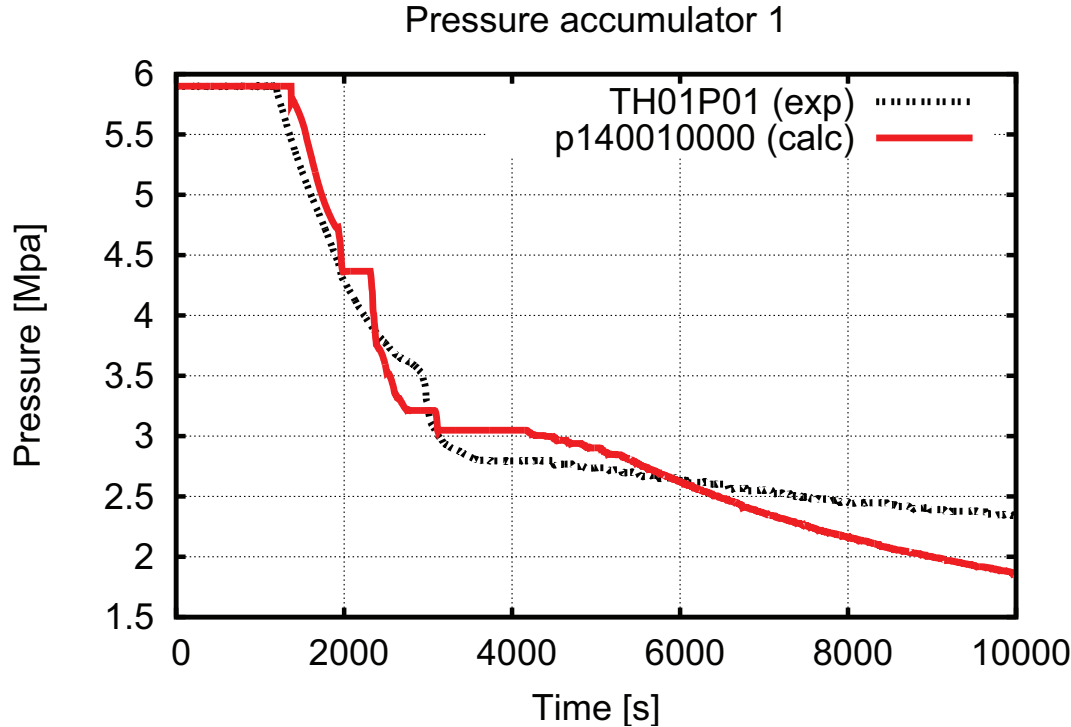


Figure 3.17: Post test 12 results, improved, pressure in accumulator 1

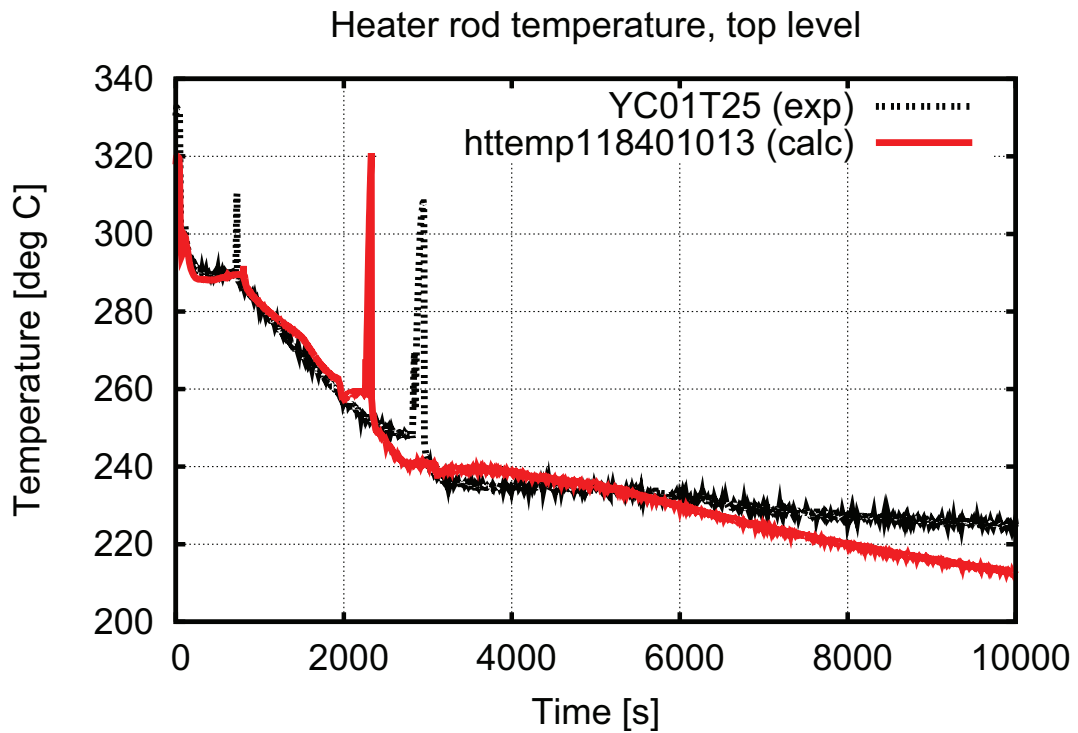
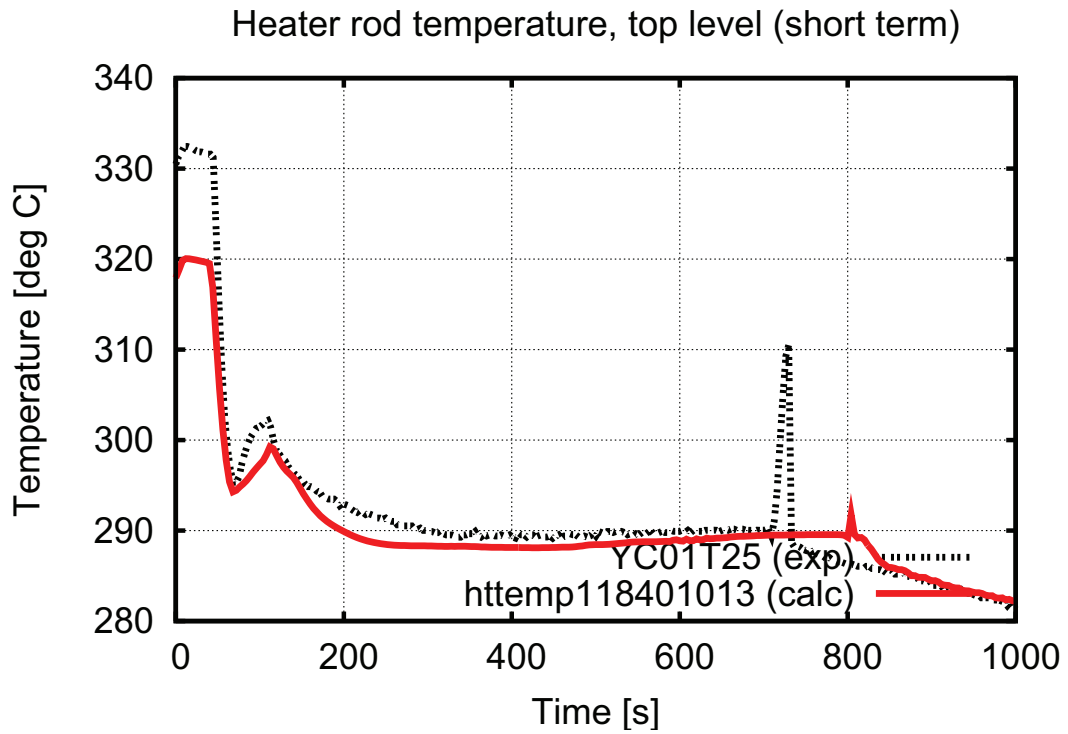


Figure 3.18: Post test 12 results, improved, heater rod cladding temperature top, short and long term

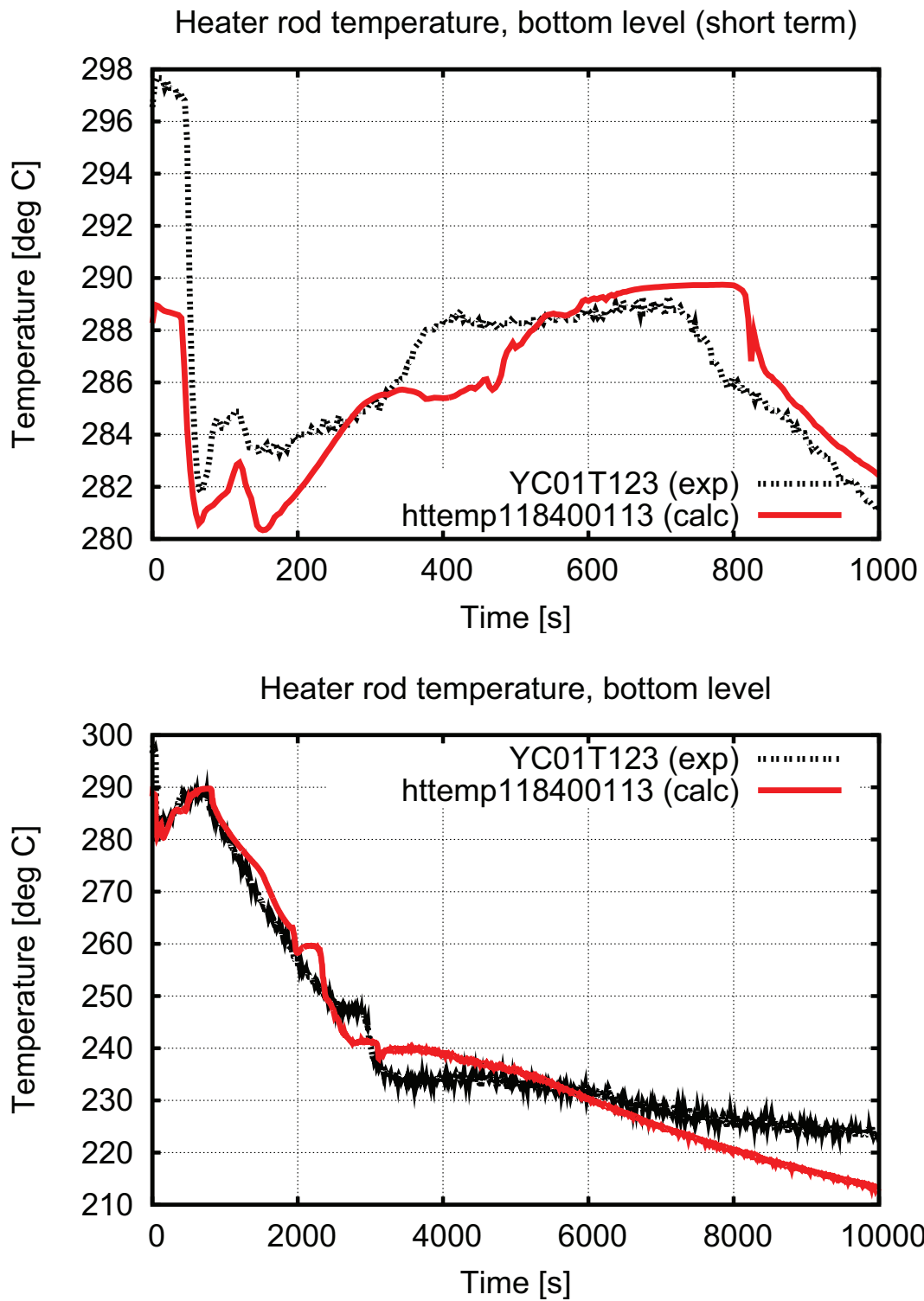


Figure 3.19: Post test 12 results, improved, heater rod cladding temperature bottom, short and long term

3.1.3 Post test analysis 11 - 0.7% CL break

Full title of the Test is “SB-LOCA 0.7% with failure of HPIS cool-down through secondary circuit and HPIS train in affected loop” The section presents the post test analysis of the SB-LOCA experiment CL-0.7-12 (cold leg), the 11th of the TM. The test simulates a small break in cold leg (0.7% equivalent break area in the plant) with failure of HPIS and LPIS and use of normal operation systems of water supply to primary side.

Description of the experiment The test 11 specifications and scenario can be found in detail in Andrioutschenko [2004] and Elkin [2004a]. Initial event is a break of the cold leg (break size 0.7% of CL). Failure of all HPIS, cooldown through secondary circuit, recovery of one HPIS train in affected loop is assumed.

Please refer to table 3.8 for the configuration of the facility.

Equipment	Connection status
Pressurizer	Connected to loop #2
Core by-pass	2 diaphragms with 2 orifices of diameter 7 mm are installed at inlet and outlet of core by-pass
ECCS hydroaccumulators	ACC #1 and #3 are connected to the outlet plenum, ACC #2 and #4 are connected to the inlet chamber
Make-up system of primary side and system TQ14	Both systems are modeled by one make-up system of a primary side.
Work of a make-up system is not modeled in a steady state	The system is connected to cold leg of all loops on an output from steam generators
Steam generators	Under steady state all SGs are connected to each other by steam header. The pressure is adjusted by one steam dumping valve RA06S01
Feed water heater	On. SG level under steady-state conditions is maintained by supply of feed water with a temperature of ≈ 218 °C
ADS simulation system	ADS are connected to each SG. In each ADS line, throttle channel - diameter 12.1 mm and L=50 mm is installed. Actuation set points are 7.16/6.28 MPa
Leak simulation system	Break is located in the cold leg in loop #4 between MCP and DC entrance and oriented upward. Leak channel: $\varnothing 4$ mm, L = 40 mm.
Simulation system of primary side cooldown by mean of ADS	For simulation of primary side cooldown by means of ADS with a rate 30 °/h a throttle with a diameter 2 mm and a length 20 mm is installed in the common ADS line.
UP warming-up line	Under steady state the line is open. The warming-up of the UP top part is stopped about 2 min before opening break line.
Warming-up line of break line	Under steady state the line is open. The warming-up of the break line is stopped about 1 min before opening break line.

Table 3.8: Test 11 facility configuration, taken from Elkin [2004a]

Description of the experiment Please refer to table 3.9 for an overview over the imposed events. Table 3.10 presents the main events during the experiment. The following description of the experiment as taken mainly from Elkin [2004a].

The transient as a whole may be divided into four main stages:

Ph1 blowdown of subcooled coolant (0-300 s);

Ph2 primary side pressure stays at secondary side pressure and the first initial heating of the core model (300-717 s);

Ph3 decreasing the primary coolant mass under saturated coolant discharge and second core heat up (717-2914 s);

Ph4 primary side refilling after the primary side make up system actuation and primary side cooldown under the alternation of saturated and subcooled coolant discharge (2914- 10014 s).

Phase 1 The experiment was started by opening the break valve. A sharp decrease in PS pressure was observed. The PRZ level started to decrease. At 45 s PRZ level was lower than 2.32 m (according to the transducer YP01L02) and the PRZ heaters were turned of.

At 41 s the primary side pressure was lower than 13.7 MPa and the scram was simulated - the program for core and core by-pass electric power decrease was started. At 1200 s the core simulator power had decreased to 202 kW. The core simulator power was kept at this level until the end of the experiment. Ten seconds after the scram the turbine shut valve simulator was closed, and the feed water temperature was changed from 220 °C to 150°C . After the start of RA06S01 valve closure the pressure increased in the secondary side in the SGs SG-1, SG-3 and SG-4. In SG-2 the pressure started to increase earlier due to the hot coolant inflow from pressurizer at the SG inlet. As a result of core power reduction the primary side temperature at the SG inlet lowered and due to the decrease of temperature decrease between the primary and the secondary sides the SGs pressure increase stopped at 130 s, and the set values for the BRU-A valves simulation were not reached.

Due to the pressure decrease the PRZ coolant started to boil and was completely moved to the hot leg of loop #2. It may be deduced by the temperature changes at SG and UP inlet that almost the whole coolant coming from pressurizer moved towards SG. At first relatively cold water reached the SG from surge line (2 sec), then the hotter fluid coming from the pressurizer (3 sec). Due to hot fluid from PRZ at the inlet of SG-2 the temperature started to increase and at 52 sec the saturation margin became less than 10 °C . 15s later, at 67s, the coast-down of the MCPs started continued up to 299 s.

After the coolant reached the saturation point and began to boil the stage of phase's separation in the primary side started. At 111s a level was formed in UP, at 124s the levels started forming in hot legs and SG collectors. In the hot leg and collector of loop #2 connected to PRZ the levels were forming earlier than in other SGs at 82s and 84s correspondingly.

At 249s the upper plenum level decreased to hot legs mark and continued to decrease slowly until 580 s. The UP head (above the upper grate) was completely dry at 246s, which was caused by the lower temperature of the coolant (292°C in the UP head and 308°C at hot legs level). Simultaneously with UP voiding the levels decreased in SG collectors, in hot and cold legs.

Phase 2 At 300s the primary side pressure decreased to the secondary side pressure. The primary circuit pressure decrease stopped at this point. Between 300s and 717s the primary side pressure stabilized at the secondary side pressure level. At 561s the SGs hot collector voided (cold collectors voided by 370s), which led to the break down of the natural circulation in the primary side. Following hot collectors the hot legs of all four loops voided completely at 582s and a rapid decrease of the UP level could be seen a second time. At 700s the level decreased to the upper part of the core and at 710th s the cladding heat-up in the upper plenum of the test facility began.

Phase 3 At 729s the test facility heat-up stopped due to the loop seals clearance in loop-2 and partially in loop-1. The loop seal of the loop-2 was cleared completely at 777s. From 729s the break flow changed from liquid to two phase. This can be seen from the pressure change in the primary side. From this moment on energy was no longer removed by the secondary side - at 731s the primary side pressure dropped beneath the secondary side pressure and the heat transfer was reversed (SS supplied heat to the PS). At 755s the DC level decreased to the cold legs and continued decreasing slowly up to 900s. Thus from 760s on saturated coolant was flowing out of the leakage. Between 990s and 2742s the coolant mass decreased in DC and UP. The level was constant in the core model and in the circulating loops until 2742 s. At 1187s the primary circuit pressure decreased to 5.9 MPa and starting at 1193s the water from ECCS accumulators was fed to the primary circuit.

At 1800s the simulation of the operator action “cool down of the PS via SS with a cool down rate of 30K/h” was simulated by opening the isolation valve of the installed cool down system. The complete opening of isolation valve was at 1811s. The primary and secondary side was not affected by this measure. At 1928s primary side make-up system actuated spuriously for 43s. Water from this system was entered in primary side during 43s.

Phase 4 The upper plenum was completely voided at 2741s. Immediately after the core level began to drop. At 2816s the upper part of the fuel rod simulator uncovered and a second heat up began. At 2914s the set point for the second operator action was reached (the cladding temperature reached 302 °C), and the make up and TQ(1,2,3)4 system was taken into operation. The make-up system cold water supply into the primary side led to acceleration of the primary pressure decrease rate and resulted in water flow rate increase from ACCs. The total water flow rate coming from the passive ECCS and make-up system exceeded the coolant flow rate discharged from the leakage and therefore at 2922s the refilling of the downcomer and core regions began. At 3456s it reached the cold legs. From this moment up to the end of the experiment there was alternating discharge of saturated and unsaturated coolant into the leakage. As a result the rate of the primary pressure decrease slowed down again and there appeared pressure pulsation in the primary side and pulsation of other parameters caused by the status change of the coolant discharged from the break. Between 3456s and 10014s there was a slow pressure and primary side temperature decrease. The coolant flow rate discharged from the break was comparable to the coolant flow rate coming from ACCs and make up system which led to the level stabilization in the reactor model and circulating loops. This state was kept until 10014s.

EVENT	pre-set	actual
Leak opening	0 s	0 s
SCRAM signal	UP pressure < 13.7 MPa + 1 s	UP pressure < 13.7 MPa + 2 s
PRZ heaters switched off	PRZ level = 4.21 m	PRZ level = 4.17 m
Turbine valve simulation closure begins	UP pressure < 13.7 MPa + 11 s	UP pressure < 13.7 MPa + 11 s
SG SS isolated - Turbine valve simulation closure ends		71 s
Transition to the AFW	UP pressure < 13.7 MPa + 11 s	UP pressure < 13.7 MPa + 11 s
MCP coast-down onset	Difference between saturation temperature (UP pressure) and HL temperature < 10 °C + 15 s	Difference between saturation temperature (UP pressure) and HL temperature < 10 °C + 15 s
Start of ACC 1 operation	UP pressure < 5.9 MPa	UP pressure < 5.9 MPa + 1 s
Start of ACC 2 operation	UP pressure < 5.9 MPa	UP pressure < 5.9 MPa - 5 s
Start of ACC 3 operation	UP pressure < 5.9 MPa	UP pressure < 5.9 MPa - 3 s
Start of ACC 4 operation	UP pressure < 5.9 MPa	UP pressure < 5.9 MPa - 7 s
Primary side cool-down procedure	1800 s	1801 s
Start of HPIS operation	Core cladding temperature = 350°C and $\tau > 1800$ s	Core cladding temperature = 338°C and $\tau > 3018$ s
Start of HPIS operation	UP pressure = 2.43 MPa	UP pressure = 2.45 MPa

Table 3.9: Imposed sequence of main events for PSB Test 11, CL-0.7-12, taken from Elkin et al. [2004]

EVENT	Time (s)
Leakage opening (opening isolation valve XL10S01)	0
YC01P17=13.7 MPa	41.2
Switching off PRZ heater	45
Start of power reduction on FRS bundle and core by-pass	45.9
Start closing of steam discharge valve RA06S01	52.1
Ts(YC01P17) - YA02T04 < 10 °C	52
Start of MCPs coast-down (YD01-04R11)	67.1
Stopping of SGs steam discharge (full closing of RA06S01 valve)	69.6
Complete closing of feed water valves to SG	
- RL01S06,- RL02S06	167, 380
- RL03S06, - RL04S06	176, 316
Coolant reaching of saturation in hot legs at SG inlet	
- in loop #1, #2	124,84
- in loop #3, #4	123,127
Complete switching off of MCP	299
Coolant reaching of saturation in cold legs at SG outlet:	
- in loop #1, #2	308, 287
- in loop #3, #4	314, 320
Start of the first bundle heat up	710
Pressure in the primary side is lower than in the secondary one:	
- in SG -1, -2	731, 730
- in SG -3, -4	721, 731
Pressure in the primary side 5.9 MPa	1187
Start of Acc operation:	
-TH01B01,-TH02B01	1198, 1193
-TH03B01, -TH04B01	1200, 1195
Coolant reached saturation at the core inlet	1283
Start of cooldown procedure (opening of RA15S01)	1801
Start of the second bundle heat up	2816
Start of operation of primary side make-up system	
-RL16F01, -RL17F01	2914, 2914
-RL18F01, -RL19F01	2914, 2914
Stop of experiment	10014

Table 3.10: Sequence of the principal events in the experiment 11 [Elkin, 2004a]

Calculation results

Primary Pressure

The primary side pressure trend is generally very well predicted. It can be seen in Figure 3.20. The overall non-dimensional error for the pressure trend, which was calculated using the FFTBM, is 0.09, which is a good result (see Table 3.11). The acceptability limit of the University of Pisa for a qualified nodalisation is 0.1.

In the first phase, about 0 to 300s, the primary pressure trend is very well predicted. The next phase, 300s-800s, in which the upper plenum and the loops are in saturation, the primary pressure rests on the secondary pressure. The pressure in this phase is slightly overpredicted. The end of the subcooled blowdown, which is marked by again a decrease in the PS pressure, is predicted to be at about 800s, while the experiment shows that this event takes place about after 720s. The next phase, 800s-2300s, shows about the same depressurization rate as the experiment. At about 2300s the second-dryout occurs in the calculation and some parts of the ECCS are recovered. This is one of the main differences between calculation and experiment - in the experiment this event occurs at about 3000s. A difference of 700s is just within the acceptability range for a transient like this - one has to consider that local phenomena like comparably small dry-outs are very difficult to predict, and that this is certainly an aspect of test 11 which is very challenging for the code. The last phase, from accident management to the end of the experiment, shows qualitatively the same behavior. Cold water from the recovered ECCS systems cools the primary side inventory and causes a visible drop in the primary side pressure - which in turns enhances ECCS intervention.

Secondary side temperatures

The secondary side pressure trend for SG1 is reported in Figure 3.21. The non-dimensional error of the FFTBM analysis is reported for SG1 and SG4 in Table 3.11. The pressure trend from 0s - 700s is well predicted. The end of the subcooled blowdown is calculated to be 800s, while in the experiment it turned out to be at 720s. This is the reason why the SS pressure trend starts to drop later in the calculation than in the experiment. Up to 1800s the rate of the SS pressure decrease is slightly underpredicted. At 1800s the SS cool down system, designed to realize a cool down rate of 30K/h, is taken into operation by opening the correlated valve. Although a big effort was made the catch this event with the calculation, there is still a visible distortion. From 1800s the cool down rate predicted by the calculation is bigger than the experimental one.

Temperatures

The fluid temperatures are reasonably well predicted, see Figure 3.22 for the core inlet temperature and Figure 3.23 for the core outlet temperature. The disagreements in the fluid temperature between calculation and experiment can mainly be explained by the differences in the pressure. The trend of the clad temperature at several elevations is reported in Figure 3.28 (bottom), Figure 3.27 (middle) and Figure 3.26 (top). While the middle and bottom range follow closely the fluid temperature, the top range shows a dry-out at 730s in the experiment and 800s in the calculation. This is a good agreement between calculation and experiment. The second dry-out occurs earlier in the calculation than in the experiment (at about 2300s in the calculation, 3000s in the experiment). This is a minimal agreement between calculation and experiment, and shows the fact that local small dry-out phenomena are very challenging for the code and difficult to predict. Figure 3.26 shows the temperature for the two top nodes of the heater rods for the relap calculation. Please note that the dry-out occurs after the accumulator intervention, and that the accumulators quench the dry-out in the top-node. So the second dry-out occurs in the first node after the top node.

Break mass flow rate and primary side mass

The experimental and calculated mass flow through the break are in excellent agreement during all phases of the experiment (see Figure 3.25).

Pressure drops

All pressure drops between different points of the primary circuit are compared in figures. All of the comparisons, with different extent, suffer of the limitation connected to the fact that the pressure taps are not

coincident with the center of the volumes of the nodalization. Pressure drops in the loops are reasonably well predicted by the code: notwithstanding the code predicts the occurrence of loop seal clearing in one loop, as in the experiment, this loop is not the correct one. This confirms the difficulty, already emphasized in previous analyses, see D'Auria et al. [1999] and D'Auria et al. [2003], in correctly predicting a critical phenomenon like loop seal clearing. The distribution of pressure drops in the initial steady state, both direct and reverse (in this last case calculated data can not be qualified), are responsible for the misprediction of loop seal clearing phenomena. This is a well known limitation, resulting from several code applications to SBLOCA analyses, that does not affect the code capability in predicting the overall transient scenario D'Auria et al. [1999] and D'Auria et al. [2003].

Conclusions The primary pressure follows very close the experimental one. Even the secondary pressure is in good agreement with experimental data at the beginning of the transient. Regarding the cladding temperature, relap calculation shows a good agreement with the experimental data for the first dryout occurrence - the second dryout is predicted to happen earlier. The reason might be that the mass flow through the break for two phase flow is overpredicted (see also the mass inventory). It has also to be noted that the heat losses of the PSB facility, especially the heat losses of the MCP, are not precisely known and may introduce a source of error. Nevertheless, the prediction is close enough to the experiment to achieve a FFTBM-Score within the acceptability limit, which means that the calculation can be considered as qualified calculation.

Parameter	AA	WF
0 PRZ pressure	0.0903	0.030
1 SG1 pressure	0.2495	0.048
2 SG4 pressure	0.2546	0.048
3 ACC1 pressure	0.1514	0.034
4 ACC4 pressure	0.1651	0.035
5 Core inlet temperature	0.0896	0.034
6 Core outlet temperature	0.0833	0.039
7 Upper head fluid temperature	0.1360	0.026
8 Integral break flow	0.2648	0.166
9 Active eccs integral flow rate	0.3971	0.041
10 ACC1 level	0.2330	0.043
11 ACC4 level	0.2472	0.060
12 Heater rod bottom	0.1300	0.050
13 Heater rod middle	0.1256	0.052
14 Heater rod top	0.3597	0.039
15 Primary side mass	0.1923	0.093
16 Core power	0.3615	0.121
17 DP core	1.5532	0.082
18 DP loop seal	0.6970	0.031
19 DP across DC and UH bypass	2.3407	0.054
20 DP sg1 inlet and top	0.8209	0.086
21 DP SG4 inlet and top	0.8888	0.069
TOTAL	0.26	0.049

Table 3.11: Post test 11 results, accuracy evaluation following the FFTBM

EVENT	EXP (s)	R5 base (s)
Leakage opening	0	0
YC01P17=13.7 MPa	42.2	37
Start closing of steam discharge valve RA06S01	53	47
Start of MCPs coast-down (YD01-04R11)	68.5	60
Stopping of SGs steam discharge (full closing of RA06S01 valve)	70.6	67
Complete switching off of MCP	300.4	300
Start of the first bundle heat up	703	780
Pressure in the primary side is lower than in the secondary one:	725	850
Pressure in the primary side 5.9 MPa	1188	1160
Coolant reached saturation at the core inlet	1220	1245
Start of cooldown procedure (opening of RA15S01)	1801	1800
Start of the second bundle heat up	2805	2150
Start of operation of primary side HPIS system	3018	2300
Stop of experiment/calculation	4780	5000

Table 3.12: Relap5 comparison experiment/calculation, test 11

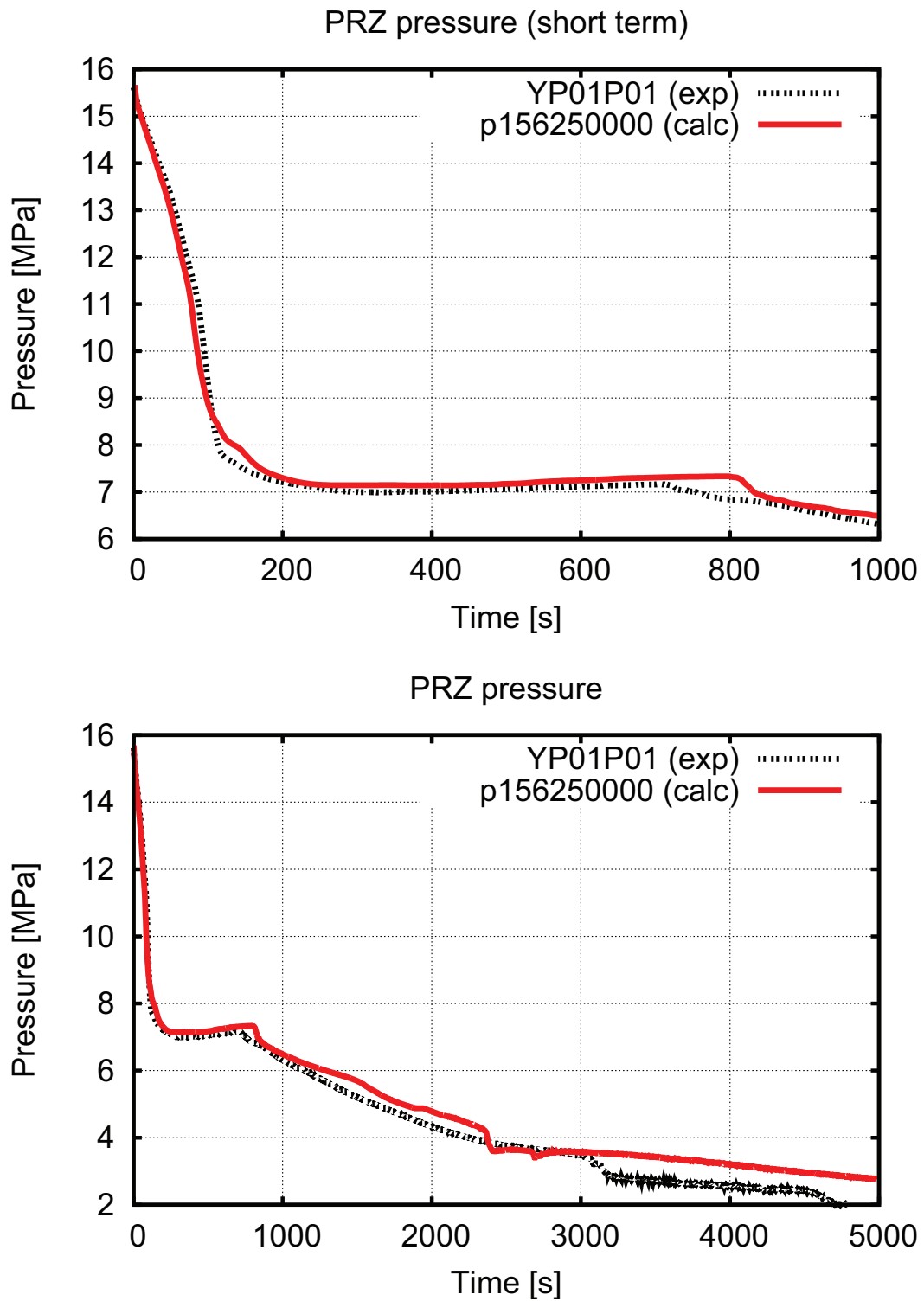


Figure 3.20: Post test 11 results, primary side pressure, short and long term

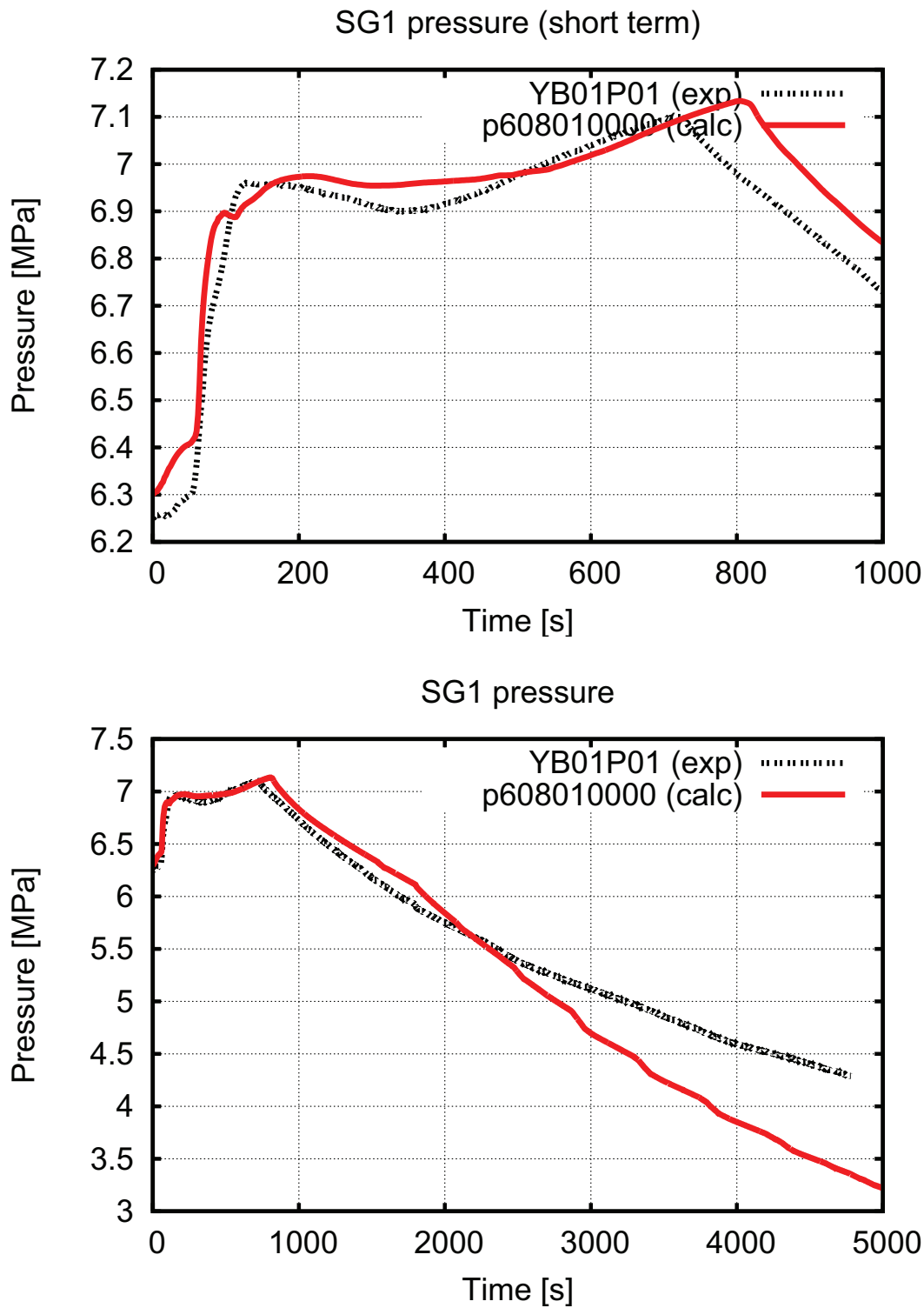


Figure 3.21: Post test 11 results, secondary side pressure, short and long term

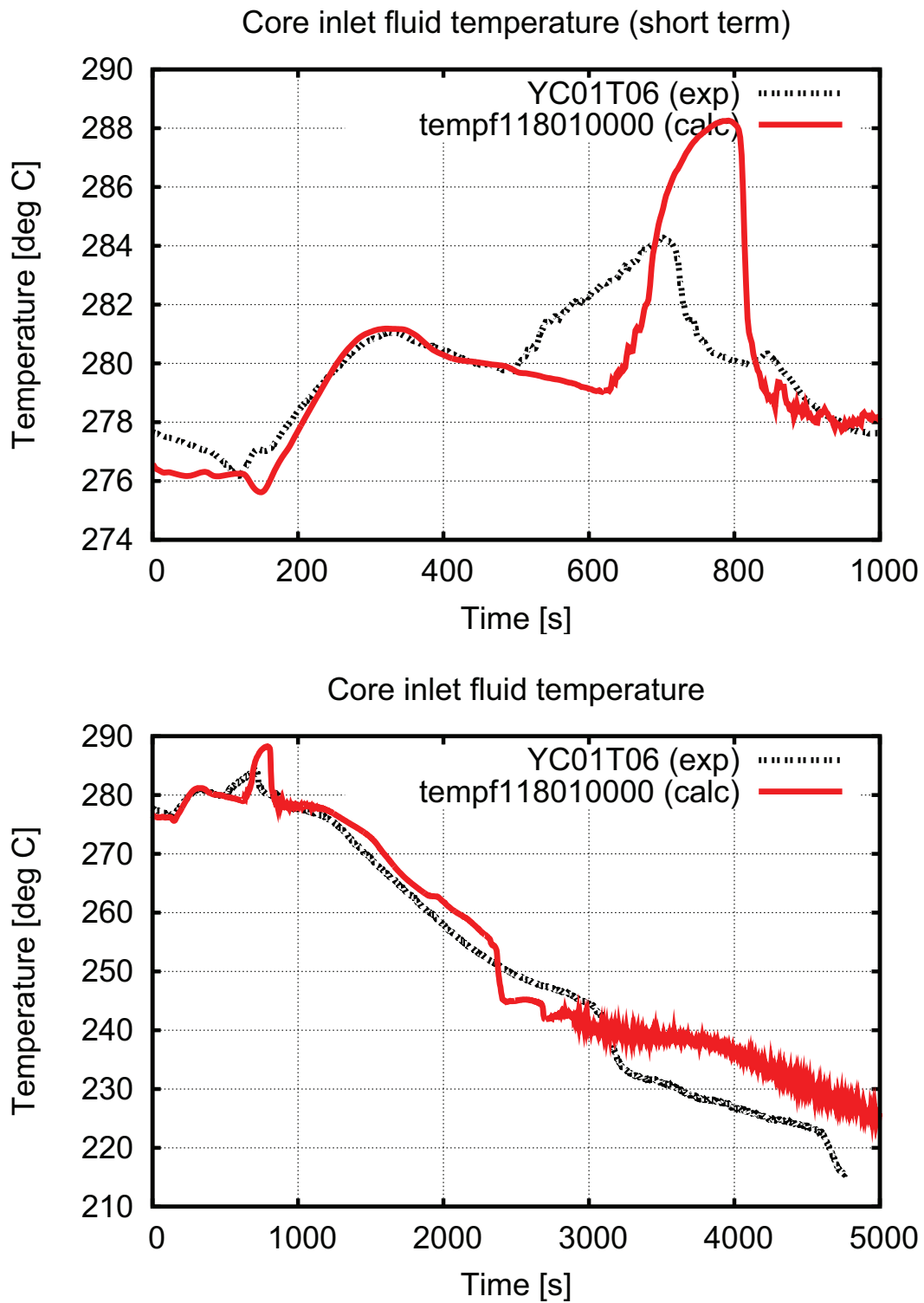


Figure 3.22: Post test 11 results, core inlet temperature, short and long term

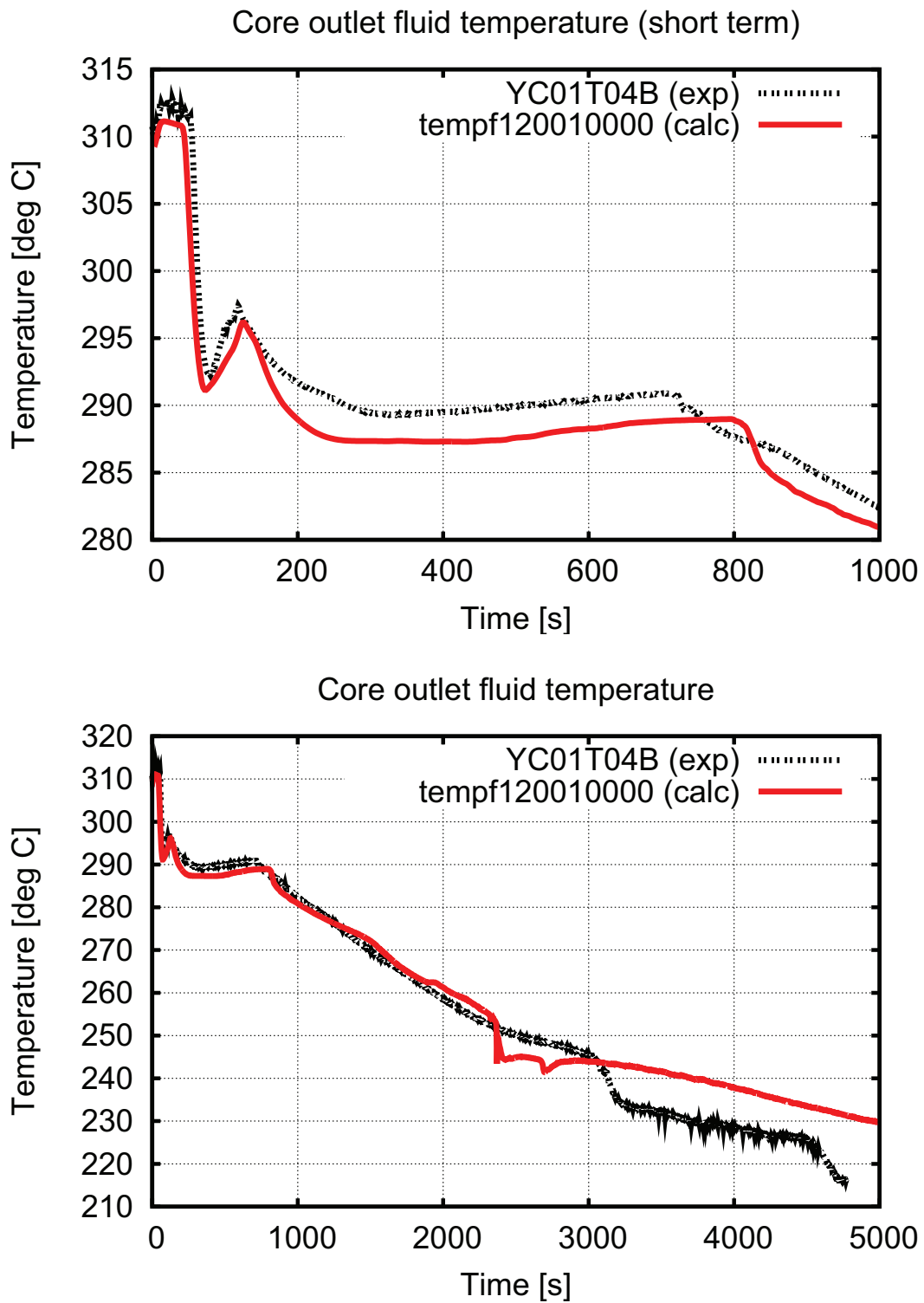


Figure 3.23: Post test 11 results, core outlet temperature, short and long term

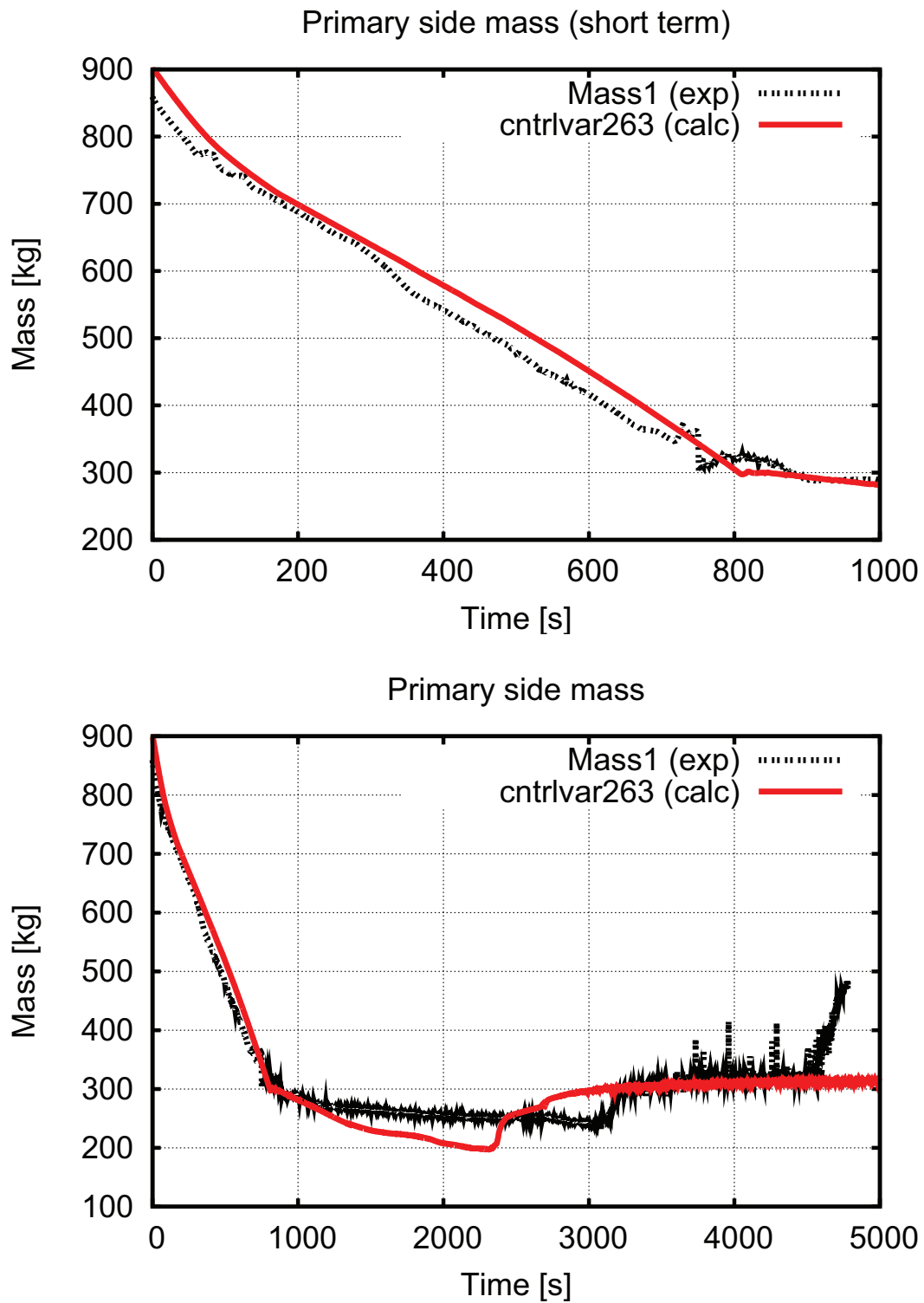


Figure 3.24: Post test 11 results, primary mass, short and long term

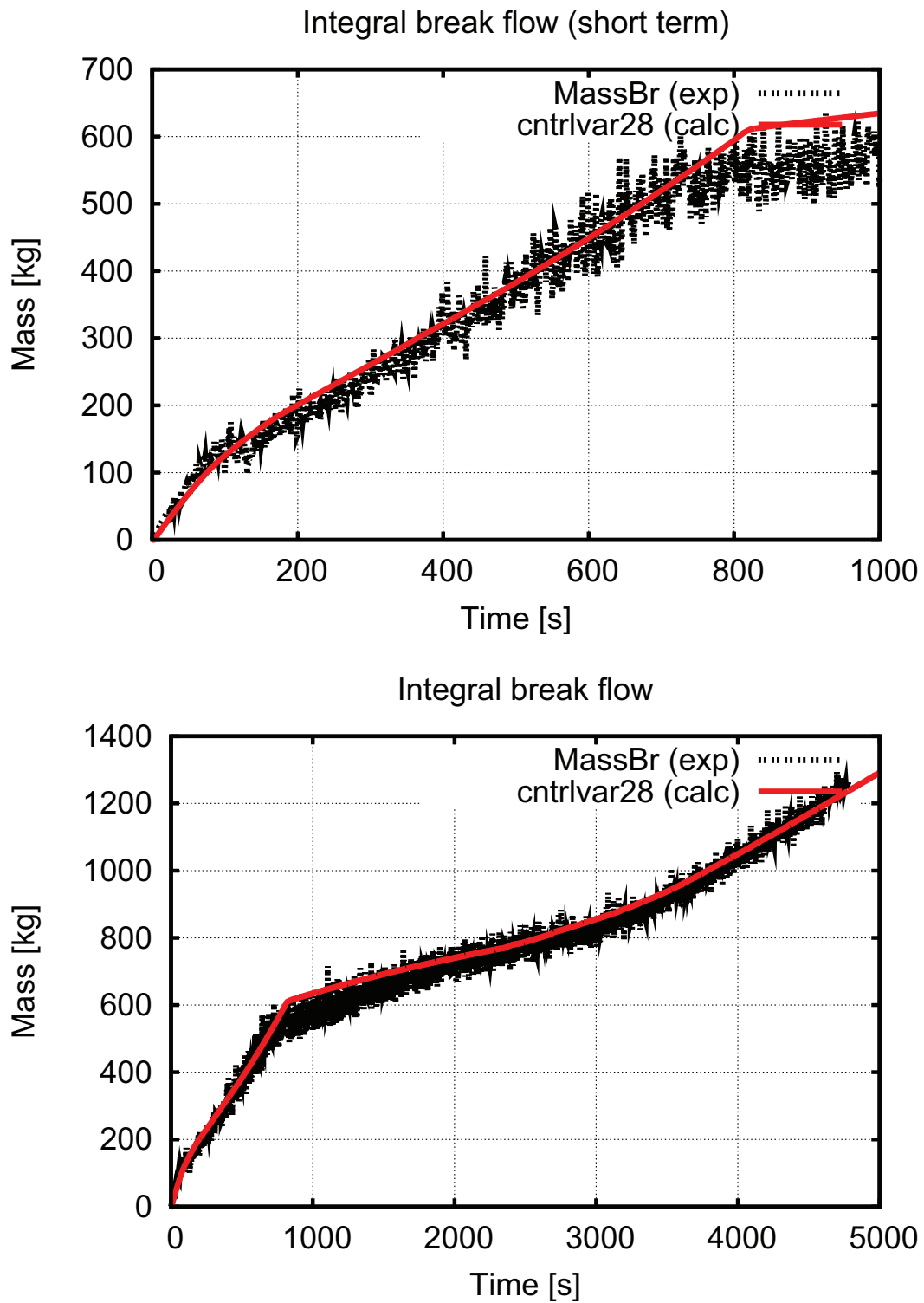


Figure 3.25: Post test 11 results, integral flow rate through the break, short and long term

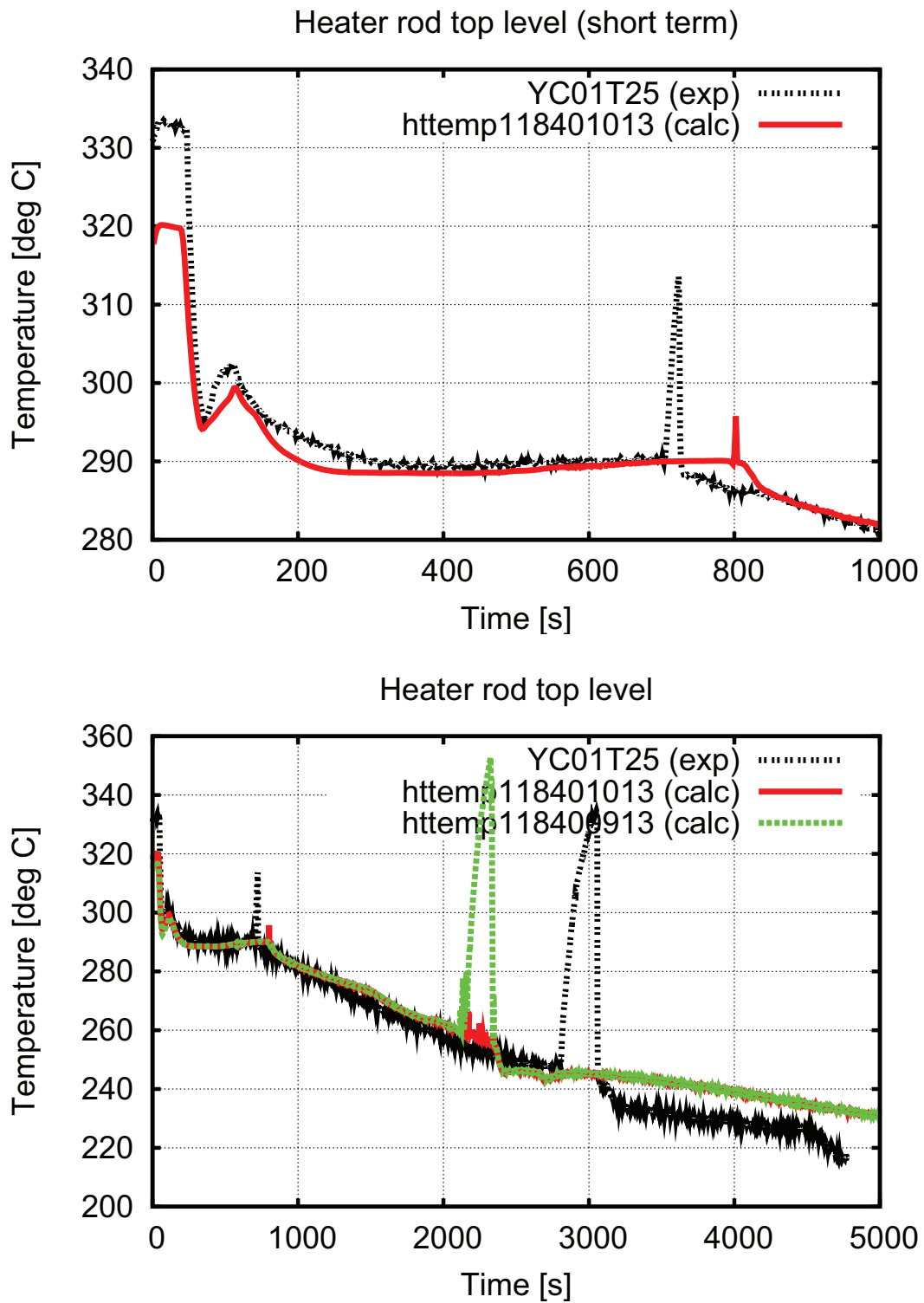


Figure 3.26: Post test 11 results, heater rod cladding temperature top, short and long term

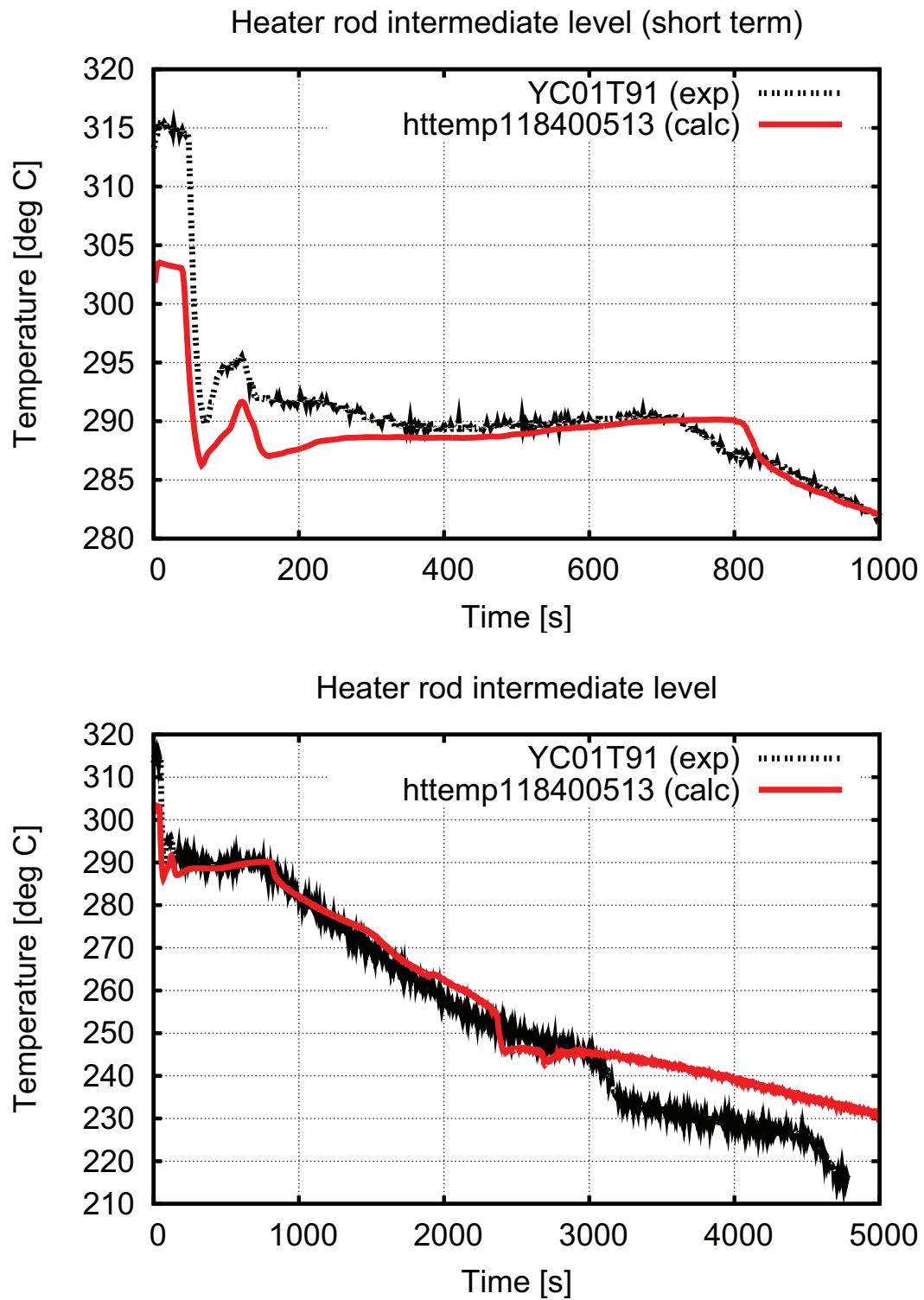


Figure 3.27: Post test 11 results, heater rod cladding temperature middle, short and long term

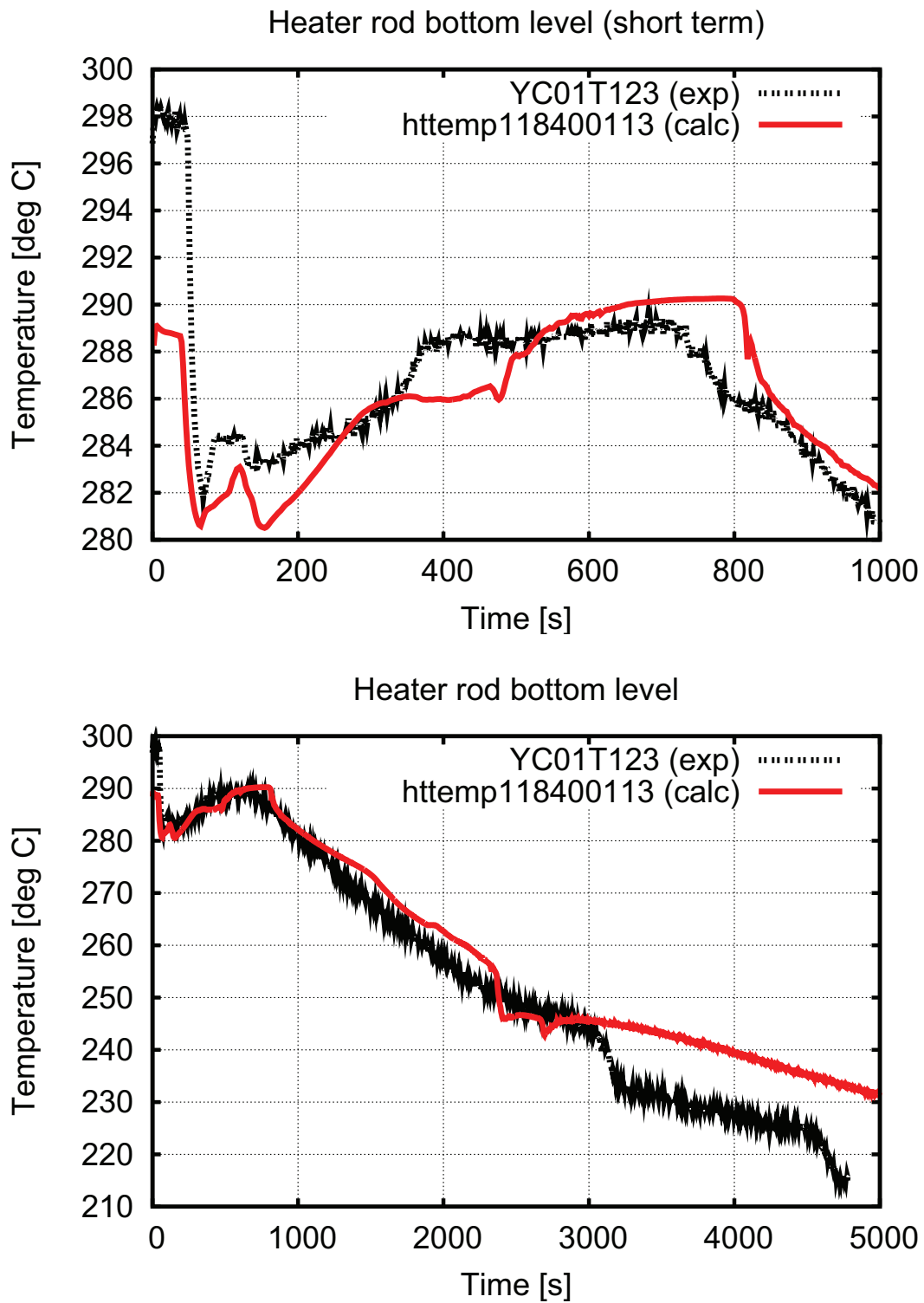


Figure 3.28: Post test 11 results, heater rod cladding temperature bottom, short and long term

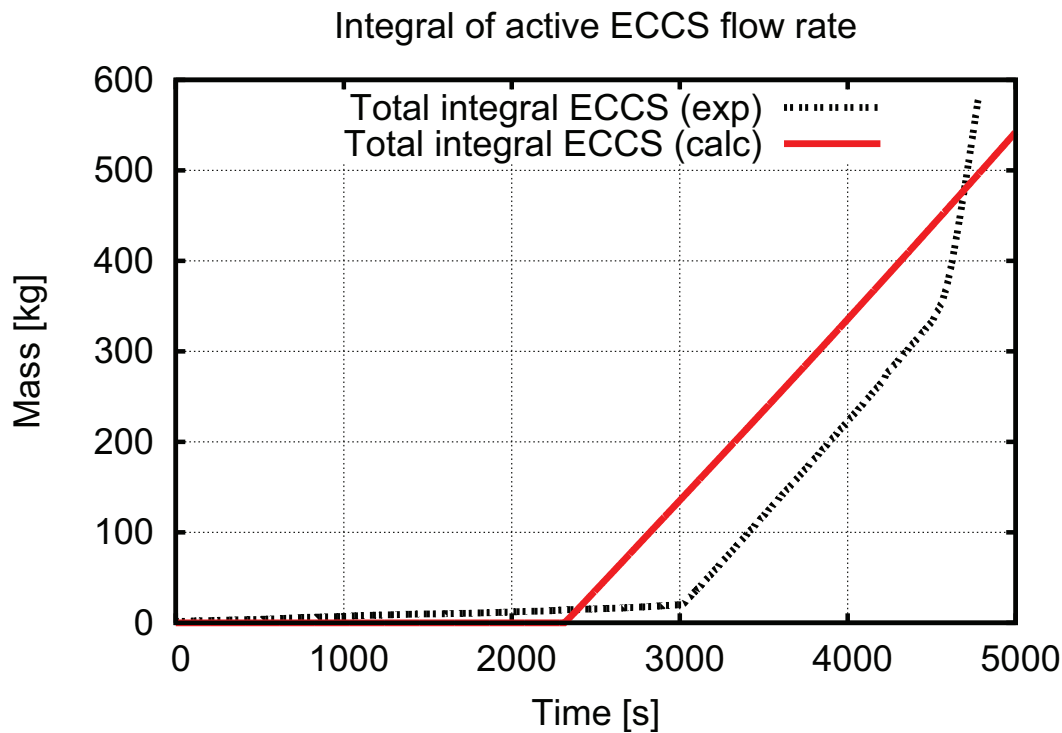


Figure 3.29: Post test 11 results, integral eccs flow rate

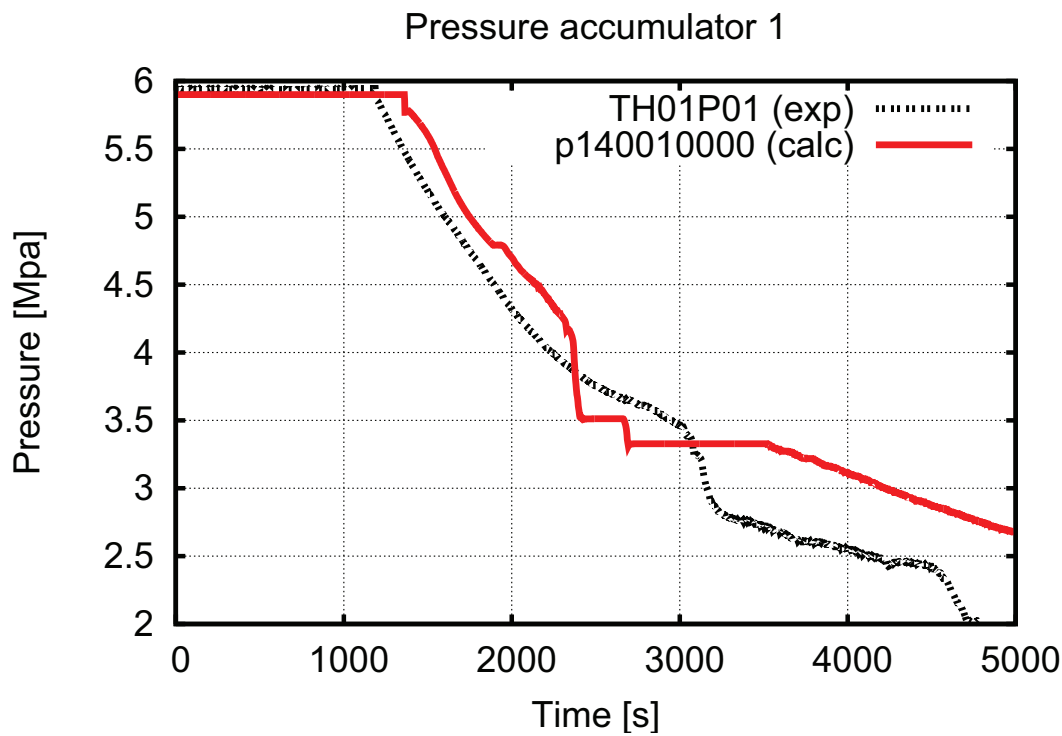


Figure 3.30: Post test 11 results, pressure in accumulator 1

		UNIT	EXP	CALC R5	Judg. R5
RTA: Pressurizer emptying					
TSE	emptying time*	s	64.5	70	E
	scram time	s	46	37	E
IPA	integrated flow from Surge Line (from 0 up to emptying)	kg	-	-	-
RTA: Steam generators secondary side behavior					
TSE	main steam line valve closure	s	70.6	52	M
	feed water valve closure	s	-	-	-
	difference between PS and SS pressure at 100 s	MPa	2.3	2.0	E
SVP	SG level · at the end of subcooled blow- down · when PS pressure equals SS pressure when HPIS starts	m	2.25,2.30 2.31,2.38 2.32,2.27 2.32,2.37 2.29,2.27 2.27,2.24	2.29,2.41 2.41,2.46 2.29,2.41 2.41,2.46 2.35,2.33 2.27,2.27	R,R R,R R,R R,R E,E E,E
SVP	SG pressure · at the end of subcooled blowdown · when PS pressure equals SS pressure · when HPIS starts	MPa 7.15	6.84,6.85 6.84,6.85 7.1,7.1 7.1 5.14,5.15 5.19,5.15	7.1,7.1 E,E 7.1,7.1 E,E 7.1,7.1 E,E 7.1,7.1 5.5,5.5 R,R 5.5,5.5 R,R	 E,E
RTA: Subcooled blowdown					
TSE	upper plenum in sat. conditions	s	140	130	E
	break two phase flow	s	758	820	E
IPA	break flow up to 30 s	kg	48	41	R
RTA: First dryout occurrence (+)					
TSE	time of dry out	s	703	798	R
	range of dry out occurrence at various core levels	s	703-712	798-804	E
	peak cladding temperature	°C	314	295	R
SVP	average linear power	kW/m	0.39	0.38	E
	core power / primary mass	kW/kg	0.65	0.76	R
IPA	integral of dry out at 2/3 of core height	°C s	2480	-	-
NDP	primary mass / initial mass	%	40	33	R
RTA: Rewet by loop seal clearing					
	time of loop seal clearing	s	717 Loop #2	800 Loop #1	R R
TSE	range of rewet occurrence	s	-	-	-
	time when rewet is completed	s	-	-	-

Table 3.13: Test 11 - judgement of code calculations on the basis of RTA (part 1)

		UNIT	EXP	CALC R5	Judg. R5
RTA: Saturated blowdown					
TSE	PS pressure equal to SS pressure	s	725	825	R
IPA	integrated flow from 400 to 1000 s	kg	277	315	R
RTA: Mass distribution in primary side					
TSE	time of minimum mass occurrence	s	3000	2315	M
SVP	minimum primary side mass	kg	230	195	R
	av. linear power at min. mass	kW/m	0.34	0.32	E
	minimum mass/ITF volume	kg/m ³	191	158	R
RTA: Accumulators behavior					
TSE	accumulators injection starts	s	1180	1360	R
IPA	total mass delivered by accumulators	kg	71	152	M
NDP	minimum primary mass/initial primary mass	%	50	84	M
	primary mass/initial accumulator mass	%	133	132	E
RTA: Final dryout occurrence					
TSE	time of dry out	s	2802	2110	M
	range of dry out occurrence at various core levels	s	2802-3000	2110-2350	R
	peak cladding temperature	°C	336	352	E
SVP	average linear power	kW/m	0.34	0.34	E
	maximum linear power	kW/m	-	-	-
	rate of rod temperature increase	K/s	0.35	0.5	R
	core power / primary mass	kW/kg	0.82	1.0	R
IPA	integral of dry out at 2/3 of core height	°C s	-	-	
NDP	primary mass / initial mass	%	28	22	R
RTA: HPIS intervention					
TSE	HPIS start	s	3000	2315	M
	range of rewet occurrence		3040 - 3047	2325 - 2350	M
	final rewetting	s	3040	2350	M
IPA	integrated flow from start to end of rewet	kg	5.5	6.7	R
NDP	primary mass/initial mass	%	25	22	E

Table 3.14: Test 11 - judgement of code calculations on the basis of RTA (part 2)

3.1.4 Post test analysis 7 - SBO with operator actions

Full title of the Test is “SBO with operator actions on SS depressurization for FW supply” Experiment 7 specifications can be found in detail in [Elkin et al., 2005c]. The experiment is the 7th of the TM, simulating a SBO. It is assumed that the operator is able to attach an external supply of feed water to SG1 after the upper plenum temperature exceeds 350°C. In the experiment the flow rate of 67g/s of feed water is sufficient to slowly cool down the primary circuit, although primary side pressure remains at a high level.

Description of the experiment The test 7 specifications and scenario can be found in detail in Elkin et al. [2005c] and Elkin et al. [2005d]. Initial event is a SBO, which means a loss of all off-site and on-site power. After the initial event natural circulation together with the cycling BRU-A valves is capable to remove the residual heat, until the SGs are boiled dry. Approximately at this moment the temperature in the PS starts to rise. This in turn causes the PRZ level to rise, and the PS pressure to increase. The PS pressure increase becomes severe once the pressurizer is solid. The PORV valve starts to cycle.

When the UP fluid temperature reaches a value of 350°C (about 10000 s from the beginning of the transient), the operator succeeds in connecting an external source of feed water to the feed water line: he closes all four MSIV and depressurizes SG1 and SG4. When the pressure in SG1 drops below 1MPa, the mobile pumps are able to furnish feed water with a flow rate of 67 g/s into SG1. The procedure is successful - the primary side pressure increase can be stopped, and the UP fluid temperature starts to decrease. At 15000 s after the beginning of the transient the experiment is terminated.

Configuration of the PSB-VVER facility Please refer to table 3.15 for the configuration of the facility. A more detailed description on the configuration of the facility and the initial and boundary conditions can be found in Elkin et al. [2005c] and Elkin et al. [2005d].

Equipment	Connection status
Pressurizer	Connected to loop #2
Core by-pass	2 throttle with 2 orifices of diameter 7 mm are installed at inlet and outlet of core by-pass
ECCS hydroaccumulators	Not used
HPIS&LPIS	Not used
Steam generators	Steam dump of all SG is connected to one steam collector during steady state. Steam discharge and valve RA06S01
Feed water heater	On. SG level under steady-state conditions is maintained by supply of feed water with a temperature of ≈ 220 °C
ADS simulation system	ADS are connected to each SG. In each ADS line, throttle channel (L/d=10) diameter 12.1 mm in diameter. Actuation set points are 7.16/6.28 MPa
PRZ relief valve simulation system	System is located in the PRZ. Actuation set points are 18.14/16.67. Leak channel: 3 mm diameter, L = 20 mm.
UP warming-up line	Under steady state the line is open. The warming-up of the UP top part is stopped about 2 min before the SBO.

Table 3.15: Test facility configuration, taken from Elkin et al. [2005d]

Description of the experiment Please refer to table 3.16 for an overview over the imposed events. A more detailed description of the initial and boundary conditions, as well as the experimental results can be found in Elkin et al. [2005c] and Elkin et al. [2005d]. Table 3.17 presents the main events during the experiment. The following description of the experiment is taken mainly from Elkin et al. [2005d].

The following description is mainly following [Elkin et al., 2005c]:

The transient may be divided into three main stages:

- evaporation of SGs by opening of ADS valves (0 - 5146 s);
- depressurization of primary side by opening PRZ relief valve (5146 - 10014 s);
- accident management procedure for primary side cooldown (10014 - 15016 s).

The experiment was started issuing a scram-signal (the core simulator power was decreased to 300 kW and further it was practically constant till the end of experiment) and by closing the feed water and steam dump valves. The MCP coast-down began at the 0 s and continued until 232 s, the PRZ heaters were set to 12 kW and kept constant at that value to compensate for the PRZ heat losses.

Since the steam flow rate was reduced faster than the feed water flow rate, the SG level was increasing in the first 15 s, as was the SG pressure.

By 200 s the secondary pressure reached the value of 7.16 MPa and the ADS valves were the first time actuated. They were effective in reducing the SS pressure, and at a pressure of 6.28 MPa they were closed again. They cycled until 7833 s. With every cycle the SG inventory was decreased. The SG level trend shows a step function.

As a result of the evaporation of water of the secondary side and the reduction of the SG level the heat transfer surface primary-secondary was reduced, and therefore the efficiency of the SGs. The coolant temperature at SGs primary side outlet started to increase. By 5146 s the primary pressure was at 15.4 MPa - after that the primary pressure started to increase. By 6315 s the primary pressure reached the value of 18.14 MPa and PRZ relief valve was opened, succeeding in reducing the ps pressure, was closed, and kept on cycling from that time on.

At 10014 s the cladding temperatures increased to 350°C and the AM procedure was initiated. It started with the closure of the FASIVs in SG2 and SG3. At 10029 s, after the MSIVs were closed, the ADS in SG-1 and SG-4 were fully opened. The decreasing of the secondary pressure in SG-1 and SG-4 continued until it reached the value of 1 MPa and at 10282 s; this was the signal for the opening of isolation valve RL01S06 (simulating the operator intervention - start the primary side cooldown through ADS of SG-1). Water was supplied into SG-1 with flow rate of 67 g/s.

The cold water supplied into the SG-1 led to a decrease in primary pressure. From this moment and up to the end of the experiment there was the decreasing of the PRZ level due to primary side cooldown. The level of SG1 started to increase. Between 10282 s and 15016 s slow pressure and primary side temperature decrease could be observed. At the 15016 s the primary side pressure was at 14.3 MPa and the coolant temperature 320°C - the experiment was terminated.

The result of the calculation with the code Relap5 are presented. Table 3.3 shows the time of occurrence of important events, comparing the experimental data with the Relap5 results.

Relap5 results The results of the calculation are summarized in Figures 3.31 to 3.38 and in Table 3.18, which reports the timing of main events.

Conclusion The analysis shows that the code is capable of reproducing the most important phenomena of the test. However, due to uncertainties in the boundary conditions (heat losses which cannot be exactly given), the code run shows significant differences in the timing. From a formal point of view, the calculation would fail to pass as “qualified calculation” according to the standards of the University of Pisa, because the primary side pressure FFTBM results are above the threshold of 0.1. But one should keep in mind that the FFTBM has been developed and tested mainly for LOCA calculations; the high value of 0.37 for the primary pressure trend derives mainly from the discrepancies during the cycling of the PRZ safety valve simulator. In the experiment the valve opens and closes eight times, while the calculation predicts eleven cycles. Judging from the primary pressure trend, this difference is owed to the fact that the primary pressure in the experiment drops with every opening of the valve to 16 MPa, while in the calculation only the first opening shows a drop to 16 MPa, for all following openings the PP stays closer to the closure set-point. Therefore, the time to reach again the opening set point is lower in the calculation than in the experiment. From a qualitative point of view, this is an acceptable difference; the overall behaviour is well caught - the start of primary pressure increase and the primary temperature trends (which is the set point for the operator action) agrees reasonably well.

EVENT	pre-set	actual
Start blackout	0 s	0 s
Beginning of RA06S01 closing	0 s	0 s
Finishing of RA06S01 closing		16 s
Beginning of RL01-04S07 closing	0 s	0 s
Finishing RL01S07 closing		6 s
Finishing RL02S07 closing		11 s
Finishing RL03S07 closing		15 s
Finishing RL04S07 closing		7 s
Start of PCS program of the electric power reduction at core and core by-pass	0 s	0 s
MCP coast down onset	0 s	0 s
Stop PRZ heaters power change	0 s	0 s
Cycling of ADS valves	pressure set point	
Cycling of the PRZ valve	pressure set point	
Closure of the MSIV in SG2 and SG3	YC01Tmax=350°C	YC01T09=350°C
Finishing of RA08S01 closing		TMSIV + 16s
Finishing of TA09S01 closing		TMSIV + 10s
Opening of BRU-A in SG1 and SG4	TMSIV + 15s	TMSIV+15s
Finishing of RA11S01 opening		TMSIV + 19 s
Finishing of RA14S01 opening		TMSIV + 20 s
Water supply from external source into SG1 with flow rate of 67g/s	YB01P01 = 1 MPa	YB01P01 = 1 MPa

Table 3.16: Imposed sequence of main events for PSB Test 7

EVENT	Time (s)
Start of SBO	0
Stop of PRZ heater change	0
Start of closing steam discharge valve RA06S01	0
Start of MCPs coast down	0
Start of core and core by-pass power reduction	5.6
Complete closing of feed water valves	
RL01S06	6
RL02S06	11
RL03S06	15
RL04S06	7
Stopping of SG steam discharge (full closing of RA06S01 valve)	16
Beginning of ADS cycling	200
Complete switch off of MCPs	232
Start of primary pressure increase	5146
Begin of PRZ relief valve cycling	6315
Closure of MSIV in SG2 and SG3 (YC01T09=350°C)	10014
Opening of ADS in SG1 and SG4	10029
Water supply into SG1, G=67g/s, YB01P01=1MPa	10282
Stop of experiment	15016

Table 3.17: Sequence of the principal events in test 7 taken from Elkin et al. [2005c]

EVENT	EXP (s)	R5 (s)
Start of station blackout	0	0
Stop of PRZ heater change	0	0
Start of closing steam discharge valve RA06S01	0	0
Start of MCPs coast down	0	0
Start of core and core by-pass power reduction	5.6	0
Complete closing of feed water valves		
RL01S06	6	5
RL02S06	11	10
RL03S06	15	15
RL04S06	7	5
Stopping of SG steam discharge (full closing of RA06S01 valve)	16	21
Beginning of ADS cycling	200	114
Complete switch off of MCPs	232	232
Start of primary pressure increase	5146	5123
Beginning of PRZ relief valve cycling	6315	6726
Closure of MSIV in SG2 and SG3 (YC01T09=350°C)	10014	10439
Opening of ADS in SG1 and SG4	10029	10445
Water supply into SG1, G=67g/s, YB01P01=1MPa	10282	10541
Stop of experiment/calculation	15016	15000

Table 3.18: Post test 7 comparison experiment/calculation

	Parameter	AA	WF	ω_i
1	PRZ pressure	0.37	0.011	0.070
2	SG1 pressure	0.54	0.010	0.046
3	SG2 pressure	0.65	0.016	0.046
4	SG4 pressure	0.53	0.010	0.046
5	core inlet temperature	0.14	0.014	0.107
6	core outlet temperature	0.11	0.013	0.107
7	upper head fluid temperature	0.34	0.013	0.107
8	heater rod bottom	0.16	0.019	0.075
9	heater rod middle	0.17	0.018	0.075
10	heater rod top	0.16	0.021	0.075
11	core power	0.18	0.027	0.022
12	DP core	0.20	0.011	0.017
13	DP loop seal	0.63	0.003	0.017
14	DP across DC and UH bypass	0.20	0.007	0.017
15	DP SG1 inlet and top	0.16	0.013	0.017
16	DP SG4 inlet and top	0.17	0.020	0.017
17	DP UP and core outlet	0.18	0.004	0.017
18	SG1 level	0.18	0.027	0.030
19	SG2 level	0.11	0.022	0.030
20	SG4 level	0.18	0.016	0.030
21	PRZ level	0.34	0.010	0.030
	TOTAL	0.26	0.015	

Table 3.19: Post test 7 results, the accuracy evaluation following the FFTBM

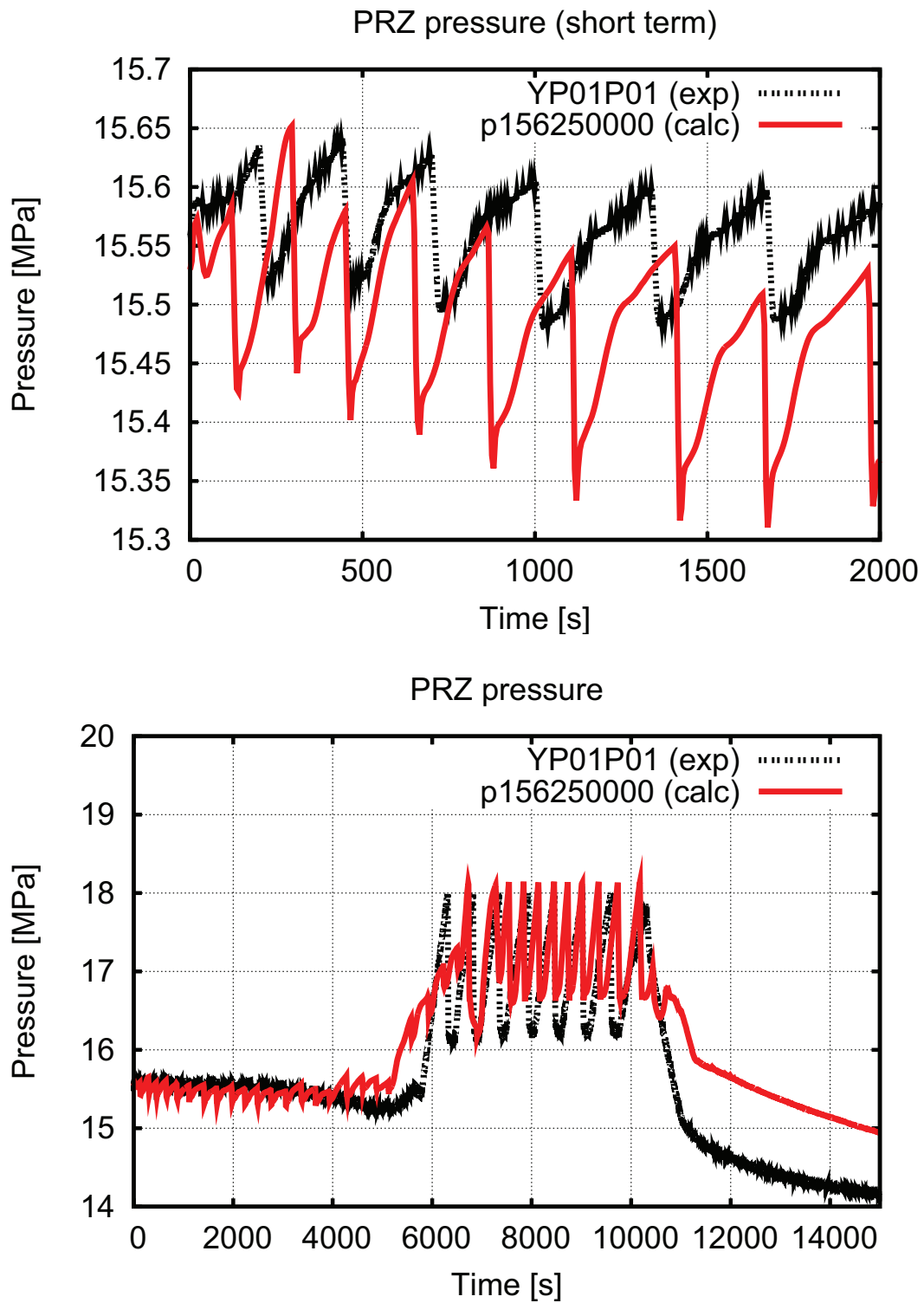


Figure 3.31: Post test 7 results, primary side pressure

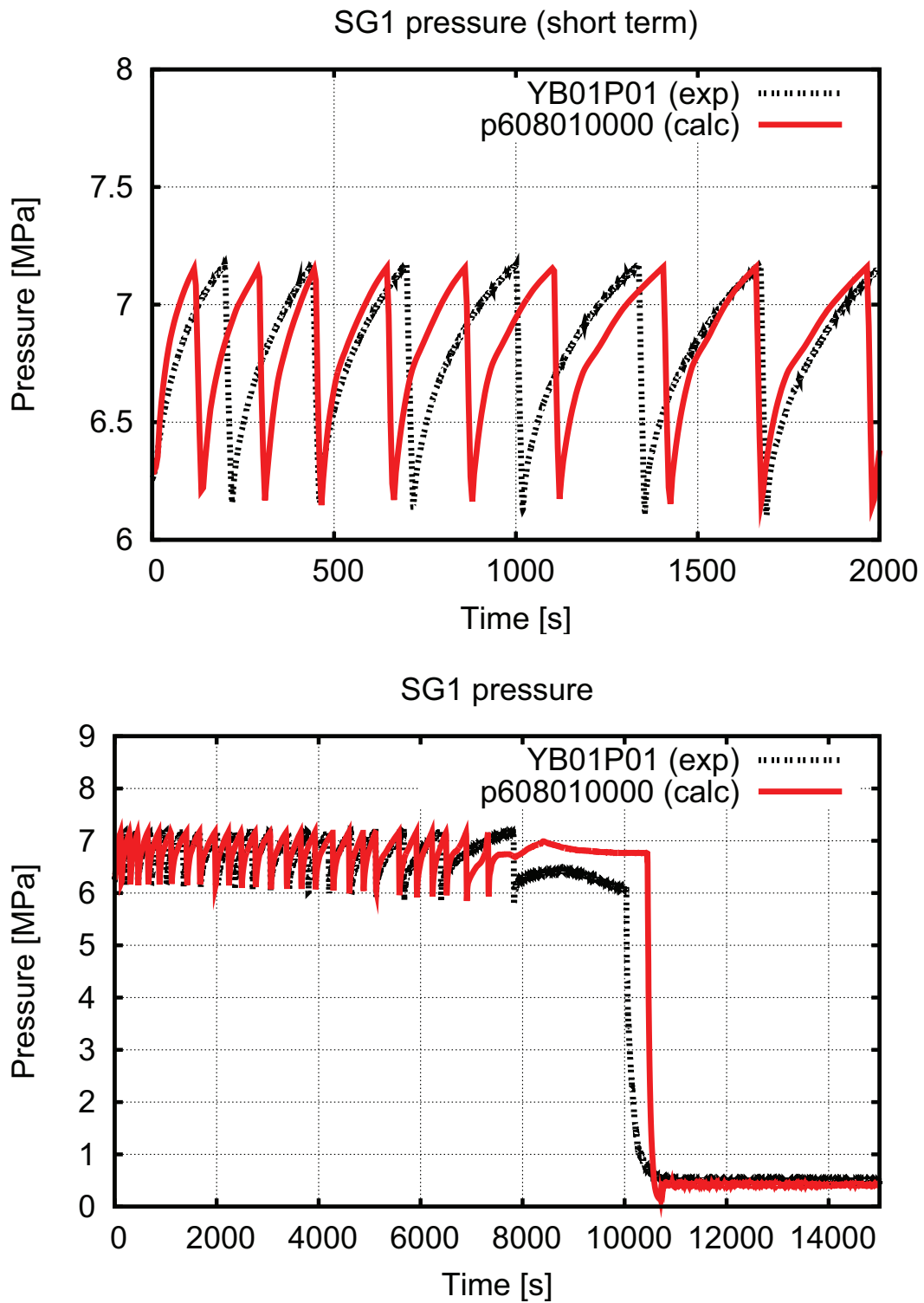


Figure 3.32: Post test 7 results, SG1 pressure

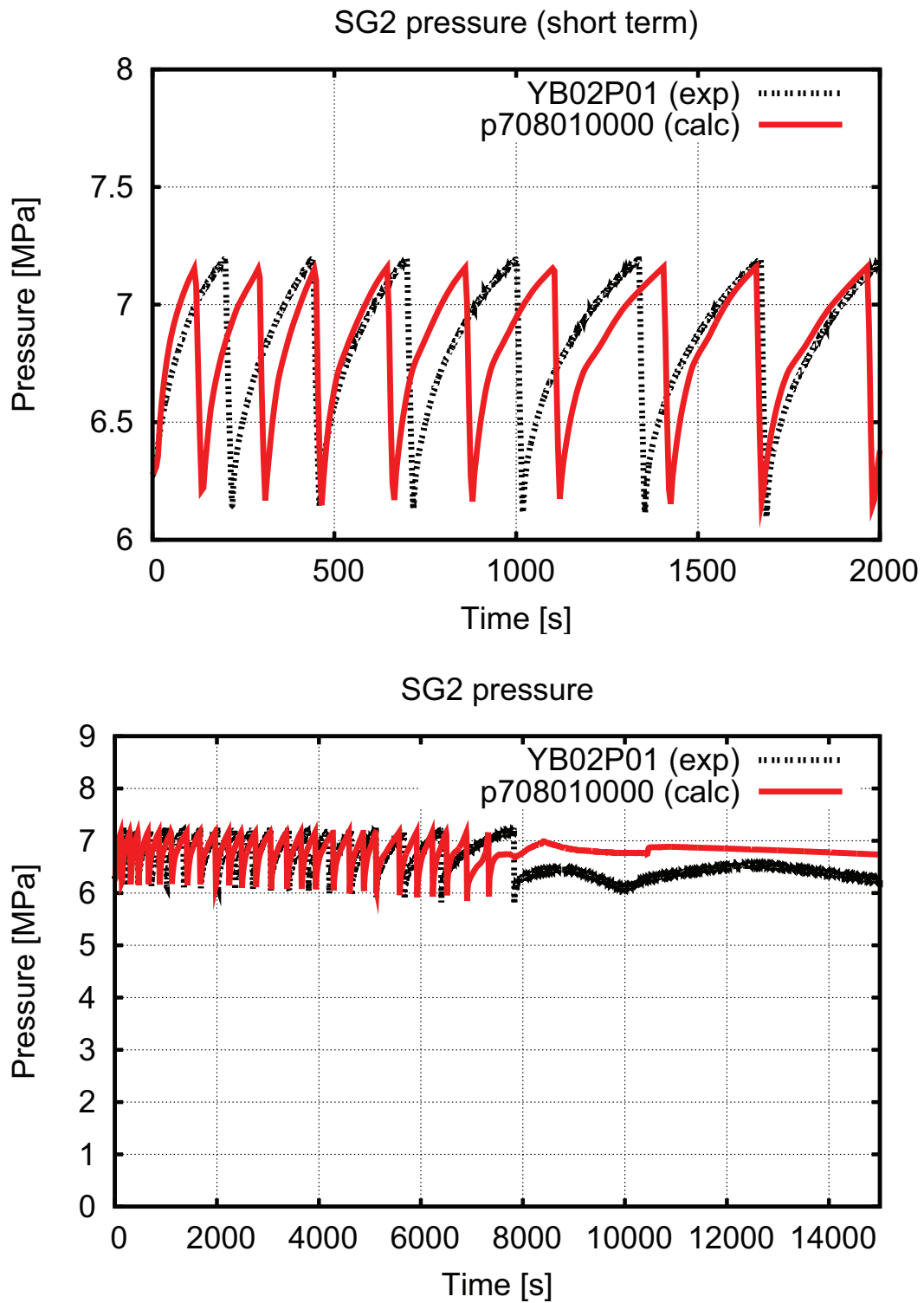


Figure 3.33: Post test 7 results, SG2 pressure

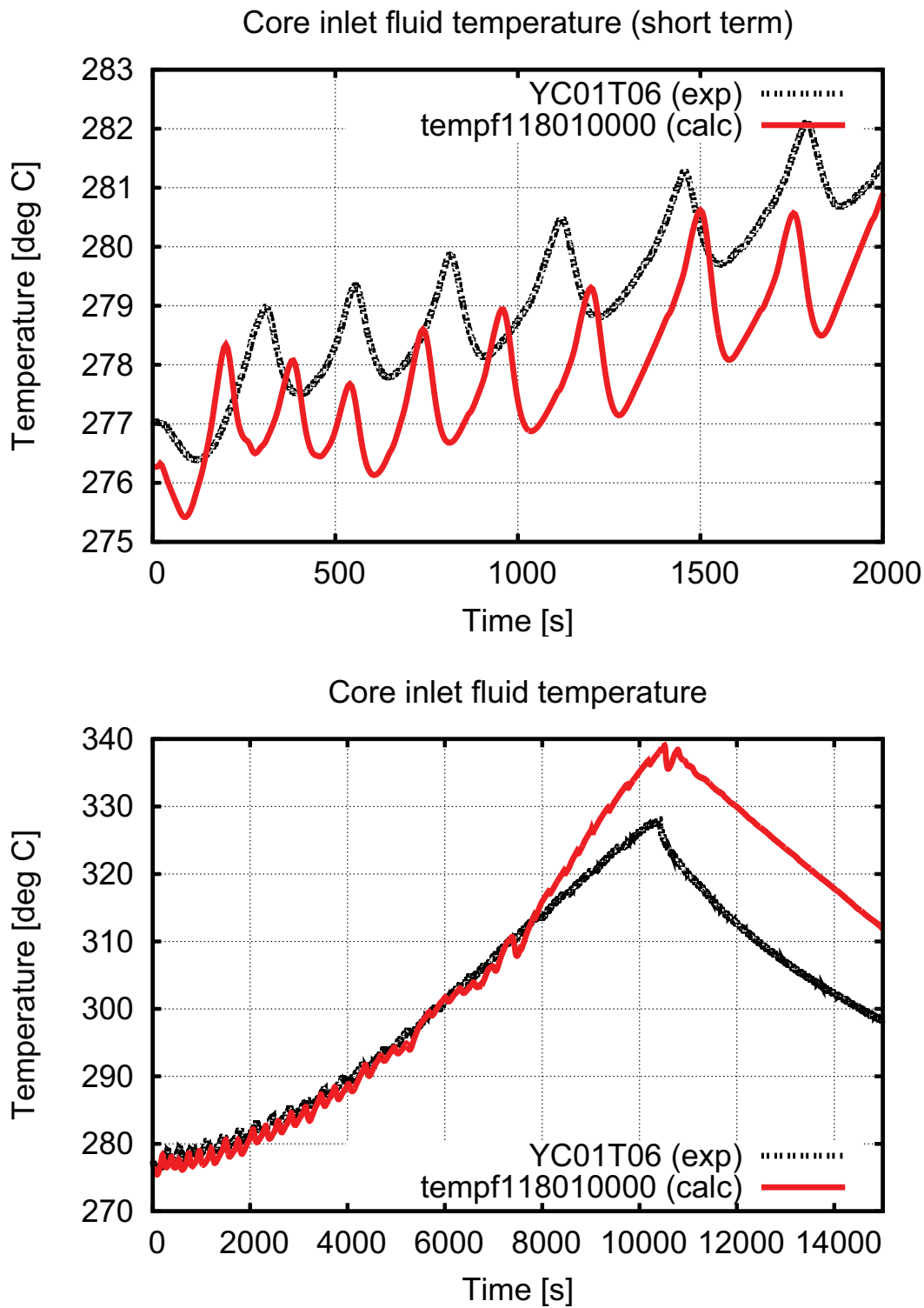


Figure 3.34: Post test 7 results, core inlet temperature, short and long term

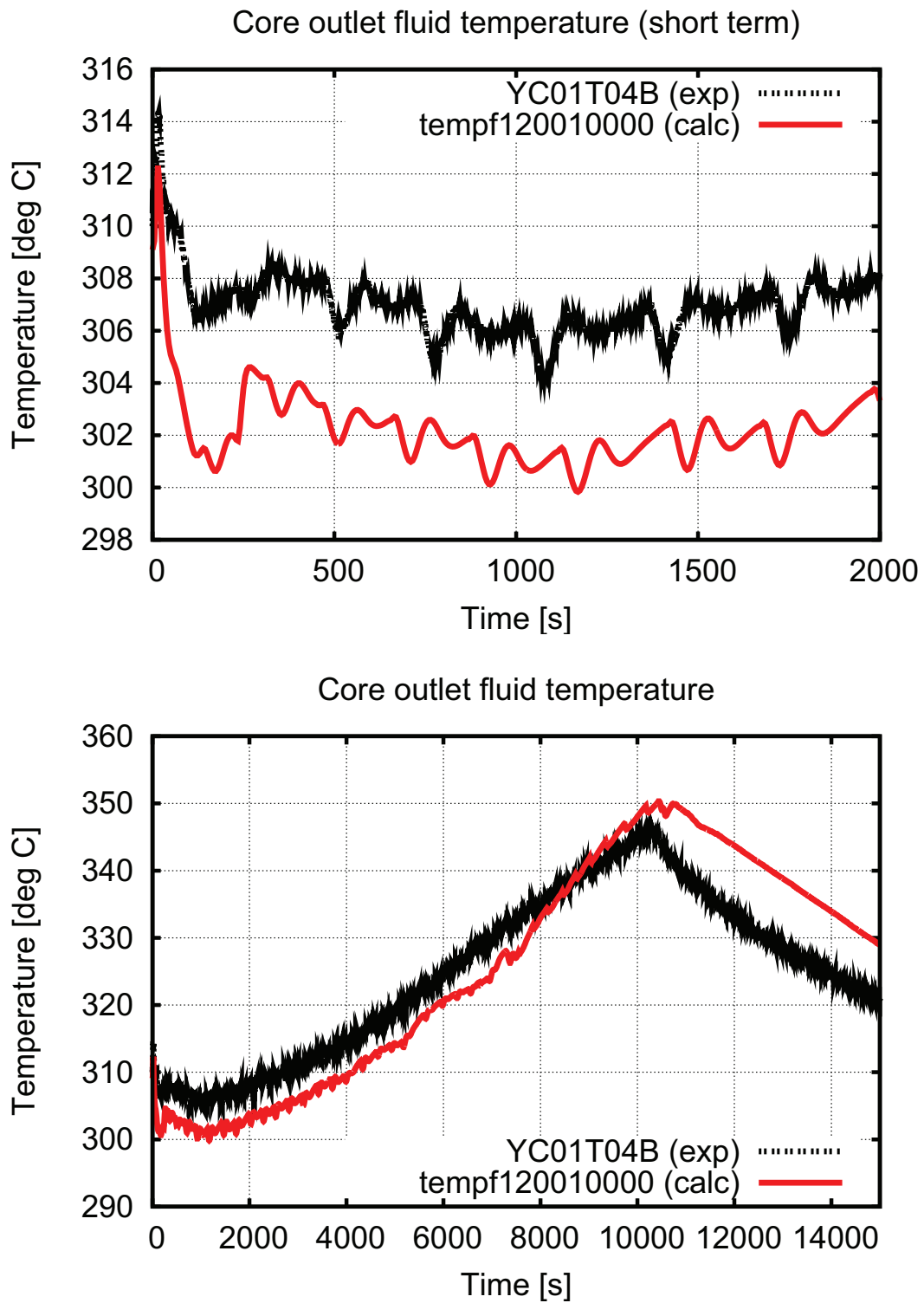


Figure 3.35: Post test 7 results, core outlet temperature, short and long term

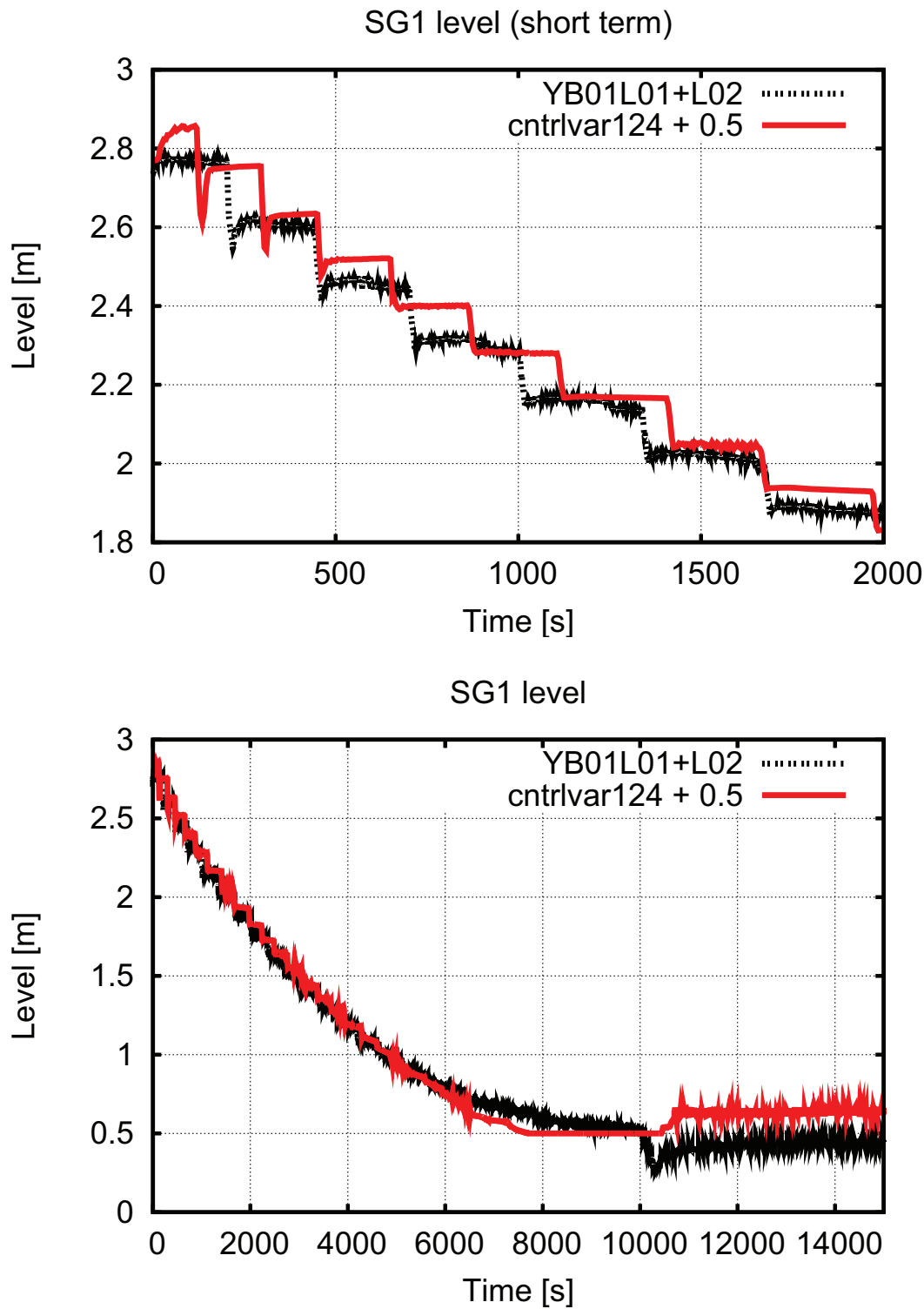


Figure 3.36: Post test 7 results, level SG1, short and long term

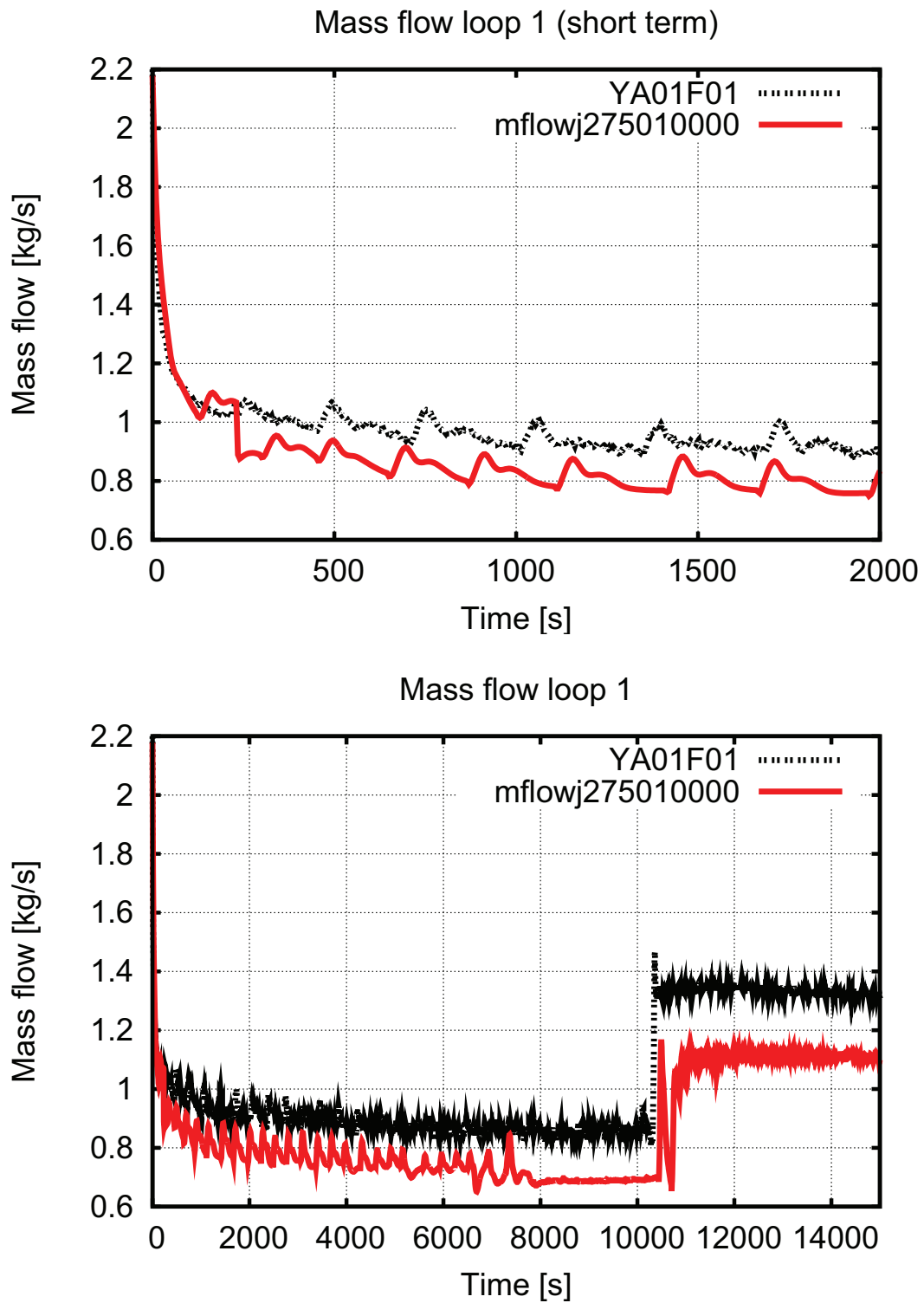


Figure 3.37: Post test 7 results, loop 1 mass flow rate, short and long term

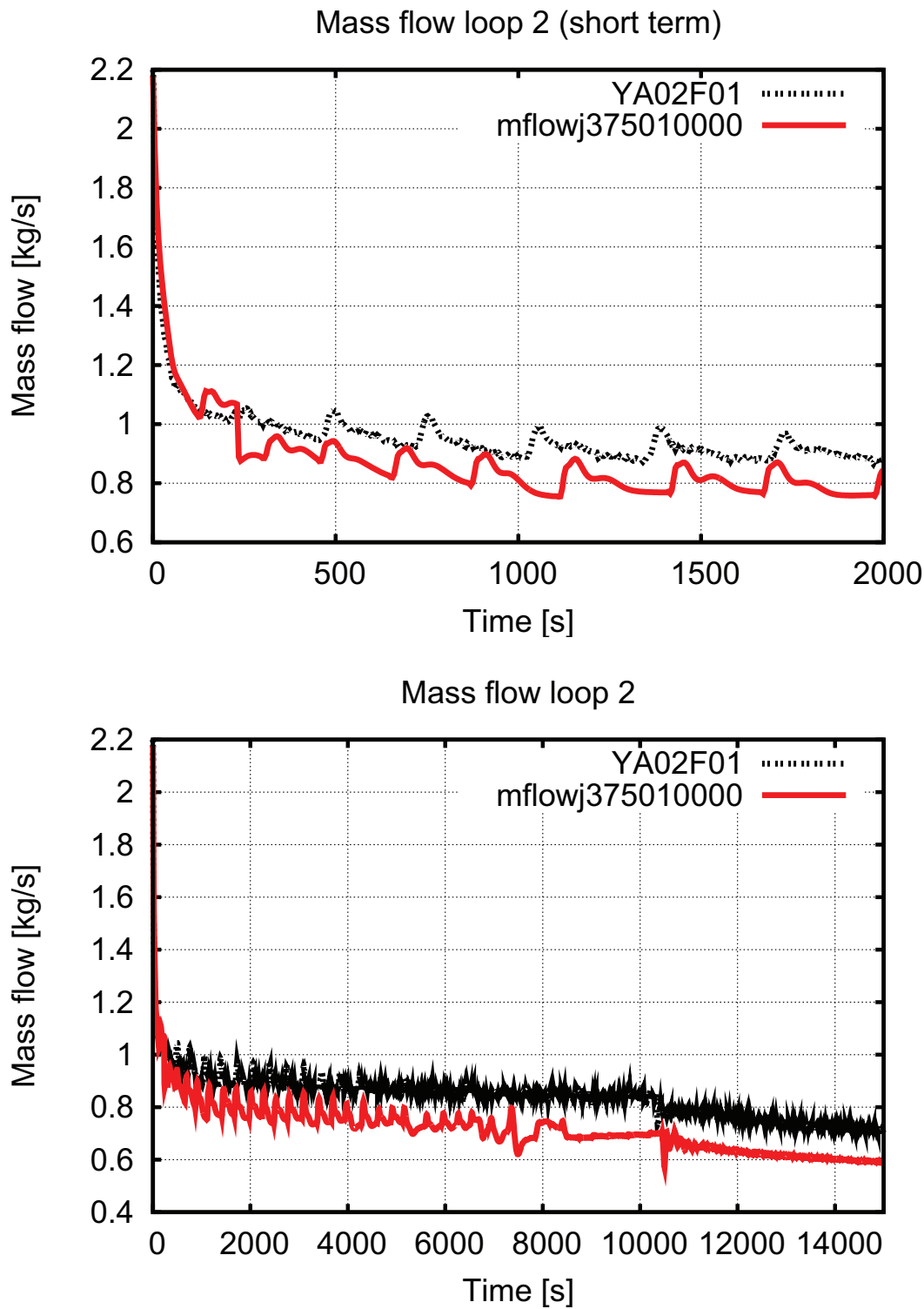


Figure 3.38: Post test 7 results, loop 2 mass flow rate, short and long term

3.1.5 Post test analysis 1 - LOFW with operator actions

The experiment is the 1th of the TM, simulating a total LOFW. It is assumed that the operator is able to attach an external supply of feed water to SG1 and SG4 after the upper plenum temperature exceeds 350°C. In the experiment the flow rate of 33 g/s of feed water is furnished into each of the two SG, and is sufficient to slowly cool down the primary circuit. The primary side pressure decreases at first slowly - then, after the PRZ heaters are switched off on PRZ low level signal, the PS depressurization rate increases.

Description of the experiment The test 1 specifications and scenario can be found in detail in Elkin et al. [2005a] and Elkin et al. [2005b]. Initial event is a LOFW, which means a loss of all sources of feed water (main, auxillary and emergency feed water). Together with the feed water pumps the TSV is closed. The MCP trip occurs on low level in the SG, and the reactor scram is simulated after three out of four pumps are tripped. Natural circulation together with the cycling BRU-A valves is soon ineffective in removing the residual heat. Average PS temperature and in turn the PRZ level start to increase. When the PRZ is full and the PS is solid, PS pressure increases fast. The PORV valve starts to cycle.

When the UP fluid temperature reaches a value of 350°C (about 11300 s from the beginning of the transient), the operator succeeds in connecting an external source of feed water to the feed water line: he closes all four MSIV and depressurizes SG1 and SG4. When the pressure in the SG drops below 1MPa, the mobile pumps are able to furnish feed water with a flow rate of 33 g/s into each of SG1 and SG4. The procedure is successful - the primary side pressure increase can be stopped, and the UP fluid temperature starts to decrease. At 21760 s after the beginning of the transient the experiment is terminated.

Configuration of the PSB-VVER facility Please refer to table 3.20 for the configuration of the facility. A more detailed description on the configuration of the facility and the initial and boundary conditions can be found in Elkin et al. [2005a] and Elkin et al. [2005b].

Equipment	Connection status
Pressurizer	Connected to loop #2
Core by-pass	2 diaphragms with 2 orifices of diameter 7 mm are installed at inlet and outlet of core by-pass
ECCS hydroaccumulators	ACC #1 and #3 are connected to the outlet plenum, ACC #2 and #4 are connected to the inlet chamber
HPIS&LPIS	Two lines of LPIS are connected to the hot and cold legs of loops #1, #3 and #4
Steam generators	Under steady state all SG are connected to each other by the steam header. The pressure is adjusted by one steam dumping valve
Feed water heater	On. SG level under steady-state conditions is maintained by supply of feed water with a temperature of ≈ 216 °C
ADS simulation system	ADS are connected to each SG. In each ADS line, throttle channel L=50mm, diameter 12.1 mm. Actuation set points are 7.16/6.28 MPa
Pressurizer spray	The injection water is supplied from the feed water header Actuation set points are 16.08/15.98 MPa
PRZ relief valve simulation system	System is located in the PRZ. Actuation set points are 18.14/16.67. Leak channel: 3 mm diameter, L = 20 mm.
Line for UP warming-up	Under steady state the line is open. The warming-up of the UP top part is stopped about 2 min before the start of the test.

Table 3.20: Test 1 facility configuration, taken from Elkin et al. [2005b]

Please refer to table 3.21 for an overview of the imposed events. A more detailed description of the initial and boundary conditions, as well as the experimental results can be found in Elkin et al. [2005a] and Elkin et al. [2005b]. Table 3.22 presents the main events during the experiment. The following description of the experiment is taken mainly from Elkin et al. [2005b].

The transient may be divided into five main stages:

- primary pressure increase (0-71s);

- warming-up of the primary side coolant and water evaporation from SGs in the secondary side (ADS operation) (71-6146 s)
- warming-up of the primary side coolant and periodical coolant discharge from the primary side through PRZ relief valve;
- primary side cool down through ADS of SG-1 and SG-4 with PRZ electric heater being switched on (11600-17524 s);
- primary side cool down through ADS of SG-1 and SG-4 with PRZ power being switched off (17524-21769 s).

The experiment was started with the signals generated simultaneously by PCS to close isolation valves of feed water supply in SG (RL01-04S06) and to close the control valve of the steam dumping from SGs (RA06S01).

First phase 0 - 71 s

Steam dumping and feed water supply were totally stopped by 15 s and 12 s accordingly. After starting the closure of the corresponding valves and as a result of the balance between the quantity of steam discharged and water supply, it was observed a SG level increase lasting till 25 s. When the steam dumping is stopped SG pressure and temperature begin growing. As a result of decreasing of temperature difference between the primary and secondary side, primary pressure and temperature start to increase. Temperature increase in the cold legs at the SG outlet causes the reduction of the flow rate in circulation loops of the test-facility. At 71 s secondary pressure reaches the set point of ADS actuation. ADS actuation was observed 17 times during the whole experiment

Second phase 71 - 6146 s

Every ADS actuation leads to a short time intensification of heat removal from the primary side and as a consequence to the reduction of primary pressure and temperature. Temperature decrease at SG outlet results in a short time growing of the flow rate in circulation loops of the test-facility (≈ 0.1 kg/s). At the time of every regular ADS actuation secondary pressure after closure of ADS valve differs greatly from the low actuation set point. Such behavior of secondary pressure is explained by a fast pressure reduction under ADS actuation due to the decrease of steam generation intensity caused by the diminution of secondary coolant mass and by the progressive reduction of the heat exchange surface.

Because the speed of valve simulating ADS operation during its opening and closure remains constant, secondary pressure has time to diminish till a lower value.

Nearly simultaneously with ADS actuation a set point is reached to actuation the PRZ spray (YC01P16=16.08 MPa) at 73 s. The injection in PRZ of coolant with a temperature 30 °C and a flow rate 35 g/s is performed during the period between the 77 and 98 s.

ADS operation and injection in PRZ leads to the primary pressure decrease. Further during ADS actuation, primary pressure at the time of MCP operation does not reach the set point of actuation PRZ spray.

As a result of ADS operation SGs levels reduce. At 256 s as a consequence of the level decrease in SG-1 on 0.5 m from the nominal value MCP coast down begins in this loop. In the third loop MCP coast down begins at 259 s and in the other ones at 260 s. The coasts down of all MCPs are finished at 491 s and after that a singlephase natural circulation is set in the primary side. As MCP-1 coast down is the first one the flow rate of the natural circulation in the first loop is set two times less than in other loops ≈ 0.45 and ≈ 1 kg/s accordingly.

At the moment of the third pump coast down the signal is generated to simulate SCRAM which leads to the beginning of electric power decrease in the core and bypass zones at 265.5 s. At the same time with the beginning of the fourth pump coast down the signal is generated to stop the operation of PRZ spray.

The start of electric power reduction at the core model effects to a short time cessation of pressure increase in the primary side of the test-facility under ADS valves closed.

As a result of secondary side voiding and decrease of SG level there is a voiding of heat exchange surface. It leads to the reduction of cooling efficacy for the primary side coolant. In spite of absence of temperature growing at the core outlet during the period between 285 and 1500 s (it is even observed its little decrease caused by electric power reduction) cold legs temperature of the test-facility grows.

During the period between 1500 and 4000 s there is a monotone increase of coolant temperature in the primary side accompanying the slow pressure increase. The increase of coolant temperature occurs with the reduction of its density. It leads to the ousting of the coolant in PRZ and as a consequence to the level increase in it.

By 4000 s the PRZ is nearly totally filled with water. It effects the sharp speed increase of pressure growing at the primary side of the test-facility. As a result at 5396.5 s the set point of PRZ relief valve actuation is reached. Totally PRZ relief valve actuation was observed 10 times during the experiment.

Third phase 6146 - 11600

PRZ relief valve operation did not influence greatly the development of the accident process. The coolant warming-up rate in the primary side did not changes and was about 15 °C /h .

At 11294 s coolant temperature at the core outlet reached 350°C and there was a start of simulation of operators actions for accident management. At 11294 and 11300 s, FASIVs of SG-3 and SG-4 were totally closed (closure of valves RA09S01 and RA08S01) and at 11302 and 11304 ADS of SG-1 and SG-4 were totally opened (opening of valves RA14S01 and RA11S01). As a result of ADS opening in SG-1 and SG-4 secondary pressure in these SG decreased till the value of 1 MPa. At 11569 and 11601 s accordingly the feed water started to be supplied to SG1 and SG4 with a temperature of ≈ 45 °C and a flow rate ≈ 35 g/s .

Forth phase 11600 - 17524

The feed water supplying in SG-1 and SG-4 led to the intensification of heat removal from the primary side which resulted in decrease of primary temperature and pressure. Temperature reduction at the outlet of SG-1 and SG-4 led to the increase of natural circulation flow rate in these loops. Further during the whole experiment it was observed a slow flow rate decrease in all loops effected by the total cooling of the primary side. At 12062 s the speed of primary pressure decrease slowed down which was probably explained by a short time coolant boiling in the hot legs of loops #1 and #4 as well as at the core outlet, and also by the formation of a steam blanket in PRZ, as a consequence of its level reduction due to the growing of coolant density in the primary side.

During the period between 12062 and 17526 s there was a slow cooling of the installation (≈ 14 -15 °C /h) accompanied by a smooth fall of primary pressure and PRZ level.

Fifth and last phase 17524 - 21769

At 17524 s an automatic switching off of PRZ heater occurred according to the set point to have reached the minimum PRZ level. PRZ power switching off led to the sharp increase of primary pressure decrease rate. However primary temperature decrease rate did not change. PRZ power switching off also effected the reduction of PRZ level decrease rate as a result of its cooling. During the period between 17524 and 21769 s the slow cooling of the installation in the primary side continued and at the 21769 s under the primary temperature ≈ 312 °C the experiment was stopped.

EVENT	pre-set	actual
Test start	0 s	0 s
Beginning of RA06S01 closing	0 s	0.0 s
Finishing of RA06S01 closing		16.6 s
Beginning of RL01S06 closing	0 s	4.9 s
Finishing of RL01S06 closing		6.4 s
Beginning of RL02S06 closing	0 s	4.4 s
Finishing of RL02S06 closing		10.8 s
Beginning of RL03S06 closing	0 s	9.3 s
Finishing of RL03S06 closing		11.7 s
Beginning of RL04S06 closing	0 s	5.4 s
Finishing of RL04S06 closing		7.3 s
MCP1 coast down onset	YB01L01=1.20m	YB01L01=1.21m
MCP2 coast down onset	YB01L01=1.18m	YB01L01=1.19m
MCP3 coast down onset	YB01L01=1.20m	YB01L01=1.20m
MCP4 coast down onset	YB01L01=1.19m	YB01L01=1.19m
Start of PCS program of the electric power reduction at core and core by-pass	3/4 pumps tripped	3/4 pumps tripped
Cutting off electric load at PRZ	YP01L02=2.32m	YP01L02=2.42m
Cycling of ADS valves	pressure set point	
Cycling of the PRZ valve	pressure set point	
Closure of the MSIV in SG2 and SG3	YC01T04b=350°C	YC01T04b=350°C
Opening of BRU-A in SG1 and SG4	TMSIV + 15s	TMSIV+15s
Water supply from external source into SG1 with flow rate of 33g/s	YB01P01 = 1 MPa	YB01P01 = 1 MPa
Water supply from external source into SG4 with flow rate of 33g/s	YB04P01 = 1 MPa	YB04P01 = 0.96 MPa

Table 3.21: Imposed sequence of main events for PSB Test 1

Event	Time (s)
Test start	0
Beginning of RA06S01 closing	0
Beginning of RL01S06-RL04S06 closing	0.0
Finishing of RL01S06-RL04S06 closing	4.9 - 11.7
Finishing of RA06S01 closing	16.6
Start of closing steam discharge valve RA06S01	0
Start of MCP1-4 coast down	255-260
Start of core and core by-pass power reduction	265
Beginning of ADS cycling	76
Begin of PRZ relief valve cycling	5396
Closure of MSIV in SG2 and SG3 (YC01T09=350°C)	11294
Opening of ADS in SG1 and SG4	11302-11304
Water supply into SG1, SG4 G=33g/s each, YB01P01=1MPa	11569 / 11601
Switching of PRZ heaters on low level	17524
Stop of experiment	21769

Table 3.22: Sequence of the principal events in the experiment 1 taken from Elkin et al. [2005a]

Post test calculation results The results of the calculation with Relap5 for Test 1 are presented. Table 3.23 shows the time of occurrence of important events, comparing the experimental data with calculated results.

EVENT	EXP (s)	R5 (s)
Begin to stop feed water supply and steam dumping from SG	0	0
Steam discharge valve RA06S01 fully closed	15	16
Beginning of ADS cycling	76	54
Start of core and core by-pass power reduction	265.5	275
Beginning of PRZ relief valve cycling	5396.5	3850
Closure of MSIV in SG2 and SG3 (YC01T04b=350°C)	11294	7130
Opening of ADS in SG1	11302	7145
Opening of ADS in SG4	11304	7145
Water supply into SG1, G=33g/s, YB01P01=1MPa	11569	7240
Water supply into SG4, G=33g/s, YB04P01=1MPa	11601	7240
Switching of PRZ heaters	17524	12400
Stop of experiment/calculation	21769	21500

Table 3.23: Relap5 test1 comparison experiment/calculation

Table 3.24 shows the quantitative accuracy avaluation for the Relap5 calculation results. The overall accuracy is well below the acceptability limit of 0.4, while the primary side pressure is outside. This calculation is not qualified according to the standards of the University of Pisa.

Parameter	AA	WF	ω_i
1 PRZ pressure	0.50	0.009	0.070
2 SG1 pressure	0.77	0.006	0.046
3 SG2 pressure	0.62	0.014	0.046
4 SG4 pressure	0.76	0.006	0.046
5 core inlet temperature	0.16	0.008	0.107
6 core outlet temperature	0.18	0.011	0.107
7 upper head fluid temperature	0.27	0.004	0.107
8 heater rod bottom	0.13	0.008	0.075
9 heater rod middle	0.14	0.008	0.075
10 heater rod top	0.16	0.011	0.075
11 core power	0.24	0.020	0.022
12 DP core	0.22	0.007	0.017
13 DP loop seal	0.70	0.003	0.017
14 DP across DC and UH bypass	0.26	0.009	0.017
15 DP SG1 inlet and top	0.25	0.007	0.017
16 DP SG4 inlet and top	0.26	0.007	0.017
17 DP UP and core outlet	0.26	0.004	0.017
18 SG1 level	0.47	0.012	0.030
19 SG2 level	0.15	0.013	0.030
20 SG4 level	0.26	0.012	0.030
21 PRZ level	0.56	0.008	0.030
TOTAL	0.31	0.009	

Table 3.24: Relap results test 1, the accuracy evaluation following the FFTBM

The results of the calculation are summarized in Figures 3.39 to 3.56 and in Table 3.23, which reports the timing of main events.

Conclusions The analysis shows that the code is capable of reproducing the most important phenomena of the test. However, due to uncertainties in the boundary conditions (heat losses which cannot be exactly given), the code run show significant differences in the timing of main parameter trends such as primary side pressure (the phenomena are well foreseen, only at different times - which can be adjusted by utilising the

range of possible heat losses from the facility. However, this has not been done to stay with the heat losses close to the other tests. The run fail to pass as “qualified calculations” according to the standards of the University of Pisa, because the primary side pressure FFTBM-evaluation result is well above the threshold.

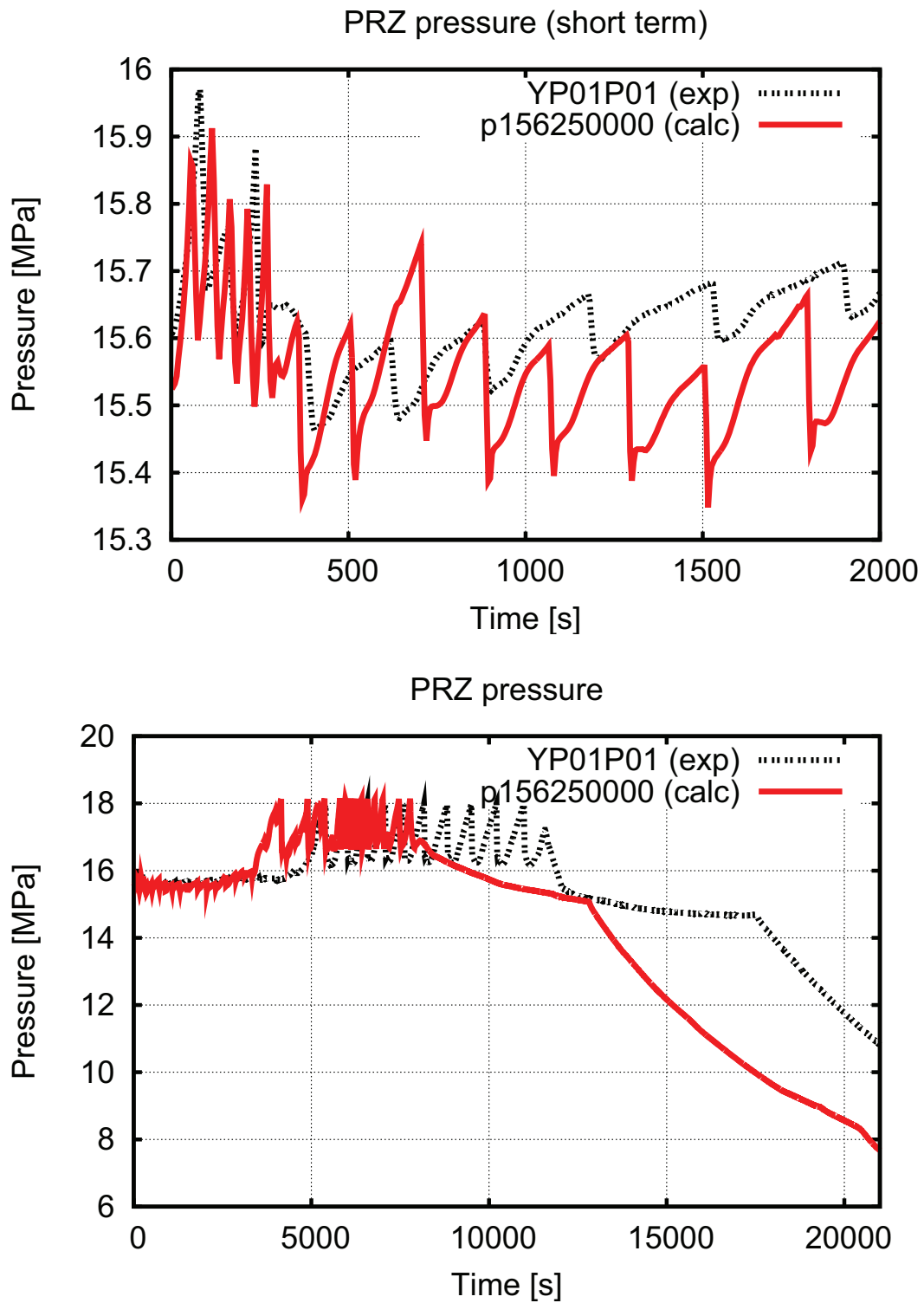


Figure 3.39: Relap results test 1, primary side pressure, short and long term

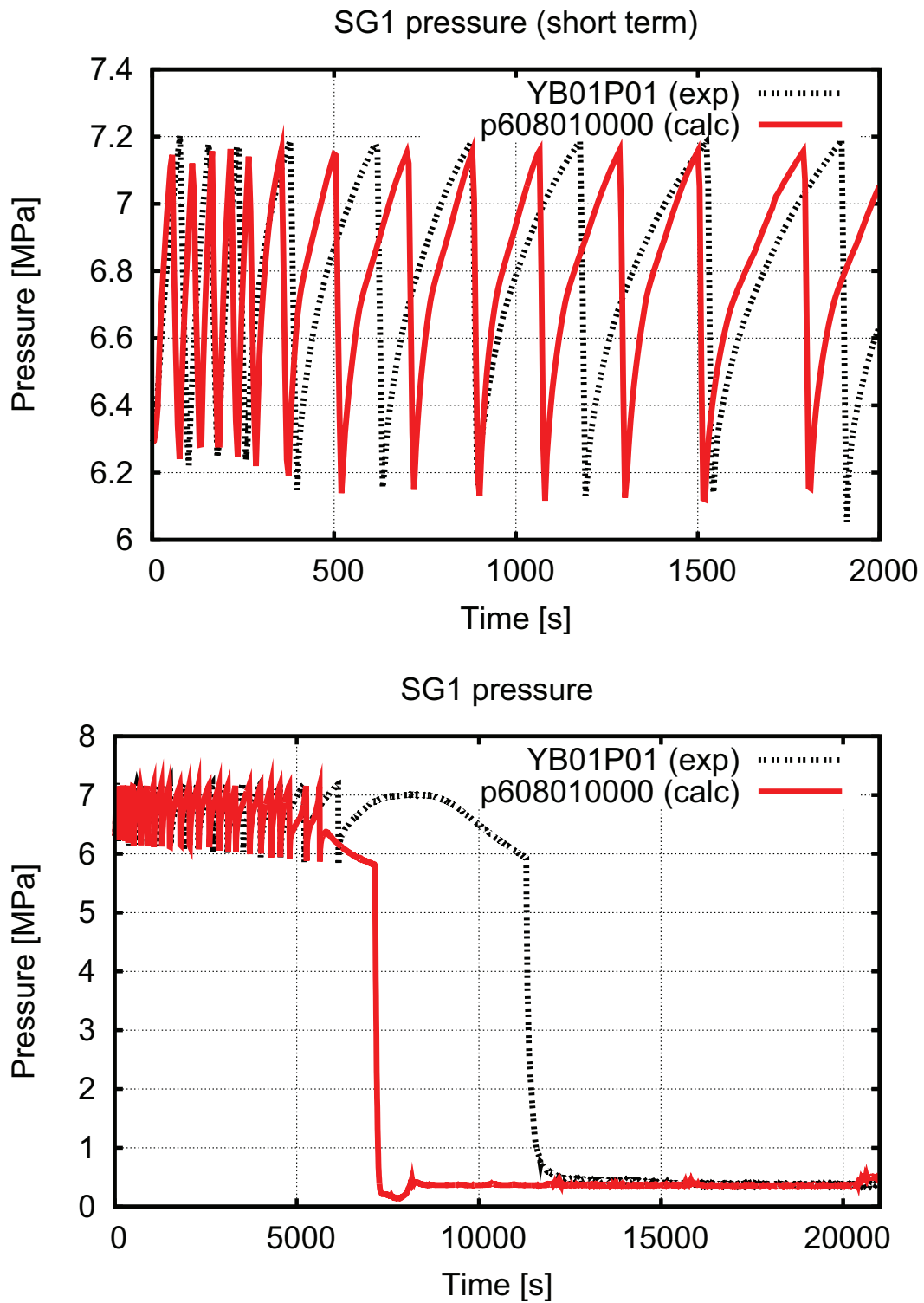


Figure 3.40: Relap results test 1, SG1 secondary side pressure, short and long term

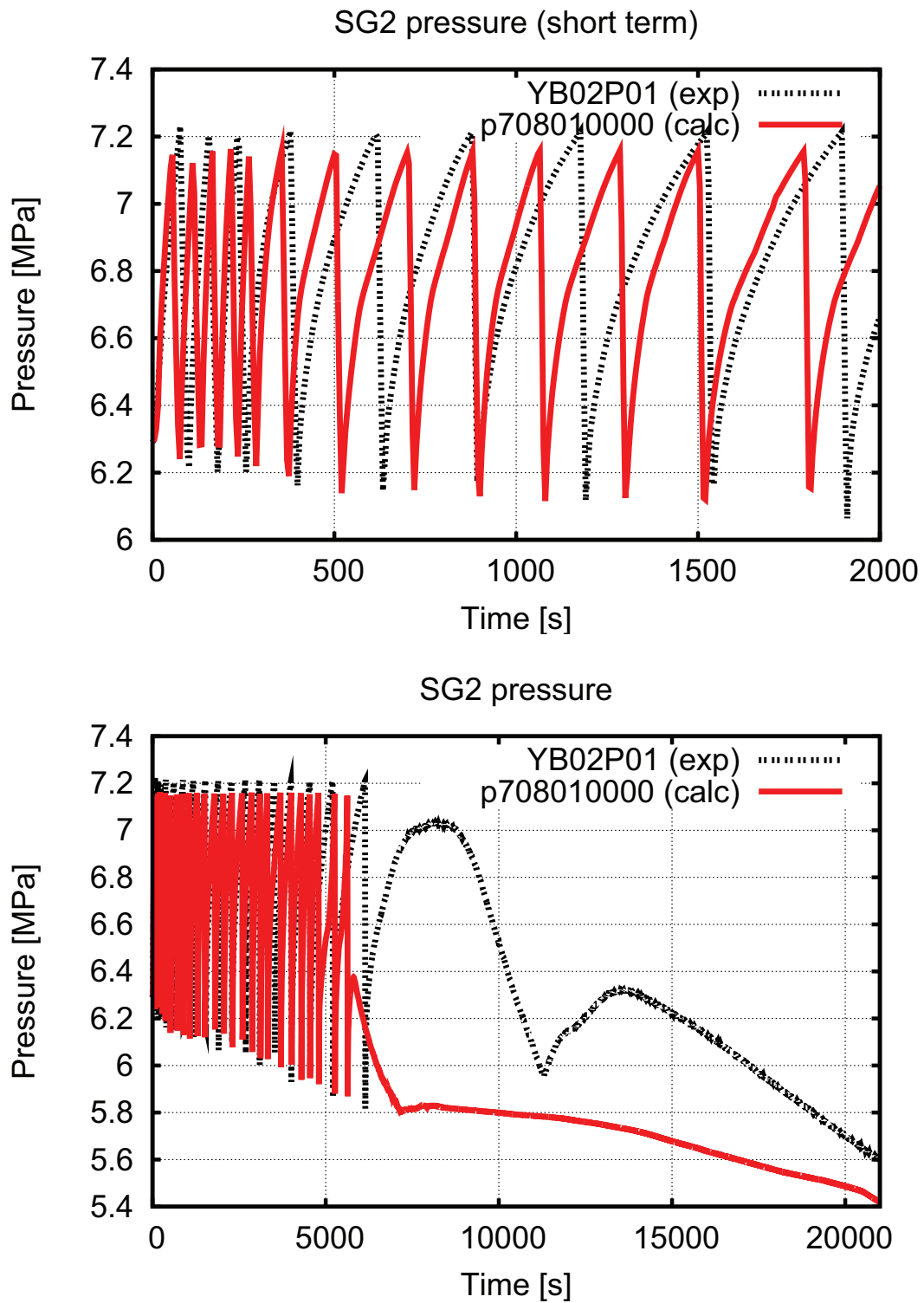


Figure 3.41: Relap results test 1, SG2 secondary side pressure, short and long term

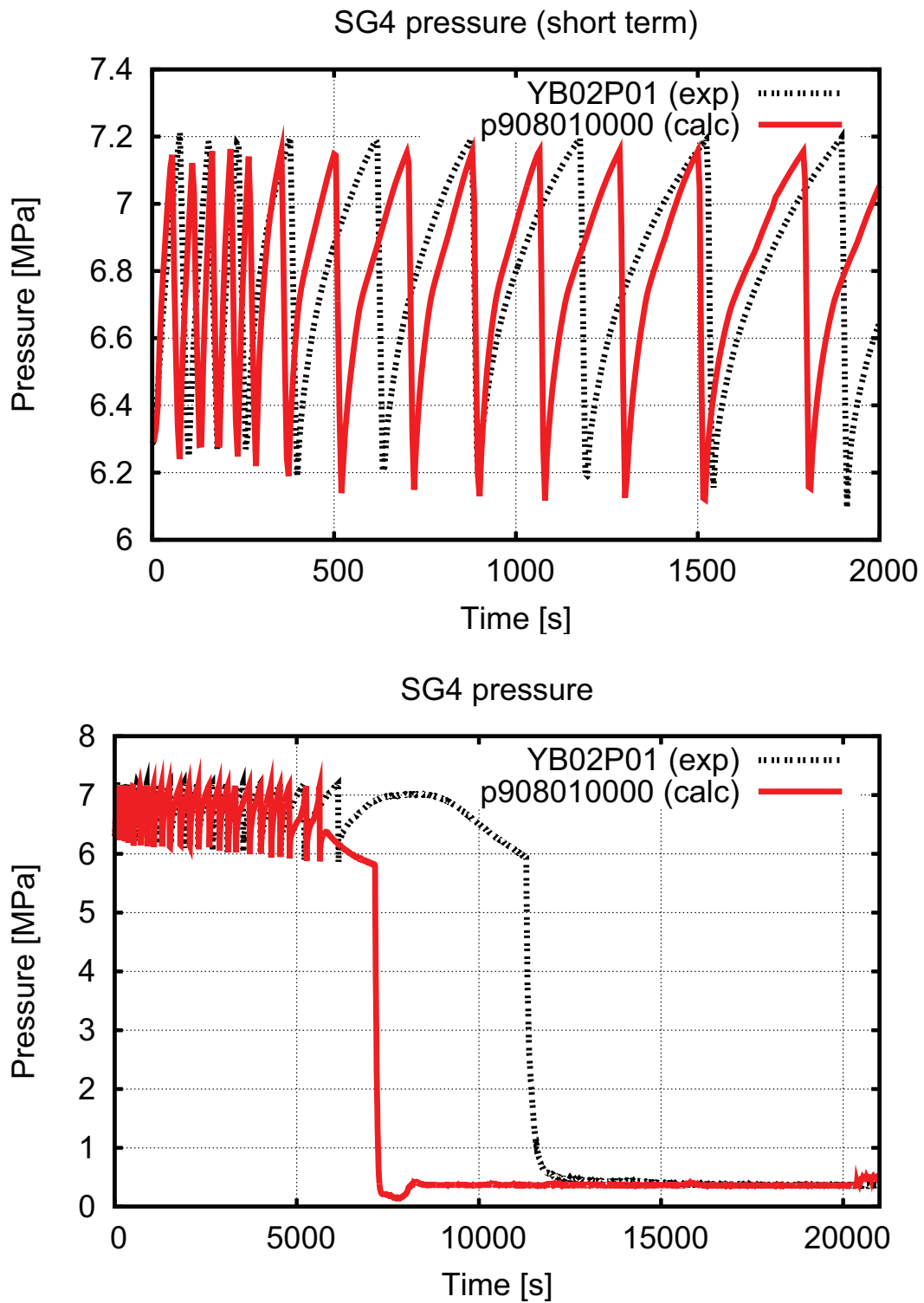


Figure 3.42: Relap results test 1, SG4 secondary side pressure, short and long term

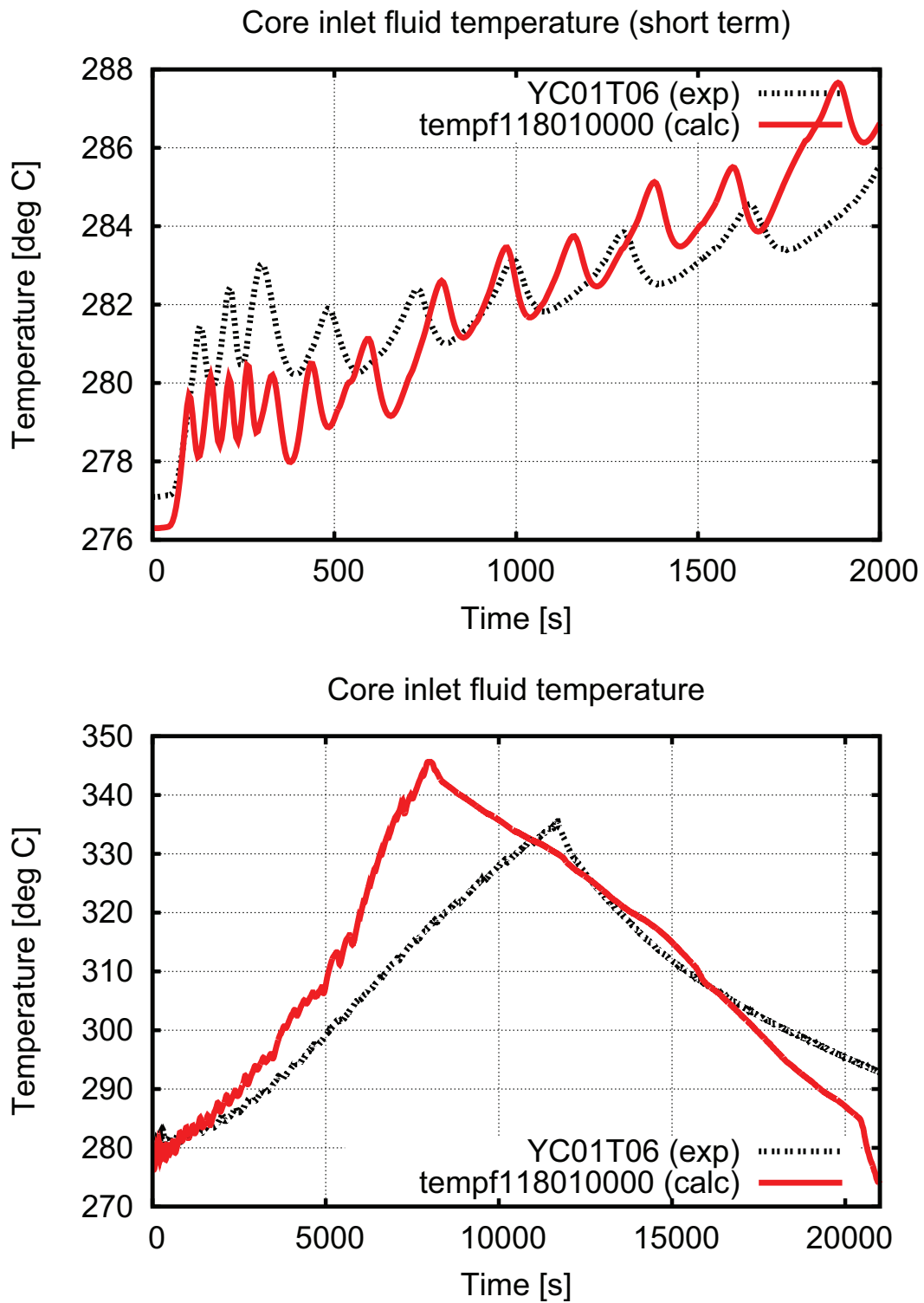


Figure 3.43: Relap results test 1, core inlet temperature, short and long term

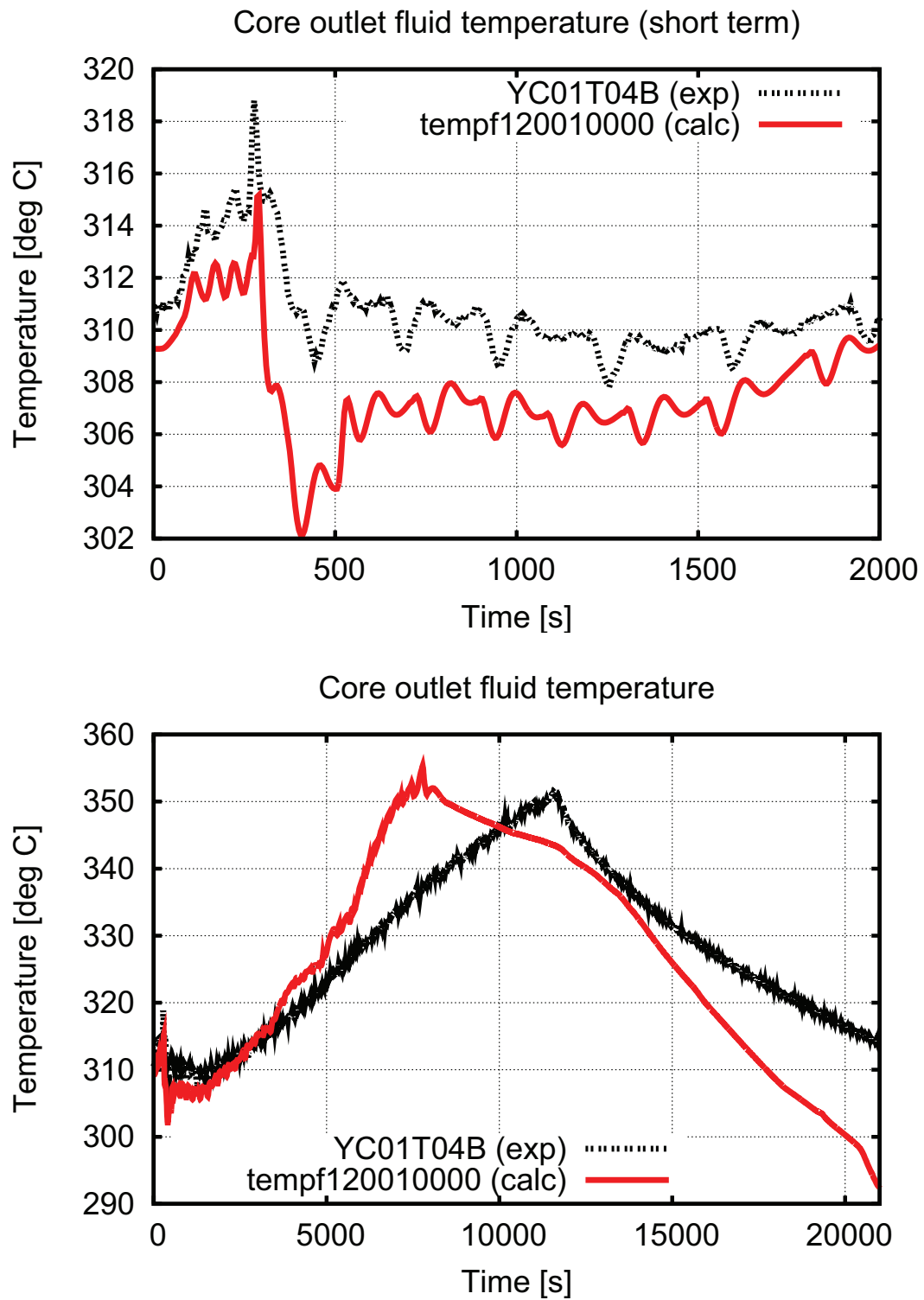


Figure 3.44: Relap results test 1, core outlet temperature, short and long term

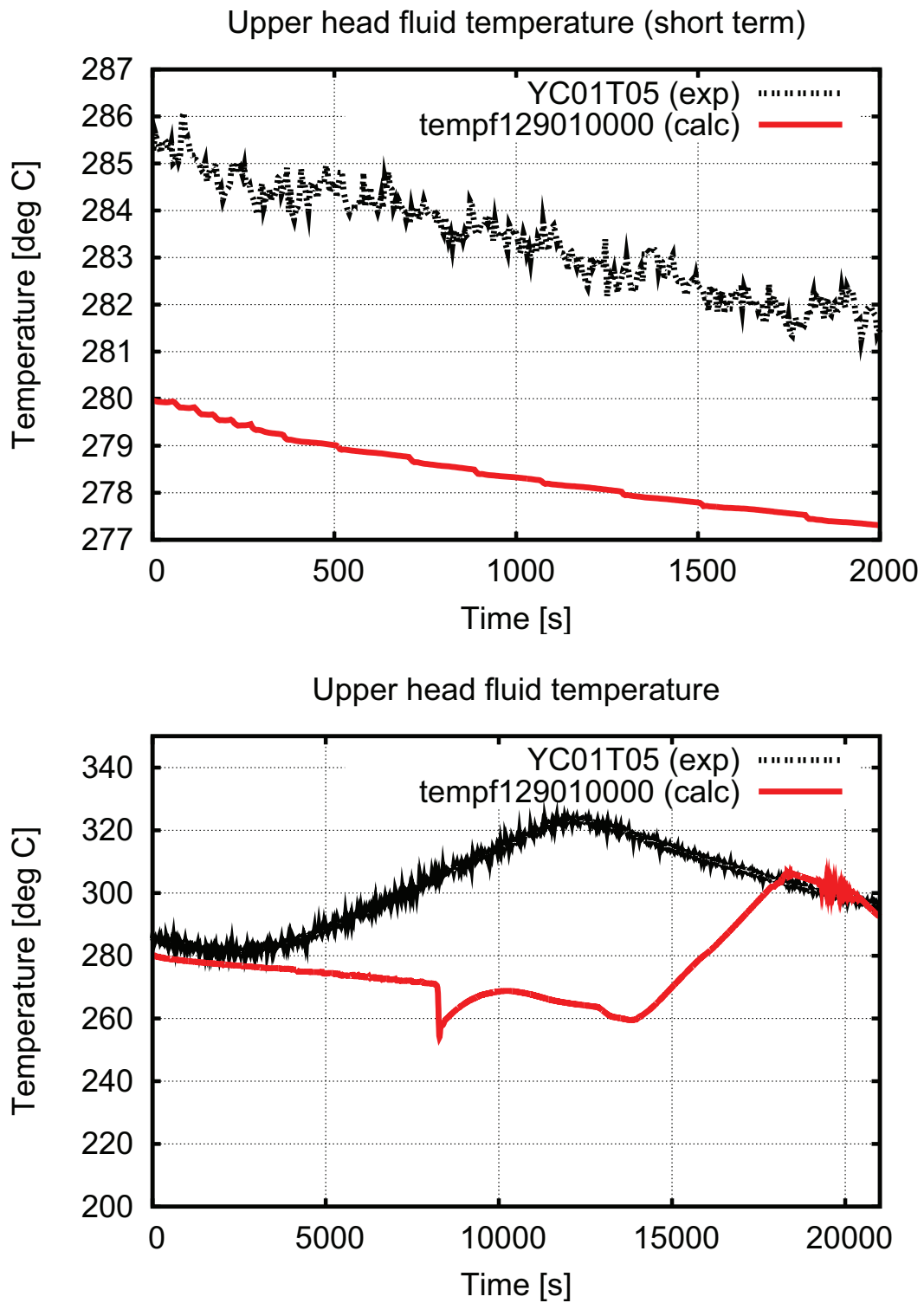


Figure 3.45: Relap results test 1, upper head temperature, short and long term

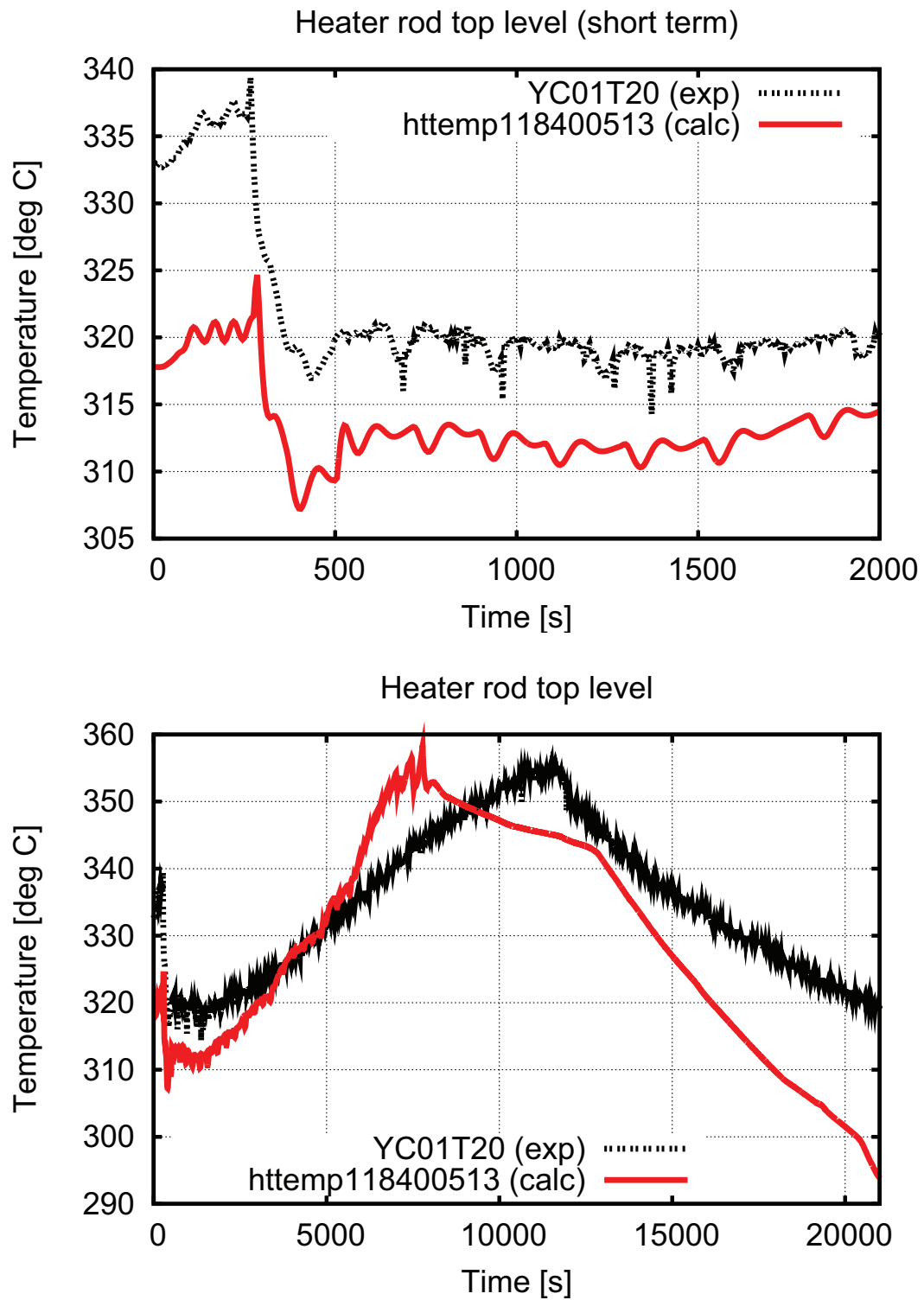


Figure 3.46: Relap results test 1, heater rod cladding temperature top, short and long term

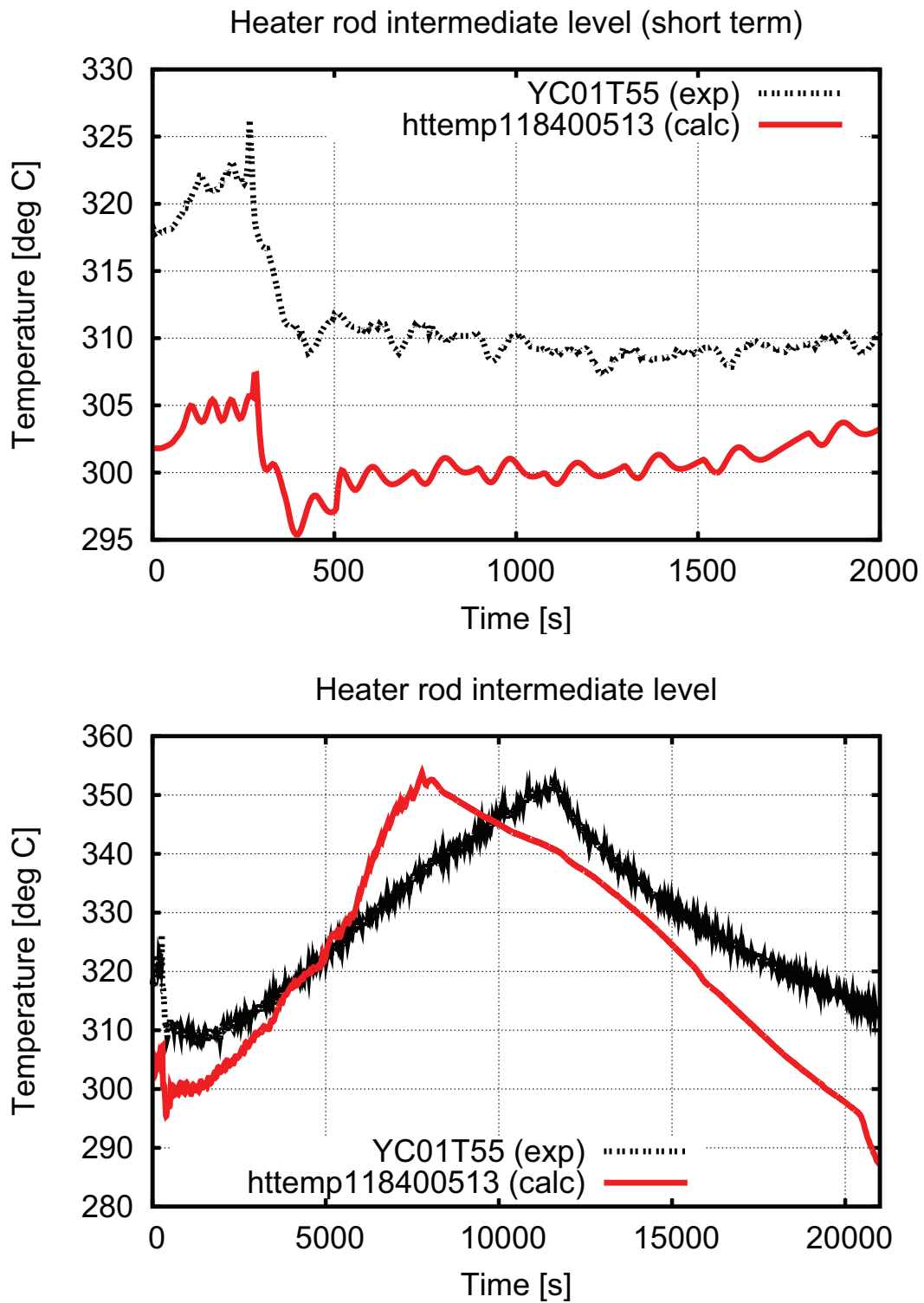


Figure 3.47: Relap results test 1, heater rod cladding temperature middle, short and long term

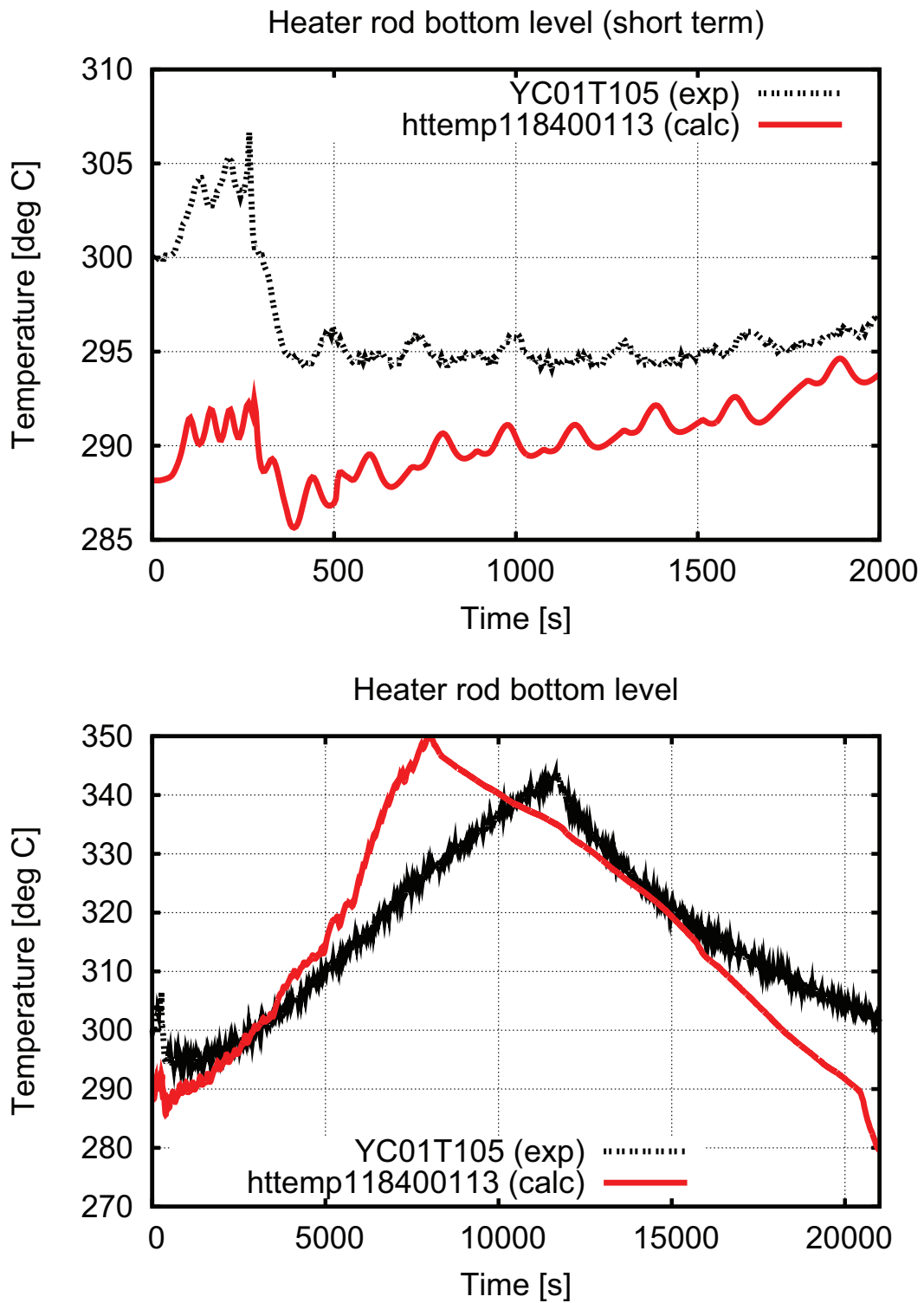


Figure 3.48: Relap results test 1, heater rod cladding temperature bottom, short and long term

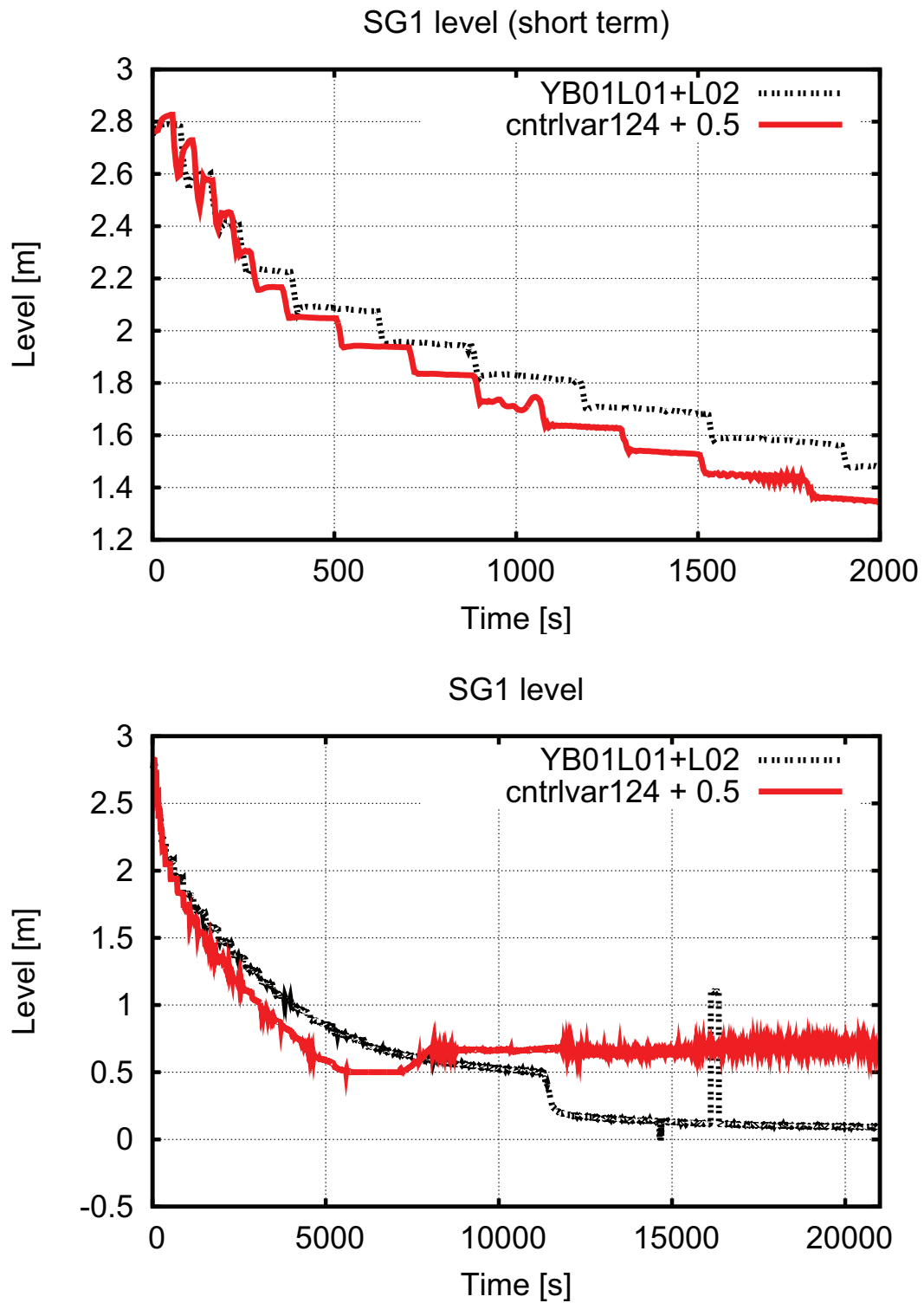


Figure 3.49: Relap results test 1, level SG1, short and long term

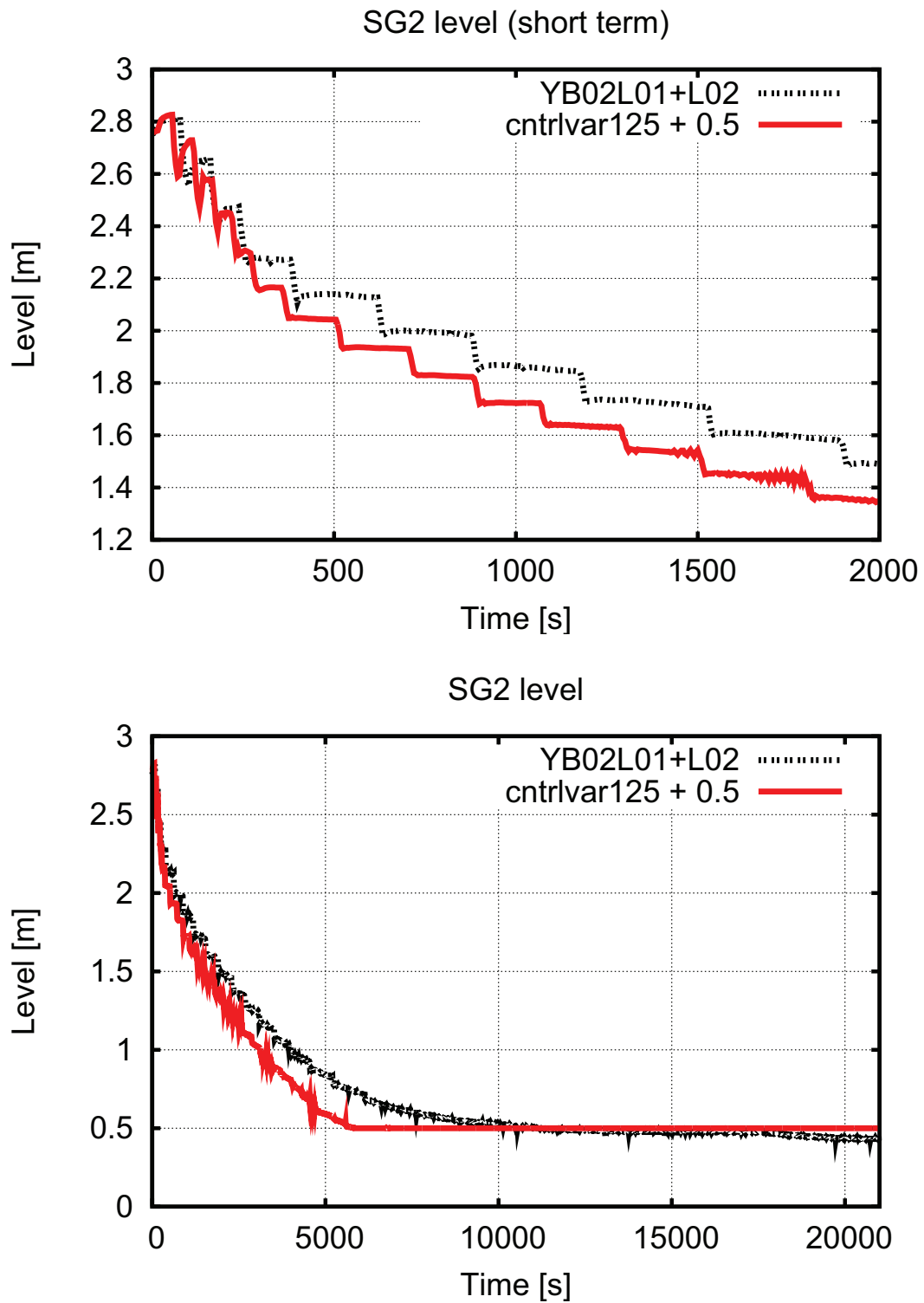


Figure 3.50: Relap results test 1, level SG2, short and long term

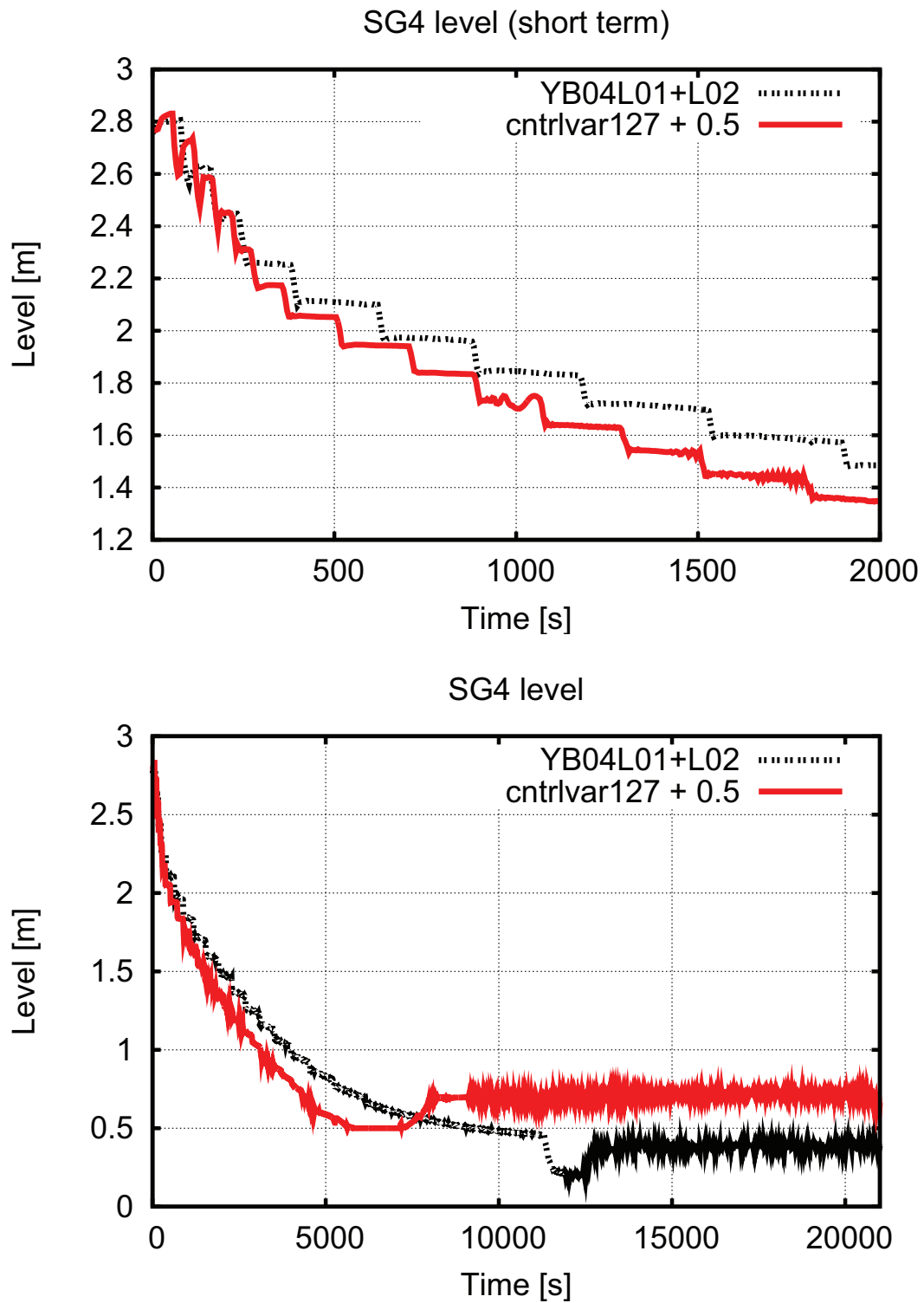


Figure 3.51: Relap results test 1, level SG4, short and long term

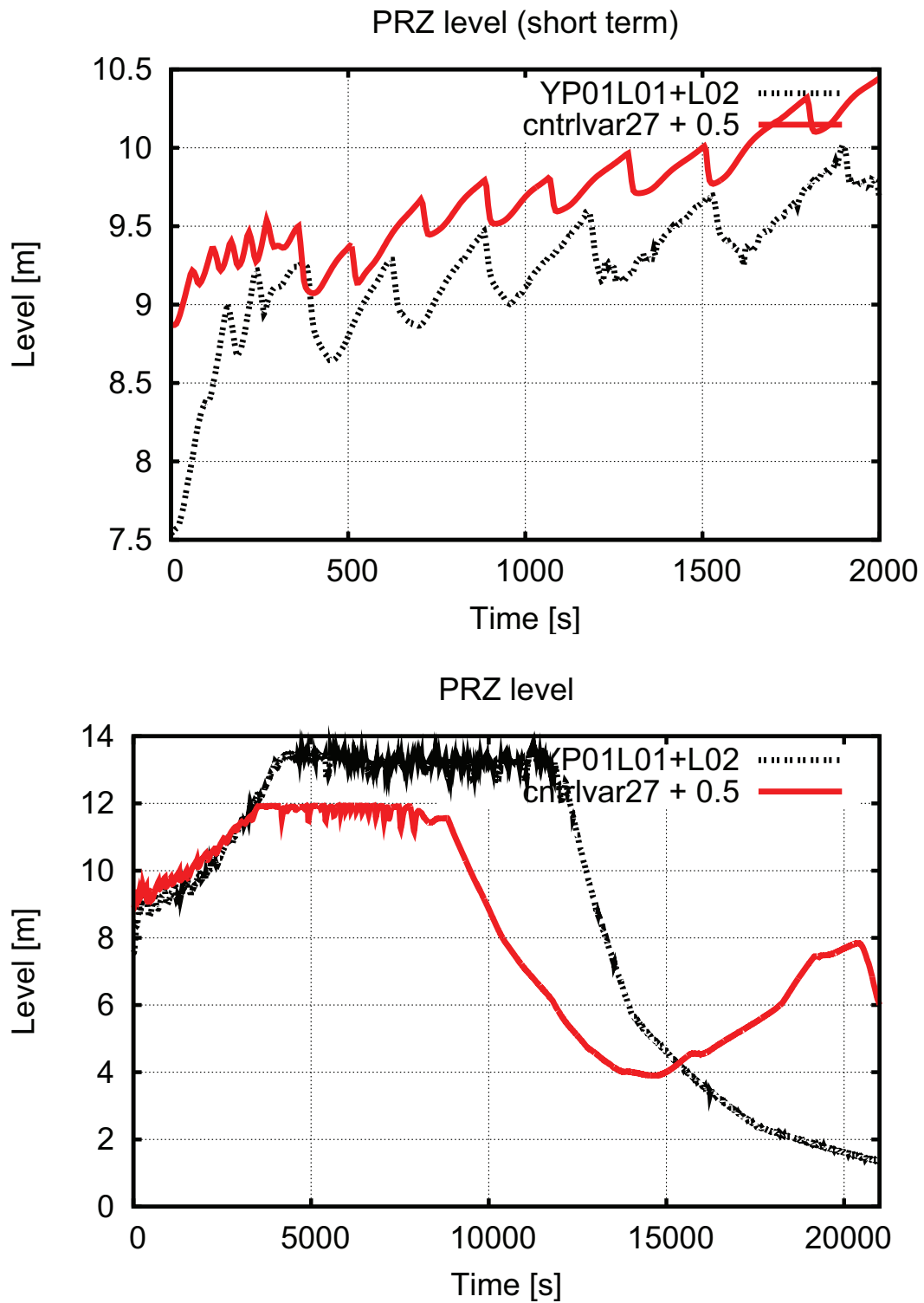


Figure 3.52: Relap results test 1, level PRZ, short and long term

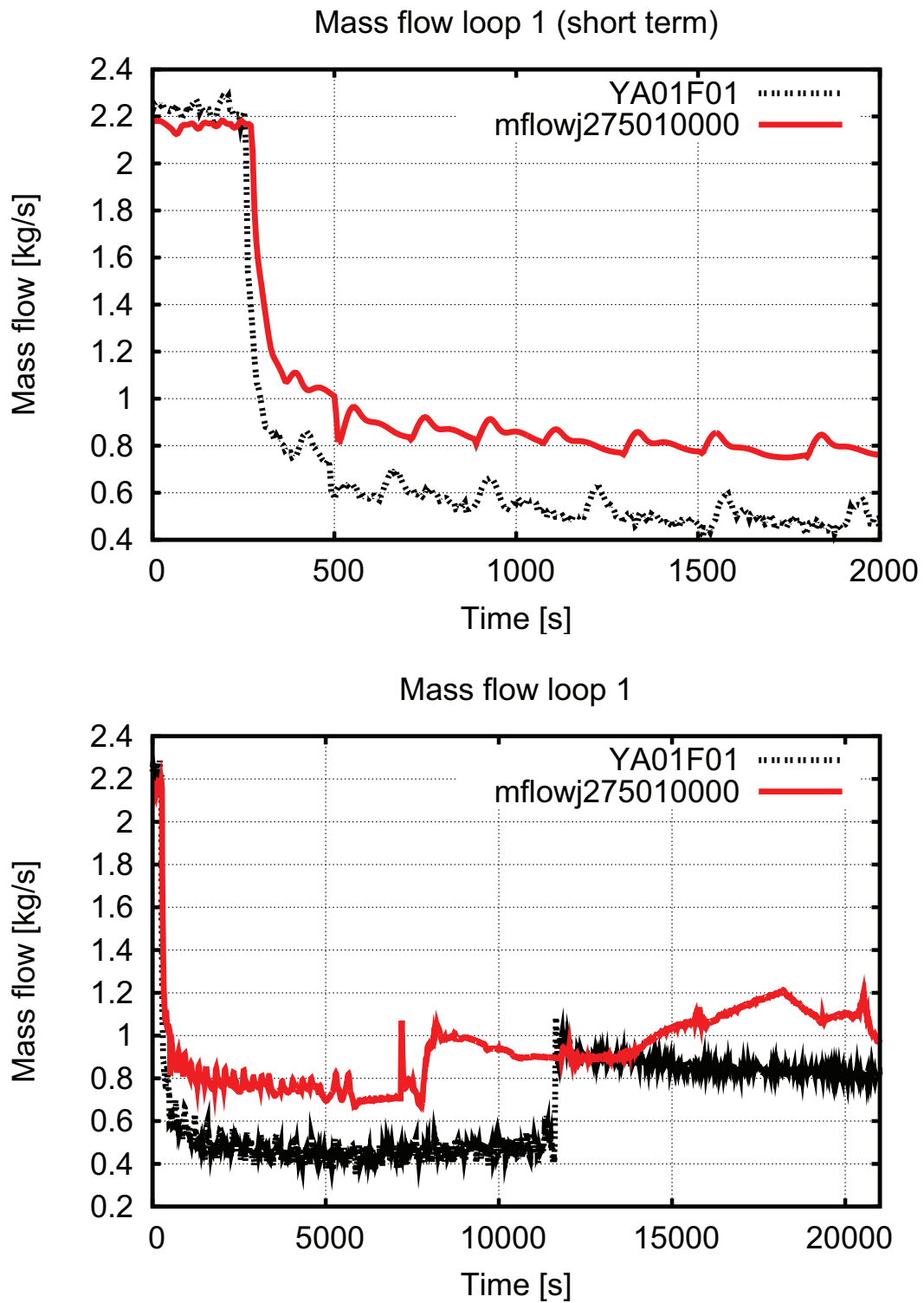


Figure 3.53: Relap results test 1, loop 1 mass flow rate, short and long term

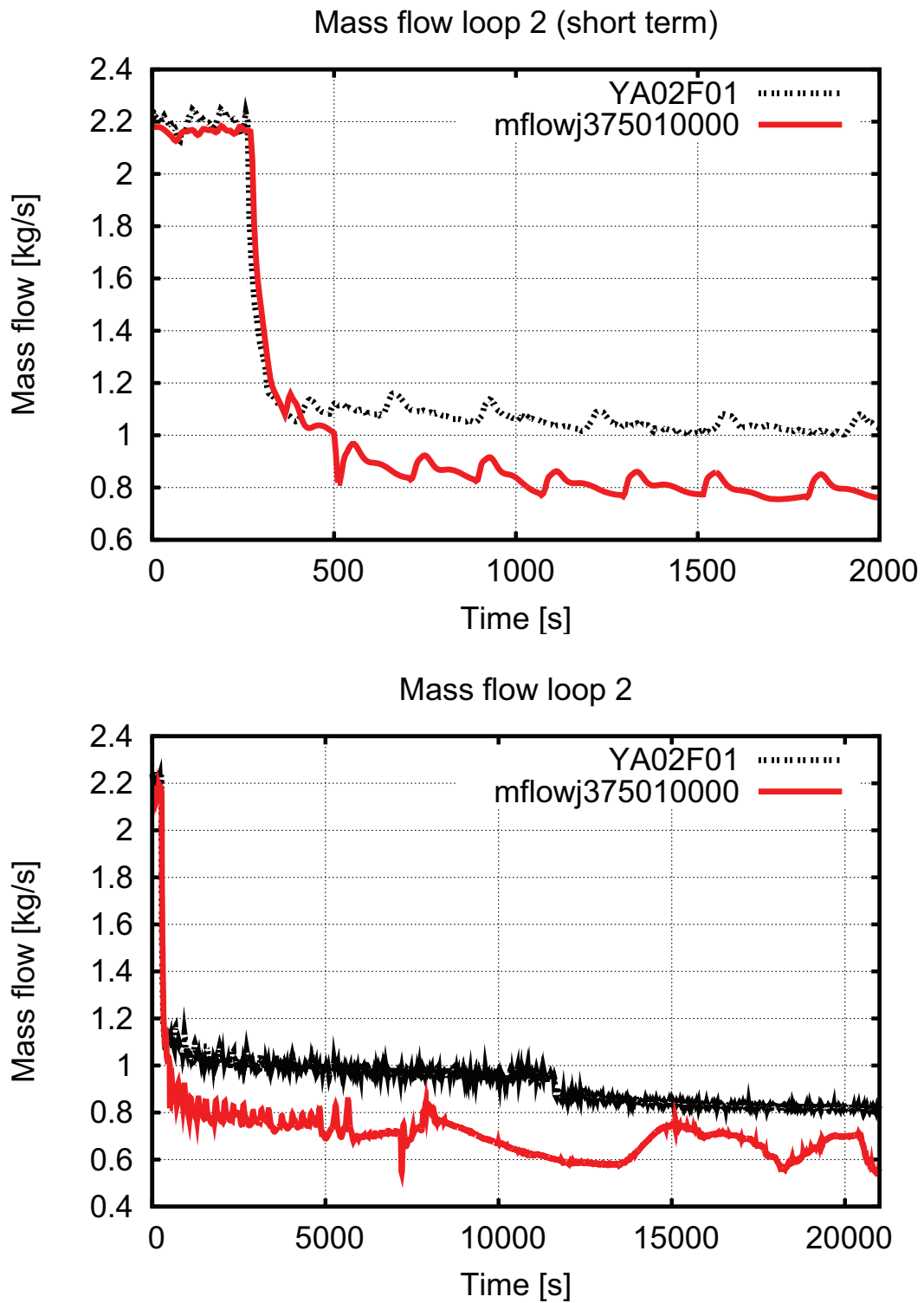


Figure 3.54: Relap results test 1, loop 2 mass flow rate, short and long term

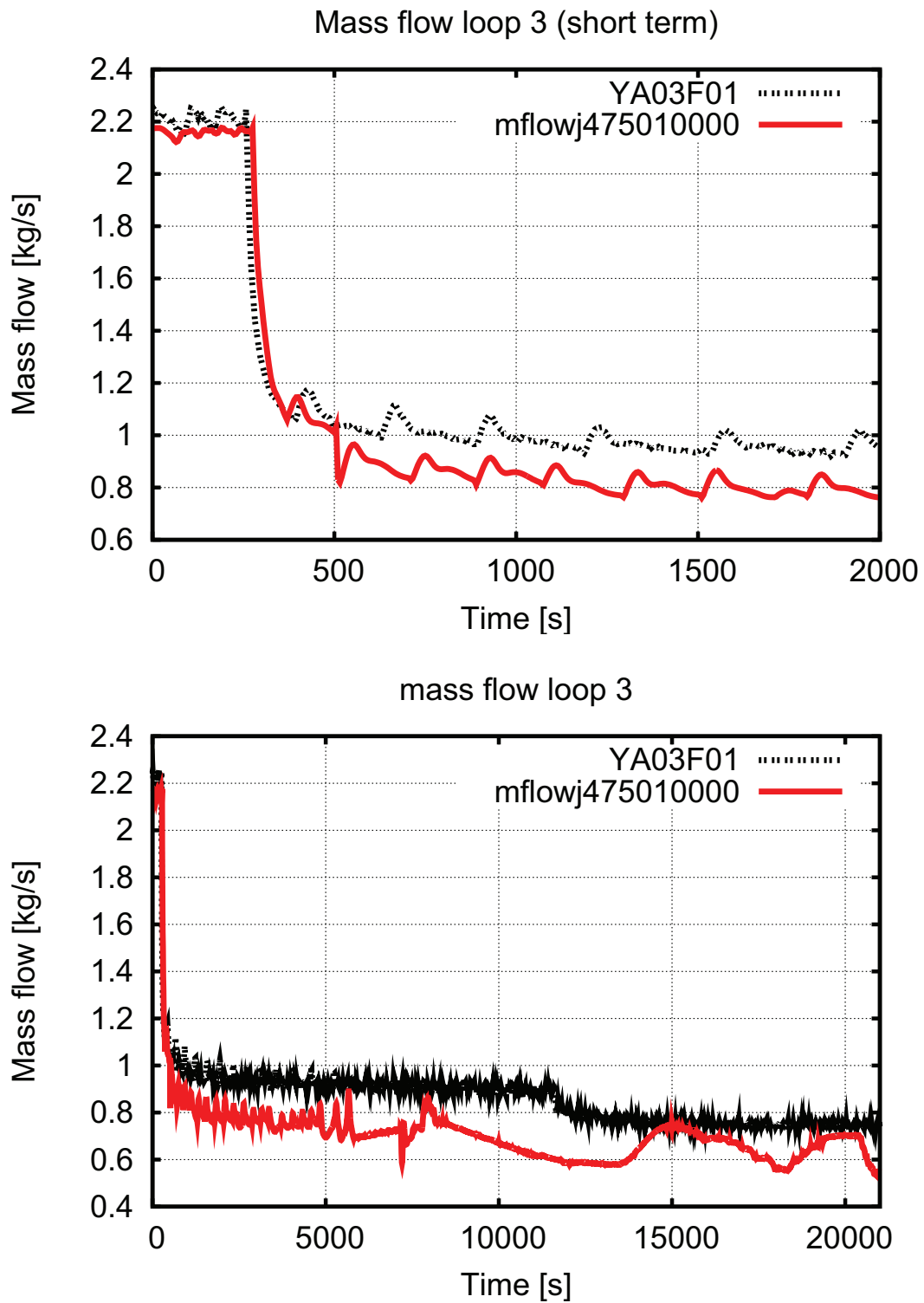


Figure 3.55: Relap results test 1, loop 3 mass flow rate, short and long term

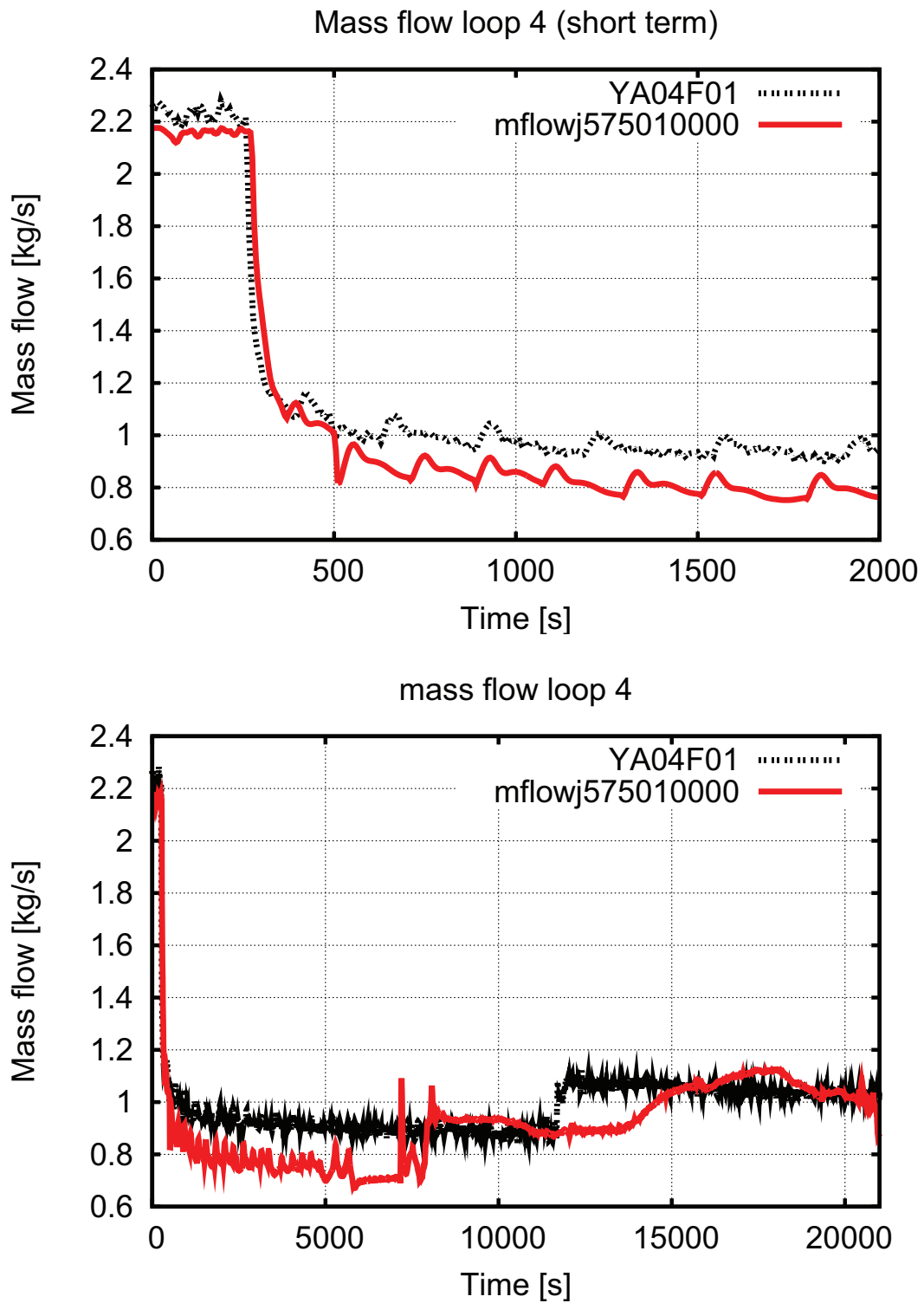


Figure 3.56: Relap results test 1, loop 4 mass flow rate, short and long term

3.2 Nodalisation

At the beginning of the work, a “general” VVER-1000 nodalisation was available at the University of Pisa. The nodalisation was developed and matured over years. The “general” or generic VVER-1000 nodalisation was also used in several international exercises, and commercial projects.

The generic VVER-1000 nodalisation was the bases to develop a nodalisation specific for the VVER-1000/320, Unit 3 Balakovo.

The University of Pisa uses the UMAE method to “qualify” a nodalisation (see 2.4.2). Both nodalisations, the generic and the specific one, have been qualified using the mentioned method.

This section describes the steps that have been performed to derive a qualified nodalisation for Balakovo from the generic nodalisation which was already present at the University of Pisa.

3.2.1 Description of the nodalisation

The nodalisation which was used is very detailed, the total number of heat structures is 1255, with a total number of 7919 mesh points; 1311 thermo hydraulic volumes have been used (the number of junctions is 1369). A “slicing” technique was adopted, meaning that the RCS has been cut horizontally in slices; the distance between two slices is the height that was chosen tentatively for the volumes. The technique ensures that the center of the volumes between two slices are at the same elevation, thereby avoiding to create artificial gravitational driving forces.

The model of the **primary side** comprises the core, four independent modeled loops, pressurizer and valves subsystem with steady state pressure control, ECCS and make-up.

The **core** comprises the volumes from 0 to 199. The upper downcomer region is modeled with eight volumes (133-138,176,178). The cold legs are attached to 133,134,136 and 138. The four volumes are joint on the top and on the bottom. On the bottom they lead into the volumes 139 and 130, modeling the major part of the downcomer and ending in the lower plenum (volume 100), on the upper part volume 131 and 132 join them, and model the core-bypass (to volume 146). The active (inner) part of the RPV is modeled with three volumes (113,110,120). Volume 113 models the core bypass for the guiding tubes, leading to the upper head. Volume 110 (and on top of it, volume 140) models the active part of the core (all active heat structures are connected to this volume). Volume 120 (and on top of it, 121) model the outer region of the core. Volume 121 and 140 join in the upper plenum, volume 141. The upper plenum is modeled with two separate stacks to allow for circulation in the upper plenum (an inner region, 141-148, and an outer region, 190, 185 and 180). The four hot legs are connected to volume 148. Volumes 150, 155, 156, 160-162, and 170 model the upper head (with two stacks, allowing for circulation). Figure 3.57 shows the nodalisation scheme of the core.

The **four loops** are modeled separately, but identically except for the pressurizer (surge line and spray line are attached to loop 4), the HHPIS and HPIS (connected to loop 1,3 and 4). volumes of loop one are taken from 200-299, of loop two from 300-399, of loop three from 400-499, and of loop four from 500-599. The hot leg consists of the volumes (X has a value between 2 and 5, depending on the loop) X00, X01, X03, X05. The primary side of the SG comprises the hot collector, volumes X09, X10, X12, X14, X16, X18, X20, X22 and X24, the SG tubes (the 11000 tubes are divided into six groups, each of which is modeled by one of the volumes X13, X15, X17, X19, X21 and X23. The groups model different elevations of SG tubes. Volumes X31, X60, X62, X64, X68, X70, X72 and X74 represent the cold collector, to which the SG tubes are connected. The cold leg including loop seal to the MCP is modeled with volume X33 - here is also, in every loop, the injection point of the make-up system. Volume X39 models the pump. The CL between MCP and RPV is modeled by the volumes X41, X43, X45, X47 and X50. Here is the connection point for HPIS and HHPIS. Figure 3.58 shows the nodalisation scheme for loop one.

The **pressurizer** subsystem consists of the surge line, volume 36 (attached to the hot leg of loop number four, volume 503), a connection volume between the pressurizer vessel and the surge line, volume 32, the pressurizer vessel itself, volume 30, the top of the pressurizer (volume 26) and the spray line (volume 22, 20), which is attached to the cold leg of loop number four, volume 541. The PORV and two safety relief valves are modeled on top of the pressurizer (23, 24, 25) which discharge into the time dependent volumes 27, 28, 29. The four groups of pressurizer heaters are modeled by a single heat structure with variable power. During steady state valve 33 opens a connection to the time dependent volume 34, which imposes the pressure for the primary side. The time dependent junctions 42 and 48 stabilize the pressurizer level during state at 8.47 meters by injection and suction of water respectively. Figure 3.59 shows the pressurizer nodalisation scheme.

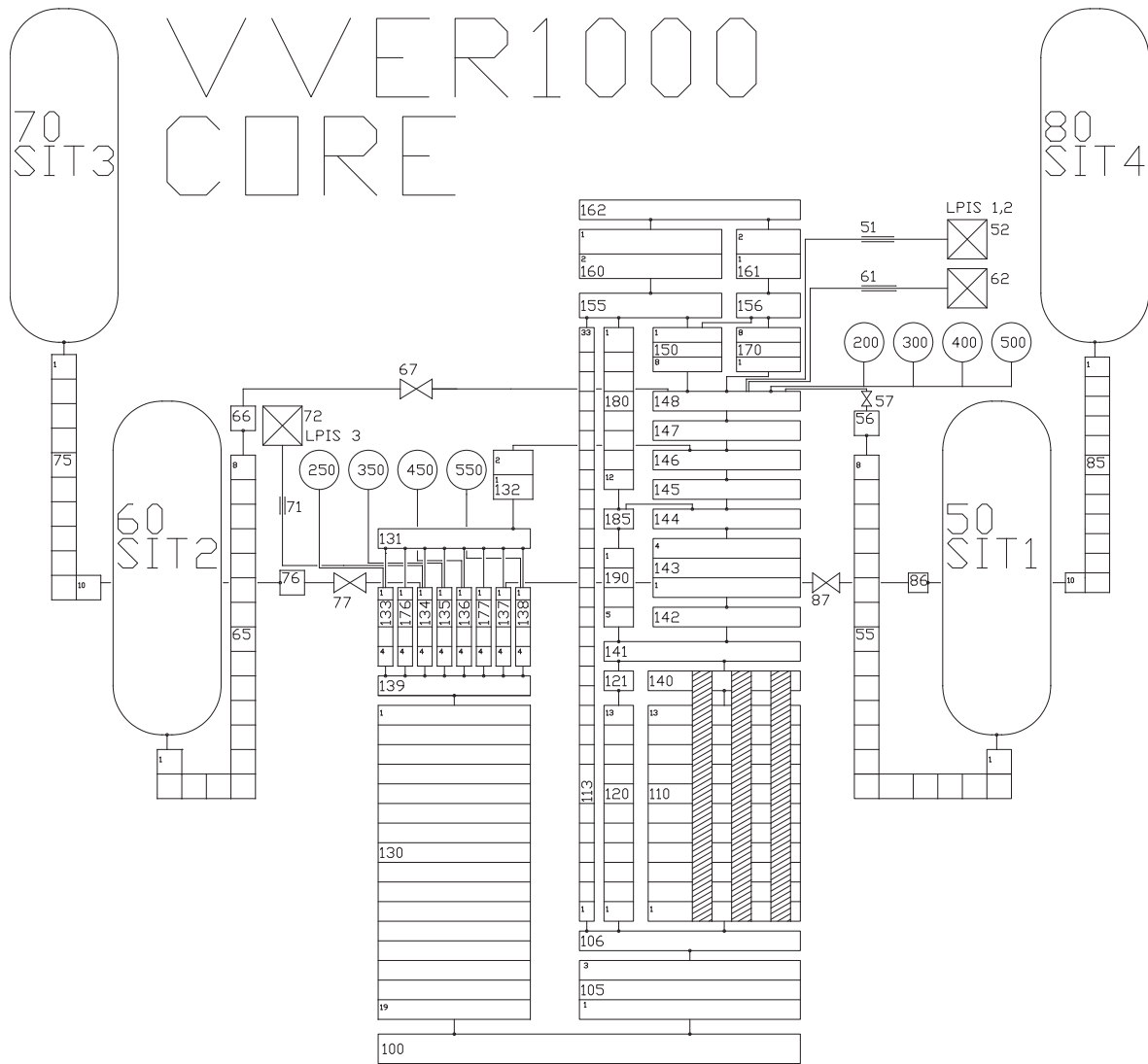


Figure 3.57: Relap5 nodalisation scheme - core

The **ECCS and Make-up** consist of three trains of the low pressure injection system, which takes suction from the containment sump. Train one of the LPIS injects into hot- and cold leg of loop one (line modeled starting from time dependent volume 52, which is connected via the time dependent junction 51 to volume 280. Time dependent junction injects following a pressure - flow rate curve which simulates the LPI pumps. Volume 281 and the junctions 282 and 283 model the connection to cold- and hot leg. Train two of the LPIS (volume 62, junction 61) injects directly into the upper plenum (volume 148) and train three (volume 72, junction 71) injects into the downcomer. A control variable keeps track of inventory which goes out and which enters the sump. The emergency heat exchangers for the ECCS and residual heat removal system are assumed to be always available. The initially the sump is filled with about 450 m³ of water, with 16g of boric acid per kg of water.

The four accumulators (accumulator component 60,70,80,90) are connected via the accumulator lines 55,56,57 - 65,66,67 - 75,76,77 and 85,86,87 in pairs to the downcomer (134,137) and the upper plenum (148). They are set to a initial pressure of 60 MPa and 16 g of boric acid per kg water .

The HPIS is simulated by the time dependent volume and junction 246, 248 (loop one) 446, 448 (loop three) and 546, 548 (loop four). The time dependent junctions simulate the pressure - mass flow rate curve. This system injects up to 15 m³ of water with 40 g/kg of boric acid, to simulate water supply from the tanks (see VVER 1000 ECCS, section 2.2.3). If more water is necessary, volumes and junctions 238, 242 (loop one) 438, 442 (loop three) and 538, 542 take over. The amount injected is debited to the sump inventory, and injection takes place only if there is still water in the sump.

The HHPIS is simulated by the time dependent volume and junction 244, 249 (loop one) 444, 449 (loop three) and 544, 549 (loop four). Up to 15 m³ of water with 40 g/kg boric acid are injected.

The Make-up system for chemical and volume control during normal operation is modeled with the time dependent volume and junction 291, 290 (loop one), 391, 390 (loop two), 491, 490 (loop three) and 491, 490 (loop four). The normal operation of the system is not simulated. Some of the investigated transients assume that the make up system is used as emergency system. It is assumed that the operator uses the full capacity of the system to inject water into primary side. The injection points can be seen in Figure 3.58.

The **secondary side** model comprises steam generator, feed water system (FW, AFW, EFW), steam line and valves. The deaerator system has also been simulated for a few cases (see Figure 3.60). The feed water line never used during steady state calculations. Its sole purpose was to verify the feasibility of passive feed of the steam generators using the operating pressure of the deaerator tanks. When the system was included in the calculations, it was connected after loss the main feed water.

The secondary side of the four **steam generators** are, like the primary side, modeled equally, but separately. The volumes (X stands for 6, 7, 8, and 9, meaning loop one, two, three and four respectively) X00 and X01 model the steam generator bottom, below the steam generator tubes. Three stacks of volumes (X10, X20 and X30) model the SG heat exchanging region. X10 the outer “downcomer” region of the SG, X20 and X30 are connected with heat structures to the primary side SG tubes. X20 models the region close to the hot collector of the SG, X30 the region close to the cold collector. The volumes X11, X21, X31 and X12, X35, X40 and X45 model the top of the SG. The volumes X50, X55 and X60 model the connection to the main steam header, volumes X65, X70 and X75. Please refer to Figure 3.58 for details.

The main steam header connects to the **main steam line**, volume X80, X82, X84, X86 and X88, and attached valves. The BRU-A valves, X90 are attached at X86, and discharge to the time dependent volume X92. The BRU-A valves model can discharge at nominal opening pressure 250 kg/s of steam. Two safety valves (X94 and X72) are attached to the volumes X82 and X84. The main steam isolation valve, also called fast acting isolation valve, connects to volume 997, which joins the four steam lines X88.

Comment on code models While it is questionable to what extend results of an experimental facility in scale can be transferred to the plant, the UMAE (uncertainty method based on accuracy extrapolation) assumes that the accuracy of code prediction can be extrapolated, provided that the same nodalisation approach has been used for facility and plant. Therefore the basic choices on the use of code models for the plant is the same one as the one adopted for the facility (please, refer to section 3.1).

This is true for the basic choices on Relap5 control volumes and junctions. Again, momentum flux calculation between SG hot- and cold collector and SG-U-tubes has been restricted, and the vertically stratified flow model in the volumes simulating the U-tubes has been disabled. Reflood calculation has been turned off.

The same model for critical heat flux calculation, the Groeneveld look-up table based method, has been used.

Heat losses, on the other hand, are specific to the PSB-VVER facility, and are modeled differently in the plant calculations. Mainly due to the difference in the volume to surface ratio heat losses play almost no role in the plant. Heat structures are assumed to be isolated - no heat transfer to the environment is assumed.

Plant logic

A list of the most important systems to control the unit follows. The first table describes the status quo in the Generic VVER1000 input deck, the second table the conditions present at Balakovo3

MSIV Main steam line isolation valve - fast acting isolation valve FAV

MSIV - one for each loop

Area (m2)	Set Point	During normal operation		
		Open/closure time (s)		
				Lay Out
0.2827	Closure logic	open	1	steam line, upstream BRU-K
	1 Pressure MSL < 4.9 MPa AND			
	2 $T_{SAT}(core_{out}) - T(MSL) > 75^{\circ}C$ AND			
	3 $T(coolant) > 200^{\circ}C$			

BRU-A valves

One BRU-A valve for each loop:

Area (m2)	Set Point	Configuration during normal operation		
		closed	Open and Closure time (s)	
				Lay Out
0.0415	open at 7.16 MPa close at 6.28 MPa	closed	< 16	steam line, upstream BRU-K

SG safety valves MSSV/SV

SG safety valves, two for each loop:

Area (m2)	Set Point	Configuration during normal operation		
		closed	Open and Closure time (s)	
				Lay Out
0.0299	open /close 1 open at 8.43 MPa close at 6.86 MPa 2 open at 8.24 MPa close at 6.86 MPa	closed	1	steam line, upstream MSIV

BRU-K valves

Area (m2)	Set Point	Configuration during normal operation		
		closed	Open and Closure time (s)	
				Lay Out
0.0415	open /close open at 6.67 MPa close at 5.59 MPa	closed	16	steam line, downstream MSIV

Pressurizer relief and safety valves

Pressurizer PORV:

Area (m2)	Set Point	Configuration during normal operation		
		closed	Open and Closure time (s)	
				Lay Out
0.078	open /close (1) open at 18.14 MPa close at 17.26 MPa (2) open at 18.63 MPa close at 17.26 MPa	closed	1	discharge line

(1) via electromagnetic device

(2) via spring

Pressurizer safety valves:

Area (m2)	Set Point	Configuration during normal operation		
		closed	Open and Closure time (s)	
				Lay Out
0.078	open /close SRV1 open at 19.03 MPa close at 17.85 MPa SRV2 open at 19.03 MPa close at 17.85 MPa	closed	1	discharge line

Reactor Scram signals:

Scram signals:

1	$Power > 107\%$	OR
2	Does not exist	
3	$SG_{level} < 1.60m (\Delta SG_{level} < -0.65m)$	OR
4	$P(PS) > 17.65MPa (17.6MPa)$	OR
5	$PRZ_{level} < 4.6m (may not exist)$	OR
6	$P(SG) > 7.84MPa$ in any of the four SGs	OR
7	Does not exist	
8	$P(MSL) < 4.9MPa$ AND $T_{sat}(core_{out}) - T(MSL) > 75^\circ C$	OR
9	$T(HL) + 10^\circ C > T_{sat}(HL)$ in any HL	OR
10	$P(MCP_{upstream}) - P(MCP_{downstream}) < 0.245$ for any (running) MCP	OR
11	$P(core_{out}) < 13.73MPa$ AND $T(HL) > 260^\circ C$ for any HL	OR
12	$T(HL) > 324^\circ C (+8^\circ C \text{ above nominal})$ (delay of 8s)	OR
13	$Power > 75\%$ of nominal AND two (or more) MCPs tripped (6s/1.4s delay)	OR
14	$Power > 75\%$ of nominal AND $P(core_{out}) < 14.7MPa$ (14.51 Riskaudit)	

SGs balakovo collapsed level 2.25, water mixture level 2.65. For all SCRAM signal 0.5s delay, plus 0.5s for signal propagation time (total delay of 1s)

MCP Characteristics

Pump trips:

1	$SG_{level} < 1.75m (\Delta SG_{level} < -0.5m)$ for each SG	OR
2	$P(MSL) < 4.1MPa$ AND $T_{sat}(core_{out}) - T(MSL) > 75^\circ C$ AND $T(coolant) > 200^\circ C$	
3	MSIV closing signal	OR
4	$SG_{level} > 2.5 (\Delta SG_{level} > 0.25)$	

The logic for the trips of the MCPs was derived from the chapter "set-points and interlocks" from Mikhaltchuk [1997]. For the trip in question the report states that the signal YBF04(1,2,3) corresponds to the MCP trips: 1-trip of MCP1, 2-trip of MCP2, 3-trip of MCP3 and 4. Further in the report it is stated that YBF04(1,2,3) is composed from signals YZS01, and YBS03(1,2,3). YBS03(1,2,3) is connected with a loss of pressure in the steam lines 1,2,3 and 4. See p.98 to p.121.

Feed water system (normal fw, auxiliary fw and emergency fw)

Feed water (2 pumps for all loops) logic: feed water is tripped when

1	$SG_{level} > 2.25m (\Delta SG_{level} > 0.0m)$	OR
2	$P(MSL) < 4.1MPa$ AND $T_{sat}(core_{out}) - T(MSL) > 75^\circ C$	

Auxillary feed (2 pumps for all loops) water logic:

AFW activation

1	$SG_{level} < 2.15m, (\Delta SG_{level} < -0.1m)$ AND T in any of the loops $> 150^\circ C$	
---	-----------------------------------------------------------------------------------------------------	--

AFW stop

	feed water level recovered	
--	----------------------------	--

Emergency feed water, three independent trains:

AFW activation (three trains)

train 1:	$SG_{level}inANYSG < 1.5m(\Delta SG_{level} < -0.75m)$	
train 2:	$SG_{level}inSG1ORS4 < 1.5m(\Delta SG_{level} < -0.75m)$	
train 3:	$SG_{level}inSG2ORS3 < 1.5m(\Delta SG_{level} < -0.75m)$	

AFW stop

	$T(coolant) < 150^{\circ}C$	
--	-----------------------------	--

Active ECCS Logic

HPIS:

activation

	$T_{sat} - T(coolant) < 10^{\circ}C$ AND $P < 10.8MPa$	
--	--------------------------------------------------------------	--

flow rate/train

11.0 MPa	0.0 kg/s	
9.0 MPa	41.6 kg/s	
0.1 MPa	69.3 kg/s	

Water supply

Tank	15 m ³	per train
Sump	500 m ³	for all trains HPIS/LPIS

Injection point CL loop 1,3,4

LPIS:

activation

	$T_{sat} - T(coolant) < 10^{\circ}C$ AND $P < 2.5MPa$	
--	-------------------------------------------------------------	--

flow rate/train

2.5 MPa	27.8 kg/s	
1.93 MPa	111.0 kg/s	
0.1 MPa	212.0 kg/s	

Water supply

Tank	15 m ³	per train
Sump	500 m ³	for all trains HPIS/LPIS

Injection point HL loop 1, Acc.line DC and UP

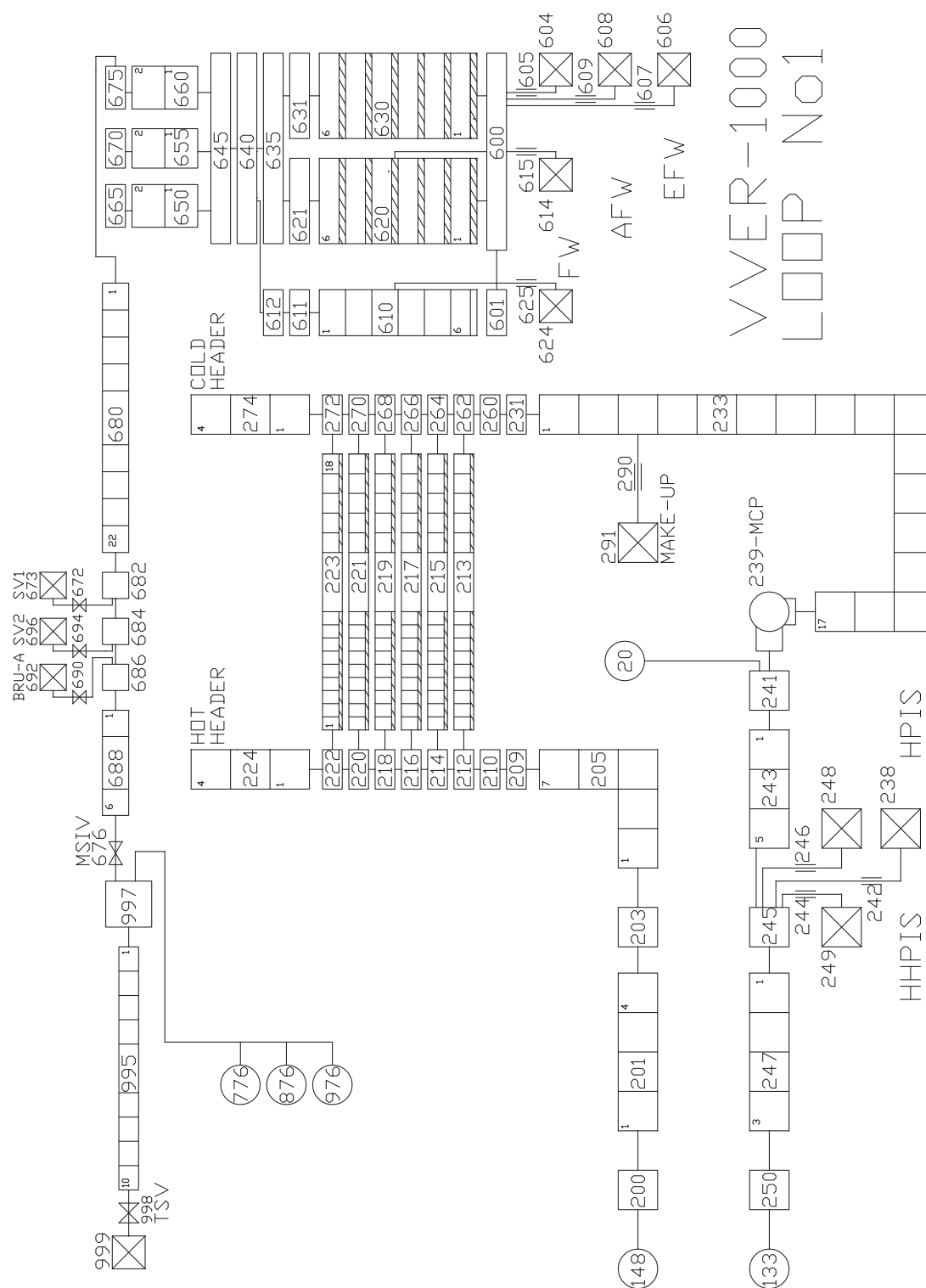


Figure 3.58: Relap5 nodalisation scheme - loop

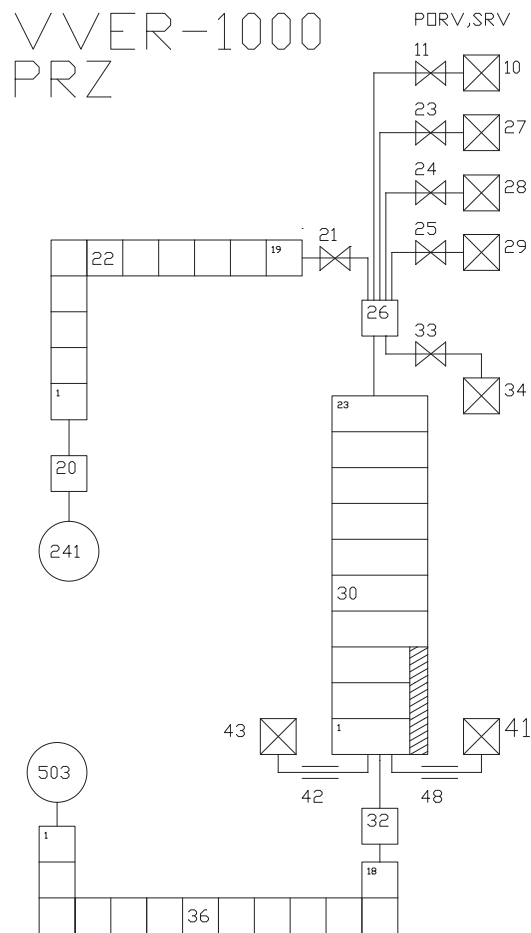


Figure 3.59: Relap5 nodalisation scheme - pressurizer

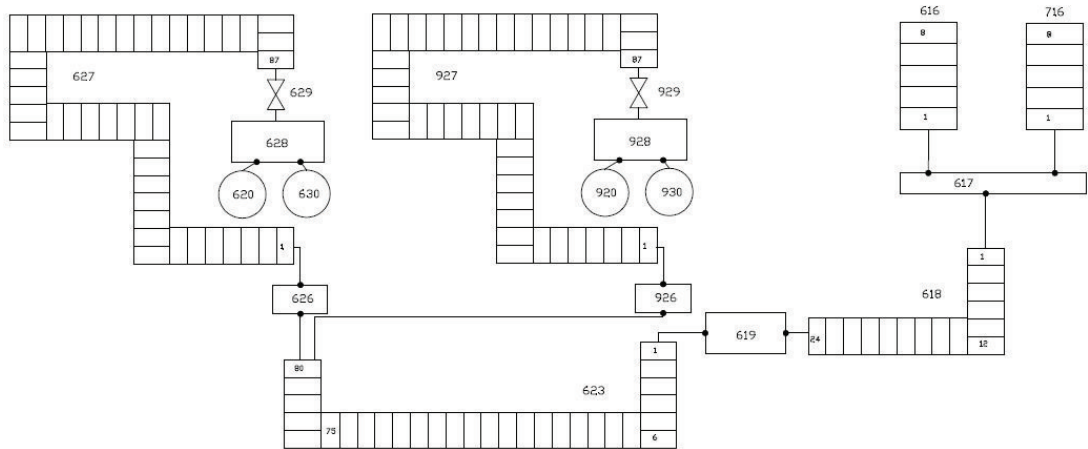


Figure 3.60: Relap5 nodalisation scheme - feed water line and deaerator tanks

3.2.2 Qualification of the nodalisation

Steady state qualification

One steady state calculation was run. The time from -100 to 0 designates the “official” steady state time, in which several artificial systems to control the steady state are in use (e.g. a control variable for reactivity control, two tmdpvols to control the level in the PRZ, one tmdpvols to control the initial pressure in the PS). After 100s they are all switched off, and the calculation runs for further 900s on its own. A summary of main parameters of the steady state calculation are reported in 3.25.

Parameter	Unit	VVER1000/320 input deck Balakovo3		Difference	Comment
Power	Mw	3000	3000 ± 60	0	
Core inlet temperature	°C	289	289.7	-1	
Core Dtemperature	°C	29	30	-1	
Core outlet temperature	°C	318	320	-2	
Coolant pressure outlet core	MPa	15.7	15.7	0	In UP
One loop flow rate	m ³ /h	21717	21200	517	Core flowrate/4
Core flow rate	m ³ /h	86871	84800 ±4000	0	
Pump rotation speed	rev/min	995	995	0	
PRZ pressure	MPa	15.7	15.7	0	
PRZ temperature	°C	346	346	0	
Pump flow rate	m ³ /h	21717	21200	517	pump capacity
SG exchanged power	MW	750	750	0	
SG steam production	kg/s	408	408	0	
SG pressure	MPa	6.3	6.27	0.03	
SG steam temperature	°C	278	279	-1	
FW temperature	°C	220	220	0	

Table 3.25: Parameters of the steady state calculation

On transient qualification

Test No 4 (not of the TACIS project, but of the PSB-OECD project) was used as K_v -scaled analysis for the on-transient qualification. Test No 4 OECD-PSB-Project simulates a SBLOCA in the CL. The following chapter is quoted from Cherubini et al. [2005]:

A requirement of the UMAE methodology constituted by the 'demonstration of similarity' block k in figure 1. The available qualified nodalisation of the VVER1000 NPP must be capable of simulating the selected transient. This requirement is relevant in order to applied the nodalisation to the selected transient in nominal condition and to use the extrapolation of the accuracy (this phase is not the scope of this paper).

A K_v -scaled calculation is carried out with the following steps:

1. calculation of the K_v -ratio considering the primary system volumes of the concerned facilities or plants;
2. achievement of steady state in the NPP nodalisation, 'scaling' the relevant quantities on the basis of the related values;
3. performing the K_v -scaled calculation with the scaled boundary conditions, comparison between calculated and reference (experimental in this case) data and conclusion about the acceptability of the results.

The results of step one shows that the generic VVER1000 primary system is 300 times bigger than PSB primary system volume. This value is used for scaling, to preserve the break area and the ratio of core power over primary system volume. Given the consideration above mentioned initial and boundary conditions are strictly derived from the corresponding parameters of the considered test in the PSB facility. It must be stressed that this step has been fulfilled easily because the PSB is a VVER simulator scaled 1 to 300.

The steady state conditions (step two), envisaged by the target values of the ' K_v -scaled' calculation, have been reached running a transient calculation for 100 s. During this time the various time trends are stabilized before starting the CL-4.1-03 test in VVER1000. The relevant results regarding initial and boundary conditions of the experiment and of NPP calculation are given in table 3, where the values reported in the fifth column are related to the end of steady state.

The main results of step three are given in table 4 and 5. A systematic procedure consisting in the identification of phenomena and of Relevant Thermal-hydraulic Aspect (RTA) has been applied. In details:

- subdivision of the considered transient into "phenomenological windows" (i.e. time spans in which a unique relevant physical process mostly occurs and a limited set of parameters controls the scenario): phenomena consequent to the physical process characterize each phenomenological window;
- for each Ph. W. the identification of the RTA (events or phenomena consequent to the physical process and characteristic of each transient) and the selection of the parameters characterizing the RTA have been taken into account;
- qualitative analysis of results obtained by evaluating and ranking the comparison between measured and calculated values.

The qualitative analysis, is based on five levels of judgment (E, R, M, U and -) whose meaning is essentially derived from a visual observation of the experimental and predicted trends:

E	the code predicts qualitatively and quantitatively the parameter (Excellent - the calculation is within experimental data uncertainty band);
R	the code predicts qualitatively, but not quantitatively the parameter (Reasonable - the calculation shows only correct behavior and trends);
M	the code does not predict the parameter, but the reason is understood and predictable (Minimal - the calculation lie within experimental data uncertainty band and sometimes does not have correct trends);
U	the code does not predict the parameter and the reason is not understood (Unqualified - calculation does not show correct trend and behavior, reasons are unknown and unpredictable)".

N.	Parameter/System	Unit	PSB CL-4.1-03 test	VVER1000 Dem. of Similarity
1	Primary system volume	m ³	1.23	370 (1)
2	Break: - area - - Ar/V	m ² CL with PRZ m ⁻¹	7.85E-5 CL with PRZ 6.38E-5	2.355E-2 6.36E-5
3	Primary system: - HL temperature - CL temperature - mass flow rate - GLoop/Core power	°C °C kg/s kg/s/MW	308-311 282-283 7.9 6.99	309 283 2416 7.12
4	PRZ - pressure - level	MPa m	15.6 4.94	15.7 4.95
5	Core - initial power - decay power - ΔT - average linear power - core power/vol.	MW - °C KW/m MW/ m ³	1.130 - 27 1.905 0.919	339 - 26 1.878 0.916
6	SG SS: - pressure - SL flow rate - DC level - FW temperature - GFW/Core power - MSIV closure - FW stop - SRV set point	MPa Kg/s m °C kg/s/MW - - MPa	6.93-6.88 0.11 (1) 2.48-2.52 170 -3 - 13MPa(4) 7.4	6.88 34 (1) 2.00(2) 170 -3 - 13MPa(4) 7.4
7	Accumulators: - no. - position - total volume - pressure - liquid mass - liquid mass/PS vol. - total vol./PS vol. - temperature - isolation	- - m ³ MPa kg kg/m ³ - °C -	2 DC 0.2 4.08-4.14 157 127.6 0.162 26-32 Lev.=1.3m	2 DC 60 4.1 47000 127.0 0.162 25 Tot. M=36tons
8	LPIS: - no. - position - fluid temperature - delivered flow rate - flow rate/PS volume - actuatuion set point	- - °C kg/s kg/s/m ³ -	3 CL 1, 3, 4 - 0.248 0.20 CL T = 500°C	3 CL 1, 3, 4 50 -1 - CL T = 500°C
9	HPIS and AFW	-	not active	not active
10	Reactor coolant pump: - trip - coastdown	- -	13MPa(1) 4 s	13MPa(1) 4 s
11	SCRAM	-	13MPa(1)	13MPa(1)
12	CMT, PRHR and RHR	-	-	-
13	TEST END	s	2591	2694

Table 3.26: Relap5 nodalisation qualification - key parameters

		UNIT	EXP	VVER CALC	Judg. VVER
RTA: Pressurizer emptying					
TSE	emptying time	s	10	13	R
	scram time	s	57.6	63	E
IPA	integrated flow from SL (from 0 up to emptying)	kg	-	-	-
RTA: Steam generators secondary side behaviour					
TSE	main steam line valve closure	s	17.5	10	R
	difference between PS and SS pressure at 100 s	MPa	0.33	0.27	E
SVP	SG level:	m			
	end of subcooled blowdown		2.44;2.44; 2.49;2.38	2.11;2.11; 2.12;2.01	R
	- when PS pres. equals SS pres.		2.43;2.44; 2.49;2.37	2.12;2.12; 2.13;2.05	R
	- when ACC starts		2.40;2.41; 2.47;2.33	2.13;2.13; 2.13;2.05	R
	- when LPIS starts		2.35;2.26; 2.34;2.30	2.09;2.10; 2.10;2.02	R
SVP	SG pressure	MPa			
	- at end of subcooled blowdown		7.31;7.34; 7.36;7.31	7.28;7.28; 7.28;7.28	E
	- when PS pres. equals SS pres.		7.30;7.34; 7.37;7.30	7.28;7.28; 7.28;7.28	E
	- when ACC starts		6.79;6.81; 6.83;6.79	7.12;7.12; 7.12;7.12	R
	- when LPIS starts		5.36;5.39; 5.41;5.37	6.61;6.61; 6.61;6.61	R
RTA: Subcooled blowdown					
TSE	upper plenum in sat. conditions	s	16	24	R
	break two phase flow	s	113	147	R
IPA	break flow up to 30 s	kg	183.7	38768	M
RTA: First dryout occurrence					
TSE	time of dry out	s	97	-	-
	range of dry out occurrence at various core levels	s	97 - 102	-	-
	peak cladding temperature	K	589	-	-
SVP	average linear power	kW/m	1.416	-	-
	maximum linear power	kW/m	1.416	-	-
	core power / primary mass	kW/kg	2.01	-	-
IPA	integral of dry out at 2/3 of core height	K s	-	-	-
NDP	primary mass / initial mass	%	47.6	-	-
	time of loop seal clearing	s	109 loop 1&4	-	-
RTA: Rewet by loop seal clearing					
TSE	range of rewet occurrence	s	102 - 107	-	-
	time when rewet is completed	s	109	-	-
TSE	PS pressure equal to SS pressure	s	150	149	E
SVP	break flow at 200 s	kg/s	-	317.5	-
	break flow at 1000 s		-	35.9	-
IPA	integrated flow (200 - 1000 s)	kg	236.52	62878	R
RTA: Mass distribution in primary side					
TSE	time of minimum mass occurrence	s	430 2430	325 2570	M R
SVP	minimum primary side mass	kg	171.3 140.6	40458 27068	R M
	av. linear power at min. mass	kW/m	0.304	0.27	R

continued on next page

		UNIT	EXP	VVER CALC	Judg. VVER
RTA: Second dryout occurrence					
TSE	time of dry out	s	405	236	M
	range of dry out occurrence at various core levels	s	401-478	236-315	M
	peak cladding temperature	K	590	723	M
SVP	average linear power	kW/m	0.425	0.628	M
	core power / primary mass	kW/kg	1.41	2.09	M
IPA	integral of dry out at 2/3 of core height	K	-	-	-
NDP	primary mass / initial mass	%	21.6	22.9	E
RTA: Accumulators behavior					
TSE	accumulators injection starts	s	406 - 414	325	R
	accumulators injection stops	s	1365- 1452	1230	R
IPA	total mass delivered by accumulators	kg	-	-	-
NDP	minimum mass/initial mass	%	20.7	17.1	R
	primary mass (acc. start)/initial mass	%	21.3	17.1	R
RTA: Final dryout occurrence					
TSE	time of dry out	s	2077	2171	E
	range of dry out occurrence at various core levels	s	2077-2313	2171-2540	R
	peak cladding temperature	K	783	855	R
SVP	average linear power	kW/m	0.304	0.274	R
	rate of rod temperature increase	K/s	0.8	1.1	R
	core power / primary mass	kW/kg	1.06	1.356	M
IPA	integral of dry out at 2/3 of core height	K s	-	-	-
NDP	primary mass / initial mass	%	20.6	15.4	R
RTA: LPIS intervention					
TSE	LPIS start	s	2432	2565	R
	range of rewet occurrence	s	2482-2518	2570	R
	final rewetting	s	2559	2620	E
IPA	integrated flow from start to end of rewet	kg	96.7	9687	M
NDP	primary mass (LPIS start)/initial mass	%	16.8	11.7	R

Table 3.27: Relevant thermalhydraulic aspects on-transient qualification

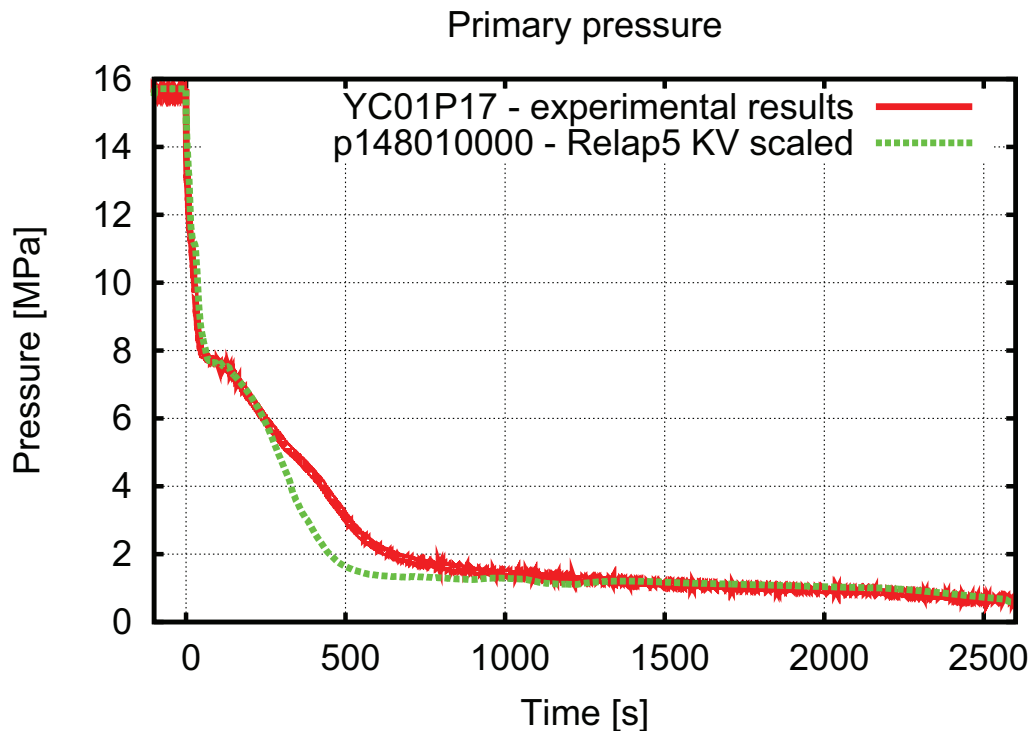


Figure 3.61: KV scaled calculation, OECD test No3, primary pressure

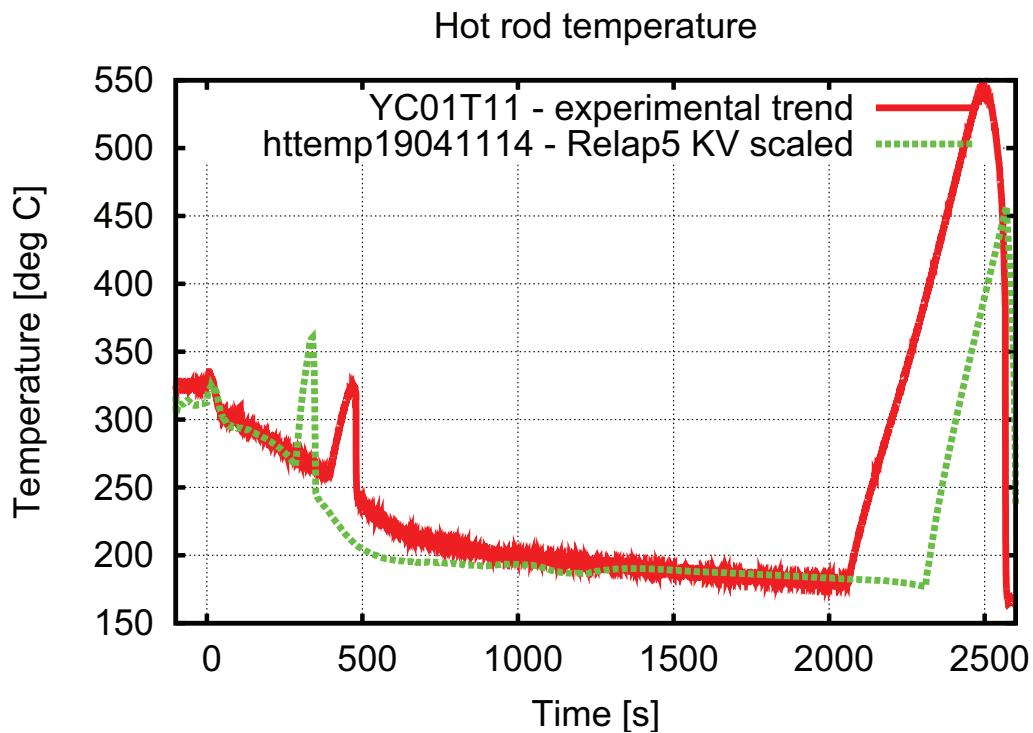


Figure 3.62: KV scaled calculation, OECD test No3, hot rod temperature

3.2.3 Matrix of performed calculations

Please refer to Table 3.28 to see an overview on all presented calculations using the code Relap5. An Appendix to the present work reports a bigger number of parameters for each of the calculations.

No	Initiating event/type	ECCS used	ECCS unavailable	Operator actions
1	Loss of all feed water (LOFW)	4 SITs	All trains HHPIS, HPIS	Full opening of BRU-A 1 and 4, closing MSIV 2 and 3, supply of 10kg/s into SG 1 and 4
2	Loss of all feed water (LOFW)	4 SITs	All trains HHPIS, HPIS	1.) Full opening of BRU-A 1 and 4, closing MSIV 2 and 3, supply of 10kg/s into SG 1 and 4 2.) Manual opening and closing of the PORV based on the available saturation margin
3*	PORV stuck open (SBLOCA)	all HHPIS, HPIS, all SITs	none	none (initial conditions hot standby)
4	Cold leg break loop No 4 with equivalent diameter of 70mm (SBLOCA)	4 SITS, All trains LPIS	All trains HHPIS, HPIS	Cooldown of PS via SS by fully opening BRU-A valves of SG 1 and SG 4 after core exit temperature exceeds 350°C
5	Main steam line break and simultaneous double-ended guillotine break of one steam generator tube in loop 4 (PRISE)	all trains of LPIS, SITs	all trains of HHPIS and HPIS	after 30min isolating of SITs, primary depressurization by opening the PORV, cool down (60°C /h) of primary with BRU-A valves
6	total loss of feed water (LOFW)	two trains of HPIS, all SITs and all trains of LPIS	failure of one train HPIS, all trains HHPIS	On Δ SG level $< 0.9m$ from nominal depressurize the PS by fully opening the PORV
7	loss of off-and on site power - full station black out (SBO)	SITs, fire brigade trucks	all active systems (only power from batteries available)	depressurization of all four SG and supply of feed water from fire brigade trucks after core outlet temp. exceeds 350°C
8	small break equivalent to a diameter of 60mm in cold leg of loop 4 (SBLOCA)	SITs	failure of all trains of HPIS	No accident management

continued on next page

No	Initiating event/type	ECCS used	ECCS unavailable	Operator actions
9	primary to secondary leak equivalent to 100 mm - SG header break, BRU-A stuck open after first opening	HPIS, SITS	none	after 30 min two trains of HPIS switched off, SITS isolated, cool down of primary via secondary with 60°C /h after 45 min last train HPIS switched off, make-up switched on
11	small break equivalent to a diameter of 70 mm in cold leg of loop 4 (SBLOCA)	SITS, LPIS, HPIS after 30 min	initial failure of all HPIS pumps	recovery of one train of HPIS (injecting into loop 4), cool down of primary via secondary with a rate of 30°C /h
12	small break in loop No 4 equivalent to 70 mm	HHPIS and make up	failure of all trains of LPIS and HPIS	after 30 min cool down of primary via secondary with 30°C /h, switching on of HHPIS and make up

Table 3.28: Overview on presented Relap5 calculations.

3.3 LOFW and SBO

The section contains three loss of all sources of feed water sequences, and one station black out sequence. The station black out in the first phase is also characterized by high pressure in the primary side and a challenge to the heat removal from the primary by the secondary side, therefore it was included in this section.

3.3.1 Scenario 1

Initiating event is a total loss of feed water. The all trains of HPIS are considered to fail, LPIS and accumulators are available. Accident management consists in SS depressurization: the operator isolates SG2 and SG3 by MSIV closure, depressurizes SG1 and SG4 to supply water with a flow rate of 10 kg/s at 1 MPa into SG1 and SG4. The accident management is considered to be successful if the core exit coolant temperature decreases to 300 °C .

First 100s: the imposed initial event is a LOFW. FW, AFW and EFW fail at time 0 s, the TSV closes at the same time. A rapid increase in the SS pressure is the immediate result. Since the BRU-K valves are assumed to be not operational, the set point of the BRU-A valves opening is reached after 3 s. The PS pressure follows, and the spray line fully opens after 3 s. The BRU-A valves have a capacity of 250 kg/s of steam, which is lower than the 408 kg/s of steam usually produced by each SG. So only a fraction of the produced heat is removed, which leads to an increase in the PS temperature at the SG outlet of almost 10 °C . This in turns leads to a negative reactivity feedback due to the reduced moderator density and a reduction in power of almost 30%. A rapid decrease in the PS pressure occurs after 13 s, the spray line closes and after 14 - 15 s all groups of the pressurizer heaters are switched off. At 46 - 47 s the MCPs are tripped on a low level signal of the steam generators (0.5 m less than the nominal level), the reactor SCRAM follows at 48 s (All MCP tripped, scram with 1s delay for signal propagation time).

100s up to the AM: the upper part of the SG tubes are uncovered, thus the heat exchange (PS to SS) is here reduced almost to zero. The SG outlet temperature is a result of the mixture of the hotter coolant from

the upper part of the SG, and the lower part, which is cooled to the SS saturation temperature. So the PS temperature at the SG outlet is increasing constantly, its rate depends on how many SG tubes are uncovered. A nodalisation effect can be seen here - if one looks closely on the primary side pressure, one can detect a step-wise pressure increase (which, as analysis showed, corresponds to the event when the SG-SS level drops below one of the SG-tube-bundle simulations). The increasing of the PS pressure causes the increase of PS temperature. Between 280 and 325 s the four groups of the PRZ heaters are switched off and at 555 s the PORV opens and starts to cycle.

From accident management to the end of the transient: at 3530 s the core exit temperature reaches 350 °C and the operator starts the accident management. The MSIV valves of SG2 and SG3 are closed to isolate them, while the BRU-A valves for SG1 and SG4 are fully opened soon after. An external sources (e.g. Fire brigade trucks) are connected to the feed water lines of SG1 and SG4 and supply feedwater having a flow rate of 10 kg/s into each SG up to 1 MPa. The tested countermeasure is effective in reducing the PS temperature and pressure. Namely after 7700 s the core outlet temperature drops below 300 °C, which was set as criteria for successful accident management.

No	Event	Time (s)
1	LOFW (FW, AFW, EFW) and closure of the TSV	0
2	First opening of the BRU-A valves (failure of the BRU-K valves assumed)	3
3	spray line opens	3
4	spray line closes	13
5	prz heaters group 1 switched on	14
6	prz heaters group 2,3,4 switched on	15
7	MCP 1 trip (on SG low level)	46
8	MCP 2,3,4 trip (on SG low level)	47
9	scram (4 pumps tripped, 1s delay)	48
10	switch off PRZ heaters group 3	280 - 285
11	switch off PRZ heaters group 2,4	310 - 315
12	switch off PRZ heaters group 1	320 - 325
13	beginning of PORV cycling	555
14	core exit temperature reaches 350 °C	3530
	AM strategy: SG 1 and 4 refilled, SG 2 and 3 isolated	
15	switch on PRZ heaters group 1,3	4400
16	switch on PRZ heaters group 2,4	4410
17	switch off PRZ heaters group 1,2,3,4 (low level PRZ)	7350 - 7400
18	core outlet temperature drops below 300oC	7700

Table 3.29: Resulting events, test 1

3.3.2 Scenario 2

Short description of the test: Initiating event is a total loss of feed water and all the trains of HPIS are considered to fail. On the contrary LPIS and accumulators are available. The AM consists in SS depressurization, followed by PS depressurization: the operator isolates SG 2 and SG 3 by MSIV closure, depressurizes SG 1 and SG 4 supplying water with a flow rate of 10 kg/s at 1 MPa (into SG 1 and SG 4). This action should decrease the PS pressure below 16 MPa and the PS coolant temperature down to 300 °C. When this plant state is reached the operator opens the PORV to accelerate the PS depressurization. The saturation margin at the core exit is used as set-point for the PORV operation. The accident management is considered to be successful when the core exit coolant temperature drops below 200 °C.

First 100s: The initial phase develops exactly as in test 1, section 3.3.1. The imposed initial event is a LOFW. FW, AFW and EFW fail at time 0 s, the TSV closes at the same time. A rapid increase in the SS pressure is the immediate result. Since the BRU-K valves are assumed to be not operational, the set point of the BRU-A valves opening is reached after 3 s. The PS pressure follows, and the spray line fully opens after 3 seconds. The BRU-A valves have a capacity of 250 kg/s of steam, which is lower than the 408 kg/s of steam usually produced by each SG. So only a fraction of the produced heat is removed, which leads to an

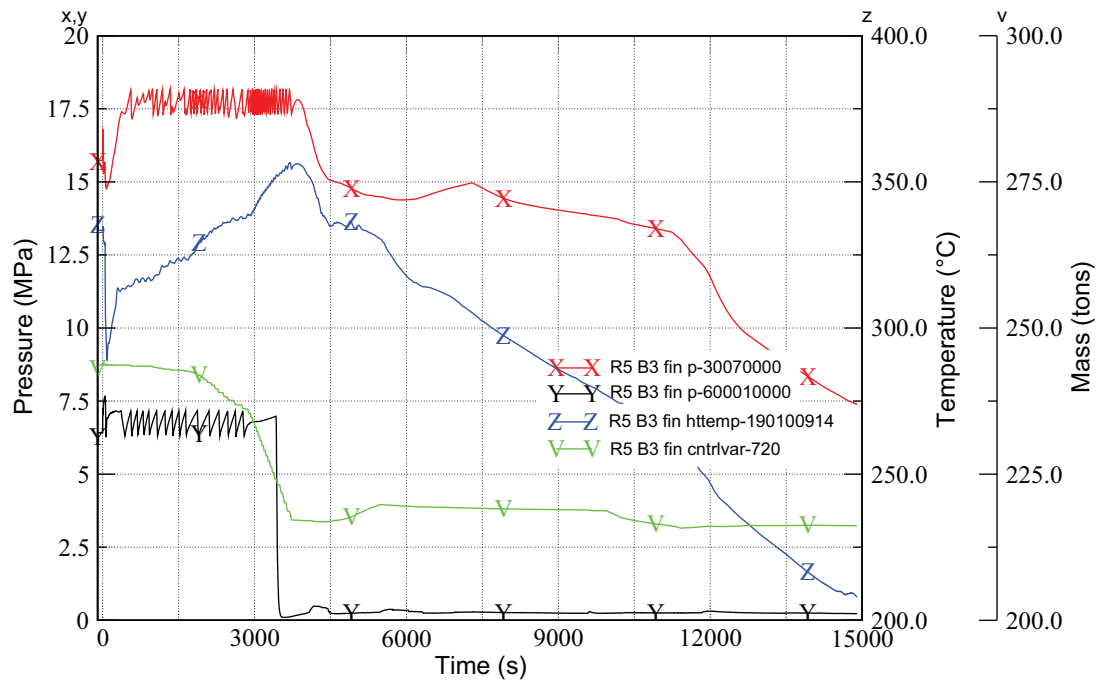


Figure 3.63: Relap5 primary and secondary side pressure, temperature and mass inventory, calculation 1

increase in the PS temperature at the SG outlet of almost 10°C . This in turns leads to a negative reactivity feedback due to the reduced moderator density and a reduction in power of almost 30%. A rapid decrease in the PS pressure occurs after 13 s, the spray line closes and after 14 - 15 s all groups of the pressurizer heaters are switched off. At 46 - 47 s the MCPs are tripped on a low level signal of the steam generators (0.5 m less than the nominal level), the reactor SCRAM follows at 48 s (All MCPs tripped, scram with 1s delay for signal propagation time).

100 s up to the AM: the upper part of the SG tubes are uncovered, thus the heat exchange (PS to SS) is here reduced almost to zero. The SG outlet temperature is a result of the mixture of the hotter coolant from the upper part of the SG, and the lower part, which is cooled to the SS saturation temperature. So the PS temperature at the SG outlet is increasing constantly, its rate depends on how many SG tubes are uncovered. Between 280 and 325 s the four groups of the PRZ heaters are switched off and at 555 s the PORV opens and starts to cycle.

From the AM to the end of the transient: at 3530 s the core exit temperature reaches 350°C and the operator starts the accident management. The MSIV valves of SG 2 and SG 3 are closed to isolate them, while the BRU-A valves of the SG 1 and SG 4 are fully opened soon after. An external sources (e.g. Fire brigade trucks) are connected to the feed water lines of SG 1 and SG 4 and supply feedwater having a flow rate of 10 kg/s into each SG up to 1 MPa. The tested countermeasure is effective in reducing the PS temperature and pressure. Namely after 7650 s the core outlet temperature drops below 300°C , the PS pressure drops below 16 MPa thus the second part of the AM strategy is actuated. The PORV is openend, at 7900 s the PS saturation margin above the core drops below 15°C and the PORV is closed. The PORV is opened and closed again at 9500 s and 9950 s respectively and again at 11200 s and 11600 s. At this time the PS pressure drops below 6 MPa, the set point for the HA injection. The PORV is opened for the last time at 13700 s, at about 14000 s the core exit temperature is below 200°C and the LPIS starts to inject. The calculation is stopped after 20000 s.

3.3.3 Scenario 6

Short characterization of the test: Initial event is a total loss of feed water. All ECCS are considered to be available. As accident management the operator opens the PORV when the core exit temperature increases to 310°C , but not earlier than 1800 s. The measure is successful if the core exit coolant temperature decreases below 200°C .

First 100 s: Also Test 6 repeats, due to the same conditions at the The imposed initial event is a LOFW.

No	Event	Time (s)
1	LOFW (FW, AUX FW, EFW) and closure of the TSV	0
2	First opening of the BRU-A valves (failure of the BRU-K valves assumed)	3
3	Spray line open	3
4	Spray line closure	13
5	PRZ heaters group 1 switched on	14
6	PRZ heaters group 2,3,4 switched on	15
7	MCP 1 trip (on SG low level)	46
8	MCP 2,3,4 trip (on SG low level)	47
9	Scram (4 pumps tripped, 1s delay)	48
10	Switch off PRZ heaters group 3	280 - 285
11	Switch off PRZ heaters group 2,4	310 - 315
12	Switch off PRZ heaters group 1	320 - 325
13	Beginning of PORV cycling	555
14	Core exit temperature reaches 350 °C	3530
	AM strategy: SG1 and 4 refilled, SG2 and 3 isolated	
15	Switch on PRZ heaters group 1,3	4400
16	Switch on PRZ heaters group 2,4	4410
17	Switch off PRZ heaters group 1,2,3,4 (low level PRZ)	7350 - 7400
18	Core outlet temperature drops below 300 °C	7650
	operator opens the PORV	
19	Saturation margin 15 °C, PORV closed	7900
20	Saturation margin 30 °C, PORV opened	9500
21	Saturation margin 15 °C, PORV closed	9950
22	Saturation margin 30 °C, PORV opened	11200
23	Accumulators injection	11500
24	Saturation margin 15 °C, PORV closed	11600
25	Saturation margin 30 °C, PORV opened	13150
26	Core exit temperature less than 200 °C	13700
27	LPIS start to inject	14000
28	Calculation stop	20000

Table 3.30: Resulting events, test 2

FW, AFW and EFW fail at time 0 s. The TSV closes at the same time. A rapid increase in the SS pressure is the immediate result. Since the BRU-K valves are assumed to be not operational, the set point of the BRU-A valves is reached after 3 s and the BRU-A valves open. The PS pressure follows, and the spray line fully opens after 3 seconds. The BRU-A valves have a capacity of 250 kg/s of steam, which is lower than the 408 kg/s which are usually produced. So only a fraction of the produced heat is removed, which leads to an increase in the PS-SG outlet temperature of almost 10 °C. This in turns leads to a negative reactivity feedback due to the reduced moderator density and a reduction in power of almost 30 %. A rapid decrease in the PS pressure is the result. after 13 s the spray line closes and after 14-15 s all groups of the pressurizer heaters are switched off. At 46-47 s the MCPs are tripped on a low level signal of the steam generators (0.5 m less than the nominal level) - reactor SCRAM follows at 48 s (All MCPs tripped, scram with 1s delay for signal propagation time).

100 s up to accident management: The upper part of the SG - U-tubes are uncovered. The heat exchange PS to SS here is reduced to almost zero. The SG outlet temperature is a result of the mixture of the hotter coolant from the upper part of the SG, and the lower part, which is cooled to the SS saturation temperature. So the temperature of the PS SG outlet is increasing constantly, with a rate increasing depending on how many of the SG U-tubes are uncovered.

From accident management to the end of the transient: After 30 minutes the operator decides to depressurize the PS by opening the PORV. At the same time he switches off the PRZ heaters. The aim is to decrease the PS pressure below the set point of the HPIS. Two trains of HPIS are available - train No 2 and No 3. At 2200 s the set point for the HPIS is reached and train 2 and 3 start to inject. At 2800 s the

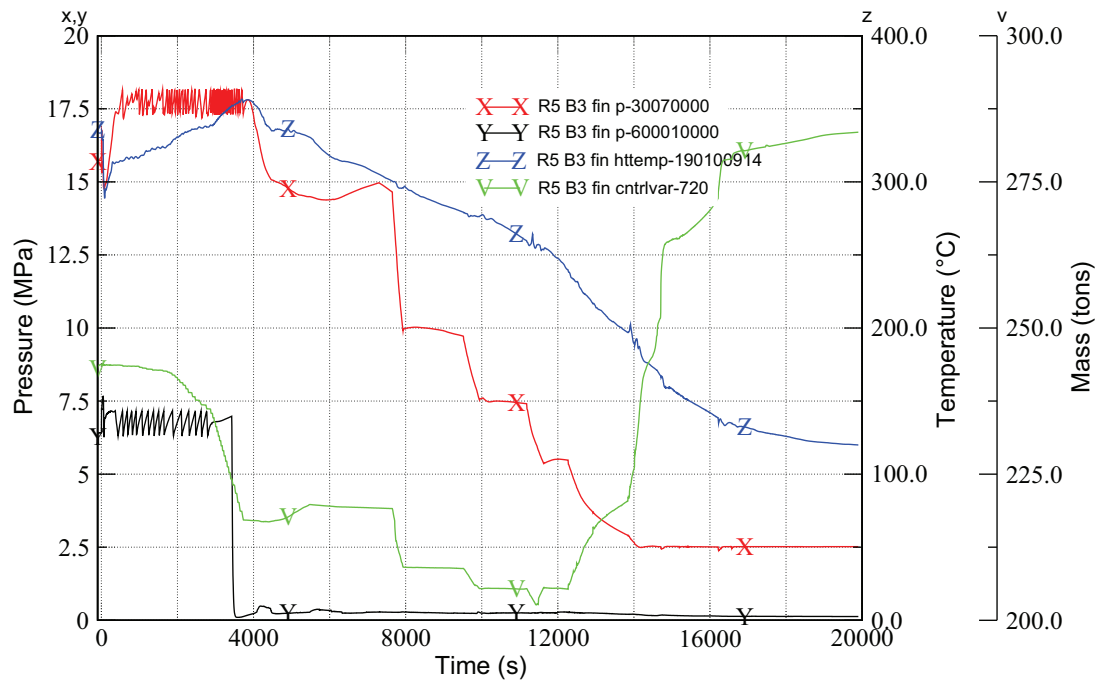


Figure 3.64: Relap5 primary and secondary side pressure, temperature and mass inventory, calculation 2

HPIS tanks are empty, and supply is switched to the sump. The HPIS helps to further cool down and thereby depressurize the PS, so that at 4800 s the HA start to inject. The pressure stays constant near to the HA set point, while at 6800 s the core outlet temperature drops below 180 °C .

Primary and secondary system pressure, the primary system mass and the clad temperature are reported in Figure 3.65

3.3.4 Scenario 7

Short characterization of the test: Initial event is a station blackout. Only passive ECCS is available (the accumulators). After the rod cladding temperature rises up to 350 °C the operator depressurizes SG 1 and SG 4, and isolates SG 2 and SG 3 as accident management. Water supply from an external source starts with a flow rate of 20 kg/s into SG 1. Should the temperature increase of the cladding proceed up to 400 °C despite of this measure, the operator splits the total available amount of feed water flow equally to SG 1 and SG 4. The accident management is considered to be successful if the process stabilizes (PORV no longer cycling, primary pressure stagnating or decreasing).

First 100 s: The initiating event is a loss of off- and on site power (station blackout). So reactor SCRAM, closure of the TSV, MCP trip, loss of all sources of feed water occurs at 0 s. Due to the coast down time of the pumps (232 s) the SG remove more power than the scrammed reactor produces for the first 75 s. The PS temperature pressure and temperature drop. The SG levels start to decrease.

100 s up to accident management: The upper part of the SG - U-tubes are uncovered. The heat exchange PS to SS here is reduced to almost zero. The SG outlet temperature is a result of the mixture of the hotter coolant from the upper part of the SG, and the lower part, which is cooled to the SS saturation temperature. So the temperature of the PS SG outlet is increasing constantly, with a rate increasing depending on how many of the SG U-tubes are uncovered. After 2890 s the PS pressure increases to the set point of the PORV (start of PORV cycling). After 5000 s the SG level drops below 15cm, which marks the beginning of the U-tubes.

From accident management to the end of the transient: After 5650 s the cladding temperature in the upper part of the core exceeds 350 °C . This is a sign for the operator to take action: SG 2 and SG 3 are isolated, SG 1 and SG 4 are depressurized. Feed water from mobile pumps (fire brigade trucks) with a flow rate of 20 kg/s are furnished into SG 1. This measure is successful in reverting the temperature trend: the PS temperature starts to decrease, so does the PS pressure. After 20000 s (end of calculation) the PS temperature at the core outlet is about 170 °C , the PS pressure about 8 MPa.

No	Event	Time (s)
1	LOFW (FW, AUX FW, EFW) and closure of the TSV	0
2	First opening of the BRU-A valves (failure of the BRU-K valves assumed)	3
3	spray line opens	3
4	spray line closes	13
5	prz heaters group 1 switched on	14
6	prz heaters group 2,3,4 switched on	15
7	MCP 1 trip (on SG low level)	46
8	MCP 2,3,4 trip (on SG low level)	47
9	scram (4 pumps tripped, 1s delay)	48
10	switch off PRZ heaters group 3	280-285
11	switch off PRZ heaters group 2,4	310-315
12	switch off PRZ heaters group 1	320-325
13	beginning of PORV cycling	555
14	beginning of operator action: opening of porv	1800
15	HPIS supplying to loop 3 and 4 start to inject	2200
15	HPIS tanks are empty, supply is switched to the sump	2800
17	Accumulators start to inject	4800
18	Core outlet temperature less than 180oC	6800

Table 3.31: Resulting events, test 6

Primary and secondary system pressure, the primary system mass and the clad temperature are reported in Figure 3.66.

No	Event	Time (s)
1	Loss of on- and offsite power. Scram, closure of TSV, MCP trip, loss of all feed water	0
2	BRU-A valves open for the first time	4
3	first opening of the PORV	2890
4	SG1,SG2,SG3,SG4 level drops below 15cm (no U-tubes)	5000
5	peak cladding temperature exceeds 350oC , operator isolates SG2, SG3, and depressurizes SG1 and SG4 after. Feed water with a flow rate of 20kg/s is furnished into SG1	5650
6	last opening of PORV	5950
7	Core outlet temperature is less than 200oC	16620
8	pressurizer empty	17700
9	End of calculation	20000

Table 3.32: Resulting events, test 7

Influence of the SG model: Scenario 7 shows a numerical effect - the influence of the detail in the SG Relap5 model on the calculation ([Muellner et al., 2008]). Dominant phenomena during the first phase of the accident is the heat transfer from primary to secondary system. The VVER-1000 Relap5 model divides the SG-U-tubes in six vertical levels. Each level is represented by one (horizontal) Relap5 pipe-component (with 18 subvolumes), which is connected to two (vertical) pipe-components on the secondary side. The secondary side of the SG is modelled by two pipes with six subvolumes (one for each level) which are connected to the primary system, one to the first 12 sub-volumes of the SG-U-tubes, one to the sub-volumes 13-18, the hot-and cold riser. A third pipe of six subvolumes models the SG downcomer (to allow for recirculation). The three pipes lead at the top in the SG dome, and are joint by one branch component at the bottom.

During a station blackout primary system parameters stay relatively stable, while the SG secondary side inventory boils off. Once the SG U-tubes are uncovered, the heat transfer surface between primary and secondary side decrease. This means, that part of the primary coolant passes through SG U-tubes which are

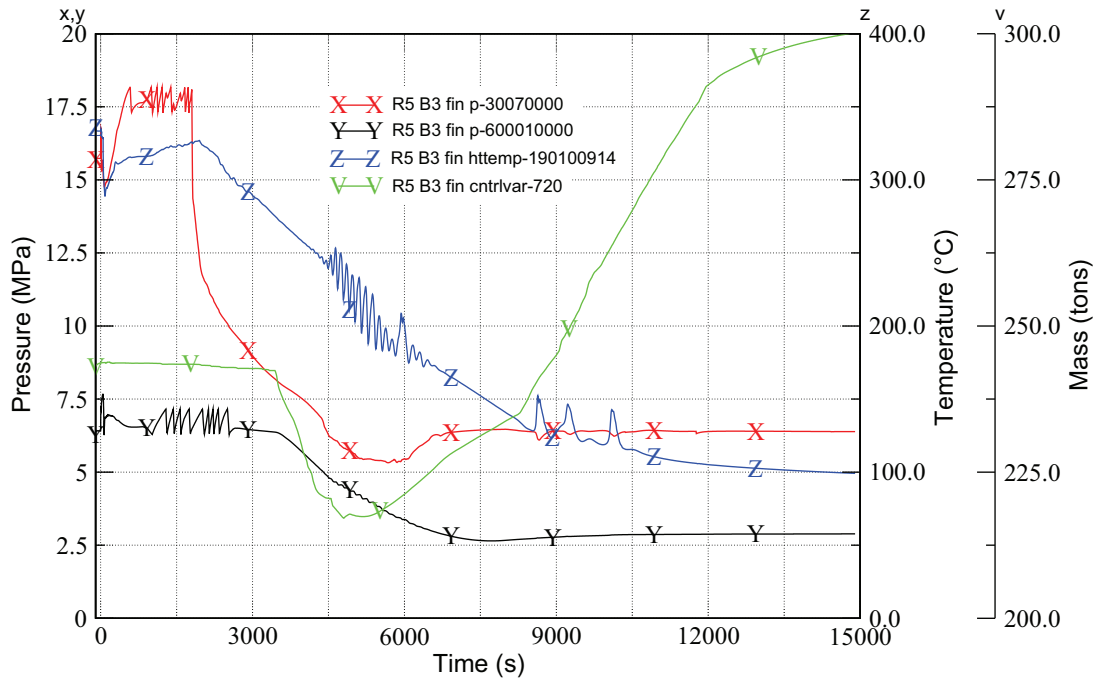


Figure 3.65: Relap5 primary and secondary side pressure, temperature and mass inventory, calculation 6

completely uncovered (and is therefore not cooled). At the steam generator outlet coolant from covered and uncovered SG U-tubes is mixed, and the SG-outlet temperature will be dependent on the relation of covered to uncovered U-tubes. One would expect a continuous process of ps coolant increase and SG-level decrease.

However, this is not what the calculation result is showing. If one looks close on the primary system pressure for the first phase of the transient (until opening of the PORV), one can identify six steps of pressure increase (corresponding to the six levels of the SG). To understand the both, the physical phenomena and how it is simulated by the code, the SG model has been cut out from the whole nodalisation, and an investigation on heat transfer primary to secondary has been made. The following two paragraphs aim to explain where the effect comes from, to estimate what might be the physical situation, and to quantify the difference to the calculated results.

Heuristic approach To analyze the main phenomena (the heat transfer primary to secondary) during the first hours of an SBO, a number of simplifying assumptions have been made.

Main interest was on the effect of the SG-model in a bulk-properties code on the heat transfer. The conditions, that were established 500 s after beginning of the calculation in scenario 7, have been taken as boundary conditions for a reduced input, modeling just a single loop. The nodalisation of just a single loop can be seen in Figure 3.69, the boundary conditions (line 1-3, line 4 and 5 are for information) in Table 3.33).

No	Parameter	Unit	Value
1	Loop flow rate	kg/s	200
2	Loop pressure between SG and MCP	MPa	15
3	Loop temperature upstream SG	°C	300
4	Core power	MW	80
5	Feed water needed	kg/s	10-15

Table 3.33: BC for analysis

The small set-up should be sufficient to study the dominant phenomena during the initial phase of a station black out in a NPP with a horizontal type SG, i.e. the declining heat transfer in time.

At first a heuristic analysis of the situation should give an idea what is to be expected. Figure 3.67 shows the situation. One can assume a more or less constant mass flow in natural circulation regime for several thousands of seconds once the coast down of the pumps is complete. For simplicity, the temperature of the

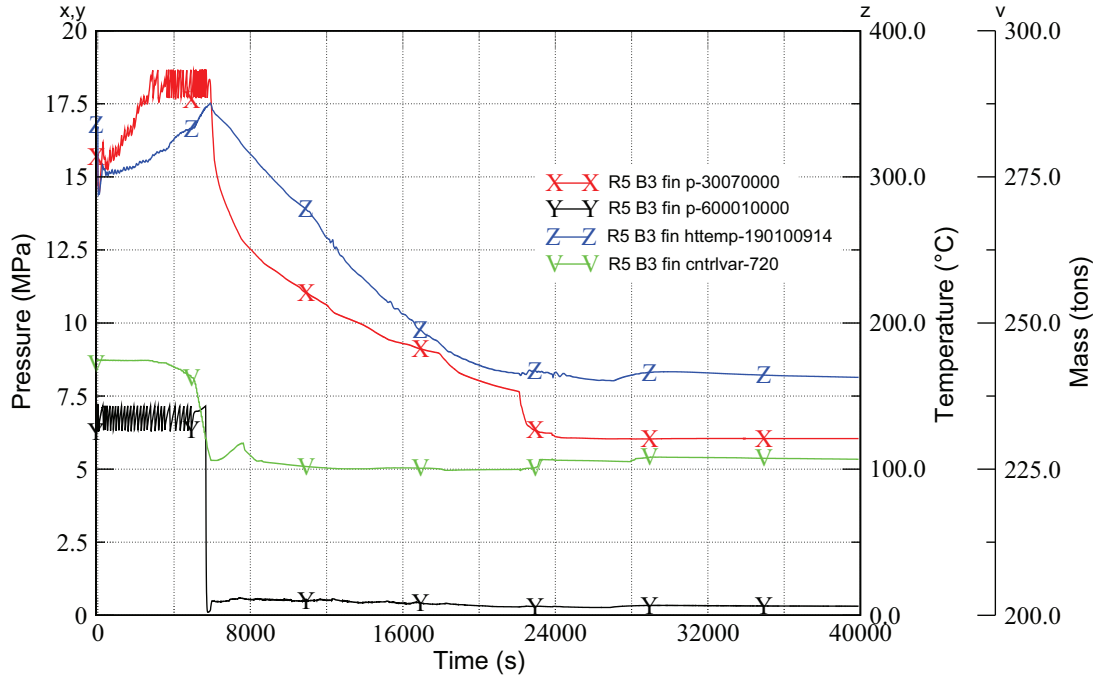


Figure 3.66: Relap5 primary and secondary side pressure, temperature and mass inventory, calculation 7

fluid at the core outlet is also assumed to be constant. This is not the case in a “real” SBO, but allows to study the phenomena. So for the primary side one can assume a given mass flow \dot{m}^{ps} and specific enthalpy h_{in}^{ps} upstream of the SG.

During normal operation, all SG tubes are covered with water from the secondary side. Once the feed water is lost, the level on the secondary side of the SG will start to drop, and the SG tubes will uncover. One can assume that the heat exchange PS to SS takes place only in the SG-tubes, and can neglect the SG hot- and cold header. If the SG-tubes are covered with water on the secondary side, the primary fluid will cool down to the saturation temperature of the secondary side (natural circulation). If the SG-tubes are not covered with water, their contribution to the heat exchange again is negligible - due to the low heat capacity of steam. The only significant contribution to heat exchange will come from the SG-tubes covered with water - the specific enthalpy at the end of the SG-tubes is designated with h_{out}^{ps} .

The number of SG-tubes covered with water is proportional to the Volume of feed water still available at the secondary side. This means, the flow that passes through the SG-tubes covered with water, and further the total heat removed by the SG secondary side can be approximately described as

$$\dot{m}_{tc}^{ps} = \dot{m}^{ps} \cdot \frac{V}{V_{2m}} \quad (3.1)$$

$$P = \dot{m}^{ps} \cdot \frac{V}{V_{2m}} (h_{out}^{ps} - h_{in}^{ps}) = \dot{m}^{ps} \cdot \frac{V}{V_{2m}} \cdot \Delta h^{ps} \quad (3.2)$$

- \dot{m}_{tc}^{ps} Total mass flow of primary side coolant through SG-tubes covered with water on the secondary side
- \dot{m}^{ps} Total loop primary side mass flow
- V Volume of secondary side liquid fluid
- V_{2m} Volume of secondary side liquid fluid, at which all SG-tubes are covered, corresponding to a level of 2 m (nominal collapsed level is 2.25 m)
- P Exchanged power

The Power is removed by the secondary by boiling off the still available feed water, which is then released to the environment through the BRU-A valves as steam:

$$P = \dot{m}^{sg} (h_{out}^{sg} - h_{in}^{sg}) = \dot{m}^{sg} \cdot \Delta h^{ss} \quad (3.3)$$

The decrease in volume of the secondary side fluid is equal to the mass leaving the SG, so

$$\rho_{fw} \cdot \dot{V} = -\dot{m}_{sg} \quad (3.4)$$

Resolving equation 3.3 for \dot{m}^{sg} , substituting P from equation 3.2, and substituting finally for \dot{m}_{sg} in equation 3.4 leads to

$$\dot{V} = -V \left(\frac{\dot{m}^{ps}}{\rho_{fw} \cdot V_{2m}} \cdot \frac{\Delta h^{ps}}{\Delta h^{ss}} \right) = -V \left(\frac{\dot{m}^{ps}}{M_{2m}} \cdot \frac{\Delta h^{ps}}{\Delta h^{ss}} \right) = -kV \quad (3.5)$$

Which, assuming that at $t = 0$ the level in the SG is equal to 2 m, leads to a rough estimate for the decrease of SG side inventory according to p

$$V(t) = V_{2m} \cdot e^{-k \cdot t} \quad (3.6)$$

The relation between SG liquid level and SG liquid volume unfortunately can not be written in an easy way (assuming the SG is a cylinder). With L being the SG length, l the level, r the radius

$$V = L \left(r^2 \cdot \arccos \left(\frac{r-l}{r} \right) - (r-l) \sqrt{2rl - l^2} \right) \left(1 - \frac{V_{tubes}^{ps}}{V_{2m}^*} \right) \quad (3.7)$$

The formula was checked against real-plant data from Balakovo3 [Mikhailchuk, 1997]. So in the end, the heuristic approximation for the level in time will be an implicit equation. Substituting numbers for all quantities leads to the equation

$$55.16 \text{ m}^3 \cdot e^{-4.04 \cdot 10^{-4} s^{-1} \cdot t} = 11.4m \left(4 \text{ m}^2 \cdot \arccos \left(\frac{2m-l}{2m} \right) - (2m-l) \sqrt{2m \cdot l - l^2} \right) \cdot 0.77 \quad (3.8)$$

r	2 m	
L	11.4 m	
\dot{m}^{ps}	200 kg/s	
M_{2m}	37 tons	
V_{2m}	55.16 m ³	without volume occupied by PS in SS
V_{2m}^*	71.5 m ³	half of SG volume
Δh^{ss}	1.5528 MJ/kg	
Δh^{ps}	0.1160 MJ/kg	
k	$4.04 \cdot 10^{-4} s^{-1}$	
V_{tubes}^{PS}	23.4 m ³	

Figure 3.68 shows a plot of function 3.8. To have also the exchanged power, one simply substitutes the result 3.6 into 3.4 and further into 3.3:

$$P(t) = -M_{2m} \Delta h^{ss} k e^{-kt} = 23MW \cdot e^{-4.04 \cdot 10^{-4} s^{-1} t} \quad (3.9)$$

Numeric analysis In the current analysis, the horizontal steam generators are modelled with six levels for heat transfer. The U-tubes are during station black out conditions the primary side shows a more or less constant mass flow and stays subcooled, while secondary side mass inventory is still available. The water still available on the secondary side boils off in the course of two to three hours.

The situation described in the heuristic considerations is now analysed using the code Relap5. A nodalisation with six, three and one level for the steam-generator U-tubes has been set up.

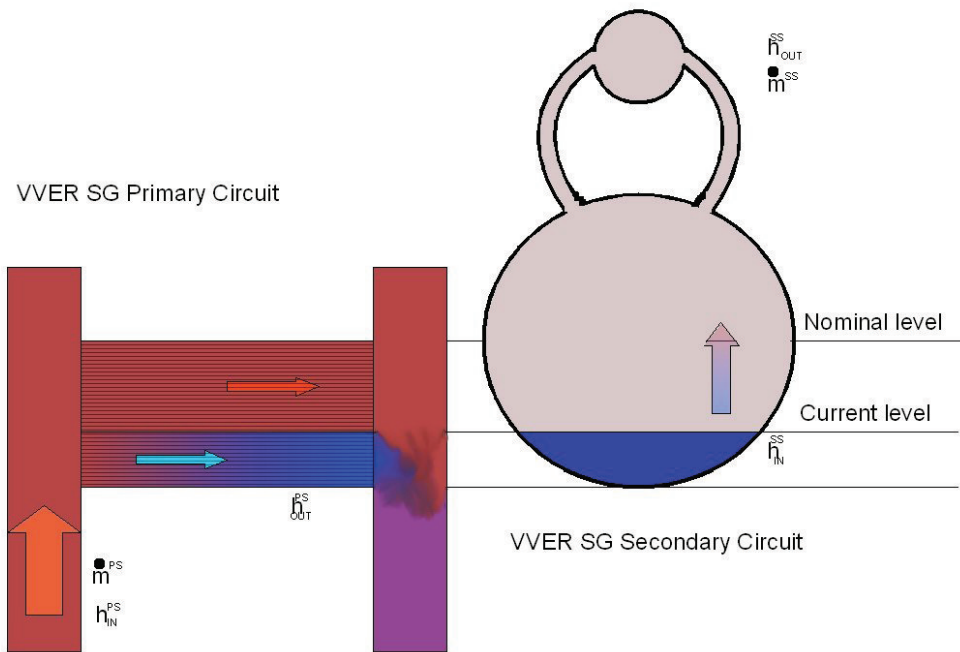


Figure 3.67: SG heat transfer, heuristic

On the primary side inlet (hot leg) a flow rate of 200 kg/s at a temperature of 300 °C has been imposed. At the outlet of the SG a pressure of 15.0 MPa has been imposed. On the secondary side the SG is filled up to the nominal level with water. Feed water was injected up to 500 s (10-15 kg/s) to keep the level constant, and then switched off (steady state time). In the Cathare calculations no feed water has been injected. A pressure of 6.27 MPa has been imposed at the end of the volumes simulating the steam line.

In real physics, the drop of the liquid level in the steam generator, the decrease of heat transfer area and the deterioration of the heat transfer are continuous processes. A TH-SYS code, on the other hand, will typically model the secondary side with volumes of 0.25 m to 0.5 m height. The heat transfer correlations are chosen depending on the bulk properties of the volumes (see Section 2.4.1. The conditions during a station black out are such that the code uses first subcooled/saturated nucleate boiling, “mode 3 and 4” correlations listed in Table 2.13 (Chen). Then, when the void fraction drops below a certain threshold, the code jumps suddenly into single phase gas and uses “mode 9” heat transfer correlations from Table 2.13 (e.g. Dittus-Boelter). As a consequence, the transferred heat, instead of deteriorating slowly, shows a step-function. Furthermore, since the heat transfer drops to zero only when the control-volume average void fraction is close to zero, the heat transfer is calculated correctly only when the control-volume is full of liquid. For intermediate stages, with void fractions between 0 and 1, the heat transfer seems to be overestimated (since equal to the heat transfer when the volume is full of liquid).

The result of the six level nodalisation, Figure 3.69, shows a not physical step-function for the transferred power. The function shows six steps, which, as can be seen in the Figures, take place when the void-fraction of one of the sub-volumes drops to zero.

The calculated power is compared to the “heuristic” result. One can see that the transferred power is overestimated, and that the heat-transfer therefore completely ceases to take place earlier than predicted by the heuristic calculation. The heuristic calculation assumed that the level of the SG is at 2 m (height of the U-tubes). The heuristic power curve therefore is shifted, to start when the level in the numerical calculations reaches 2 m. This is the case at 445 s for Cathare, and 1440 s for Relap.

The nodalisations with three volumes for the heat transfer show the same behavior, refer to Figure 3.70. Now, as expected, the power-curve shows only three steps. The error in calculating the heat-transfer is larger, therefore the SG-level drops faster compared to the 6-node calculation.

The nodalisations with only one volume confirm the trend, see Figure 3.71. Using just one large volume,

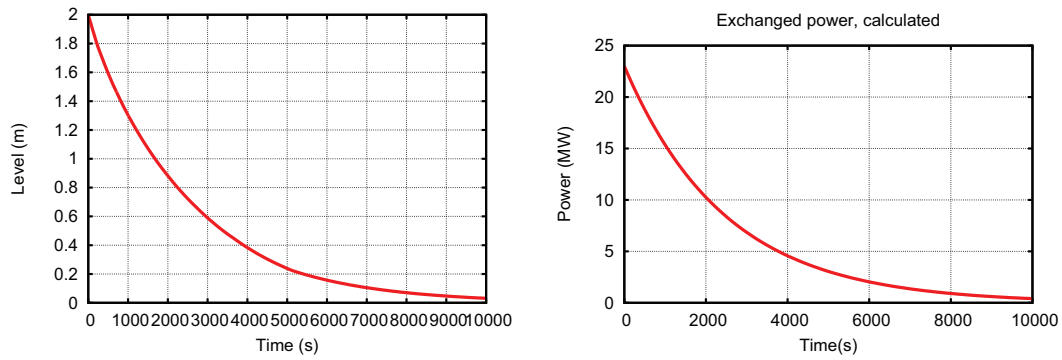


Figure 3.68: Level of the SG and heat transfer, heuristic evaluation

the heat transfer degrades at a sudden.

Figure 3.72 summarizes the levels for the three Relap nodalizations. The comparison of the level with the heuristic result should be used with care. The results should be seen more on a qualitative level. But one can conclude that the level of detail when noding the SG has a significant influence on the heat-transfer during SBO conditions. The time to boil off the SG inventory is significantly lower using a 1-node nodalisation than using a 6-node nodalisation. It can be assumed that the time at which the SG is empty in the real situation would be even further in time.

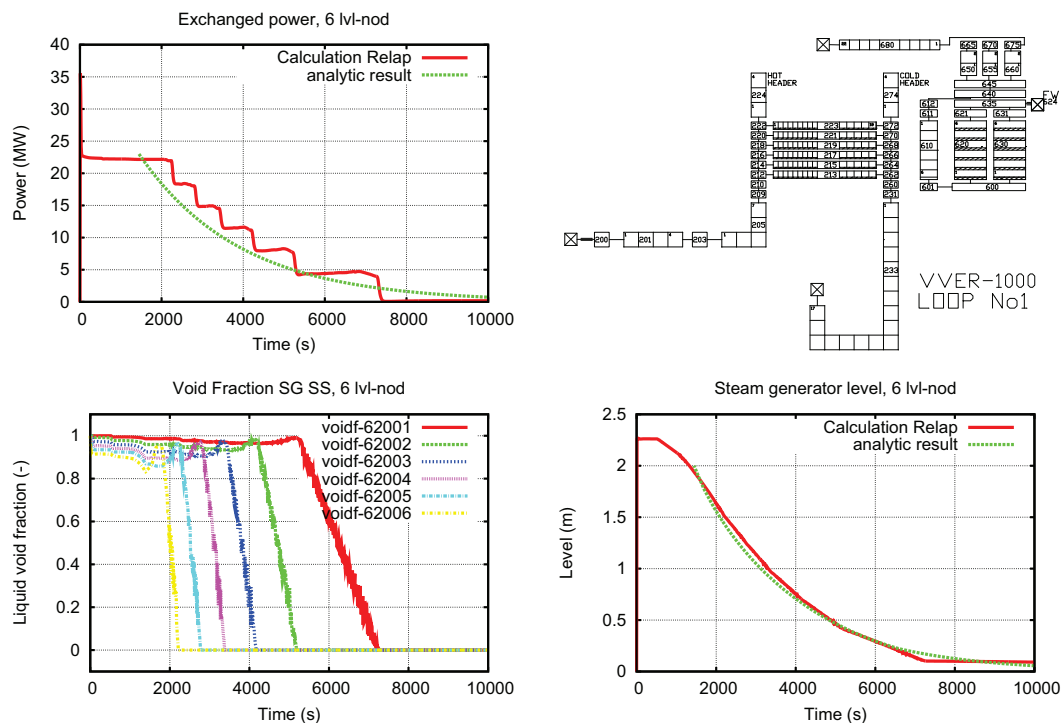


Figure 3.69: Sc 7 heat transfer across SG, six levels, nodalisation, exchanged power, level, void fraction (Relap)

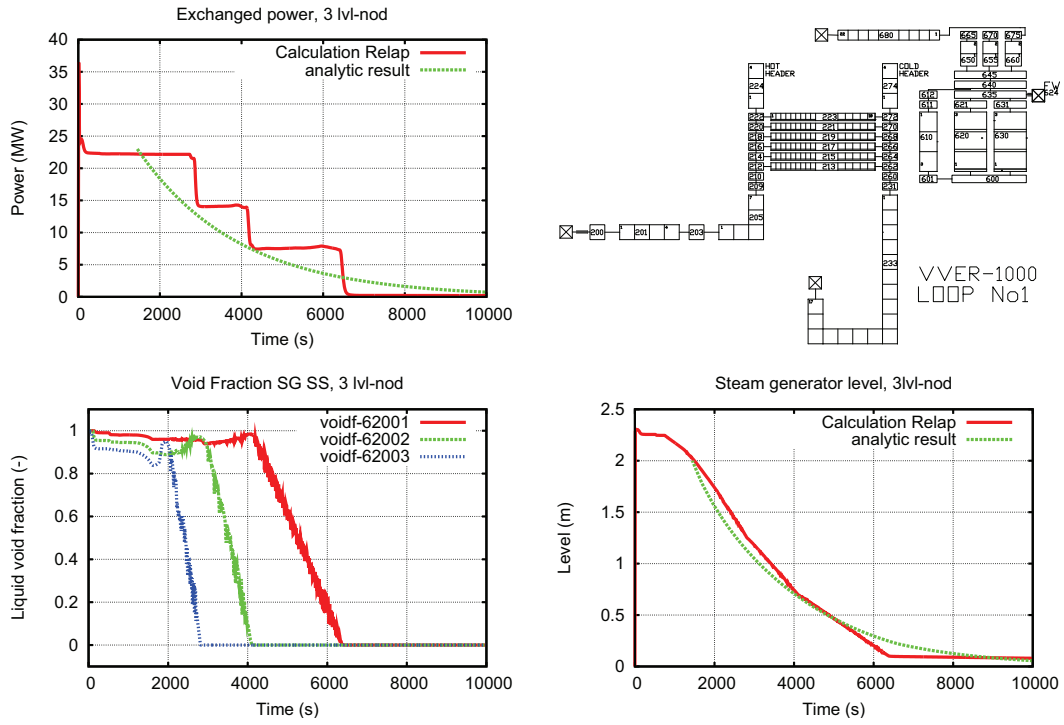


Figure 3.70: Sc 7 heat transfer across SG, three levels, nodalisation, exchanged power, level, void fraction

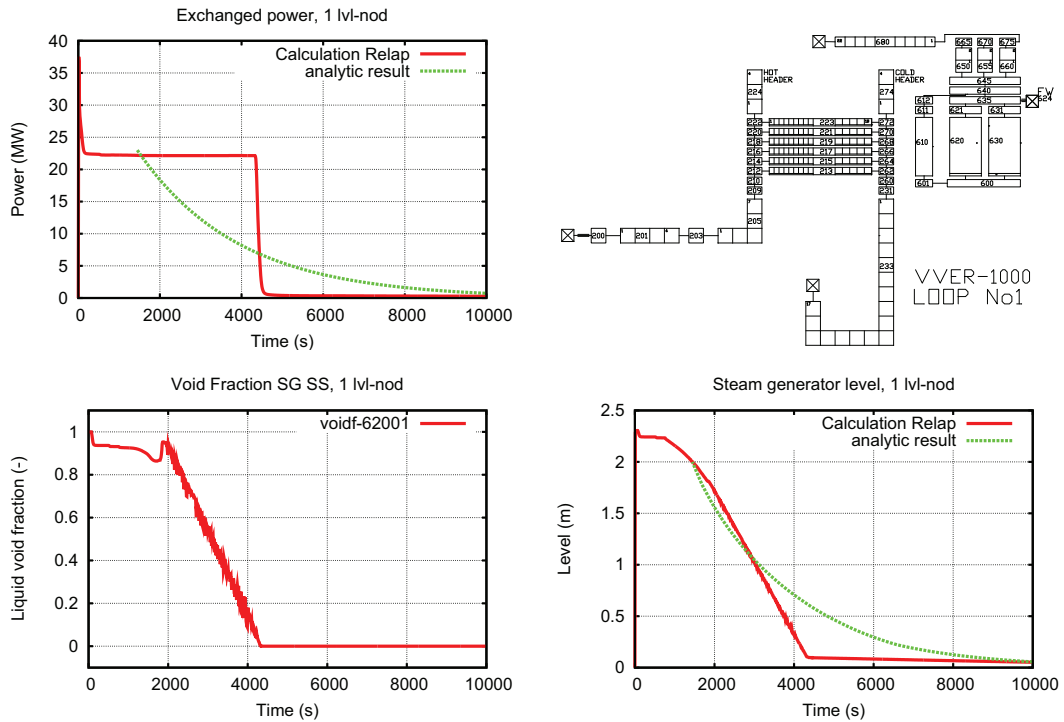


Figure 3.71: Sc 7 heat transfer across SG, one level, nodalisation, exchanged power, level, void fraction

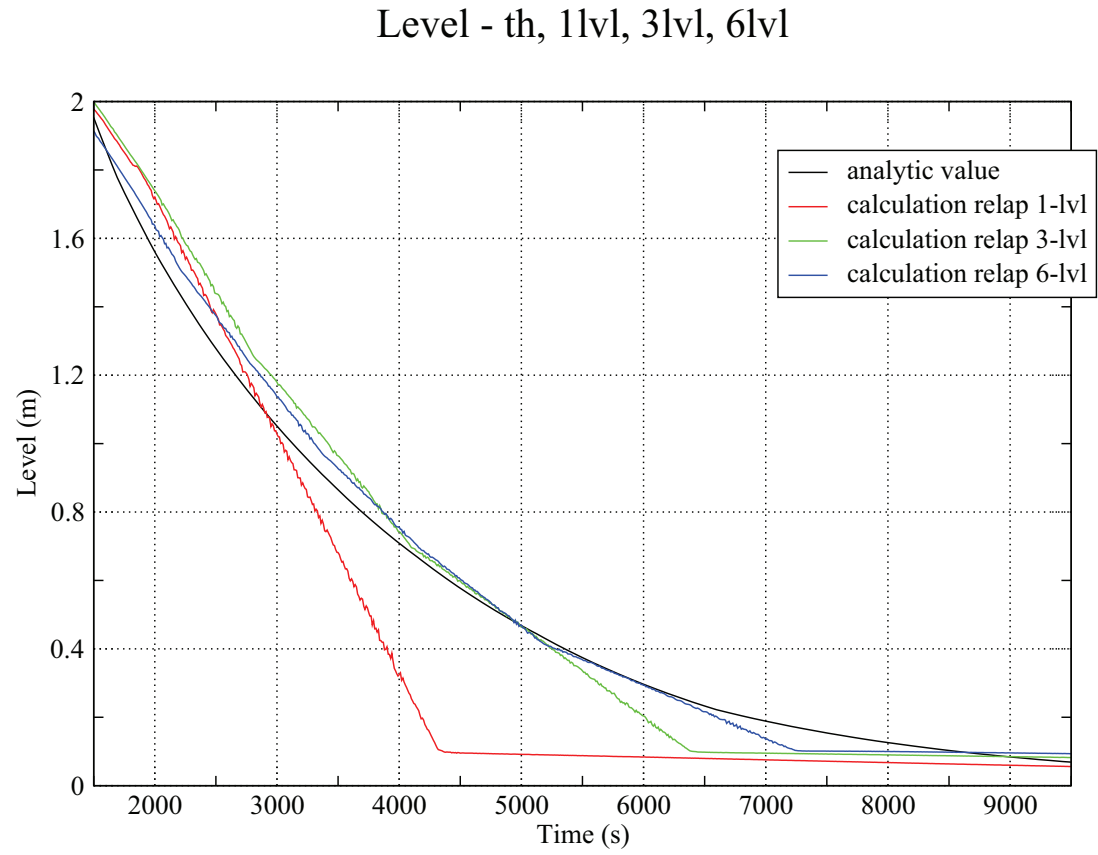


Figure 3.72: Sc 7 heat transfer across SG, SG levels

rm

3.4 SBLOCA

A series of calculations to investigate the effect of a loss of coolant accident have been performed. The break area was in most cases equivalent to 70 mm or less, and assumed to be a small break in loop No 4.

Two calculations are in a certain sense special small breaks - one is calculation No 3, the investigation of PORV-stuck open as initiating event (Zaphorshye VVER 1000 Unit 1, 1995 - for details please refer to Blinkov et al. [2004]). The other one is calculation No 10, which is actually the case corresponding to a natural circulation experiment. Coolant is continuously drained from the lower plenum during natural circulation conditions.

The calculations have been performed in the frame of an EC project, and are therefore also reported in D'Auria et al. [2006].

3.4.1 Scenario 3 - Zaphorshye

The Zaporoshye test and plant calculation aims at reproducing the Zaporoshye PORV stuck open accident from 1995. The plant was in shut down condition, put at full pressure, 23 h after shut down. During a routine test of the PORV and safety valves (PS pressure was increased with the pressurizer heaters up to the set point of the valve), one of the three PRZ relief valves failed to close. Within 1000 s the PS pressure dropped down to the set point of the ECCS, and HPIS and HA injection was observed. The dangerous point in this transient was the cool down rate the conditions were such that the PS temperature dropped from 289 °C to 50 °C within 1000 s.

Primary and secondary system pressure, the primary system mass and the clad temperature are reported in Figure 3.73.

No	Event	Time (s)
1	Opening of the PORV	0
2	HPIS injection	257
3	HA injection	461
4	End of the calculation	800

Table 3.34: Resulting events, test 3

3.4.2 Scenario 4

Short description of the transient: Initiating event is a small break in the cold leg of loop 4 with an equivalent diameter of 70 mm (Bethsy). Failure of all trains of HPIS is assumed, while accumulators and LPIS are available. Accident management consists in cooldown of the primary side with the secondary side by full opening of the BRU-A valves of SG2 and SG3 after the core exit temperature exceeds 350 °C, but not earlier than 1800 s. Accident management is considered to be successful if the core exit temperature drops below 200 °C.

First 200 s: The imposed initiating event is a break in the cold leg near RPV with an equivalent diameter of 70 mm. Due to the depressurization a reduction in the moderator density can be observed, which in turns leads to a reduction in power to about 2850 MW. After 21 s the SCRAM signal occurs on the signal pressure in the PS lower than 14.5 MPa while reactor power is larger than 75 closed and the normal FW is switched off. From the closure of the TSV the SS pressure starts to increase. After 58 s MCP1, MCP2 and MCP3 are tripped on high SG level (it is assumed that 30 s are needed to fully stop injection of feedwater). After 87s the BRU-A valves open the first time. At 134 s MCP4 is tripped due to low saturation margin in this loop.

200 s up to accident management: The PS mass inventory decreases. At 725 s DNB occurs in the upper part of the core and the cladding temperature starts to rise. This first dry-out is quenched by loop seal clearing in the loops 1 to 3. At 750 s the PS mass decreased such that the break is no longer covered with liquid. A reduction of the mass flow through the break is the consequence. At 1150 s a second dry-out of the core can be observed. At 1500 s the PS pressure decreased so far that the accumulators start to inject, but they are unable fully quench the dry-out.

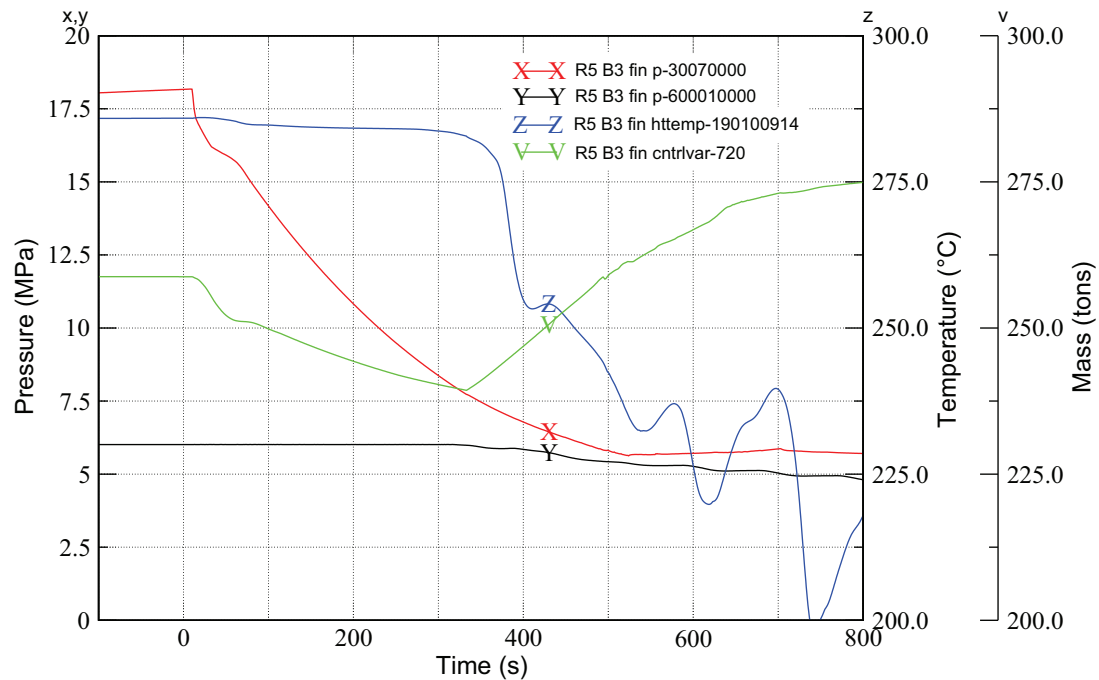


Figure 3.73: Relap5 primary and secondary side pressure, temperature and mass inventory, calculation 3

From accident management to the end of the transient: Half an hour after beginning of the transient (1800 s) the operator decides to isolate SG1 and SG4 while fully depressurizing SG2 and SG3 by opening the BRU-A valves. 200 s later the two SG are completely depressurized. The PS pressure follows the SS pressure, so that the injection of the accumulators is enhanced, and soon after the set point for the LPIS is reached. The PS pressure drop stops at the LPIS set point. The combined accumulator and LPIS injection are quickly able to restore the PS mass inventory, to quench the second dry out and to lower the PS coolant temperature below 200 °C .

Primary and secondary system pressure, the primary system mass and the clad temperature are reported in Figure 3.74.

No	Event	Time (s)
1	break of cold leg 4 with 70mm equiv. diameter	0
2	scram (PS pressure less than 14.5 MPa)	21
3	closure of the TSV, stop of FW (10s after scram)	31
4	MCP 1,2,3 trip (steam generator high level)	58
5	Set point for opening the BRU-A valves is reached for the first time	87
6	Pressurizer empty	100
7	MCP 4 trip (low saturation margin)	134
8	dry out in the core, quenched by loop seal clearing	725
9	break covered with steam only	750
10	start of second dryout	1150
11	accumulators start to inject	1500
12	operator isolates SG1 and SG4 and fully opens the BRU-A valves of SG2 and SG	1800
13	all train of LPIS start to inject	1850
14	core outlet temperature drops below 200oC	1900

Table 3.35: Resulting events, test 4

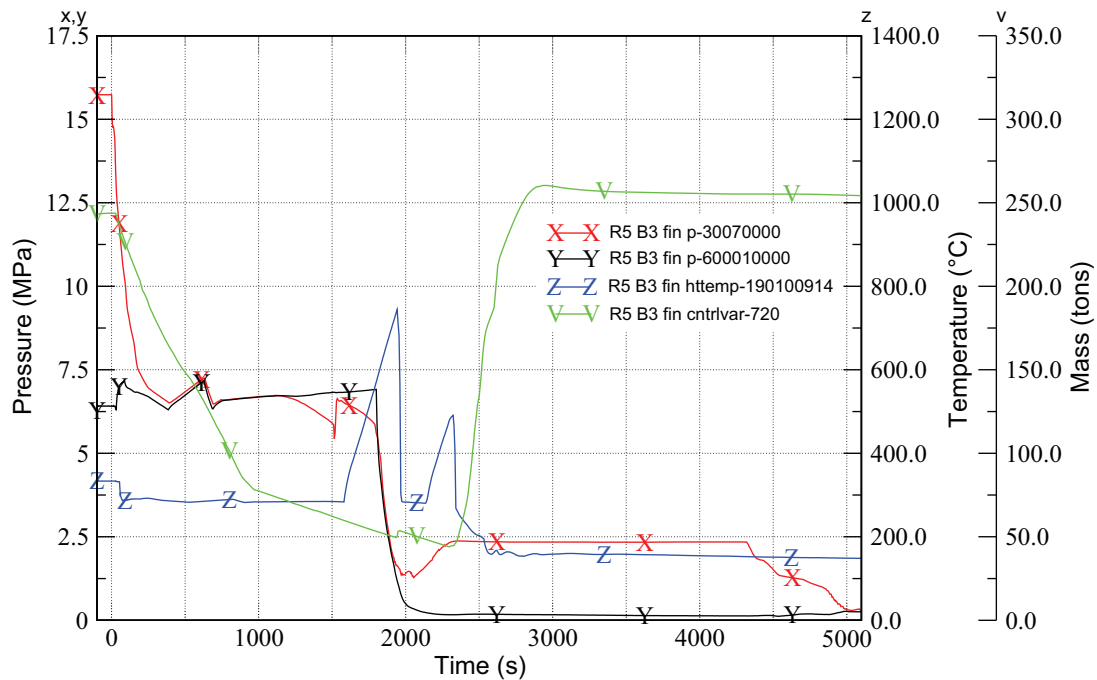


Figure 3.74: Relap5 primary and secondary side pressure, temperature and mass inventory, calculation 4

3.4.3 Scenario 8

Short description of the transient: Initiating event is a break in the cold leg near the reactor inlet with an equivalent diameter of 60 mm. All HPIS and LPIS are assumed to fail. As accident management the operator opens the PORV after 1800 s, or a peak cladding temperature of 450 °C, what ever comes first.

First 200 s: The initiating event is a SB in the cold leg No 4 near the RPV of 60 mm equivalent diameter. This leads to a reduction in the moderator density and this in turns to a reduction in power of 150 MW. After 49 s the scram occurs on a low pressure signal (pressure below 14.5 MPa while power above 75 % of nominal power). At 59 s the TSV closes and the feed water is switched off. After 84 s MCP1, MCP2 and MCP3 are tripped on a high SG level signal, while MCP4 is tripped after 184 s due to a saturation margin of less than 10 °C in loop No 4.

200 s up to accident management: The PS keeps losing mass. At 1000 s a first dry out in the core can be observed, which is quenched at 1030 s. At 1050 s the break is fully covered with steam and the mass flow through the break is reduced. At 1420 s a second dry out can be observed, the cladding temperature starts to rise.

From accident management to the end of the transient: At 1600 s the peak cladding temperature exceeds 450 °C. It is assumed that the operator opens the PORV valve on this signal to depressurize the PS and enhance ECCS flow as an accident management measure. The measure is not immediately effective - the peak cladding temperature continues to rise up to 600 °C (exceeded at 1730 s). At 1830 s the pressure drops below 6 MPa and the HA start to inject. At 1850 s the temperature trend can be reversed (cladding temperature starts to decrease) but not for long - after 2800 s the cladding temperature starts to increase again. At 8000 s the calculation was terminated

Primary and secondary system pressure, the primary system mass and the clad temperature are reported in Figure 3.75.

3.4.4 Scenario 10

Short description of the test:

Test 10 was designed to characterize the NC performance. The test consists out of two parts: in part 1 primary system mass is drained in steps from the lower plenum. NC flow-rate and NC regimes establishes when draining PS coolant and keeping available the SG heat sink. As Part 2, following DNB and DO occurrence, start PS refilling and observing hysteresis.

No	Event	Time (s)
1	SBLOCA in cold leg no 4	0
2	scram on low pressure signal	49
3	closure of the TSV (10s after scram), feed water switched to auxiliary feed water	59
4	MCP1, MCP2, MCP3 tripped on high SG level signal	84
5	MCP4 tripped on low saturation margin signal	184
6	Begin of the first dryout in the core	1000
7	Dryout quenched by loop seal clearing	1030
8	Break fully covered with steam	1050
9	Begin of the second dryout in the core	1420
10	peak cladding temperature exceeds 450oC , operator opens the PORV	1600
11	peak cladding temperature exceeds 600oC	1730
12	Accumulators start to inject	1830
13	Cladding temperature trend starts to drop	1850
14	Cladding temperature trend starts to increase again	2800
15	Calculation terminated	8000

Table 3.36: Resulting events, test 8

Primary and secondary system pressure, the primary system mass and the clad temperature are reported in Figure 3.76.

3.4.5 Scenario 11

Short description of scenario 11: Initial event is break of cold leg near reactor inlet with equivalent diameter of 70 mm into containment. ECCS availability: Failure of all HPIS pumps is assumed. It is assumed also that at certain time moment one HPIS train (supplying water to broken loop) is recovered. Accumulators and LPIS is assumed to be available. Accident management: Cool down of PS via SS with a cooling rate of 30 °C /h, recovery of one train of HPIS (injecting in loop no 4) after 1800 s

Primary and secondary system pressure, the primary system mass and the clad temperature are reported in Figure 3.77

Analysis shows that the operator actions are capable of returning the plant to a safe state.

3.4.6 Scenario 12

Short description of scenario 12: Initial event is break of cold leg near reactor inlet with equivalent diameter of 70 mm (to be scaled for PSB) into containment. ECCS availability: Failure of all HPIS and LPIS pumps is assumed. It is assumed also that at certain time moment the operator recovers water supply into primary circuit with makeup pumps and high pressure boron injection pumps Accident management: Cool down of PS via SS with a cooling rate of 30°C /h, supplying water to the PS via HHPIS and make-up system after 1800 s. Like in scenario 12, the operator actions are sufficient to return the plant to a safe state. Figure 3.78 shows primary and secondary system pressure, cladding temperature and primary inventory.

Comparison VVER and PSB-VVER

Hereafter the results as calculated for PSB-VVER and VVER-1000 are compared as far as phase separation phenomena in the core and the loops are concerned. The results from the PSB-VVER experiment, as far as can be seen from the measured parameters, are also considered.

Flow through core and core bypass The PSB-VVER facility simulates the reactor core of the NPP by a single hexangular fuel assembly. The fuel assembly corresponds a single FA of the 163 of the VVER-1000. In addition, by-pass flow is modelled by an additional line parallel to the core simulator (from lower to upper plenum). It can be expected that the complex three dimensional flow and void distribution, once voiding in

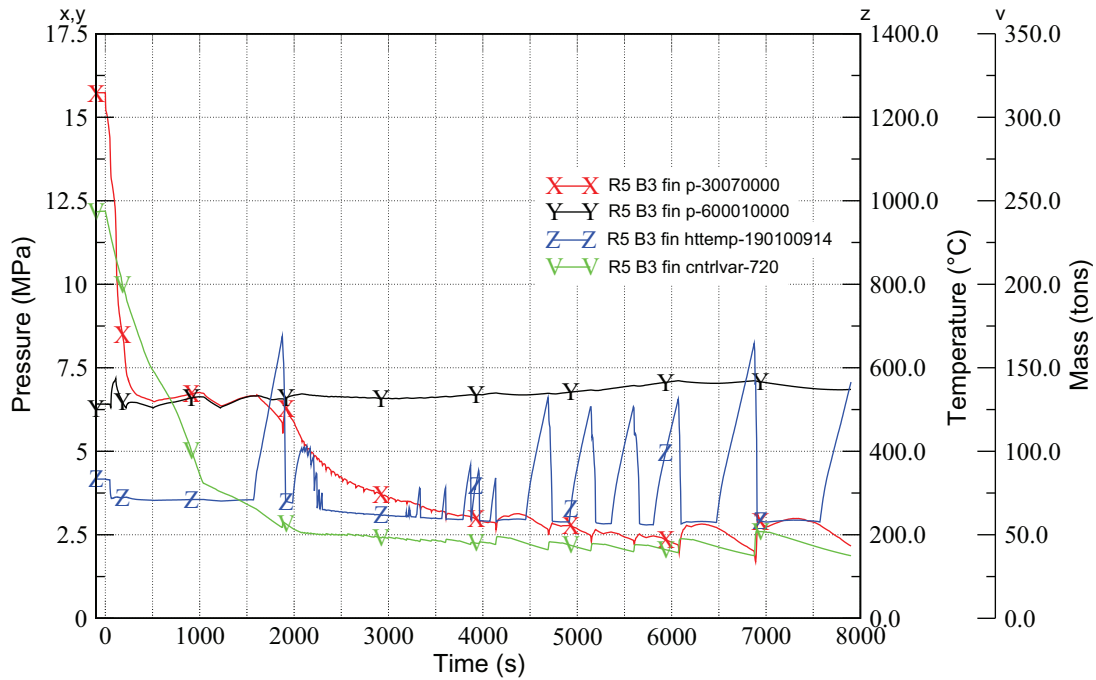


Figure 3.75: Relap5 primary and secondary side pressure, temperature and mass inventory, calculation 8

the core occurs, will not be accurately represented. Apart from the cladding temperature measurements that indicate dry out, the facility offers no possibility to gain insight on the current flow regime. Measurements of mass flows are only valid in single phase conditions. The paragraph therefore has to focus on calculated results.

The PSB-VVER nodalisation tries to represent as good as possible the facility. Therefore, the core region and core bypass are modelled with a pipe-component. The VVER-1000 nodalisation, again, does not model the complex flow paths likely to occur in a SBLOCA. A second bypass, leading from the lower plenum to the upper head to account for the control rod guide tubes is modelled. One significant difference (which leads to a significant dry-out in the plant calculation, while the experiment and post-test calculation show only comparably small, local dry-outs) is that while in the PSB-VVER nodalisation the heater rods are modelled with a single structure (axial and radial uniform power profile), the VVER-1000 has a chopped-cosine axial power profile, and three structures to account for three radial zones.

(see Figure 3.3 for the PSB-VVER, Figure 3.57 for the VVER-1000 nodalisation, Figure 2.13 for PSB-VVER, Figure 2.6 and Figure 2.9 for VVER-1000 geometry).

In the PSB-VVER nodalisation pipe-component 118 simulates the core region. It has 13 sub-components (1 at the bottom and 13 at the top). The active structures are connected to subcomponent 118-03 to 118-12. The following flow regimes have been used by Relap5 for the calculation (for a description on the Relap5 use of flow regime maps for closure equations, please refer to Section 2.4.1.)

Until 100 s “bubbly flow” is used in all subvolumes. From there on, the volumes, starting from the top, the flowregime starts to switch to slug flow (at 120 s subvolume 13, at 250 s subvolume 12, at 275 s subvolume 11). This goes on until 590 s and subvolume 5, which does not clearly switch flow regime, but oscillates between bubbly and slug flow. At roughly 800 s the subvolumes 11,12 and 13 switch to annular mist, and a few seconds later subvolume 12 (last heated subvolume) to mist pre-chf. This corresponds with the first temperature excursion, which is quenched by loop seal clearing 20 s later. Flow regimes in the experiment cannot be observed, but the temperature excursion at approximately the same time into the transient indicates that the prediction is not far away from the physics.

Until 1500 s Relap5 continues to see bubbly flow in subvolumes 1-4, and slug flow from 5 to 13. Then, the top volumes change to annular mist, mist pre-chf, the second temperature excursion takes place. In subvolumes 10 and 11 mist and mist post-chf are calculated. The second temperature excursion is quenched by the assumption that the operator manages to recover ECCS at 1800 s. The second dry out is predicted to happen earlier than can be seen in the experiment. Most likely reason is that the break flow is slightly larger

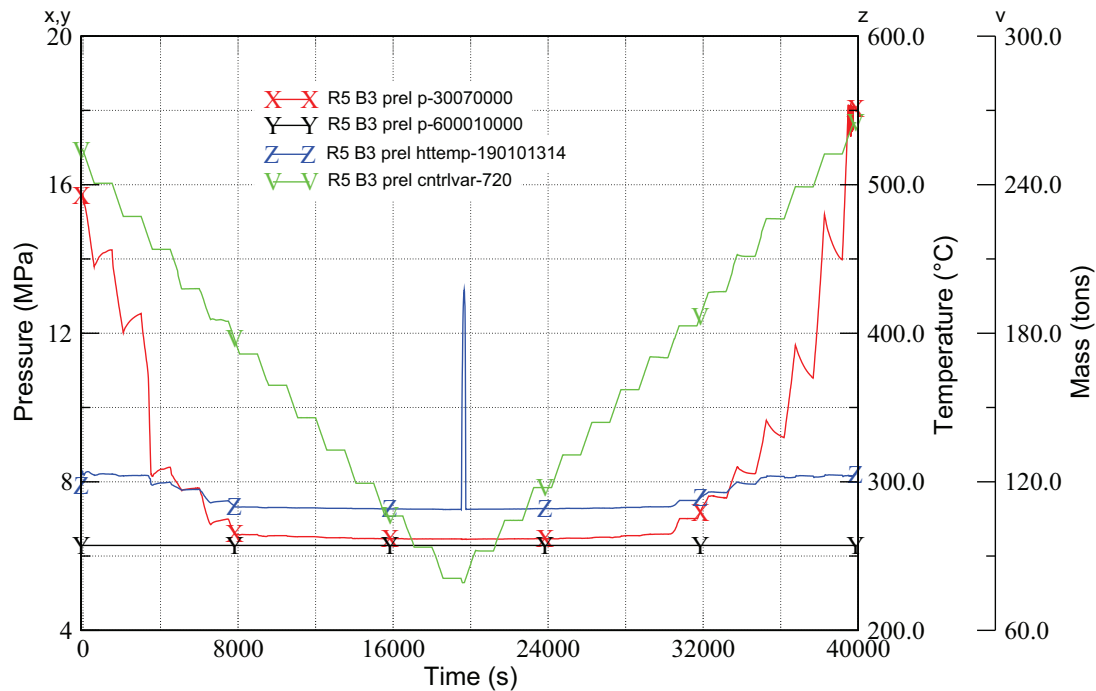


Figure 3.76: Relap5 primary and secondary side pressure, temperature and mass inventory, calculation 10

in the calculation.

In the VVER-1000 nodalisation pipe-component 110, with 13 subvolumes, and branch component 140 simulate the core region. The three active structures (and the “hot rod”) structure are connected to all subvolumes.

The situation in the VVER-1000 calculation shows a similar picture in the first phase. At roughly 150 s into the transient the flow regime starts to change from bubbly to slug flow, starting from the top volumes. At 200 s all subvolumes show slg flow. At about 700 s the three top subvolumes change to annular mist, and the connected heat structures show a mild increase in temperature. Again, the temperature rise is quenched by loop seal clearing. Then, other then in the facility, at already 1100 s the subvolumes start to switch to annular mist, to mist, and to post-chf mist. Other than in the facility calculation, this occurs not just in the top volumes, but down to subvolume 7. A large dry out at several levels is the consequence. This difference can be attributed to the different axial power profile, and the different void distribution in the primary system (the overall scaled mass parameter shows the same trend in PSB-VVER and VVER calculation, as can be seen in Figure 3.79). Again, with the partial recovery of the ECCS at 1800 s the dryout is quenched, and all subvolumes are switched back to slug flow.

Void distribution in the core and CCFL Void distribution in the core and possible counter current flow limitation (CCFL), i.e. that the steam generated in the core is inhibiting ECCS water and water from condensation in the SG to enter the core, are important for determining dry out.

Again, the complex three dimensional core is not likely to be represented by the single fuel bundle of the PSB-VVER facility. However, CCFL can occur in the facility (not necessarily representing the situation of the real plant). The capability of the code to predict CCFL can be estimated by comparing the facility experimental results to the facility Relap5 post test calculation.

Pressure differences along the RPV simulator are measured, and give an indication on the distribution of liquid and steam in the facility. Figure 3.80 shows the DP measurements at the facility during test 12. Each DP reading has been linearly transformed to correspond to the elevation over which it was measured, for elevation of DP measurements see Figure 2.16. For example, YC01DP07 pressure tap measures the ΔP from elevation 1915 mm to 2810 mm. If the section is full of liquid during nominal operating conditions, the pressure reading would be 7.7 kPa, and almost 0 kPa if the section is full of steam. In Figure 3.80 the parameter has been transformed to show 1915 if the reading is zero, and 2810 if the reading is 7.7 kPa.

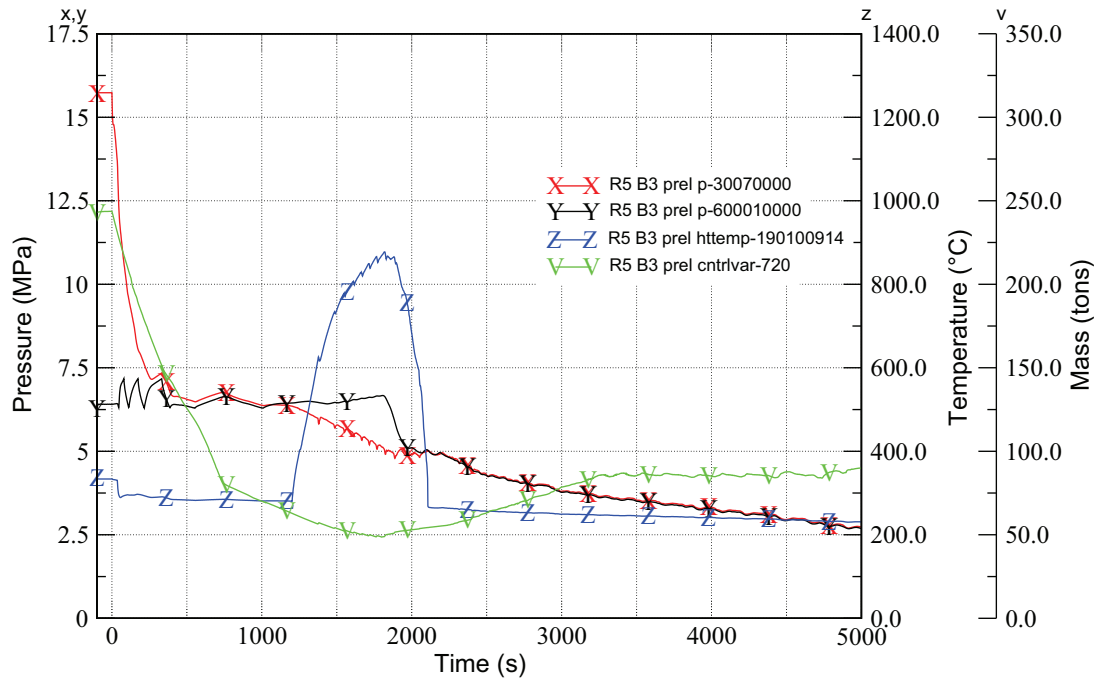


Figure 3.77: Relap5 primary and secondary side pressure, temperature and mass inventory, calculation 11

What can be seen in Figure 3.80 is, again, the two dry outs, the first at 700-800 s, quenched by loop seal clearing, and a second at 2400-2900 s, quenched by ECCS recovery. After ECCS recovery a liquid level forms above 6 m elevation in the RPV simulator, which is not fully getting into the heated section, because its held up at the upper tie plate. This indicates CCFL. To see if Relap5 predicts the same behavior, the liquid void fraction in the nodes above and below the upper tie plate are looked at in Figure 3.81. The levels cannot be directly compared to the calculation because the pressure measurement points do not coincide with the borders of the nodalisation scheme.

What can be seen is that after ECCS injection water is hold up in the uppler plenum (higher liquid void fraction). This means that the phenomena can be predicted qualitatively. The VVER-1000 calculation shows similar results.

The Relap5 models for CCFL as described in section 2.4.1 have not been used, neither in the PSB-VVER, nor in the VVER-1000 calculation. The reason is that switching on the model would hold up more water in the upper plenum, while the dry-out already occurs too early. However, sensitivity analysis switching on CCFL with user parameters taken from code-experiment comparisons (separate test facility) have been conducted, without improving the agreement between code and experiment.

Horizontal stratified flow in loops and reflux condensation Generally countercurrent horizontal stratified flow in the loops can be expected to happen in case of a SBLOCA, if the loss of coolant cannot be compensated. While steam from the core flows in the top part of the loops to steam generators, ECCS water, which might be injected into the loops, or water from the steam generators might run back into the core.

The VVER-1000 ECCS has only one loop of the low pressure injection system which injects into one pair of hot and cold leg. HHPIS and HPIS are injecting into the cold legs, and accumulators are injecting into upper plenum and downcomer. In test 12 the primary system pressure drops below the secondary system pressure until roughly 5000 s (so steam from the core is not condensed, but heated further in the steam generators). This means that for both, plant and facility calculation one would expect only marginal occurrence of water flow back into the core.

The flow regime in the hot legs in the PSB-VVER Relap5 calculation shows bubbly flow until roughly 120 s into the transient, then switches to horizontally stratified flow (described in section 2.4.1). Following the quenching of the second dry out (which occurs by recovery of ECCS/actuation of make up at 1800s in the calculation) the vapor produced in the core moved in the hot legs, and the flow regime switched to mist (pre-chf) for about 500 s.

Although the horizontally stratified flow regime in principle allows for counter current flow (i.e. hori-

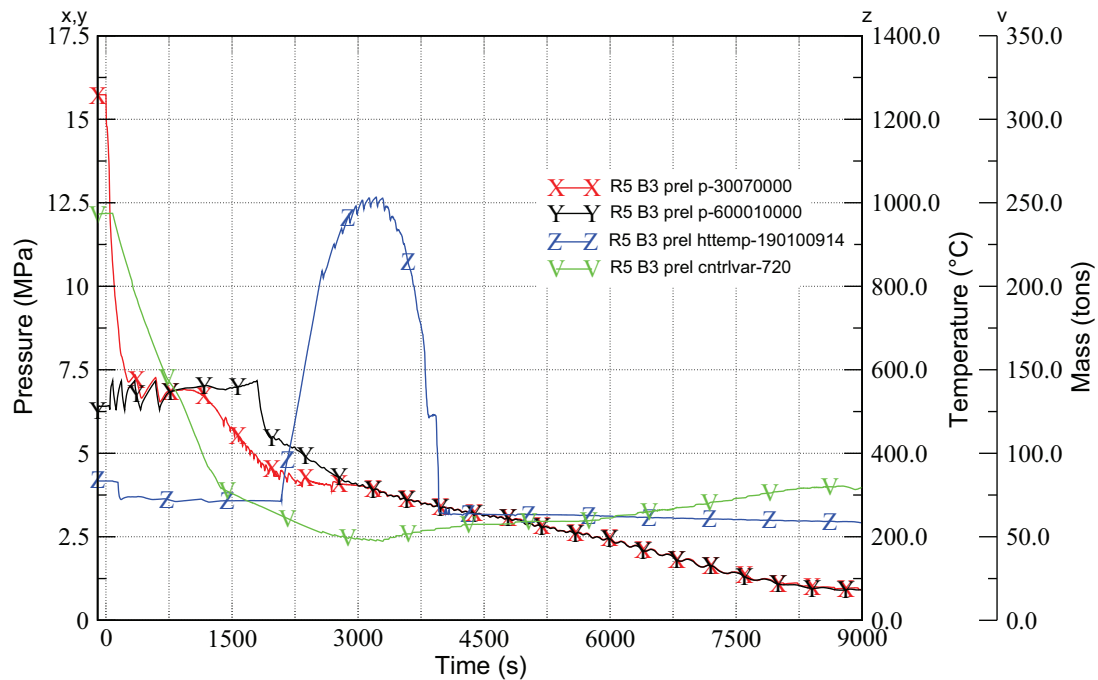


Figure 3.78: Relap5 primary and secondary side pressure, temperature and mass inventory, calculation 12

zonally stratified flow, and water and steam velocity have different signs) for the above mentioned reason practically it cannot be seen in test 12. What seems to happen occasionally is that water together with steam is pushed to the steam generators and flows back later on. For one example see Figure 3.82, which shows liquid and steam velocity of hot leg loop1, and the void fraction at the same location. Between 1300 and 1400 s one can see a positive spike in the liquid velocity, which means water and steam flow to the steam generator, which coincides with a drop in void fraction. Later on, one sees a void fraction different from 1, together with a negative water and positive steam flow for about 50 s.

Break flow Due to the large pressure difference between primary system and environment critical flow can be expected through the break. The code model for critical flow which is used therefore has a major influence on the capability to predict the behavior of the test.

As described in section 2.4.1 Relap5 offers two models for critical flow. The calculations shown here use Henry-Fauske, with default values for the two user parameters. The user defined parameters should be determined by code - experiment comparison at a separate test facility for the given break geometry. This has not been done for the PSB-VVER tests, therefore a number of sensitivities have been run, modifying the model coefficients, and also changing the critical flow model (and again, changing the three user defined coefficients for Ransom and Trapp). However, the agreement with the experimental results could not be significantly improved.

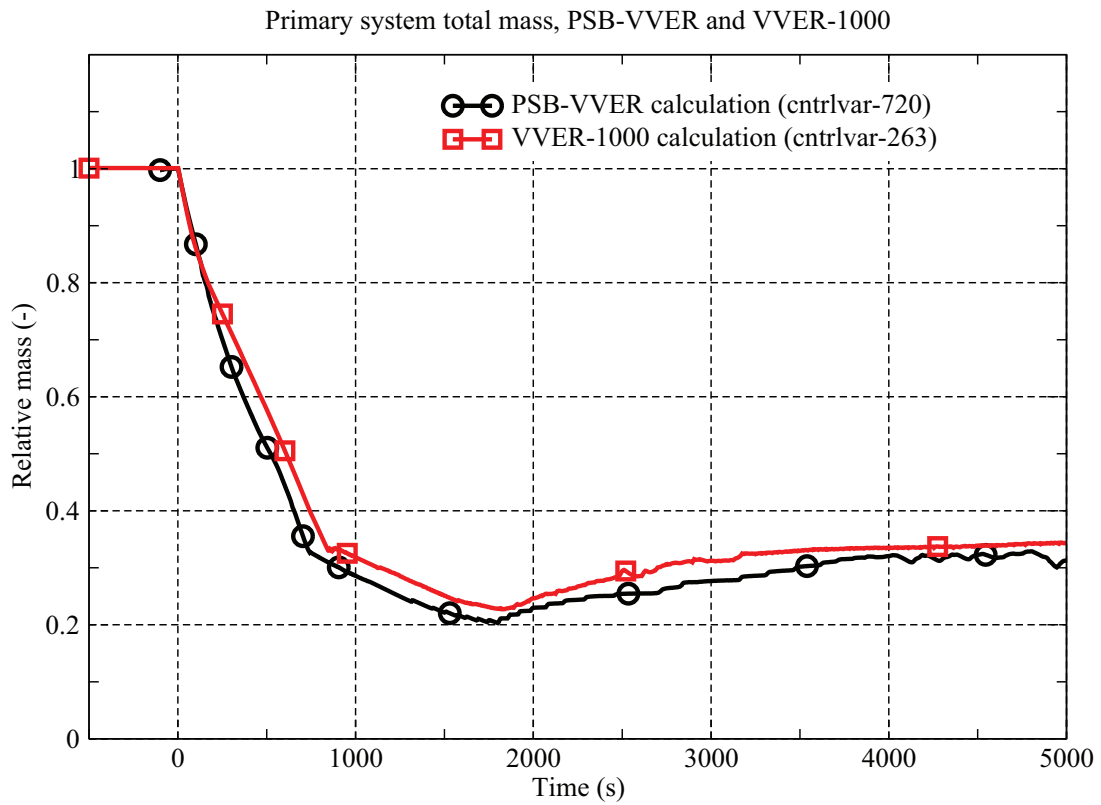


Figure 3.79: Relap5 calculation scenario 12 for PSB-VVER and VVER-1000, primary system mass

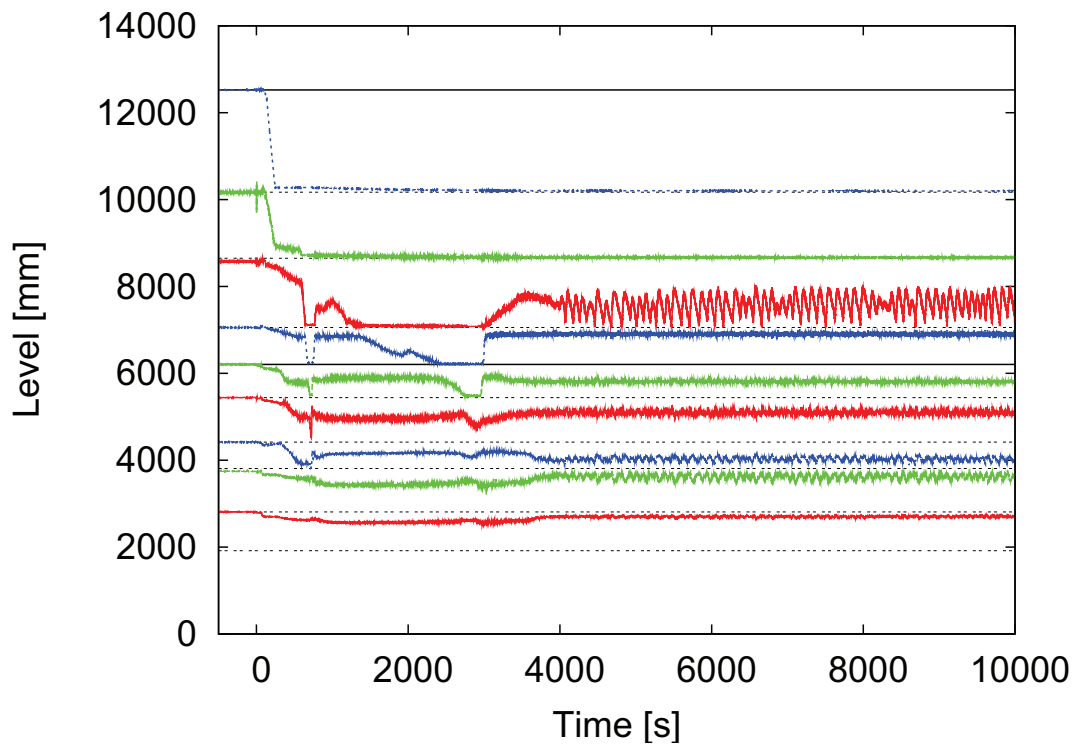


Figure 3.80: PSB-VVER test 12 RPV simulator levels

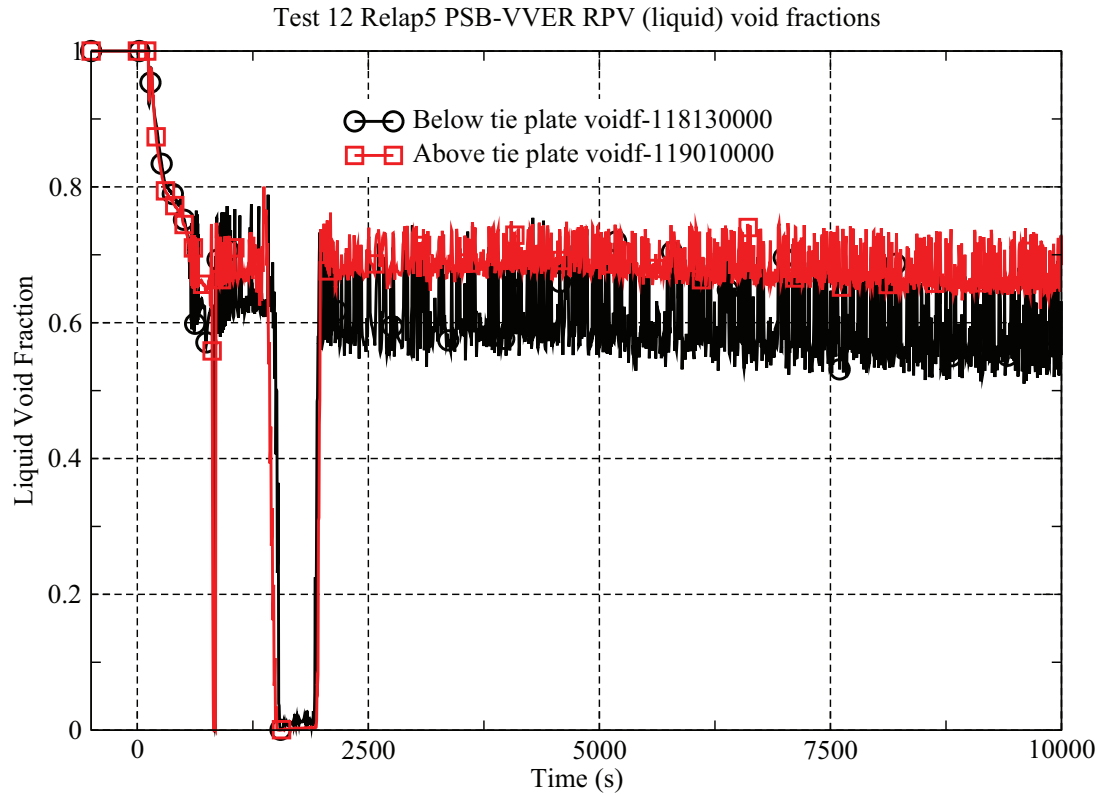


Figure 3.81: PSB-VVER post test calculation test 12 RPV liquid void fraction

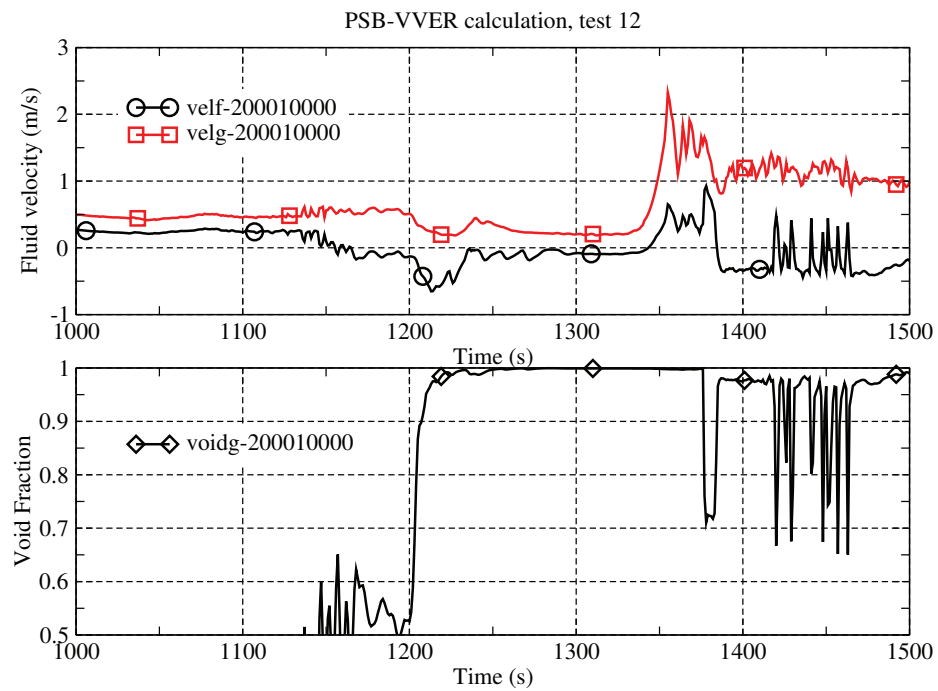


Figure 3.82: PSB-VVER Relap5 test 12 void fraction and fluid velocities

3.5 PRISE transients

3.5.1 Scenario 5

Short characterization of the test: Initial event is a double ended main steam line break with a simultaneous SG tube rupture in loop No 4. All trains of HPIS are assumed to fail, while accumulators and LPIS are available. As accident management the operator isolates the SITS, opens the pressurizer PORV, switches off the pressurizer heaters and initiates the 60 °C /h cool down mode of the BRU-A valves after 1800 s. Accident management is considered successful when the pressure drops beneath 2.6 MPa and the PS temperature is less than 180 °C .

First 100 s: The imposed initiating event is a double ended MSLB in loop No 4 between SG and MSIV, within the containment. Simultaneously one SG U-tube is assumed to break (double ended guillotine rupture) in the same loop. At 0.3 s the MSIV4 and the TSV are closed because of low pressure in the SS while the difference in the saturation margin is still larger than 75 °C . At 1 s the reactor scram signal is issued (on MSIV closure with one second delay for signaling time). Between 2-3 s all groups of pressurizer heaters are switched on. 20 s after the scram all MCP are switched off (imposed event, to account for the containment pressurization). After 58 s the PRZ level drops below 4.2 m and all PRZ heater groups are switched off.

100 s up to accident management: It takes about 200 s to depressurize SG4 to almost atmospheric pressure. During the blow down the PS coolant experiences temperatures as low as 175 °C in the cold leg of loop No 4 and 255 °C in the lower plenum. PTS phenomena or local recriticality may be an issue - this should be investigated with the appropriate tools. The rapid drop in the PS pressure at the initial phase of the transient is governed by the blow down of SG No 4. After this phase the PS pressure drop is slowed down and governed by the loss of PS inventory to the SS due to the SGTR. At 1050 s the PRZ is empty - this marks again the begin of a second phase of rapid PS depressurization, which is halted when the pressure reaches the saturation pressure of the coolant at the core outlet (HPIS is assumed not to be operational).

From accident management to the end of the transient: After 30 minutes (1800 s) the operator takes several actions: the PRZ heaters are switched off, the hydro accumulators are isolated. The PORV is fully opened (PS feed and bleed), and the intact SG are switched into 60 °C cool down mode. The operator actions are successful in drastically reducing the break flow. The PS depressurization halts at the SS pressure, and the further depressurization is governed by the 60 °C /h SS cool down. After 4900 s the PS pressure is less than 2.6 MPa, and the LPIS starts to inject. After 6650 s the core exit temperature drops and stays below 180 °C .

Primary and secondary system pressure, the primary system mass and the clad temperature are reported in Figure 3.83.

No	Event	Time (s)
1	MSLB with SGTR at the same time in loop 4	0
2	closure of MSIV 4 and TSV, stop of FW (pressure SS less than 4.9MPa), switch off MCP 4	0.3
3	scram because of MSIV closure, switch on prz heaters grp 1	1
4	switch on prz heaters grp 2,3,4	2
5	switch off MCP 1,2,3 (imposed as 20s after scram, simulating containment pressurization)	21
6	switch of all prz heaters (prz lvl j 4.2m)	58
7	pressurizer empty	1050
8	accumulators isolated, prz heaters switched off, PORV valve opened, BRU-A switched in 60oC /h cooldown mode	1800
9	PS pressure less than 2.6 MPa	4900
10	start of all trains of LPIS	4950
11	Core exit temperature stays below 180oC	6650

Table 3.37: Resulting events, test 5

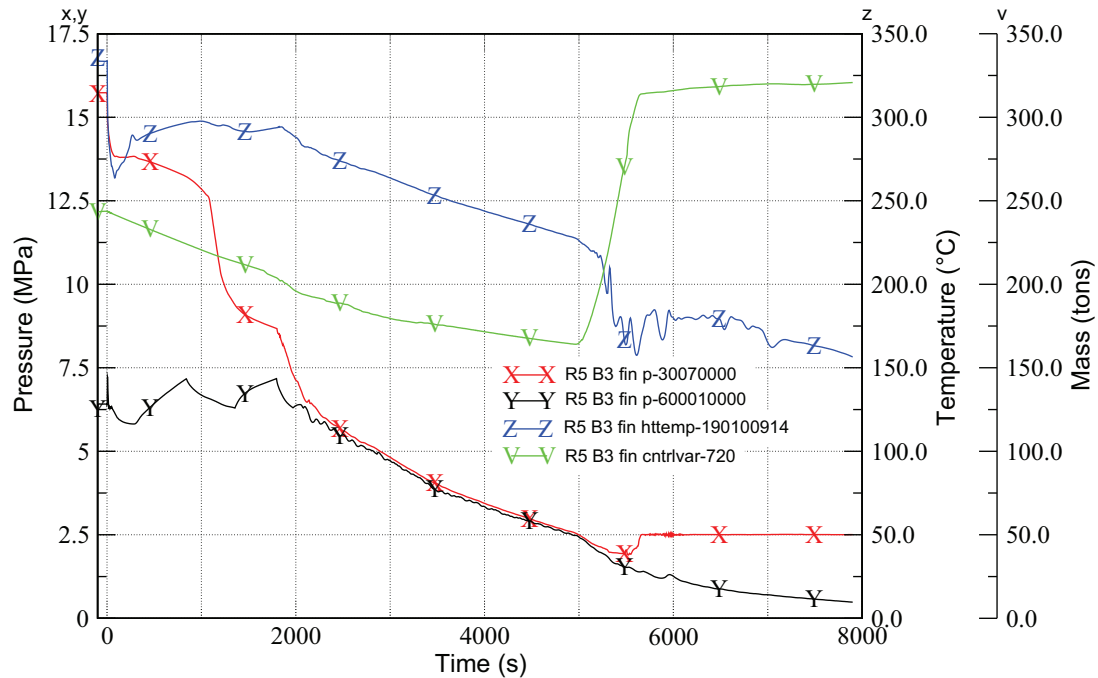


Figure 3.83: Relap5 primary and secondary side pressure, temperature and mass inventory, calculation 5

3.5.2 Scenario 9

Short characterization of the test: Initiating event is a primary to secondary side leak with an equiv. diameter of 100 mm in loop No 4. The corresponding BRU-A is considered to be stuck open after the first opening. As accident management, after 1800 s, the operator switches off two trains of HPIS (TQ13 and TQ34), isolates all hydroaccumulators, switches off all LPIS pumps, and switches the BRU-A valves of the intact SG into cool down mode with a cool down rate of 60 °C /h. After 2700 s, as a second measure, the operator switches on the make-up system, and switches the last HPIS pump off. The accident management is considered successful if the PS pressure drops below 1 MPa and the PS temperature below 180 °C .

First 100 s: The (imposed) initiating event is a primary to secondary leak in loop No 4 (SG 4 hot header break with an equivalent diameter of 100 mm). After 1 s all four groups of PRZ heaters are switched on. The level of SG 4 rises fast and after 8 s MCP4 is tripped due to high SG level. At 19 s the reactor is scrammed because the PS pressure is less than 14.5 MPa while the reactor power is larger than 75 %. At 26 s the PRZ heaters are switched off due to low level in the PRZ. Ten seconds after the scram signal (29 s) the TSV are closed. From this time on the SS pressure starts to increase and reaches the set point of the BRU-A valves (BRU-K valves are assumed fail) at 49 s. The BRU-A valve of loop No 4 is assumed to stuck in the fully open position. The MSIV valves of loops 1-3 are closed at the same time to simulate the existence of check-valves which inhibit back flow.

100 s up to accident management: The PS depressurizes to the pressure of the secondary side and follows the pressure of the intact SG. SG 4 depressurizes due to the stuck open BRU-A valve. At 108 s the MCP of loop 1-3 are tripped due to the low saturation margin in this loops. At 109 s all three trains of HPIS (TQ13) start to inject. At 396 s the HPIS tanks with borated water of 40 g/kg water are empty, and the supply is switched to the sump with 40 g/kg borated water. At about 400 s the PS depressurization continues and drops significantly below the SS pressure (intact loops). At 421 s the set point for the HA is reached and they start to inject.

From accident management to the end of the transient: Since the ECCS is fully operational, dry-out of the core is not an issue in this transient. The accident management aims to limit the PS mass lost to the SS (which means to the environment). The operator switches off two trains of the HPIS (TQ13 and TQ33), isolates the HA, switches off the LPIS, and switches the BRU-A valves of the intact steam SG into cool down mode (60 °C /h). This measure is successful: PRISE break flow is reduced from about 240 kg/s to 50 kg/s.

At 2700 s as a second AM-measure the last HPIS train is switched off, and the make-up system takes over

(2730 s). At 4000 s the PS pressure is less than 1 MPa and the core outlet temperature is less than 180 °C , so the calculation was terminated. Up to 1800 s about 500 tons of PS mass were lost to the secondary side, after that another 100 tons - so in total the integral break flow up to 4000 s was 600 tons.

Primary and secondary system pressure, the primary system mass and the clad temperature are reported in Figure 3.84.

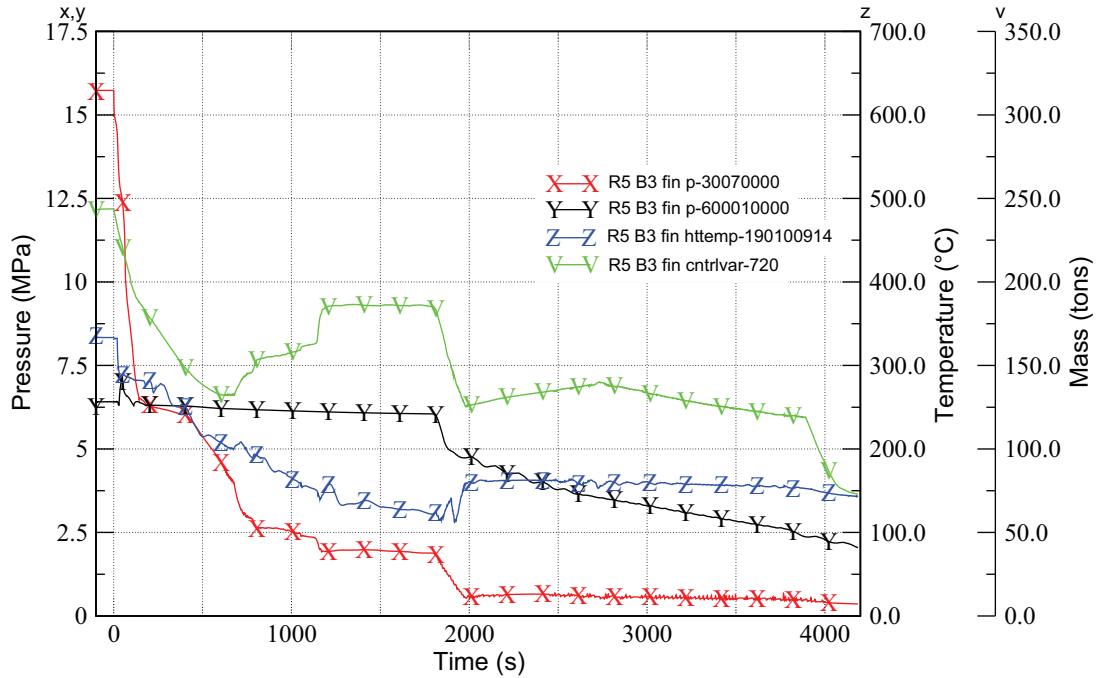


Figure 3.84: Relap5 primary and secondary side pressure, temperature and mass inventory, calculation 9

No	Event	Time (s)
1	PRISE in loop No 4	0
2	switch on prz heaters group 1-4	1
3	switch off MCP4 (SG-level too high)	8
4	SCRAM on low PS pressure signal	19
5	switch off prz heaters on low prz level	26
6	Closure of TSV (10s after scram)	29
7	BRU-A of SG 4 opens and stays stuck open (closure of MSIV in loop No 4)	49
8	PRZ empty	60
9	switch off MCP1,MCP2,MCP3 on low saturation margin	108
10	HPIS starts to inject taking suction from the tanks	109
11	HPIS supply switched to the sump	396
12	Accumulators start to inject	421
13	Accident management: switch off two trains of HPIS (TQ13,TQ33), isolation of hydroaccumulators, switch off LPIS, switch BRU-A in 60oC /h cooldown mode	1800
14	Accident management: switch on make-up pumps	2700
15	Accident management: switch off last train HPIS	2730
16	Calculation terminated (primary side pressure below 1MPa, core outlet temperature less 180 oC	4000

Table 3.38: Resulting events, test 9

Chapter 4

EOP Optimization

Chapter three investigated the effectiveness of primary and secondary depressurization based AM strategies for different initiating events. The present chapter, on the other hand, investigates possible combinations of primary- and secondary side depressurization in case of a loss of on- and offsite power (loss of connection to the grid, with failure of all diesel generators). VVER-1000, unlike e.g. German plants, have no possibility of load reduction and switch over of the turbine generator to service station operation, which means that the only available power source are batteries.

As outlined in section 2.1, accident management is step four in the IAEA “defense in depth” concept. The first level would be the design of the NPP, which by itself should be such that the reactor will not deviate from its nominal conditions. In case the first level should fail, and the reactor does deviate from normal operational conditions, the control system of the reactor should be able to lead the reactor back to a normal state. Should the control system fail and abnormal operation condition progress into a design bases accident, the reactor protection system, as third level, is there to cope with the accident.

Only in case that also the reactor protection system is unsuccessful the fourth level of “defense in depths” comes into play, accident management. This is the case of a station blackout. As part of the reactor protection system three independent trains of power from diesel generators are available, each of them sufficient (3x100% safety). But since all three are assumed to fail, the accident is beyond the design basis.

The target of accident management is to provide the plant operator with guidance on how to proceed in such cases. Accident management means that procedures are in place which tell the operator which parameters he should check to identify the plant state, and how to use the equipment that is still available to improve the situation. Accident management is to be divided in **preventive** and **mitigative** accident management. Preventive AM means that the aim of the actions is to prevent damage to the reactor core and terminate the accident. The set of preventive accident management guidance documents usually is called “emergency operating procedures”, EOPs, which are available at the control room for the operator. There are two basic approaches for EOPs - event based EOPs, and symptom based EOPs. In the first case procedures are sorted by initiating events, and the actions, that are prescribed, have been optimized for this special case. Traditionally, EOPs have been event based. The disadvantage is that the operator has to be able to clearly identify the event. This is not always possible. Therefore, “symptom based” EOPs have been introduced. Instead of identifying the event, the operator just uses “symptoms” to identify the plant state, and takes action based on the state of the plant. He continuously monitors a number of safety functions (see Table 2.1), checks if they are fulfilled, and takes action based on the outcome of his checks.

The case that is investigated here, a station blackout with failure of the DGs, can be clearly identified. Therefore the strategy can be targeted towards “event based” EOPs. Further, the analysis is restricted to the preventive part of AM - the EOPs. The mitigative part comes into play if the EOPs have not been successful. A simple, unique and clear criterion should be used to terminate the EOPs and move to the mitigative procedures, the severe accident management guidelines - usually the core exit temperature. Superheated steam of more than 650°C is commonly used as signal that the core has already been damaged, or core damage is impending and cannot be prevented. For the current work, the analysis terminates here.

To summarize, the goal of a preventive accident management strategy for a station blackout, until core damage occurred, is to prevent core damage as long as possible. Goal of the current chapter is to use the systems that are still available to the plant operator in way that core damage can be prevented as long as possible.

The next section describes the situation at the NPP Balakovo. What are the signals that the operator has

to consider for AM, and which systems are still available via batteries (or, after the batteries have finished, by hand).

A section “qualitative optimization” follows, where a number of ideas how to make the best use of the equipment which is still available has been made, where sensitivity calculations are presented to cover uncertainties in plant parameters. The time frame, in which actions have to be performed if the strategy should be successful, has been evaluated here.

The last section of the chapter “quantitative optimization”, a method aiming to optimize accident management strategies is presented. The method has been developed in the frame of the present work. The method is then used to optimize the operator interventions in case of a station blackout, and the result is presented.

4.1 Situation at Balakovo

The implementation of accident management procedures at Balakovo NPP was ongoing at the time the work has been performed. During a work visit at the NPP [Sevastyanov and Suslov, 2005] it has been confirmed that the strategy, which was to be evaluated, would close a hole in the analysis. Signals available to the operator can be deducted from [Sevastyanov et al., 2004], which is done in this section. So apart from confirming the usefulness of the analysis, goal of the visit was to find out which equipment could still be used during a station black out by the operator.

4.1.1 Strategy

Optimization of AM strategies needs considerable analytic resources. Therefore optimization and detailed analysis has been restricted to a single initiating event.

In line with previous experience and work of GRNSPG/University of Pisa in the field of analytic support in developing accident management strategies (see [Madeira et al., 2003], [Muellner et al., 2003], [Muellner et al., 2004b], [Muellner et al., 2004a], [Muellner et al., 2005a]) the initiating event has been chosen to be either a loss of feedwater, or a total station blackout. During the work visit at NPP Balakovo [Sevastyanov and Suslov, 2005] it has been decided that a station blackout would be of more interest to the NPP.

The challenge during a station black out is to recover the heat sink. Feedwater pumps and emergency feedwater pumps are lost, so alternative sources of feedwater must be procured. If feedwater can be supplied over an extended period of time, natural circulation is sufficient for decay heat removal and the plant can be kept in stable conditions for, in principle, any period of time. Alternative sources of feedwater can be fire brigade trucks, or mobile pumps which may be available at the plant. An example of the success of this strategy has been demonstrated at the Narora NPP in India, 1993. A fire in the turbine hall, caused by turbine blade failure, propagated along cables to the control room. The habitability of the control room was lost, as well as the control over the station for more than 18 hours. By feeding the SGs from fire brigade trucks the heat sink could be supplied until power was restored.

However, the current work assumes that neither mobile pumps, nor that fire brigade trucks are available. This might be possible if one considers terrorist attacks - in this case the operator may need to make use of systems which he can control from the control room, or which he can reach reasonably fast.

Goal of the strategy therefore is to make use of water which can be accessed without use of an active system. There are two main sources of water available. Firstly, the hydro accumulators which are connected to the primary system hold 200 tons of water, and inject once the primary pressure drops below 5.9 MPa. Secondly, water in the feedwater line piping is partly at 20 MPa, partly at 5.8 bar (before and after a check valve respectively). Furthermore there are two deaerator tanks for degassing of feedwater, each of them holding about 150 m³ of water. During normal operation they are pressurized at 5.8 bar. Those sources of water can be made available by primary and secondary system depressurization. Aim of the analysis is to find a sequence of primary and secondary system depressurization which utilizes at best these sources of water.

4.1.2 Signals

In [Sevastyanov et al., 2004] the safety functions, that the operator has to monitor during accident conditions, are listed. Safety functions and how the operator can verify their status at Balakovo is presented in Table

2.1. From there one can deduct that at least the following signals are available to the operator during accident conditions

- core power,
- upper plenum fluid temperature,
- steam generator level,
- feed water mass flow rate,
- steam generator pressure,
- cold leg fluid temperature,
- containment pressure,
- pressurizer level,
- pressurizer pressure,
- containment sump level.

Loss of electricity can also be detected. The parameters which are available to the operator have to be used to define the actual procedure, once the strategy has been worked out.

4.1.3 Equipment

A short description of equipment and systems that can be operated during a station black out and that are beneficial, will follow.

General comment on batteries - loss of all power means that the only available power source are batteries. All systems which are used for the strategy, i.e. the pressurizer relief valve (which could be substituted by the emergency gas removal system) and the BRU-A valves are connected to batteries. Batteries at Balakovo must provide power for at least half an hour, but in practice are able to last for a longer period of time. For the analysis it has been assumed that power from batteries is available for the whole transient. Reason for this assumption is that backfitting the plant with longer lasting batteries for the above mentioned valves is economically feasible, and can only improve safety.

Means for primary system depressurization. Primary system depressurization in a long lasting SBO transient is beneficial for two reasons. The first reason - should it be impossible to recover power, or at least to recover a stable source of feedwater, the reactor pressure vessel will fail. Failure of the RPV will release core debris to the reactor cavity - but if the failure occurs at high pressure, the subsequent blow down of saturated water, steam and hydrogen from the RCS could push the core debris out of the cavity to other regions of the containment. The heat transfer during such a process to the containment atmosphere is termed "direct containment heating", can increase the containment pressure considerably and challenge the containment integrity (see e.g. [Kirn et al., 1999]). Therefore, if it comes to RPV failure, it should happen at low pressure. The second reason is simply that by lowering the pressure water from hydroaccumulators can be furnished into the primary side.

Primary system depressurization can happen via the PORV, or via the emergency gas removal system. The PRZ safety valves only actuate when the primary pressure overpasses their pressure set point. A few comments regarding both possibilities.

The PORV (power operated relief valve) has a flow rate of 50 kg/s of steam at opening pressure (18.11 MPa). Three different pilot valves can potentially open the PORV:

- Three pilot valves can potentially open the PORV:
- Valve 1 is EM actuated. Can be controlled from MCR and ECR. In automatic mode opens 18.11, closes at 17.25

- Valve 2 is spring actuated, and is a backup for opening the PORV in case valve one is unavailable. If power is available, a solenoid increases the closing force of the spring. The open set-point for the valve is therefore 18.11/18.83 if power is unavailable/available and closure set point is 16.67/17.65.
- Valve 3 is EM actuated. Failsafe of valve 1 to close the PORV. Closes automatically at 15MPa. Possibility to override closure from CR. If electric power is unavailable, the valve closes.
- In case of an SBO, power from batteries for the PORV can be guaranteed for 30 min, although the batteries are likely to last longer.

This means, that until power from batteries is available, valve one, which can be operated from the control room, could be used to open the PORV. Should the power from the batteries finish, valve one and valve three would close the PORV, and only Valve 2 would open close the PORV at high pressure.

The EGRS (emergency gas removal system) is a mode of operation of the gas removal system. During normal operation the gas removal system is used to remove non condensable gases from top of the reactor pressure vessel, top pressurizer and steam generators. The by far biggest contribution comes from the line top of pressurizer. As emergency measure the gas removal system can be used as alternative way for primary system depressurization (steam flow rate at opening pressure 25 kg/s of steam). In case of a station blackout the emergency gas removal system is powered from batteries. Once the power from batteries is finished, the valves of the emergency gas removal system stay in there actual position (i.e. open, unlike the PORV).

Means for secondary system depressurization Secondary system depressurization can be achieved by opening the BRU-A valves. In case of a station blackout the BRU-A valves are powered by batteries. Each SG has one BRU-A valve, which can discharge 250 kg/s of steam at opening pressure.

- valves with electric power only. If the connection to the grid is lost and DGs fail, power is supplied from batteries. Once the batteries are empty, the valves stay in their current position.
- opening pressure of valve at 7.16 MPa BRU-A (valve opens 6%).
- pressure above 6.67 MPa causes BRU-A to open further, pressure below 6.67 MPa causes BRU-A to close.
- if pressure drops below 6.27 MPa, or the open area drops below 6%, valve closes.
- in case even power from batteries is lost, valve stays in its position
- comment: in case electric power is unavailable and the BRU-A are closed, spring operated SG safety valves ensure overpressure protection (open/close at 7.94/6.86 MPa)
- BRU-A can be operated manually - walking distance from control room to BRU-A valves (at 28.8 m) is roughly 5 min

The main advantage of depressurizing the steam generators is that the water from feed water lines and deaerator tanks can be furnished passively into the SG, and used for to recover at least for a limited period of time the heat sink. A couple of comments have to be made. As can be seen in Figure 4.1, the amount of water in feed water lines and deaerator is considerable. The two deaerator tanks have a liquid volume of about 300 m³, the feed water lines in addition have a volume of about 170 m³. The deaerator tanks are pressurized at 5.8 bar during normal operation (Table 4.1 reports nominal conditions and related parameters). The problem is that once the power is lost, the tanks start slowly to depressurize due to reasons - heat losses and losses of the line. Heat losses of the feedwater line, as well as steam and liquid losses during SBO conditions are, unfortunately, not well characterized. Neither are the pressure losses in the feed water line.

An idea, which is tested in later sections in calculations, was to use an existing connection between SG and steam line and the deaerator tanks to first isolate the deaerator tanks feed water side, pressurize them by connecting them to the SGs (see Figure 4.2) to a pressure of 6.6 bar. This is the pressure set point for safety valves which ensure overpressure protection for the deaerator. After that, the line to the SG should be closed again, the deaerator tanks should be again connected to the feed water side of the SG, and the SG should be further depressurized by using the BRU-A valves. As discussed in [Sevastyanov and Suslov, 2005] such a procedure would be possible in principle.

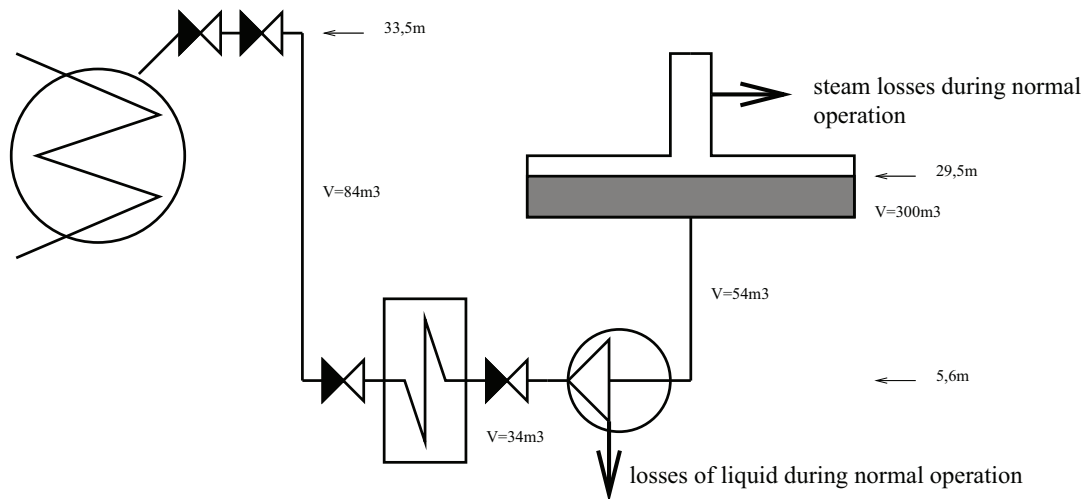


Figure 4.1: Potential reservoir of water in feed water lines and deaerator tanks

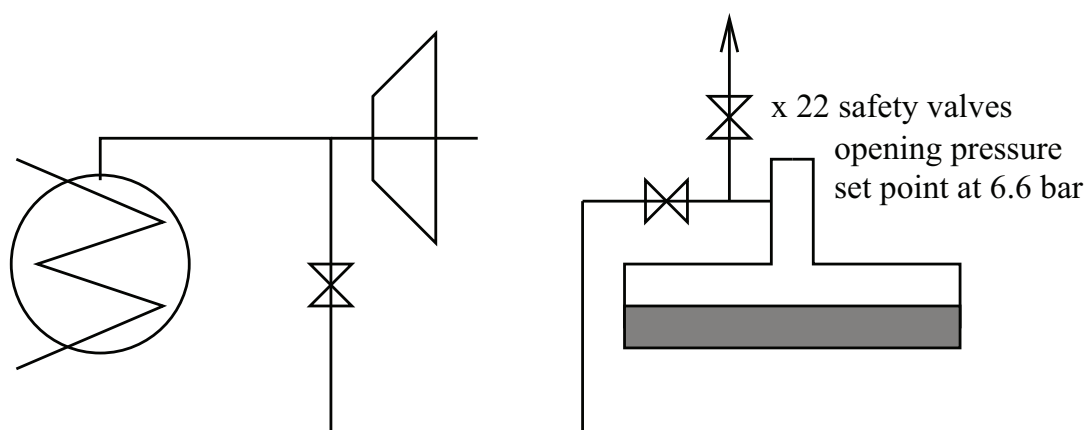


Figure 4.2: Potential connection between SG and deaerator tanks

No	Parameter	Unit	Value
RCS			
1	Power	MW	3000
2	Core inlet temperature	°C	289
4	Core outlet temperature	°C	318
5	Coolant pressure outlet core	MPa	15.7
6	One loop flow rate	m ³ /h	21200
7	Core flow rate	m ³ /h	84800
8	Pump rotation speed	rev/min	995
9	PRZ pressure	MPa	15.7
10	PRZ temperature	°C	346
13	SG steam production	kg/s	408
14	SG pressure	MPa	6.3
16	FW temperature	°C	220
Deaerator and feed water lines			
17	Nominal pressure	MPa	0.58
18	Nominal temperature		saturated
19	Deaerator water filled volume (each)	m ³	185
20	Nominal level	m	2.5
21	Feed water line volume	m ³	170
Characteristic parameters			
22	Primary side mass (without HA)	tons	253
23	HA mass	tons	198
24	PS total mass	tons	451
25	SG mass	tons	160
26	FW line mass	tons	163
27	Deaerator mass (both)	tons	337
28	SS total mass	tons	660
29	BRU-A fully open area (one valve)	m ²	$2.74 \cdot 10^{-2}$
30	PORV fully open area (one valve)	m ²	$1.53 \cdot 10^{-3}$
31	Volume SS (4xSG + FwL + 2xDeaerator.)	m ³	780
32	4xArea(BRU-A)/Volume(SS)	m ⁻¹	$1.41 \cdot 10^{-5}$

Table 4.1: Deaerator and FW lines, relevant parameters

4.2 Qualitative

The AM strategy proposed is based on two operator actions: Secondary DEpressurization (SDE) and Primary DEpressurization (PDE). The scope of SDE, performed by the complete opening of the BRU-A in all SG, is to lower the pressure in the SG below the pressure of the deaerator tanks and the feed water line and allow passive injection from the feed water line and from the deaerators. It is assumed that these two systems remain in their nominal condition as reported in Table 4.1.

PDE is foreseen to lower PS pressure below the set point of the ECC system available, to enhance ECCS flow, to keep the PS pressure low to avoid RPV failure at high pressure.

The strategy for the analysis was to perform one base calculation without operator actions (REF0). Then, a second base calculation with intuitive timing for actuation for primary and secondary depressurization. This means, that secondary depressurization is initiated after 30 min. The measure succeeds to cool down the primary system via secondary, and by contraction of coolant to lower the primary pressure - roughly to the set point of the accumulators. Then, primary depressurization is initiated, which further decreases the primary system pressure, actuates the hydroaccumulators and fills up the primary system with coolant. This is the base AM-Strategy calculation (REF1).

About thirty calculations implementing the basic strategy SDE followed by PDE were performed. One calculation is presented in detail (REF1), main results are reported briefly about selected other sensitivities. The differences among the thirty calculations and the main results of all are presented in two Tables, Table 4.3 and Table 4.4.

One note about PDE has to be made. PDE is performed in all cases with the PORV. The PORV cannot be opened manually, since it is located within the containment. The PORV relies on battery power, and would close once the batteries are finished. Power from the batteries can be guaranteed only for the first 30 min after a SBO.

This limitation was ignored. There are two reasons: firstly, the time of 30 min is the guaranteed minimum of time available. It is very likely that power from the batteries will be available for a longer time period. Secondly, it would be a small back fit to designate batteries especially and only for the PORV.

No	Event	Set point	Comment
1	SBO	0 s	reactor scram, begin of coast down of MCP, closure of feed water, closure of TSV
2	Automatic open/closure PORV	open at PRZ pressure 18.23 MPa, close at 16.67 MPa	Power from battery for PORV operation assumed to be available during the transient
3	Automatic open/closure BRU-A	open at 7.2 MPa, control the pressure to stay at 6.67 MPa, close at 6.27 MPa	Power from batteries is assumed to be available for the first half hour, then operation with batteries
4	SDE	varies	manual full opening of all four BRU-A valves
5	PDE	varies	opening of the PORV (minimum primary side pressure)
6	HPIS	none	all trains assumed to fail
7	HA	UP pressure < 5.9 MPa	
8	LPIS	none	all trains assumed to fail
9	End of calculation	Cladding Temp > 1200 °C	

Table 4.2: SBO optimization - boundary conditions

No.	ID	SDE	PDE	COMMENT
1	REF0	NONE	NONE	
2	REF1	1800 s / 4 SG	P_{MIN} (9360s)	
3	REF1a	1800 s / 4 SG	P_{MIN} (9360s)	check valve substituted

continued on next page

No.	ID	SDE	PDE	COMMENT
4	REF2	1800 s / 4 SG	P_{MIN} (7865s)	$M_{deaerator}^0 = M_{deaerator}^{nom}/2$; $P_{deaerator} = P_{deaerator}/2$ $A_{BRUA} = 2 A_{BRUA}^{NOM}$
5	REF3	1800 s / 1 SG	P_{MIN} (24380s)	
6	REF4	1800 s / 2 SG	P_{MIN} (19000s)	
7	REF5	1800 s / 3 SG	P_{MIN} (10000s)	Nominal losses of deaerator 4.4 kg/s SL4 discharges in deaerator
		5400 s / 4 SG		
8	REF6	3600 s / 4 SG	P_{MIN} (7600s)	$A_{BRUA} = 2 A_{BRUA}^{NOM}$
9	REF7	1800 s / 4 SG	$P_{MIN} - 1000s$ (8360s)	$A_{BRUA} = 2 A_{BRUA}^{NOM}$
10	REF8	1800 s / 4 SG	$P_{MIN} + 1000s$ (10360s)	$A_{BRUA} = 2 A_{BRUA}^{NOM}$
11	REF9	1800 s / 4 SG	P_{MIN} (9360s)	$A_{PORV} = 2 * A_{PORV}^{NOM}$
12	REF10	1800 s / 4 SG	P_{MIN} (9360s)	$A_{PORV} = 0.5 * A_{PORV}^{NOM}$
13	REF11	1800 s / 4 SG	P_{MIN} (18260s)	$A_{BRUA} = 0.5 A_{BRUA}^{NOM}$
14	REF12	LATEST MOMENT SDE STILL EFFEC- TIVE	$P_{UP} > 2.5$ MPa and after 15000 s	
15	REF13	1800 s / 4 SG	NONE	
16	REF14	1800 s / 4 SG	NONE	Nominal losses of deaerator 4.4 kg/s of steam
17	REF15	1800 s / 4 SG	NONE	Double losses of deaerator 8.8 kg/s of steam
18	REF16	1800 s / 4 SG	NONE	$A_{BRUA} = 0.05 A_{BRUA}^{NOM}$
19	REF17	1800 s / 1 SG	NONE	(PRE REF3)
20	REF18	1800 s / 2 SG	NONE	(PRE REF4),
21	REF19	1800 s / 4 SG	NONE	(PRE REF2)
22	REF20	3600 s / 4 SG	NONE	(PRE REF6) $A_{BRUA} = 2 A_{BRUA}^{NOM}$
23	REF21	1800 s / 4 SG	NONE	$A_{BRUA} = 0.5 A_{BRUA}^{NOM}$
24	REF102	1800 s / 4 SG	P_{MIN} (7865s)	$M_{deaerator}^0 = M_{deaerator}^{nom}/2$; $P_{deaerator} = P_{deaerator}/2$
25	REF106	3600 s / 4 SG	P_{MIN} (7600s)	
26	REF107	1800 s / 4 SG	$P_{MIN} - 1000s$ (8360s)	
27	REF108	1800 s / 4 SG	$P_{MIN} + 1000s$ (10360s)	
28	REF120	3600 s / 4 SG	NONE	(PRE REF106)
29	REF105	1800 s / 3 SG	P_{MIN} (10000 s)	Nominal losses of deaerator 4.4 kg/s SL4 discharges in deaerator
		5400 s / 4 SG		
30	REF200	1800 s / 4 SG	1800 s	PDE with GRS

Table 4.3: Performed SBO sensitivity calculations

No.	ID	Time of hot FA temperature ≥ 1200 °C (s)	PS pressure at the end (MPa)	Time interval UP pressure ≤ 2 MPa (s)
1	REF0	10040	18.1	n. A.
2	REF1	37928	3.24	18362
3	REF1a	35438	3.16	16037
4	REF2	19400	4.49	3600
5	REF3	39505	3.61	2650

continued on next page

No.	ID	Time of hot FA temperature ≥ 1200 °C (s)	PS pressure at the end (MPa)	Time interval UP pressure ≤ 2 MPa (s)
6	REF4	33111	3.67	4000
7	REF5	36010	3.34	15680
8	REF6	37344	3.33	19421
9	REF7	35463	3.37	16900
10	REF8	35614	3.27	15016
11	REF9	35857	1.61	19860
12	REF10	39504	6.69	18676
13	REF11	41829	1.83	10614
14	REF12	46667	3.62	25935
15	REF13	42730	17.8	n. A. (3.9 MPa)
16	REF14	25300	17.9	n. A. (5.54 MPa)
17	REF15	17300	18.1	n. A.
18	REF16	42700	17.7	n. A. (4.76 MPa)
19	REF17	46852	17.8	n. A. (10.04 MPa)
20	REF18	39074	17.8	n. A. (7.58 MPa)
21	REF19	20029	17.6	n. A. (9.75 MPa)
22	REF20	42033	17.7	n. A. (3.67 MPa)
23	REF21	43090	17.7	n. A. (4.66 MPa)

Table 4.4: Chosen single parameters - results

Calculation REF0 One calculation without any operator action at all has been performed, to have an idea what would be to expect. The results show that about 10000 s after beginning of the transient the hot rod temperature is reached. Figure 4.3 reports primary and secondary system pressure (X and Y respectively), primary system mass and clad temperature (V and Z respectively),

Reference Calculation SBO, no losses of the deaerator, optimized intervention of SDE and PDE - REF1a

The first 30 min. after the SBO Description of the scenario a total SBO is the initiating event. At 0 s the reactor is scrammed, the MCP are tripped, all the feed water is lost, the turbine shut valves are closed. During the coast down of the MCP more energy is removed by the SG from the PS then supplied to by the reactor core. The primary temperature and pressure drops, while the secondary side pressure shows a sharp increase. At about 230 s the MCP coast down is completed. From this time on, the inventory in the SG starts to boil down. The BRU-A control valves, which are category one equipment and supplied by batteries, maintain the SG pressure smoothly 6.67 MPa. Together with the reduction of the SG level, the heat exchange surface from the PS to SS decreases, and the heat transfer deteriorates. An increase in PS pressure and temperature is the result. After 30 min into the transient, the level of the SG is at about 1.15 m and the PS pressure at 16.1 MPa

The first operator action SDE Thirty minutes after beginning of the transient the operator has diagnosed the situation and has taken the decision to depressurize the secondary side. He fully opens all four BRU-A valves. At this time the level in the SG is still about 1.1 m, so a considerable amount of water. It takes about 3 min for the SG pressure to reach the pressure of the feed water lines and deaerator tanks. The SG level drops within 3 min to about 0.3 m and then starts to raise again, since feed water from the feed water lines and deaerator tanks is furnished passively into the SG. About one hour into the transient the SG level is at its maximum of 2.4 m. The measure lowers the temperature and pressure in the PS to about 4.5 MPa. Accumulator start to intervene, but can not yet inject effectively, since the pressure stays close to the accumulator pressure. This phase lasts until 9260 s into the transient.

The second operator action PDE After 9260 s the operator depressurizes the PS. Here the assumption was made that the PORV is still available this may require back fits to the NPP. The moment was chosen to be when the primary side pressure starts to rise again. Since the pressurizer has a large steam volume at this time, opening the PORV is very effective in lowering PS pressure. This enhances accumulator intervention and helps in further decreasing the PS pressure. Both effects fill completely the PS and lower the PS pressure to atmospheric pressure. The PS stays this way while the SG level is sufficiently high.

Final phase from increase of PS pressure to core dry out and heat up. About 23000 s into the transient the

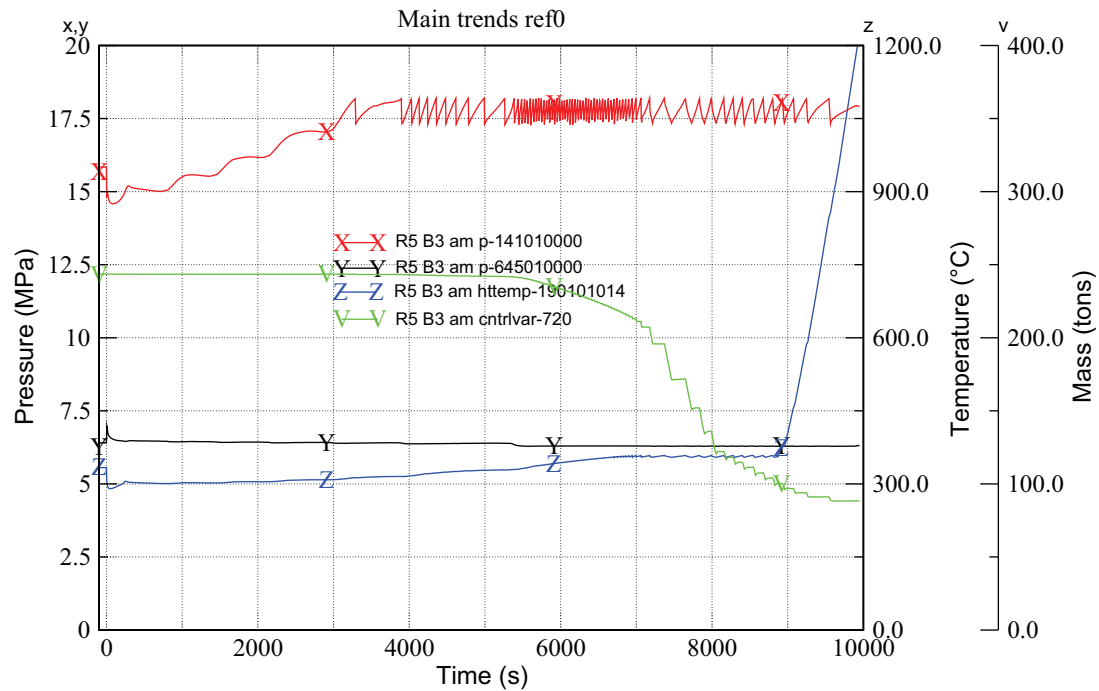


Figure 4.3: Calculation REF0, important parameters

SG are empty, and the primary side temperature starts to rise again. The PS inventory expands, and is lost through the PORV. The PORV is not capable to maintain the pressure at atmospheric level. Primary pressure continues to rise and PS inventory continues to decrease until about 30000 s. At this time a large part of the core is uncovered, the release of the energy from the core to the PS is reduced and the energy is kept in the structures of the core. As a result the PS pressure starts to decrease, and the temperature of the cladding rises sharply due to DNB. The dry out is quenched by loop seal clearing, the core is refilled again, primary side pressure continues to increase. About one hour later, at 33000 s, a second dry out occurs, which is not quenched. Primary pressure decreases slightly while the cladding temperature increases rapidly. At 33500 s the cladding temperature exceeds 1200 °C and the calculation is stopped.

Figure 4.4 reports primary and secondary system pressure (X and Y respectively), primary system mass and clad temperature (V and Z respectively). By comparing the results from REF0 and REF1 one can see that about 10 h of grace time can be won utilizing the deaerator water. Table 4.5 shows the resulting events.

No	Event	Time (s)
1	SBO	0
2	SDE	1800
3	SG level 0.25 m (local minimum)	2000
4	SG level 2.35 m (local maximum), deaerator empty	3500 - 3700
5	Accumulator intervention	4000
6	PDE	9260
7	PS pressure lower than 2 MPa	9430
8	SG empty	21500 - 22500
9	PS pressure above 2 MPa	25500
10	Begin first dry out	29250
11	Begin second dry out	33550
12	End of calculation, clad temp > 1200 °C	35350

Table 4.5: Calculation REF1 - resulting events

Conclusion and comments for the calculation REF1 SBO with SDE: In a SBO transient, the time until the clad temperature reaches 1200 °C is about 10000 s if the operator takes no action at all. The combined

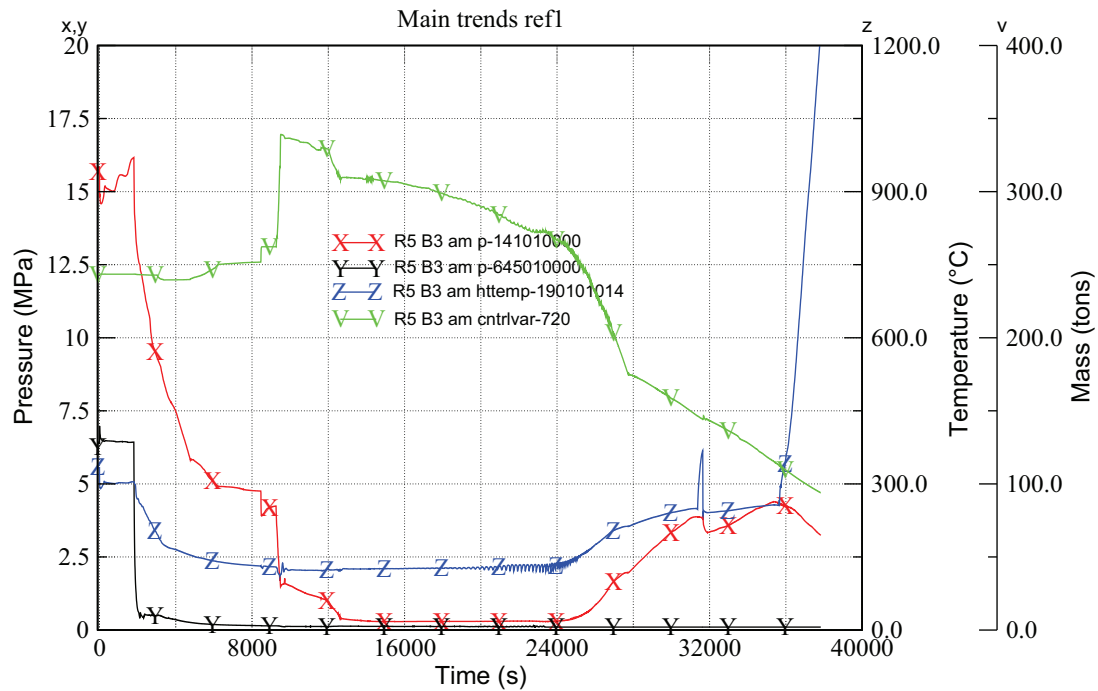


Figure 4.4: Calculation REF1 - selected parameters

action of SDE and PDE achieved three goals the time to reach the final dry out of 1200 °C could be extended to 35000 s. The PS pressure was kept below 2 MPa for about 16000 s, which means if the operator regains power, the LPIS could immediately be switched into RHR operation mode and long term controllable conditions would be achieved. The third goal which is achieved is that the PS pressure at the end of the calculation was relatively low with 3.16 MPa.

These achieve good values for these three parameters was the goal of the optimization process in the previous section, by varying the time of SDE and PDE. The method started to contract after a few iterations, which shows that the values which were chosen represent already an optimized case. This is not surprising, since the time for intervention was chosen deliberately to achieve a long grace time, while keeping PS pressure as low as possible.

Selected sensitivities

A large number of calculations have been performed, to check the effectiveness of the proposed AM procedure. Table 4.3 lists the boundary conditions for all performed calculations (i.e. the changes in respect to calculation REF1). Table 4.4 lists the chosen single parameters of the calculations, to give an idea of the effectiveness.

Calculation REF3 In this sensitivity the SDE was achieved using one SG only. The result is that the cool down rate of the primary side is about 20 /degC/h, instead of reaching up to 100 /degC/h. Other important parameters, which characterize the quality of the strategy, like the gained grace time and the primary pressure at the end of the calculation, are still comparable. Figure 4.5 shows main parameters (left, Primary and secondary system pressure denominated by X and Y, primary system mass and cladding temperature by V and Z, and right, primary system pressure and mass of calculation REF1 denominated by X and Z, primary system pressure and mass of calculation REF3 denominated by Y and V).

Calculation REF10 Calculation REF10 assumes that the PORV area is halved, which would correspond more or less to the flow rate of the gas removal system. A little bit of grace time can be won, since the primary side mass is used more effectively in terms of the removed of energy per unit mass, but at the cost of high pressure at the end of the calculation. Once the SG inventory is lost, the energy bleed through the PORV is not sufficient to maintain the primary pressure low. The results of the calculation REF9 and REF10

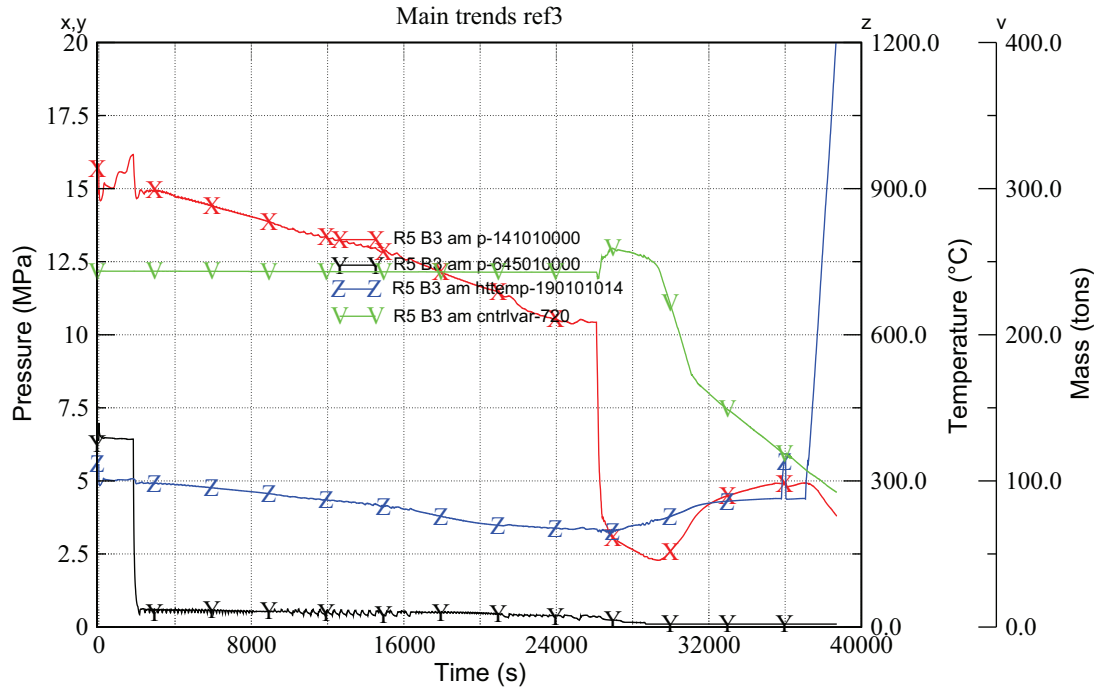


Figure 4.5: Calculation REF3 - main parameters

would suggest that a variable PORV would be an ideal solution a small area while there is still inventory in the SG, and a large area once the SG are empty. This conclusion is supported by Figure 4.6, which shows main parameters (left, Primary and secondary system pressure denominated by X and Y, primary system mass and cladding temperature by V and Z, and right, primary system pressure and mass of calculation REF1 denominated by X and Z, primary system pressure and mass of calculation REF10 denominated by Y and V).

Calculation REF14 assumes that the deaerator steam continues to consume steam after a SBO. The nominal losses of steam to the consumers are 4.4 kg/s. Apart from this, PDE was not simulated. The results show that the strategy relies heavily that the deaerator tanks stay pressurized. Also without PDE the grace time won is only half of that of the calculation REF1. But nevertheless in comparison to calculation REF0, which means no operator action, it was still possible to delay the time of occurrence of core damage from 10000 s to about 24000 s. Figure 4.7 shows main parameters (left, Primary and secondary system pressure denominated by X and Y, primary system mass and cladding temperature by V and Z, and right, primary system pressure and mass of calculation REF1 denominated by X and Z, primary system pressure and mass of calculation REF14 denominated by Y and V).

Calculation REF17 investigates SDE with one SG only. The cool down rate of the primary side is rather low, about 20 /degC/h, while the grace time gained is comparable to REF1. Figure 4.8 shows main parameters (left, Primary and secondary system pressure denominated by X and Y, primary system mass and cladding temperature by V and Z, and right, primary system pressure and mass of calculation REF1 denominated by X and Z, primary system pressure and mass of calculation REF17 denominated by Y and V).

Calculation REF18 investigates SDE with two SG only. The cool down rate is at about 60 /degC/h, while the grace time gained is still high. Figure 4.9 shows main parameters (left, Primary and secondary system pressure denominated by X and Y, primary system mass and cladding temperature by V and Z, and right, primary system pressure and mass of calculation REF1 denominated by X and Z, primary system pressure and mass of calculation REF18 denominated by Y and V).

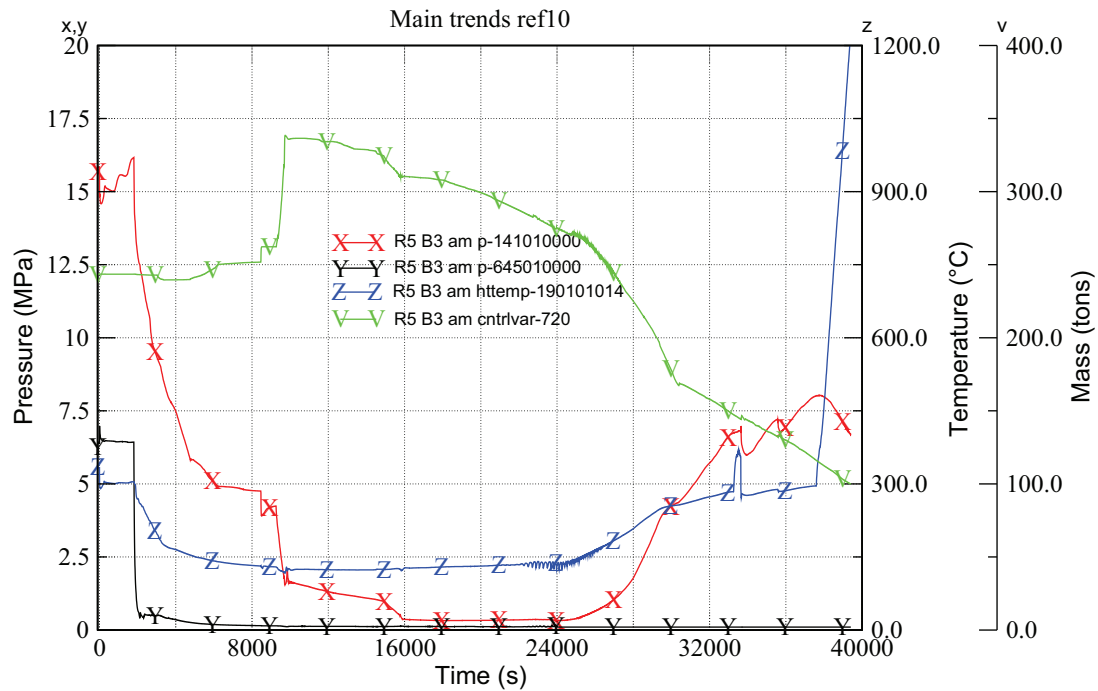


Figure 4.6: Calculation REF10 - main parameters

Calculation REF200 tries to simulate as close as possible to implement the strategy with the plant as it is now. Which means, that batteries are assumed to fail after 30 min, so the operator decides to initiate the strategy at 1800 s. Knowing that the PORV will shut close once the power supply from the batteries is lost, the operator decides to use the EGRS for PDE (the valves of the GRS will keep their current position once the power is lost). So after 30 min the operator initiates both SDE and PDE. The result is a very fast primary system depressurization, the pressure can be kept low for a long time. After the SG are empty a second time, after all water from the deaerator tanks is used up, the GRS is less effective than the PORV to keep primary pressure low, and the pressure rises again. Figure 4.10 shows main parameters (left, Primary and secondary system pressure denominated by X and Y, primary system mass and cladding temperature by V and Z, and right, primary system pressure and mass of calculation REF1 denominated by X and Z, primary system pressure and mass of calculation REF200 denominated by Y and V). As can be seen, the grace time which can be won is comparable, the pressure at the end of the calculation is almost the double in REF200.

Last possible moment - REF12 the sensitivity calculation REF12 tried to find the latest possible moment when the strategy would be still effective. Since the analysis is limited to the region where no core damage should occur, 9000, the onset of core dry out, was chosen to be a limiting calculation. So this means, that REF12 assumes the first intervention of the operator, SDE by fully opening all four BRU-A valves, at 9000 s into the transient. Just to mention, calculation REF0 shows that without any intervention at 10000 s into the transient the clad temperature locally would reach values above 1200 °C .

Surprisingly, the procedure proves to be even more effective if initiated at that time. The SG are filled on the SS and on the PS with steam. Opening the BRU-A valves leads to an almost instantaneous drop in pressure on the SS. Within 50 s the SS pressure reaches the pressure of the SL and the SG start to fill up with comparatively cold water of 150 °C . The steam on the primary side of the SG is collapsed, the NC is restarted and other hot steam of the PS is transported to the SG and collapsed. The result is that within 400 s the PS pressure, starting from about 17.5 MPa reaches the set point for intervention of the HA. Another 100 s later the pressure holds at about 1 MPa. The HA discharge 150 tons of cold water within 300 s into the PS. With the SG and the PS refilled, it takes another 30000 s to loose again all water and reach the final dry out which stops the calculation. The procedure is extremely effective from a thermal hydraulic point of view. Since the PS depressurizes so fast, not even the CSF PS integrity would show a challenge. But it is doubtful that the RCS would withstand the pure thermal shock of being cooled from 350 °C to 50 °C with 5 min.

Figure 4.11 shows main parameters (left, Primary and secondary system pressure denominated by X

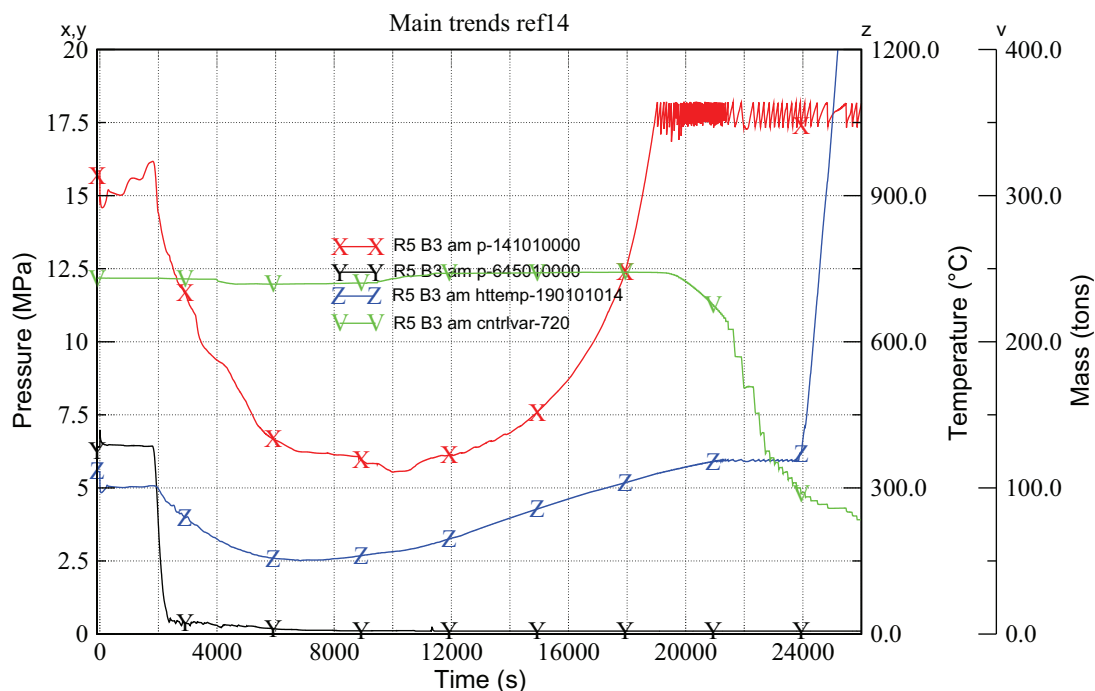


Figure 4.7: Calculation REF14 - main parameters

and Y, primary system mass and cladding temperature by V and Z, and right, primary system pressure and mass of calculation REF1 denominated by X and Z, primary system pressure and mass of calculation REF12 denominated by Y and V).

Using one SG to recharge the deaerator tanks REF5 The second sensitivity which is reported in more detail is the calculation Ref5. This calculation assumes that the deaerator tank loose their pressure (if the operator succeeds in insulating them, recharging is not necessary). This means, that at 1800 s SG1, SG2 and SG3 are depressurized, while the SG4 stays at 6.2 MPa. Until 5400 the water which is furnished passively is used. After 5400 s the last SG is depressurized, and discharges into the deaerator tanks. This succeeds in pushing the water which is still in the deaerator tanks into the SG. Ref5 should be compared to Ref14. The scenario Ref14 also assumes losses of the deaerator of 4.4 kg/s of steam after the SBO. The difference is, that in Ref14 the operator depressurizes all four SG after 1800 s. Analysis of Ref14 shows that a level of approximately 0.5 m of water stays in the SG under these conditions. Even if the safety valves to protect the deaerator tanks open, the water which still remains in the FW lines and deaerator tanks can be pushed into the SG. As a result it is possible to extend the grace time by 11000 s. As can be seen in Table, calculation Ref5 reaches 1200 °C after 36000 s, while calculation Ref12 reaches this limit after 25000 s.

Effectiveness of the procedure when the deaerator tanks are not isolated While the method is very robust against shifts in the timing of operator actions, the pressure in the deaerator tank is a crucial issue. This is shown by calculations REF2 and REF102, which show that assuming half the nominal pressure and half the nominal level reduces the effectiveness of the strategy considerably, as by calculations REF14 and REF15 which assume that the operator is not able to insulate the tanks, and that they loose 4.4 kg/s and 8.8 kg/s of steam respectively. Tab. 8.13 shows the water level of water still present in the deaerator tanks when the secondary system depressurization was fully utilized. With the assumption that the deaerator tanks are insulated after the beginning of the transient, all deaerator water can be used. With the assumption of the nominal losses of 4.4 kg/s of steam, the deaerator are still filled up to 1.25 m once SG depressurization is finished. Should the losses be higher (e.g. 8.8 kg/s of steam), only as little as the first 0.6 m of water of the deaerator tanks can be furnished into the SG.

Calculation of REF5 and REF105 show that there is a possibility to use all the water in the deaerator tanks, even if the losses can't be avoided pressure charging of the deaerator with the steam from the SG. There is a connection of the steam volume from the deaerator tanks to the steam volume of the SG. The

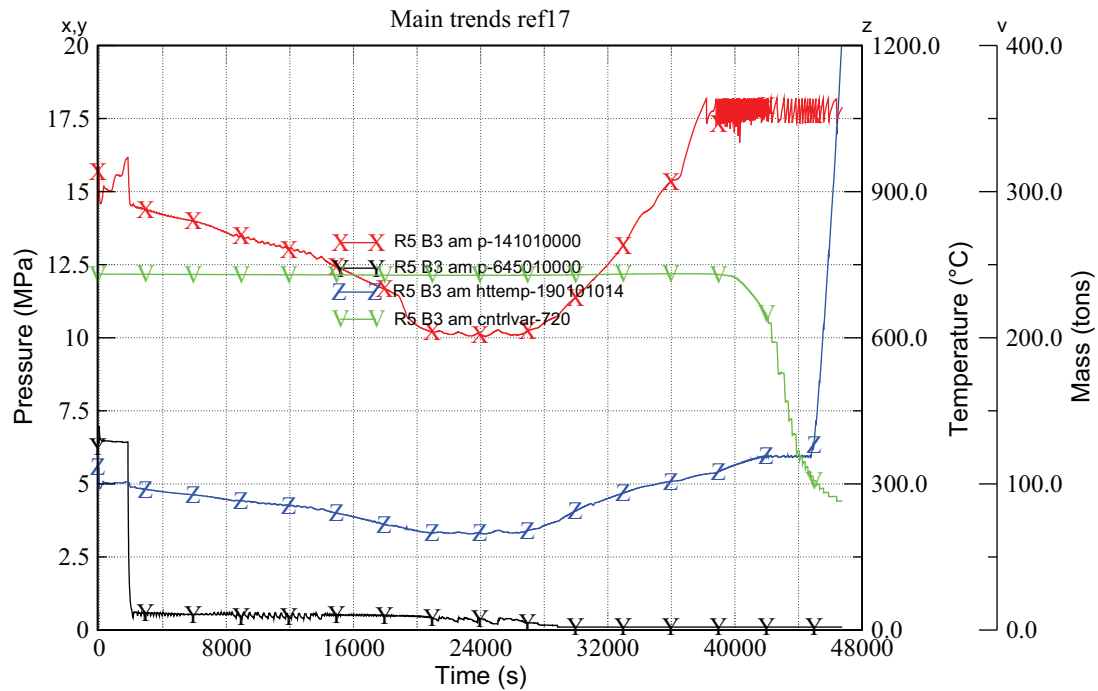


Figure 4.8: Calculation REF17 - main parameters

assumption in REF5 and REF105 was that the initial SDE is done using SG1 to SG3 only, while SG4 is kept pressurized. Once no additional water can be expected from the deaerator tanks, SG4 is connected to the deaerator. The pressurized steam at 6.2 MPa of SG4 succeeds in pushing the remaining water of the deaerator into the three depressurized SG.

Visualization of results: Figure 4.13 shows all results in a single plot. All calculations assume that power cannot be recovered, which means that the analysis has been terminated at when the peak cladding temperature exceeded 1200°C. This end point can be seen in Figure 4.13. The x-axis shows the “grace time”, while the y-axis shows primary system pressure at the end point. The scenario without AM is in the top left corner of the picture, which means early core damage (roughly 3 h) at high primary system pressure. The scenarios which assume SDE and PDE, in various variations, are all very close to each other - core damage at roughly 9 h-12 h, and primary system pressure below 2 MPa. This shows that the procedure is effective, and robust, in the sense that there is a broad time window for the operator to initiate the procedure. The violet dot in the map gives the results of a pen and paper calculation - for how long could the decay heat be removed, if all water would be used in the best possible way - i.e. evaporated directly in the core. One finds about 17 h. The comparison of 3 h without AM, 9 h to 12 h adopting the procedure and 17 h as “theoretical” optimum shows how close the procedure comes to the optimal use of the available sources of water.

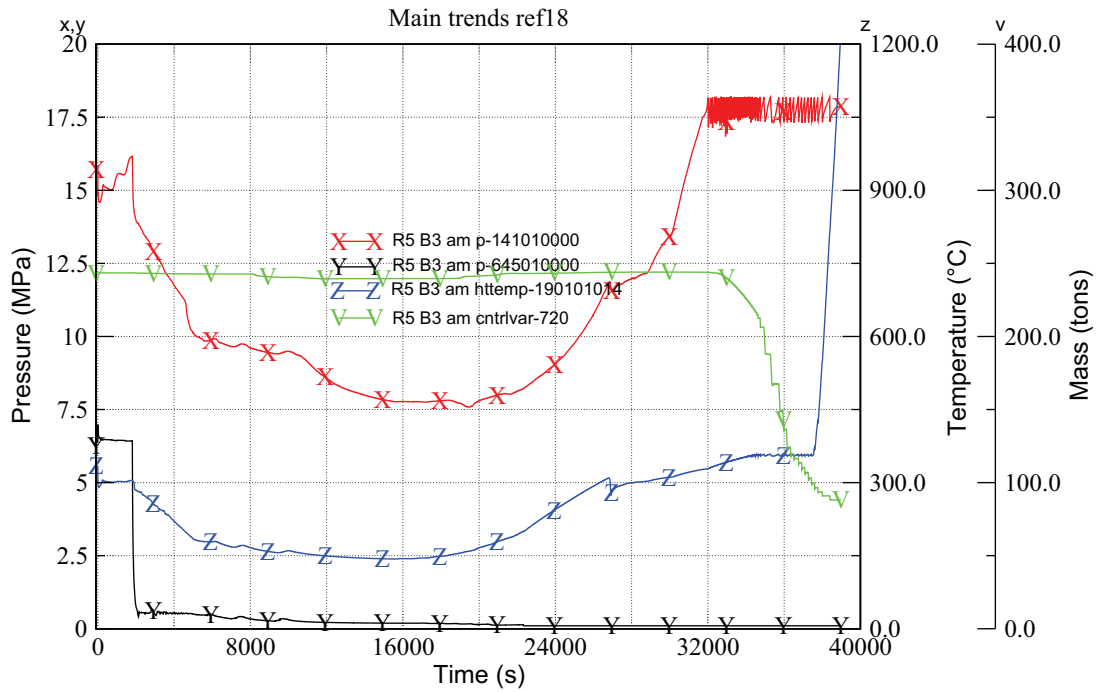


Figure 4.9: Calculation REF18 - main parameters

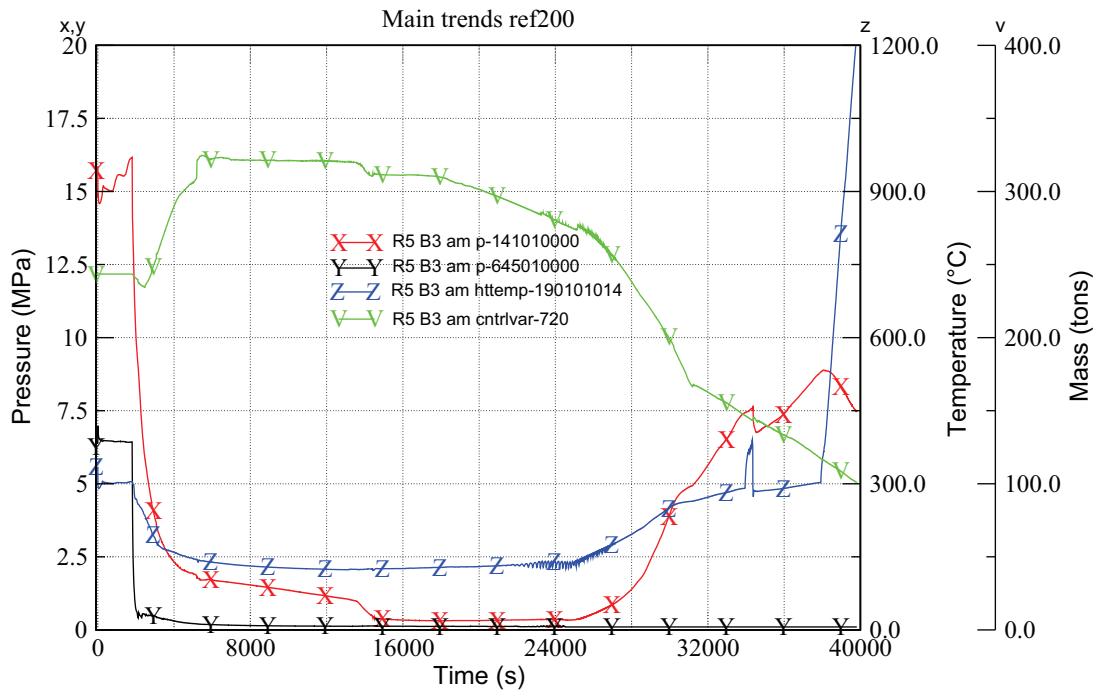


Figure 4.10: Calculation REF200 - main parameters, comparison to REF1

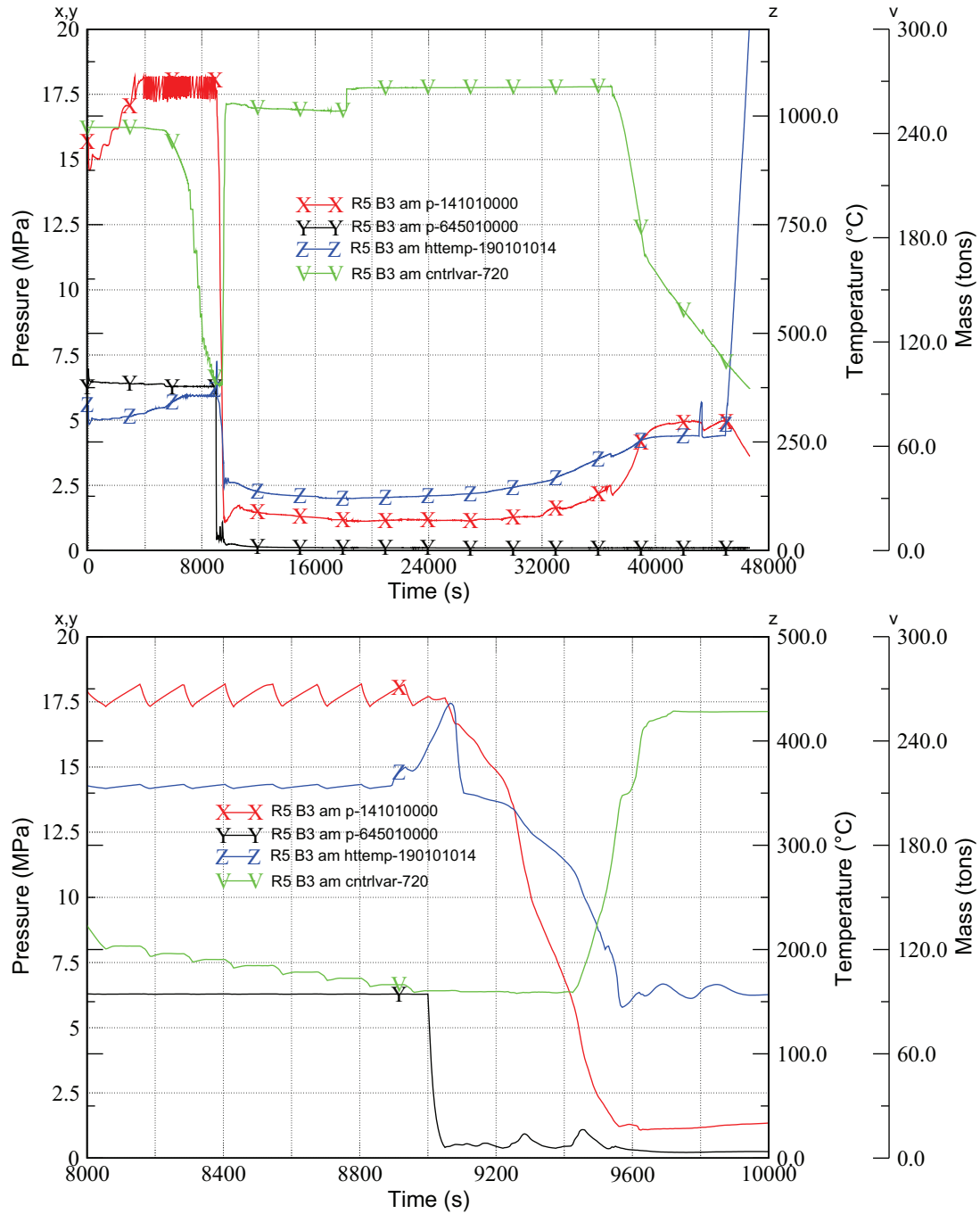


Figure 4.11: Calculation REF12 - main parameters (zoom on SDE)

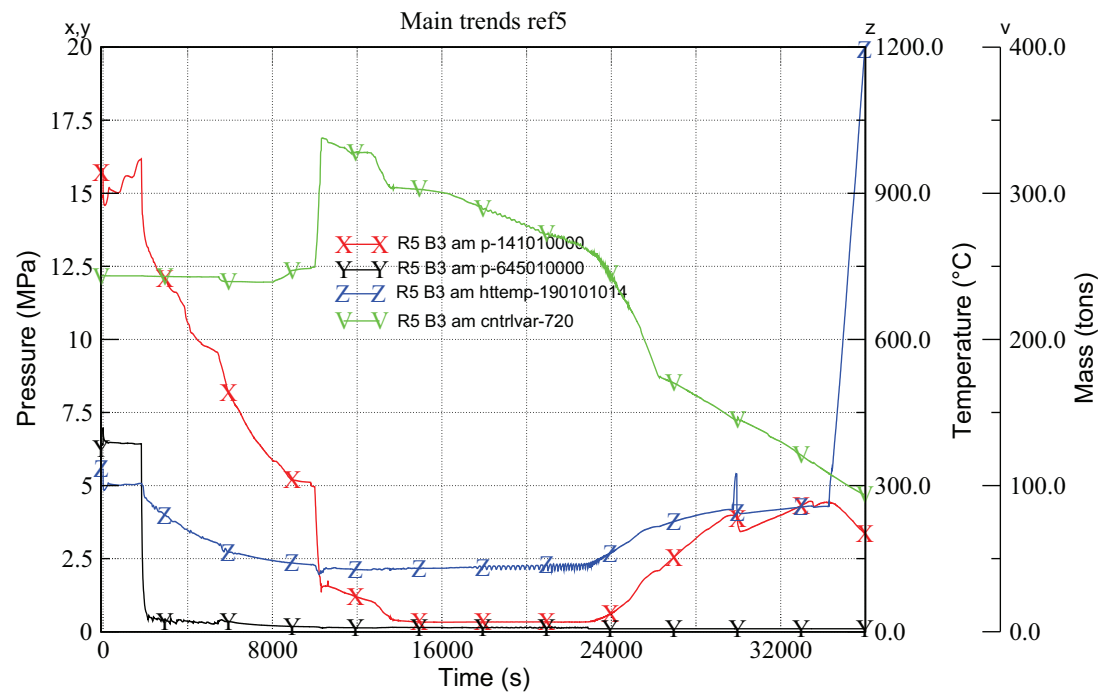


Figure 4.12: Calculation REF5 - main parameters, comparison to REF1

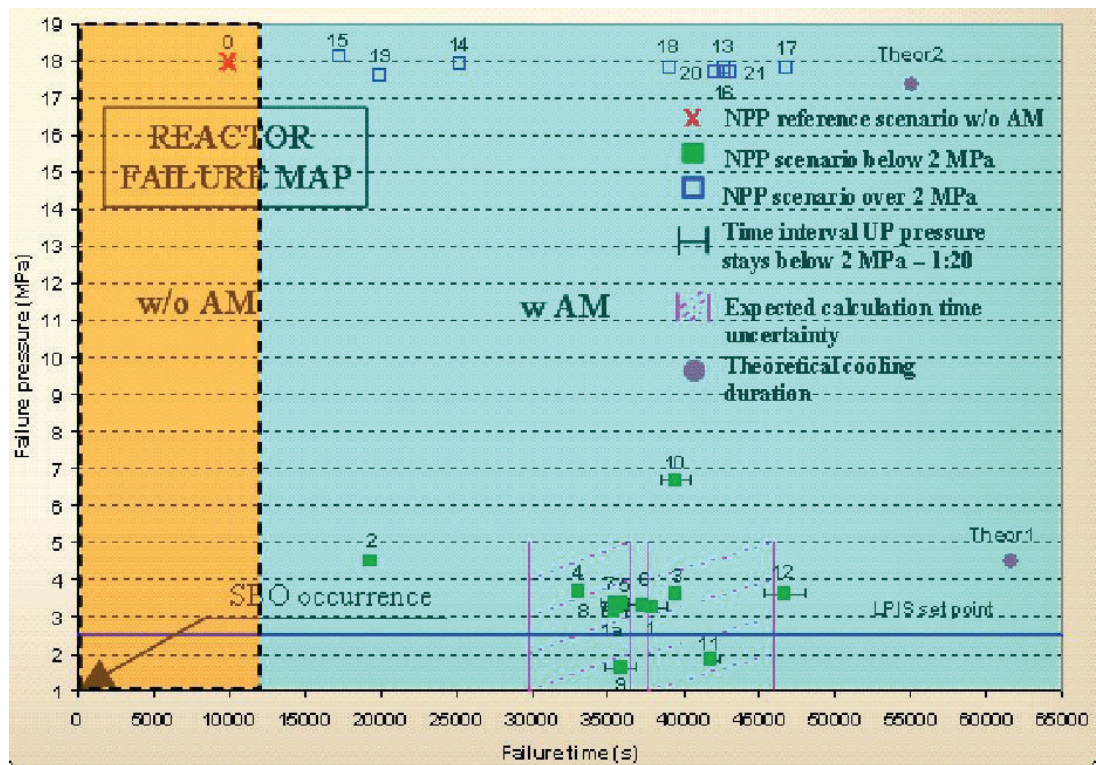


Figure 4.13: Failure map of SBO AM calculations

4.3 Quantitative

Looking at the qualitative analysis it becomes clear that primary and secondary system depressurization are beneficial in case of a SBO. Furthermore, one can see that the effectiveness depends on the timing of the action. In an accident condition it is unlikely that the operator is taking an action exactly at the moment that would be beneficial for the plant. But, nevertheless, the analyst, who is preparing and analyzing a procedure, should know when the procedure at earliest may be started, at what time in the transient it would be most beneficial and from what time it is too late.

Goal of the quantitative analysis is to work out a procedure which optimizes the use of equipment by the operator. A method which is capable to find the best moment for the actions has been worked out. This method was then applied considering a station blackout as initiating event, and secondary and primary system depressurization as possible actions, which timing should be optimized.

The procedure has been worked out by the author in the frame of this thesis - [Muellner et al., 2007].

4.3.1 Methodology

The procedure can be divided into four steps:

1. **Identify AM Parameters** find parameters which “define” the accident management procedure (non-dimensional, if possible).
2. **System availability** Decide on the system availability for the investigation. Expert judgement or a probabilistic cut-off criteria.
3. **Safety Barriers / Critical Safety Functions** identify the challenged Safety Barriers / Functions. Indicate the the state of the safety function as parameters (if possible, non - dimensional).
4. **Ideal Diagram** investigate the effect of the procedure, as analytical as possible, summarise results - e.g. using ideal diagram's of the PS pressure and temperature.

The main goal is to find a functional dependency between points one and two (independent variables of the function) and point three (the dependent variables of the function). Figure 4.14 shows how the components of the procedure act together. It is obvious that an analytical function, which can be optimized using pen and paper, will not be available for a system as complex as a nuclear power plant. Evaluating the function typically would mean to use a thermal hydraulic system code (TH-SYS) to find the effects of the chosen AM-Parameters and system availability, or an integral code, if one chooses to extend the analysis in the realm of the severe accidents.

A number of methods are available to optimize a function which can be evaluated numerically only, a summary of methods can be found in [Press et al., 2005]. The present paper chose to use the downhill simplex method [Nelder and Mead, 1965], which is known to be robust, uses only evaluation of the function without the need of calculating derivatives. The only disadvantage is that the convergence is slow.

4.3.2 Application Of The Procedure

Next step is to apply the procedure to a total SBO. As mentioned already in section 4.2, the procedure which is used to mitigate the accident is based on a procedure developed by Siemens for KONVOI type PWR for a total loss of feed water (LOFW) transient. An analysis of the procedure together with a comparison to experimental results at the LOBI facility can be found in [Madeira et al., 2003]. The basic principles of the procedure were applied to the VVER-1000 in a total LOFW [Muellner et al., 2005a].

The base scenario of section 4.2 is used for optimization, which means that the procedure consists in secondary side depressurisation (SDE) followed by primary side depressurisation (PDE).

As initiating event a loss of off-site power is assumed, together with the failure of all diesel generators (DG). Only power from batteries is assumed to be available. The minimum duration of the batteries differs from plant to plant. Figures known from certain NPPs indicate a minimum range between 15 min and several hours. PDE relies on power from the batteries (while SDE can be accomplished manually). Although the limitation from the batteries is known, it was assumed that PORV operation is always possible. Backfitting the plant with batteries which are dedicated only to the PORV is technically and economically feasible.

Together with the loss of all electric power the feed water is lost. The inventory of the steam generators can ensure decay heat removal for one to two hours. When the level in the steam generators is decreasing,

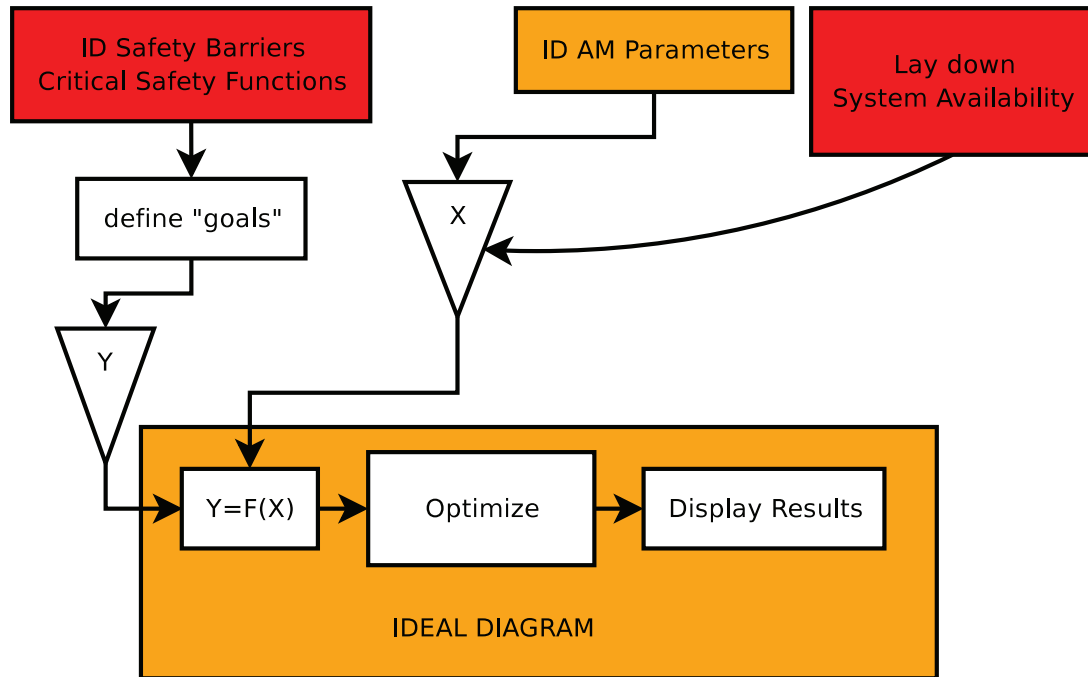


Figure 4.14: Schematic overview on the method used

and the steam generator tubes are uncovered, the heat transfer area is reduced and the heat removal from the primary side is deteriorating. The primary side pressure starts to increase, up to the set point of the pressurizer relief valve which ensures overpressure protection.

If no actions are taken, the primary side temperature will increase, the pressurizer level will rise - once the pressurizer is full and water is lost instead of steam, the primary side inventory starts to decrease and the core uncovers. After approximately 10000 s the cladding temperature exceeds 1200°C (again, please refer to section 4.2 for details).

Additional feed water can be made available by depressurising the secondary side. About 400 m³ of water in the feed water lines and deaerator tanks can be furnished passively into the steam generators.

Depressurisation of the primary side enhances the intervention of the passive parts of the emergency core cooling system, i.e. the accumulators.

Dependent Variables

The selection of the dependent variables is a crucial point, where engineering judgement comes into play. To define the success of the procedure, three parameters were chosen.

1. The “grace time” gained, i.e. the amount of time by which the grace time is extended due to the intervention of the operator.
2. The primary side pressure when the cladding temperature exceeds 1200°C .
3. The time interval in which the primary side pressure stays below 2 MPa.

The first parameter identifies the advantage of the operator action compared to no intervention in terms of time won.

The second parameter was chosen considering that direct containment heating at a vessel failure at high pressure (> 2 MPa) can not be excluded. Although calculations with integral codes (see eg [Muellner et al., 2004c]) show that from it takes still about 5000s from the time when the clad temperature exceeds 1200°C to the time when the vessel fails, the pressure at this instant was taken as indication for the pressure at the time of vessel failure. The reason is that Relap5 was used for the analysis (i.e. for every evaluation of the “plant state” - function).

The third parameter was taken because one should keep in mind that the probability for a station blackout decreases rapidly in time. If the power is recovered and the primary pressure at about or below 2 MPa, the LPIS can immediately guarantee long term coolable conditions.

Independent Variables

Since the system availability for a SBO is easy to define (only passive systems are available) the independent variables are the operator actions (time of SDE, time of PDE). These parameters are varied in the optimization process to achieve optimal values for the parameters mentioned in section 4.3.2.

However, as a second set of independent variables the time of PDE, the valve area of the PORV and the valve area of the BRU-A were chosen. This analysis might be considered academic, however, including the effect of the valve areas in to optimization process might help to identify improvements with by design changes.

Functional Dependency

Goal is to define a function which is capable of acting like a measure for the success of the intervention of the operator. A requirement for the simplex-method (see 4.3.2) is that the function should map $\mathbb{R}^n \rightarrow \mathbb{R}$. In section 4.3.2 three parameters have been chosen to characterise the final state of the transient. The goal now is to combine the three parameters to a single non-dimensional parameter using appropriate weights.

To combine parameters of different dimensions and different order of magnitude the parameters have to be normalised, i.e. have to be mapped to the interval $[0, 1]$ (the points 0 and 1 are included).

Normalisation of the Extended Grace Time

The first parameter to be normalised is the grace time which was won due to the operator actions. As normalisation function the function

$$\bar{t}_{egt} = \frac{t_{egt} - t_{egt}^{ref}}{t_{egt}} \quad (4.1)$$

was used (see figure 4.15). In the worst case the grace time is the same as the grace time of a SBO transient without intervention of the operator $t_{egt}^{ref} = 10000 \text{ s}$ - in this case the function maps to zero. The function gives more importance to grace time won at the beginning of the transient, i.e. if the grace time is 20000 s instead of 10000 s, the normalised grace time function is 1/2 instead of 0. On the other hand, if the grace time is 60000 s instead of 50000 s, normalised grace time function is 5/6 instead of 4/5.

Normalisation of the Pressure Parameter

The second parameter to be normalised is the primary pressure at the time when the cladding temperature exceeds 1200°C . The procedure requires that the transient is simulated every time the function has to be evaluated. To simulate the transient, Relap5 was used. Although a clad temperature of 1200°C by far does not indicate the failure of the vessel, the Relap5 calculation at this time was stopped, and the pressure at this time was taken as indication for the pressure at the time of RPV failure. The function (4.2) with $a = 1.1 \text{ MPa}^{-1}$, $b = 4.0 \text{ MPa}$ was chosen:

$$\bar{P}_{failure} = \frac{1 + e^{(-ab)}}{1 + e^{(a(P_{failure} - b))}} \quad (4.2)$$

To avoid direct containment heating the pressure at vessel failure should be below 2 MPa. The function therefore tries to penalise transients which end up with a pressure above 2 MPa, i.e. the function maps to $[0, 0.9]$ for pressures between zero and 2 MPa, and drops rapidly to zero for pressures bigger than 2 MPa.

Normalisation of the Time interval of Primary Pressure below 2 MPa

This parameter was selected keeping in mind that, if electricity to the unit can be recovered, it would be possible for the operator to initiate primary side feed with the LPIS immediately, and therefore keep the plant in a long term cool able state. From previous calculations it is known that this parameter is to be expected to be between 0 s and 20000 s. The normalisation function was chosen as

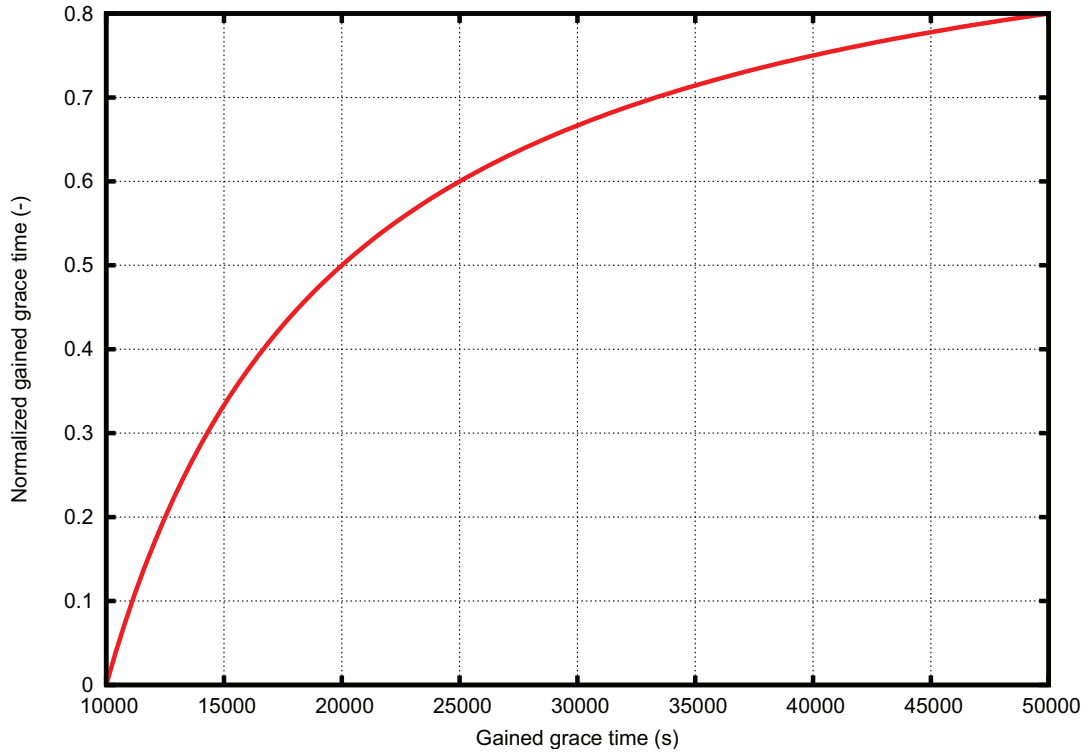


Figure 4.15: Function to normalize the extended grace time (equation 4.1)

$$\bar{t}_{below2MPa} = \frac{c}{1 + e^{(a(b - t_{below2MPa}))}} + d \quad (4.3)$$

The constants a, b, c , and d were chosen to impose the following properties on the function: the function should map a time interval of 0 (which means, the primary pressure stays always above 2 MPa) to 0. When the primary pressure can be kept below 2 MPa for about 20000 s, the function should give a value close to one. The normalisation function should approach one with the time interval approaching an infinite value. For a time interval between 0 and 20000 s the function should be close to linear. To full fill all this properties, the values were selected as following: $a = 3 \cdot 10^{-4} \text{ s}^{-1}$, $b = 10^4 \text{ s}$, $c = 1 + \exp(-ab)$, $d = -\exp(-ab)$. The function can be seen in Fig. 4.17.

Composition of the evaluation function

To summarise the results so far, three parameters were chosen to characterise the success of the operator intervention: The grace time which can be won, the primary pressure when the clad temperature exceeds 1200°C , and the time period in which the primary pressure stays below 2 MPa.

$$\bar{t}_{egt} = f_1(t_{SDE}, t_{PDE}) \quad (4.4)$$

$$\bar{P}_{failure} = f_2(t_{SDE}, t_{PDE}) \quad (4.5)$$

$$\bar{t}_{below2MPa} = f_3(t_{SDE}, t_{PDE}) \quad (4.6)$$

To combine f_1, f_2, f_3 three different weights w_1, w_2, w_3 were chosen to emphasise the difference in importance. The major weight was given the extension of the grace time with $w_1 = 0.5$. The primary pressure at the end of the calculation was found to be the second most important parameter with $w_2 = 0.3$. The weight was assigned to be $w_3 = 0.2$. The final function computes now to

$$O(t_{SDE}, t_{PDE}) = \sum_i w_i \cdot f_i(t_{SDE}, t_{PDE}) \quad (4.7)$$

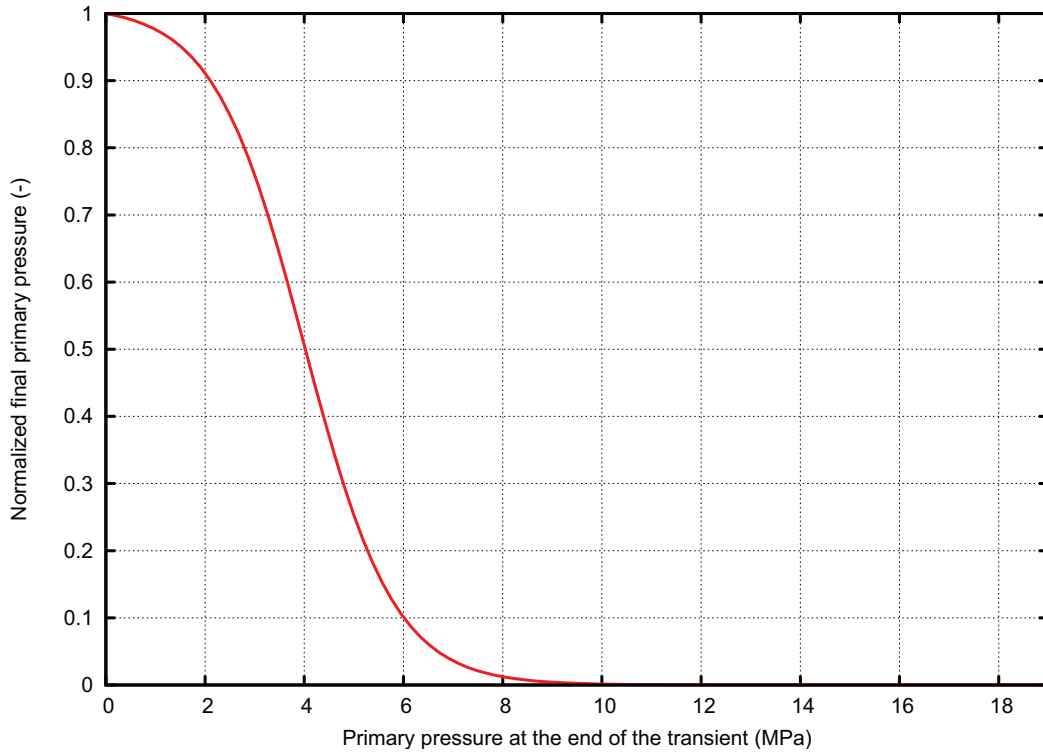


Figure 4.16: Function to normalise the final primary pressure of the transient (equation 4.2).

Optimization process - Multidimensional Downhill Simplex Method

A robust method to find local extrema of a multidimensional function, which only requires evaluation of the function, is the downhill simplex method Nelder and Mead [1965]. The efficiency of the method can be improved if a large number of parameters is needed Kaczmarczyk [1999].

The problem is how to find a multidimensional minimum of the function $f(x_1, x_2, \dots)$ such that $f(P_m)$ with $P_m = (x_1^m, x_2^m, \dots)$ becomes a minimum.

1. If the problem is N-dimensional, construct a simplex of N+1 points. Evaluate the simplex at each point. Identify the highest point of the simplex P_h . The remaining points are labelled P_i , so that the simplex consists now of the points $(P_i, P_h | i = 1, \dots, N)$.
2. Find a new point P_r by moving the highest point P_h of the simplex through the Baricenter $P_b = (1/N) \cdot \sum P_i$ of the other points, conserving the volume of the simplex. Evaluate f at this new point P_r . According to the value of $f(P_r)$ three possible ways to continue are foreseen:
 - (a) $\forall i : f(P_i) < f(P_r) < f(P_h)$: if the new point P_r is lower than the highest point of the simplex, but higher than the lowest point of the old simplex without the highest point, construct a new simplex by substituting the previous highest point with the new point (new simplex: $(\forall i : P_i, P_r)$) and start from the beginning (**reflection**).
 - (b) $\forall i : f(P_r) < f(P_i)$: if the new point P_r is the lowest point of the simplex, construct a new point P_{rr} by moving P_r further in the same direction by a factor of two. Two possible ways to proceed:
 - i. $f(P_{rr}) < f(P_r)$: the direction led further to the minimum. The new simplex will be $(\forall i : P_i, P_{rr})$. The volume of the simplex increased (**reflection and expansion**).
 - ii. $f(P_{rr}) > f(P_r)$: moving P_r did not minimise f any further. The new simplex will be $(\forall i : P_i, P_r)$, and one should start from the beginning (**reflection**).
 - (c) $f(P_r) > f(P_h)$: if the new point is higher than the previous highest point, a new point, $P_{rr'}$, halfway between P_h and P_b will be constructed and $f(P_{rr'})$ will be evaluated. Again, two possible continuations:

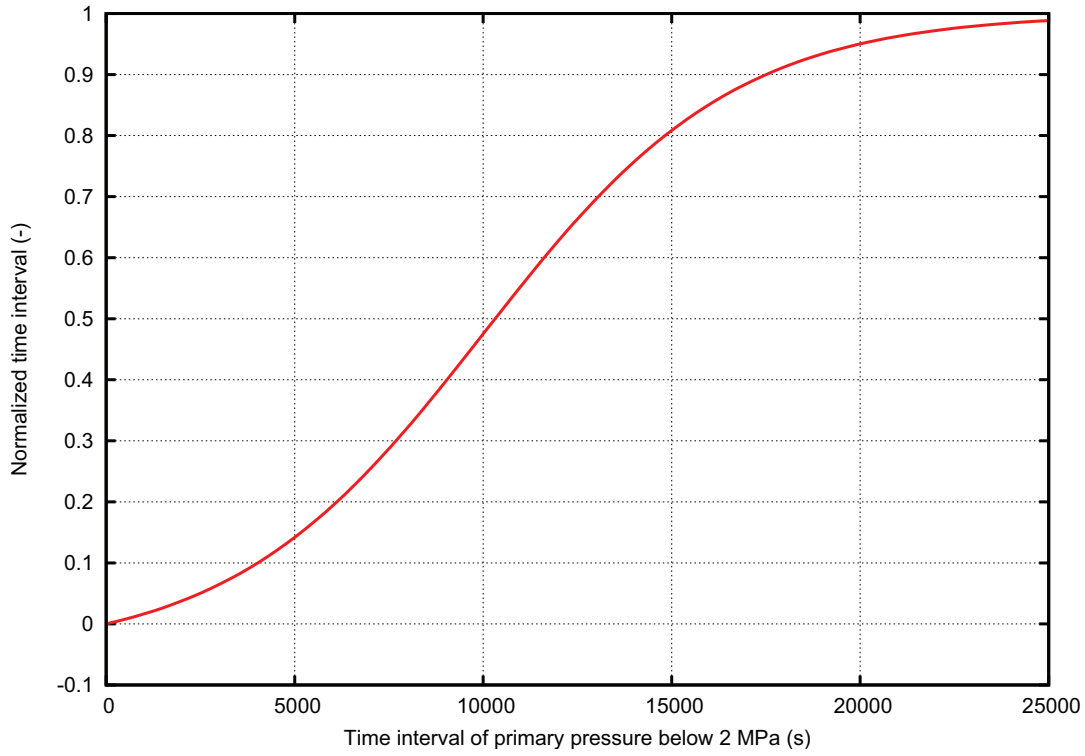


Figure 4.17: The normalisation function (4.3) for the time interval in which the primary pressure stays below 2 MPa

- i. $P_{rr'} < P_h$: the simplex already comprises the minimum and contracts. The new simplex is chosen to be $\forall i : P_i, P_{rr'}$ (**contraction**).
 - ii. $P_{rr'} > P_h$: the characteristic length of the sides of the simplex is too large - f varies too much inside the simplex. The lowest point of the old simplex is chosen $\min(\forall i : P_i, P_h)$ and all other points are moved along their sides towards the lowest point. The length all sides is reduced by a factor of two (**multiple contraction**).
3. Find an exit criteria. Possibilities are that one of the distance-values $\forall i : |P_i - P_r|$ drops below a preset threshold, or that the variation of the function $f(\forall i : f(P_i) - f(P_r))$ drops below a preset threshold.

Results

Varying t_{SDE} and t_{PDE} : Considering only two parameters the simplex has three points. The first point was chosen to be $(t_{SDE}, t_{PDE}) = (1800, 9360)$. The idea was that the operator would need 30 min to analyse the situation and to find the adequate response. The second operator action was chosen to take place when the primary pressure, due to the first action reaches a minimum. For a detailed discussion of this special case (which turned out to be the best case investigated) please refer to Cherubini et al. [2006].

Two other points were chosen, assuming as characteristic length for the first parameter 600 s, and for the second about 1000 s. The initial simplex, the following simplices and the results of the evaluation are reported in Table 4.6 and Figure 4.18.

Varying t_{PDE} , Area PORV, Area BRU-A : The next set of variables assumes that the operator initiates secondary side depressurisation at 1800 s, and just primary side, as well as the areas of the safety valves, are object to optimization. A simplex using three parameters consists out of four points and forms a tetraeder. It can be seen that increasing the PORV area helps to achieve the objectives. The results are reported in Table 4.7 and Figure 4.19, where the z-axis gives the PORV area, the x and y axis the time of PDE and area of BRU-A respectively. The red tetraeder is the first simplex, the blue the second one.

Table 4.6: Optimization of two parameters, the time of SDE and PDE

Id	t_{SDE} (s)	t_{PDE} (s)	$O(t_{SDE}, t_{PDE})$ (-)
Simplex 1			
Ref1	1800	9360	0.758
Ref7	1800	8360	0.729
Sim2	2400	10360	0.715
Simplex 2			
Ref1	1800	9360	0.758
Ref7	1800	8360	0.729
Sim1	1200	7360	0.731
Point to be evaluated			
Sim6	1200	8360	

Table 4.7: Optimization of three parameters, the time of PDE, normalized PORV area, normalized BRU-A area

Id	t_{PDE} (s)	A_P/A_0 (-)	A_B/A_0 (-)	$O(t_{PDE}, A_P/A_0, A_B/A_0)$ (-)
Simplex 1				
Ref1	9360	1	1	0.758
Ref7	8360	1	1	0.729
Ref11	9360	1	0.5	0.715
Ref9	9360	2	1	0.878
Simplex 2				
Ref1	9360	1	1	0.758
Ref11	9360	1	0.5	0.715
Ref9	9360	2	1	0.878
Sim3	10360	1.67	0.67	0.840
Point to be evaluated				
Sim5	10027	2.11	0.45	

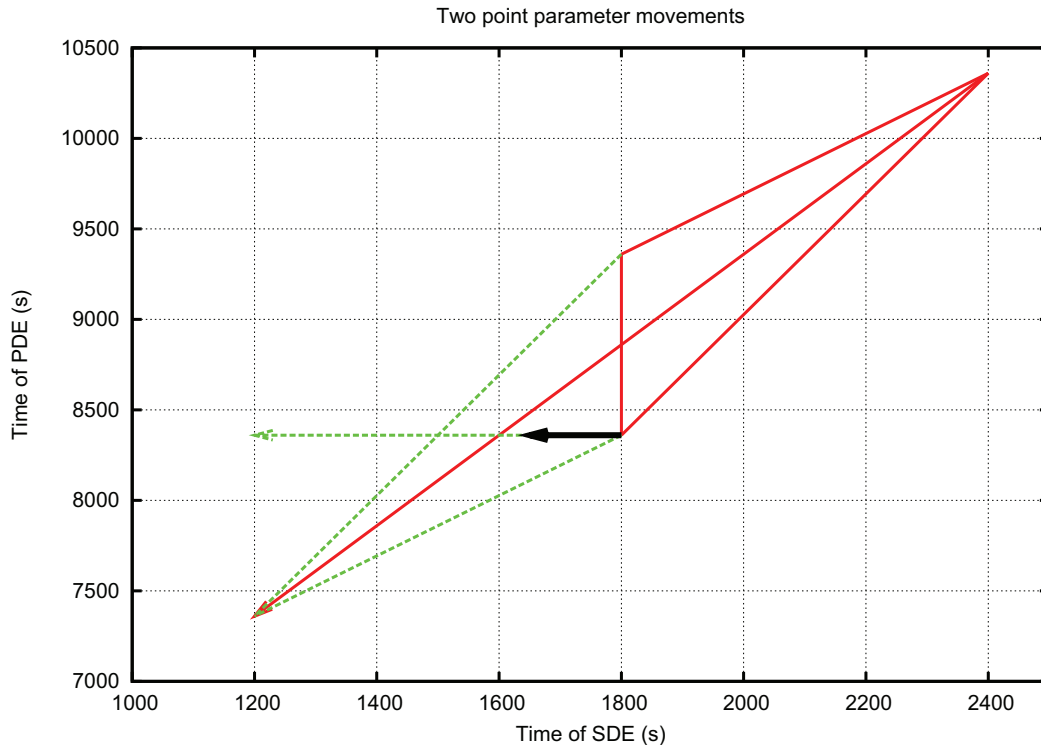


Figure 4.18: Optimization of two parameters, the time of SDE and PDE

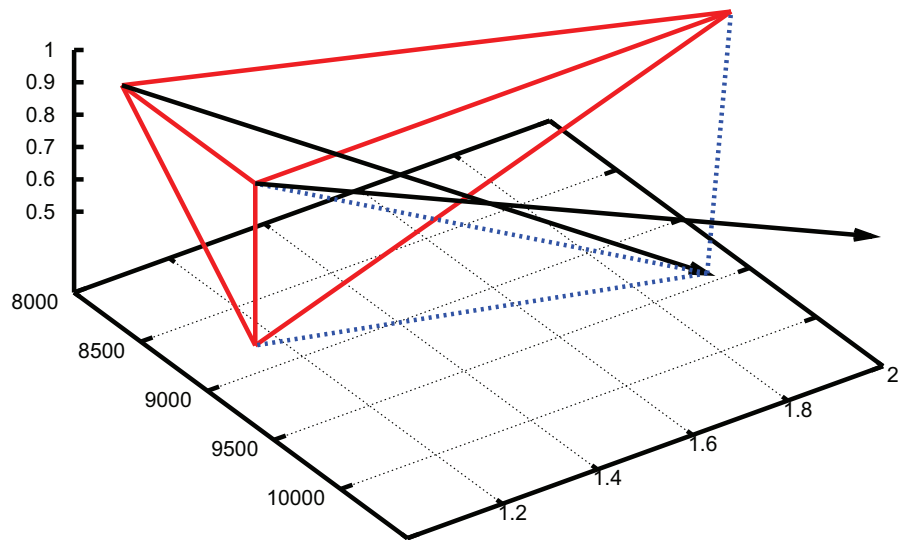


Figure 4.19: Optimization of three parameters, time of PDE, Area PORV and BRU-A

Chapter 5

Conclusions

The following section summarizes the main findings and achievements. A large number of beyond design basis accidents have been simulated. The key outcome is the following:

5.1 Code validation

After the experimental database was available, post test analysis for a number of post tests has been performed (four post test calculations performed with Relap5 are presented here). The post test analysis presented a validation step for the current work. Relap5 had been used for verification of the effectiveness of AM strategies, and for optimization of an AM strategy in case of a station blackout. To gain confidence in the results it was necessary to validate the tool by code experiment comparison.

What has been seen is that the code performs reasonably well in predicting AM relevant accident sequences for VVER type reactors. All post test calculations achieve good scores using the fast Fourier transform based method (FFTBM) for code - experiment comparison. Two small break LOCA have been analyzed - main phenomena, loop seal clearing, dry out, core heat up, quenching, counter current flow limitation, critical flow through the break, critical flow through safety valves, could be predicted by the code. Differences in the timing between code and experiment could be mainly explained by the heat losses of the pumps of the facility, which are, unfortunately, not well characterized.

Two post tests, simulating a loss of heat sink, have been analyzed, and also here the code - experiment comparison gives reasonable results. Heat removal by natural circulation, temperature increase of primary system coolant, break down of natural circulation once the SG are empty and restart of natural circulation when they are depressurized and refilled can be seen in the experiments and in the code. Again, differences in timing can be explained by heat losses, which are not well characterized.

It should be emphasized that the main goal of the experiments was to provide data for code validation. The results are not directly transferred to the NPP. It is not expected that the NPP behavior is reproduced by the experiments. If one compares test 11 and test 12 dry out at the facility with the calculation for the VVER 1000 one notices that the NPP calculation predicts a large dryout lasting several hundredths of seconds, while the experiment shows only small, local dry outs. This effect, small dry outs, has to be attributed to the PSB facility.

A second observation that has been made was that the code predictions for loss of heat sink events with natural circulation are very sensitive to the SG model (due to the horizontal steam generators). During such events the SG level slowly decreases, and SG-U-tubes are uncovered. While in vertical SG all U-tubes have the lower part covered and the upper part uncovered, horizontal SGs have some U-tubes completely covered, and some U-tubes completely uncovered. As has been shown, simplifications of the SG model lead to an error in the calculation of the transferred heat, and in consequence to a wrong timing of SG voiding. As could be seen, the model as currently adopted in the VVER-1000 nodalisation (six levels of U-tubes) introduces a small, but visible error. For PSB-VVER nodalisation (17 levels of U-tubes) a distortion due to the modeling is not even noticeable.

5.2 AM strategy evaluation

The second main outcome of the results of Chapter 3 regards the actual AM strategies that have been tested. The results from the experimental facility can tell about the qualitative evolvement of a transient, but do not provide precise predictions on the NPP response, if subjected to the same initiating event and boundary conditions. Therefore, the main goal of the experiments is to validate computer codes and give a general idea on the qualitative behavior of the plant. To gain deeper insights, one has to rely on NPP calculations, as presented in chapter 3.

Three different classes of initiating events have been assumed, each time with different AM strategies and different availability of safety systems. The initiating events, that have been assumed, are loss of feed water, station black out, small break loss of coolant accidents and primary to secondary side leaks. The following conclusions have been drawn:

- Scenario 1, loss of all feed water and unavailability of HPIS. Depressurization of the secondary system and supply of feed water of 10 kg/s to two SGs is successful in achieving a temperature decrease of primary system coolant.
- Scenario 2, as above, but with PS depressurization. Primary system depressurization (but maintaining a saturation margin) is successful in speeding up the depressurization process. No adverse effects (like interruption or break down of NC) have been observed.
- Scenario 3 for characterization purpose only (PORV stuck open in hot-shutdown conditions, Zaporoshye accident).
- Scenario 4 CL break equivalent to 70 mm diameter with failure of all HPIS. The strategy, SS depressurization, is successful to reduce the PS pressure and allow SITs and LPIS to actuate.
- Scenario 5, PRISE, with failure of all HPIS - the operator action, primary depressurization, cool down of primary via secondary with intact SGs, isolation of SITs, is successful in lowering PS pressure below SS pressure, thereby terminating the loss of PS water to the SS, and at the same time leading the PS into a long term coolable state.
- Scenario 6, total loss of feed water with one train of HPIS available and PS depressurization only. The set point of the HPIS can be reached, for a short period even the set point of hydro accumulators. One train of HPIS is sufficient to provide sufficient core cooling and lead the plant to stable conditions.
- Scenario 7, Station blackout with no active systems, as operator action secondary system depressurization plus injection from mobile pumps only. The operator actions are sufficient to lower the primary system pressure to 6 MPa (just above the actuation set point of the accumulators). Primary pressure and temperature are stable at the end of the transient.
- Scenario 8, SBLOCA without HPIS and without AM has been performed for characterization purposes. Primary depressurization is fast enough to reach the set point for accumulator intervention, but the accumulators are not effective. Periods of dryouts with core heat up follow. During core heat up the energy released to the fluid is reduced, which lowers the pressure, which, in turn actuates the accumulators, quenches the core, but stops primary depressurization and accumulator injection. The calculation is stopped after eight thousand seconds without achieving stable conditions.
- Scenario 9, PRISE equivalent to 100 mm break (SG header break) with stuck open of BRU-A of affected SG. All ECCS is assumed to be available. The strategy, isolation of SITs, switch of two trains of HPIS, cool down of primary with intact SGs, is not successful in lowering primary below secondary pressure. However, the loss of primary coolant to the secondary can be reduced, and the coolability of the core can be ensured.
- Scenario 10 for characterization purposes only (natural circulation).
- Scenario 11, a SBLOCA equivalent to 70 mm diameter, with initial failure of all HPIS pumps. Within the first 30 min the core uncovers and core heat up occurs. The (assumed) recovery of one train of HPIS together with cool down of primary by secondary with a cool down rate of 30 K/h is sufficient to quench the dry out and lead the plant to long term coolable conditions.

- Scenario 12, a SBLOCA equivalent to 70 mm diameter, with initial failure of all HPIS. Initiating event and operator actions are as in scenario eleven, but instead of one train of HPIS the operator recovers the make-up system and the HHPIS (which can provide in total a flow rate comparable to the one of the HPIS at the given pressure). Again, a dry out occurs, but the operator actions are successful in quenching the dry out and leading the plant to safe conditions.

Summarizing can be said that the investigated strategies have been proven to be successful in leading the plant to long term coolable conditions.

5.3 EOP Optimization

In close cooperation with Balakovo 3, the reference VVER 1000 unit for the implementation of AM programmes for most Russian VVER units, one special initiating event and AM strategy has been selected for optimization. As initiating event, a long term station black out has been selected, while the AM strategy was based on the use of secondary side depressurization to passively utilize the water inventory still available in the feed water lines and deaerator tanks.

A reference case, where a station black out has been assumed without operator actions, has shown that in that case, in a VVER-1000, core damage would occur after roughly 3 h. Assuming that the accident progresses further without operator actions, vessel failure and high pressure melt ejection could be expected another 1-2 h later.

This case, first of all, should be compared with the reference AM case. The reference AM case initiates after 1800 s secondary system depressurization, and after 9360 s, once the cooling effect due to the water from deaerators and feed water lines has ended, primary system depressurization is initiated (i.e. when the slope of the primary system pressure becomes horizontal). With the first measure the primary system can be depressurized just above the set point of the hydro accumulators, with the second measure the primary system can be further depressurized, and the HA fully discharge. Core heat-up occurs after roughly 10 h (compared with three!), and at comparably low primary system pressure.

The reference AM calculation assumed that the deaerator tanks would stay at their operating pressure. Unfortunately, this cannot be assured - during nominal operations there are steam- and liquid losses from the deaerator, and it is not known how much would be lost during station blackout conditions. Therefore, losses of roughly 4 kg/s and 8 kg/s of steam have been assumed (calculations Ref14 and Ref15). As result, core heat up occurs at roughly 7 h and 5 h respectively. So it has to be concluded that this variable has a major influence, and should be investigated better if the strategy is to be implemented in the Balakovo 3 accident management programme.

To cope with possible losses of the deaerator, an additional strategy has been investigated (which is, in principle, possible to be implemented): when the SGs are depressurized, not all of them depressurize through the BRU-A valves, but SG4 discharges into the deaerator tank. Such a connection exists already. Safety valves in the line, however, would limit the pressure of the deaerator tanks to 6.6 bars. It could be shown (calculation REF5) that this additional strategy allows again to fully utilize the deaerator tanks (time until core heat up was again 10 h).

A bounding case calculation assumed that the operator would initiate the procedure at the last possible moment, when dry out already occurred and cladding temperatures already started to increase (calculation REF12). The results could show that even in this case the procedure would be effective.

In addition to the qualitative analysis, a quantitative analysis has been performed. A method to optimize operator actions has been worked out. This method is easily extendible for other optimization processes, and although the method has been worked out in the frame of the work which is presented here, it has already been applied in for other applications (optimization of accumulator initial pressure and flow restrictors in the accumulator line). The method has been applied, starting from the reference AM case. After a view steps convergence has already been reached, but the improvements that could be achieved are relatively small (small compared to the uncertainty that one can expect for such calculations). It can therefore be concluded that the precise timing is of minor importance - which is positive, since it cannot be expected that the operator would initiate the procedure at just the right time.

5.4 Achievements and open issues

Summing up, the present work contributed (in frame of the Tacis-project) to drawing up a validation database, and to validation of Relap5 for analysis of long lasting transients with multiple failures and operator actions at VVER 1000 reactors. This was an open point, since experiments that were available were aiming at western type PWR (with vertical steam generators).

A second achievement was to fill a gap in the analysis of AM strategies for Balakovo 3. During a station blackout feed water from external sources should be supplied to the SG to secure the heat sink. Supplying feedwater by means of mobile pumps or fire brigade trucks has already been investigated, the present work closes a hole by extending the analysis to the passive sources of feed water, the deaerator tanks and the feed water lines. However, the analysis did not yet take the step from strategy to actual procedure. It still should be investigated to which signals the operator actions should be tied. The losses of the deaerator tanks should be characterized, and the pressure drop from deaerator tank to the steam generator should be determined experimentally at the plant. It should be investigated which valves have to be opened and closed to establish a connection from SG to the deaerator tank, in case the SG depressurization should re-pressurize the deaerator tanks. It has to be investigated how much time it would take the operator to do so. These investigations have to be performed at the station itself.

A third achievement was to work out an automated method for optimizing operator actions, which can be extended to optimizing in general set points and equipment for AM. While in the present case the optimization process was easy, and the result of the optimization could be foreseen by pen and paper analysis, other situations are more complex (e.g. initial pressure of accumulators, which should work efficiently for a wide range of initiating events) and the method could provide a tool to look for a optimal set of settings in an organized way.

Bibliography

- W. Ambrosini, R. Bovalini, and F. D'Auria. Evaluation of accuracy of thermalhydraulic code calculations. *Energia Nucleare*, 2, 1990.
- A. Andrioutschenko. Description of finalized scenarios of psb-vver-experiments. Technical report, Kurtchatov Institute Moscow, 2004.
- A. E. Bergles, J.G. Collier, J.M. Delhay, G.F. Hewitt, and F. Mayinger. *TWO-PHASE FLOW AND HEAT TRANSFER IN THE POWER AND PROCESS INDUSTRIES*. HEMISPHERE PUBLISHING CORPORATION, 1981.
- V.N. Blinkov, A.G. Kraev, O.I. Melikhov, I.V. Elkin, V.I. Melikhov, I.V. Parfenov, and R.T. Jensen. Computer code validation for transient analysis of vver and rbmk reactors. Joint Project 6 US and Minatom Nuclear Safety Centers, Project Report, 2004.
- BNPP1-DB. Db given to iaea. Excel file, 1996.
- R. Bovalini, F. D'Auria, and M. Leonardi. Qualification of the fast fourier transform based methodology for the quantification of thermalhydraulic code accuracy. DCMN Report, NT 194 (92), Pisa, 1992.
- C. E. Brennen. *Fundamentals of Multiphase Flow*. Cambridge University Press, 2005.
- E.O. Brigham. The fast fourier transform, 1974.
- M. Cherubini, A. Del Nevo, F. D'Auria, and G. Galassi. Scaling of small break loca in vver1000 system. In *4th International Conference "Safety Assurance of Nuclear Power Plants with WWER"*, Podolsk 23-25 May 2005, 2005.
- M. Cherubini, N. Muellner, F. D'Auria, and G. Petrangeli. Application of an optimized am procedure following a sbo in a vver1000. In *Proceedings Technical Meeting on Severe Accident and Accident Management Toranomon Pastoral Conference, Minato-ku, Japan, March 14-16 2006*, 2006.
- D'Auria, Galassi, and Giannotti. Update of the nodalization of the wwcr 1000 for the relap5 code to temelin model, 2003.
- F. D'Auria, N. Debrecin, and G. Galassi. Outline of the uncertainty methodology based on accuracy extrapolation. *Nuclear Technology*, 109, 1995.
- F. D'Auria, G.M. Galassi, R. Galetti, and M. Leonardi. Application of fast fourier transform method to evaluate the accuracy of sbloca data base. Technical Report DIMNP-NT 284, University of Pisa, 1996.
- F. D'Auria, M. Frogheri, and W. Giannotti. Relap5/mod3.2 post test analysis and accuracy qualification of lobi test bl-44. Technical report, US NRC, 1999.
- F. D'Auria, M. Cherubini, G. Galassi, and N. Muellner. Analysis of measured and calculated counterpart test data in pwr and vver1000 simulators. *Nuclear Technology and Radiation Protection*, XX(1):3-14, June 2005.
- F. D'Auria, O. Melikhov, V. Melikhov, I. Elkin, A. Suslov, M. Bykov, A. Del Nevo, D. Araneo, N. Muellner, M. Cherubini, and W. Giannotti. *Accident Management Technology in VVER-1000*. Pacini SRL Pisa, 2006.
- V. Denisov and G. Dragunov. *WWER Reactor Units for Nuclear Power Plants*. Izdat, 2002.

- I Elkin. Report about psb-vver heat losses, psb-vver report 04. Technical report, EREC, OECD, 2003.
- I. Elkin, S. Nikonov, I. Lipatov, G. Dremin, A. Kapustin, A. Rovnov, V. Gudkov, and A. Antonova. Cold leg sbloca 0.7% with failure of hpis and lpis and use of normal operation systems for water supply to primary circuit (test 12). Data Analysis Report Task 1.5.4, EREC, Elektrogorsk, Russia, 2004.
- I. V. Elkin. Test analysis report: Cold leg sbloca 0.7% with failure of hpis cool-down through secondary circuit, and recovery of one hpis train in affected loop (test 11)", tasis project r2.03/97. Technical report, EREC, 2004a.
- I.V. Elkin. Experimental data report: Cold leg sbloca 0.7% with failure of hpis and lpis and use of normal operation systems for water supply to primary circuit (test 12). Technical report, EREC, 2004b.
- I.V. Elkin, S.M. Nikonov, I.A. Lipatov, G.I. Dremin, A.V. Kapustin, A.A. Rovnonv, A.V. Basov, V.I. Gudkov, and A.I. Antonova. Experimental data report: Total loss of feed-water with failure of hpis pumps and operator actions on secondary circuit depressurization (test 1). Technical report, EREC, 2005a.
- I.V. Elkin, S.M. Nikonov, I.A. Lipatov, G.I. Dremin, A.V. Kapustin, A.A. Rovnonv, A.V. Basov, V.I. Gudkov, and A.I. Antonova. Test analysis report: Total loss of feed-water with failure of hpis pumps and operator actions on secondary circuit depressurization (test 1). Technical report, EREC, 2005b.
- I.V. Elkin, A.A. Rovnonv, I.A. Lipatov, G.I. Dremin, A.V. Kapustin, S.M. Nikonov, A.V. Basov, V.I. Gudkov, and A.I. Antonova. Test analysis report: Station blackout with operator actions on secondary circuit depressurization for feedwater supply (test 7). Test analysis report, EREC, 2005c.
- I.V. Elkin, A.A. Rovnonv, I.A. Lipatov, G.I. Dremin, A.V. Kapustin, S.M. Nikonov, A.V. Basov, V.I. Gudkov, and A.I. Antonova. Experimental data report: Station blackout with operator actions on secondary circuit depressurization for feed water supply (test 7). Experimental data report, EREC, 2005d.
- P. Groudev. Astec vver-1000 reference data base. word file, 2002.
- R. E. Henry and H. K Fauske. The two-phase critical flow of one-component mixtures in nozzles, orifices, and short tubes. *Transactions of ASME, Journal of Heat Transfer*, 93:179–187, 1971.
- G. Hewitt and N. Hall-Taylor. *Annular two-phase flow*. Pergamon Press, 1970.
- IAEA. Good practices with respect to the development and use of nuclear power plant procedures. Techdoc 1058, IAEA, Wagramer Strasse 5 P.O. Box 100 A-1400 Vienna, Austria, December 1998.
- IAEA. Best estimate safety analysis for nuclear power plants: uncertainty evaluation. Iaea tecdoc (in preparation), IAEA, 2007.
- IAEA-INSAG-10. Defence in depth in nuclear safety, insag 10. INSAG 10, IAEA, 1996.
- ISL. Relap5/mod3.3 code manual volume i: Code structure, system models, and solution methods. Relap5/mod3.3 manual, Information Systems Laboratories, Inc., 2003.
- ISL. Relap5/mod3.3 code manual volume ii: User's guide and input requirements. Relap5/mod3.3 manual, Information Systems Laboratories, Inc., 2006a.
- ISL. Relap5/mod3.3 code manual volume iii: Developmental assessment problems. Relap5/mod3.3 manual, Information Systems Laboratories, Inc., 2006b.
- ISL. Relap5/mod3.3 code manual volume iv: Models and correlations. Relap5/mod3.3 manual, Information Systems Laboratories, Inc., 2006c.
- ISL. Relap5/mod3.3 code manual volume v: User's guidelines. Relap5/mod3.3 manual, Information Systems Laboratories, Inc., 2006d.
- ISL. Relap5/mod3.3 code manual volume vii: Summaries and reviews of independent code assessment reports. Relap5/mod3.3 manual, Information Systems Laboratories, Inc., 2006e.
- ISL. Relap5/mod3.3 code manual volume viii: Programmers manual. Relap5/mod3.3 manual, Information Systems Laboratories, Inc., 2006f.

- ISL, A.S. Shieh, V.H. Ransom, and R. Krishnamurthy. Relap5/mod3 code manual volume 6: Validation of numerical techniques in relap5/mod3.0. Relap5/mod3.3 manual, Information Systems Laboratories, Inc., 2006.
- B. Ivanov, K. Ivanov, P. Groudev, M. Pavlova, and V. Hadjiev. Phase 1 (v1000ct-1) vol. i: Main coolant pump (mcp) switching on - final specification, 2002.
- G. Kaczmarczyk. Downhill simplex method for many dimensions. web page, 1999. URL <http://paula.univ.gda.pl/~dokgrk/simplex.html>.
- Sang-Baik Kirn, Rae-Jun Park, Kyoung-Ho Kang, and Soo-Yong Park. Evaluation of the containment integrity due to direct containment heating in korean 1300mwe pwr. In *Transactions of the 15th International Conference on Structural Mechanics in Reactor Technology, Seoul, Korea*, 1999.
- M. Leonardi, F. D'Auria, and R. Pochard. The fft based method in the frame of the uma. Spec. Workshop on Uncertainty Analysis Methods, London, 1994.
- K. Liesh and M Reocreux. Verification matrix for thermal hydraulic system codes applied for wwer analysis. Technical report, GRS, 1995.
- A. Madeira, F. D'Auria, and A. Alvim. A pwr recovery option for a total loss of feedwater beyond design basis scenario. In *NURETH-10 Conference*, 2003.
- O. Melikhov, I. Elkin, I. Lipatov, G. Dremin, I. Galchanskaya, S. Nikonov, A. Rovnov, A. Antonova, E. Chtchepetilnikov, A. Kapustin, V. Gudkov, and A. Chalych. Psb-vver report psb 09. OECD PSB-VVER project, 2003a.
- O.I. Melikhov. Report about psb-vver description (including measurement system), psb-vver report psb 03. Technical report, EREC OECD, 2003.
- O.I. Melikhov, I.V. Elkin, I.A. Lipatov, E.Yu. Chtchepetilnikov, A.V. Kapustin, and G.I. Dremin. Psb-vver report psb 06. Technical report, EREC OECD, 2003b.
- O.I. Melikhov, I.V. Elkin, I.A. Lipatov, G.I. Dremin, S.A. Galchanskaya, S.M. Nikonov, A.A. Rovnov, A.I. Antonova, E.Yu. Chtchepetilnikov, A.V. Kapustin, V.I. Gudkov, and A.F. Chalych. Psb-vver report psb 07. Technical report, EREC OECD, 2003c.
- O.I. Melikhov, I.V. Elkin, I.A. Lipatov, G.I. Dremin, S.A. Galchanskaya, S.M. Nikonov, A.A. Rovnov, A.I. Antonova, E.Yu. Chtchepetilnikov, A.V. Kapustin, V.I. Gudkov, and A.F. Chalych. Psb-vver report psb 08. Technical report, EREC OECD, 2003d.
- A. Mikhalechuk. Report on input data base for analyses on vver-1000 type npp (balakovo), final report, riskaudit report no 87. EC TACIS report, 1997.
- J. Misak. Impementation of accident management programmes in nuclear power plants. Safety Reports Series 32, IAEA, 2004a.
- J. Misak. Amp and amg in vver 1000. Tacis 30303 internal report, 2004b.
- N. Muellner, A. Petruzzi, W. Giannotti, and F.D. D Auria. Investigation of a possible emergency procedure in case of a total loss of feedwater. In *Technical Meeting to Monitor Progress in Implementation of Accident Management Programmes at NPPs Prague, Czech Republik, October 20-22*, 2003.
- N. Muellner, W. Giannotti, and F. D. D Auria. Investigation of a possible emergency procedure for the vver 440/213 npp in case of a total loss of feedwater. In *Workshop on Severe Accident Management Guidelines for VVERs, Varna, Sept 12-17*, 2004a.
- N. Muellner, W. Giannotti, and F.D. D Auria. Investigation of a possible emergency procedure for the vver 1000 npp in case of a total loss of feedwater and a main steam line break. In *Proceedings of ICONE12 2004 12th International Conference on Nuclear Engineering Arlington, Virginia, USA, April 25-29*, 2004b.

- N. Muellner, W. Giannotti, F. D'Auria, G. Kastchiev, and W. Kromp. Investigation of h2 generation during an sbo for a vver-1000 320 using the codes relap5-scdap and melcor. In *Proceedings 5th International Conference on Nuclear Option in Countries with Small and Medium Electricity Grids, Dubrovnik, Croatia, May 16-20 2004*, 2004c.
- N. Muellner, W. Giannotti, and F. D'Auria. "relap5 analysis of an eop based mobile pumps, at a generic vver-1000 npp in case of a total loss of the primary heat sink (for bdba conditions). In *NURETH-11 October 2-6 2005, Conference Proceedings*, 2005a.
- N. Muellner, E. Seidelberger, A. Del Nevo, and F. D. D Auria. Application of the fast fourier transform based method (fftbm) to assist in the qualification process of for the psb-vver1000 relap5. In *International Conference Nuclear Energy for New Europe 2005, Bled, Slovenia, September 5-8*, 2005b.
- N. Muellner, M. Cherubini, W. Kromp, F. D'Auria, and G. Petrangeli. A procedure to optimize the timing of operator actions of accident management procedures. *Nuclear Engineering and Design*, 237(22):p. 2151, 2007.
- N. Muellner, D. Araneo, M. Cherubini, and F D'Auria. Effect of sg modelling on primary side pressure and temperature trend during long term station black out conditions in vver using relap5 and cathare2 system codes. In *Proceedings of the 7th International Conference on Nuclear Option in Countries with Small and Medium Electricity Grids Dubrovnik, Croatia, Paper Ref. No. S-05.68*, 2008.
- NEA/CSNI. Bemuse phase ii report re-analysis of the isp-13 exercise, post test analysis of the loft 12-5 test calculations. Nea/csni/r(2006)2, NUCLEAR ENERGY AGENCY / COMMITTEE ON THE SAFETY OF NUCLEAR INSTALLATIONS, 2005.
- J. Nelder and R. Mead. A simplex method fo function minimization. *Computer Journal*, 7:308, 1965.
- G. Petrangeli. *Nuclear Safety*. Elsevier, 2005.
- R. Pochard and A. Porracchia. Assessment closure proposal oecd/csni sacte task group meeting. Minutes, 1986.
- W. Press, S. Teukolsky, W. Vetterling, and B. Flannery. *Numerical Recipes in C - The Art of Scientific Computing*. Cambridge University Press, 2005.
- R. Prior, V. Mitkin, V. Silin, A. Suslov, O. Traktuev, and V. Sevastyanov. Accident management measures for balakovo nuclear power plant final report. Tacis r2.06/95, Westinghouse Electric Europe s.p.rl., 2000.
- W. Riebold. Minutes of the oecd/csni sacte task group meeting. Minutes, 1987.
- R. Roumy. *Structure des ecoulements dishasiques eau-air. Etude de la fraction de vide moyenne et des configurations d'ecoulment (CEA-R-3892)*. CEA, 1969.
- V. Sevastyanov and A. Suslov. Tacis project meeting at balakovo npp, December 2005.
- V. Sevastyanov, A. Suslov, A. Andrioutschenko, and L. Gilvanov. Emergency procedures of balakovo npp units. Tacis-30303 Internal Project Report, 2004.
- S. Sholly. Consolidated notes on temelin posar & psa, review. IRF internal document, 2001.
- J.A. Trapp and V. H. Ransom. A choked-flow calculation criterion for nonhomogeneous. nonequilibrium two-phase flows. *International Journal of Multiphase Flow*, 109:669–681, 1982.
- E. Truckenbrodt. *Strömungsmechanik, Grundlagen und technische Anwendungen*. Springer-Verlag, 1968.
- Samuel J. Walker. *Three Mile Island: A Nuclear Crisis in Historical Perspective*. Berkeley: University of California Press, 2004.
- G. B. Whitham. *Linear and Nonlinear Waves*. New York: John Wiley and Sons, 1974.



Europass Curriculum Vitae

Personal information

First name(s) / Surname(s)	Nikolaus Müllner		
Address(es)	Endemanng. 6-18/2/40 1230 Vienna Austria		
Telephone(s)	+39 0502210373	Mobile:	:+43 1 388 17 53 965
Fax(es)	+39 0502210384		
E-mail	nikolaus.muellner@univie.ac.at		
Nationality	Austrian		
Date of birth	5 th of May 1973		
Gender	Male		

Work experience

Dates	From 2003 /current
Occupation or position held	Research Associate
Main activities and responsibilities	Current position Coordination of the field licensing, in particular licensing aspects of Atucha2 NPP within Contract between Na-Sa (Argentina) and Università di Pisa (2008-2010), Work as Expert in the EC Tacis Project 30303 "Safety Analysis for VVER and RBMK Reactors" (2003-2006), Project management for the Twinning Light Project "Implementation of the National Strategy for Scientific Research" (January – August 2006), project management for the Twinning Light Project "Developing the National Monitoring Institution and Certification Body for Refrigeration, Air conditioning and Heat-pump Trade" (March – October 2007).
Name and address of employer	University of Pisa, "San Piero a Grado Research Group" Via Diotisalvi 2 56122 Pisa Italy
Type of business or sector	Research and Development
Dates	From 2003/current
Occupation or position held	Research Associate
Main activities and responsibilities	Work as researcher and Ph.D, student at the University of Vienna. Currently at the University of Pisa (DIMNP) within a cooperation agreement. Work in the field of safety analysis with thermal hydraulic system codes, and severe accident analysis codes
Name and address of employer	Vienna University, IRF Tuerkenschanzstr. 17/8 A 1180 Vienna Austria
Type of business or sector	Research and Development
Dates	2002/2003
Occupation or position held	Market Researcher
Main activities and responsibilities	Work as market researcher at "H.I.Europe". My fields were IT-related business-to-business products

Name and address of employer	H.I.Europe (former Total Research), European Headquarters Watermans Park, High Street, Brentford, TW8 0BB London, United Kingdom
Type of business or sector	Market Research
Dates	2001/2002
Occupation or position held	System administrator
Main activities and responsibilities	Part time. My task was to maintain a windows NT / Linux network, consisting of approximately 20 computers, as well as to set up and maintain a Linux based firewall.
Name and address of employer	IRF, Vienna University
Dates	1991-2000
Occupation or position held	Private Tutor
Main activities and responsibilities	In the fields physics, mathematics and Russian language.
Type of business or sector	Education
Dates	October 1990
Occupation or position held	Quality assurance
Main activities and responsibilities	Practical training. My task was to look after hardness of certain components, using Vickers - and Brinells method
Name and address of employer	General Motors, Vienna
Dates	Summer 1988/89/90
Occupation or position held	Quality assurance
Main activities and responsibilities	Practical training. Menhardt Ges.m.H. specialized in production of semiconductor based heating elements. My task was to apply currency to the elements, observe the heating up process and check, whether the temperature of the elements, when settled, was in the required range.
Name and address of employer	Menhardt Ges.m.b.H, Vienna

Education and training

Dates	4-10 July 2005
Principal subjects/occupational skills covered	Post Accident Radiation Monitoring Techniques, Kyev (Training on radiation protection in the Chernobyl exclusion zone)
Name and type of organisation providing education and training	TESEC (European Center for Technological Safety) in Cooperation with the University of Vienna, Institute of Risk Research
Level in national or international classification	Higher University Education
Dates	2003-current
Title of qualification awarded	Ph.D. Student in Physics
Principal subjects/occupational skills covered	Ph.D. Student at the University of Vienna. Title of the Ph.D. thesis "Simulation of Beyond Design Bases Accidents – a Contribution to Risk Analysis of Nuclear Power Plants"
Name and type of organisation providing education and training	University of Vienna, Institute of Risk Research
Level in national or international classification	Higher University Education
Dates	1994-2002
Title of qualification awarded	Magister rer. nat. (M.Sc.) in physics, graduated with distinction

Principal subjects/occupational skills covered	Principal subjects: theoretical, computer aided physics and nuclear physics. Title of my master thesis: "Cosmological Black Holes of the Nonlinear - Sigma - Model". The goal was to find numerical solutions to the Einstein equations within certain boundary conditions. FORTRAN routines of the NAG-Libraries, C and TclTk for a GUI were used.
Name and type of organisation providing education and training	University of Vienna
Level in national or international classification	Higher University Education
Dates	1997/1998
Title of qualification awarded	Erasmus-Exchange Student
Principal subjects/occupational skills covered	Coursework included working with UNIX, differential geometry, solid state physics
Name and type of organisation providing education and training	Technical University of Berlin, Germany
Dates	1993 (March-October)
Title of qualification awarded	Improved skills in Russian language
Principal subjects/occupational skills covered	Trip to St. Petersburg to improve my Russian language skills.
Name and type of organisation providing education and training	Private Teacher in St. Petersburg, Russia
Dates	1991-1993
Title of qualification awarded	Matura (equiv. A-levels GCE), graduated with distinction
Principal subjects/occupational skills covered	Grammar school with scientific Bias
Name and type of organisation providing education and training	Bundesrealgymnasium Henriettenplatz
Dates	1979-1991
Principal subjects/occupational skills covered	Primary and grammar school based on Waldorf education principles. English and Russian lessons were held from the first to the twelfth grade
Name and type of organisation providing education and training	Rudolf Steiner Schule Wien Mauer

Personal skills and competences

Mother tongue(s) German

Other language(s)

Self-assessment

European level ()*

English

Italian

Russian

Understanding				Speaking				Writing	
Listening		Reading		Spoken interaction		Spoken production			
C2	Proficient user	C2	Proficient user	C2	Proficient user	C2	Proficient user	C2	Proficient user
C2	Proficient user	C2	Proficient user	C2	Proficient user	C2	Proficient user	C2	Proficient user
B1	Independent user	B1	Independent user	B1	Independent user	B1	Independent user	B1	Independent user

- Scripting languages:** Tcl/Tk, Perl, Python, Bash
- Enviroments:** Linux, Windows
- Applications:** Mathematica, Maple, Matlab / Octave, NAG librarys, ODE - package, LAPACK, Latex, Gnuplot, Emacs, vi, UNIX administration tools, Samba, MS-Office applications
- Security related software:** Iptables Netfilter, Snort, Nessus, nmap, pgp/gpg, ssh (Openssh 2.9 and ssh2 server).
- Programming languages:** C++, C, Fortran

Driving licence yes

List of Publications:

- Investigation of a Possible Emergency Procedure in Case of a Total Loss of Feedwater
N. Muellner, A. Petrucci, W. Giannotti and F. D'Auria
Technical Meeting to "Monitor Progress in Implementation of Accident Management Programmes at NPPs", Prague, Czech Republik, October 20-22, 2003
- Qualification and Application of Coupled Reactor Cooling System and Containment Nodalizations
F. D'Auria, G.M. Galassi, W. Giannotti, A. Petrucci, K. Moussavian, F. Pierro, A. Lo Nigro and N. Muellner
IAEA Technical Meeting, Vienna, Nov 26-28, 2003, "Progress in Development and Use of Coupled Codes for Accident Analysis"
- Investigation of a Possible Emergency Procedure for the VVER 1000 NPP in Case of a Total Loss of Feedwater and a Main Steam Line Break
N. Muellner, W. Gianotti and F. D'Auria
Proceedings of ICON12 2004 12th International Conference on Nuclear Engineering Arlington, Virginia, USA, April 25-29, 2004
- Investigation of H₂ Generation During a SBO for a VVER 1000-320 Using the Codes RELAP5-SCDAP and MELCOR*
N. Muellner, W. Giannotti, F. D'Auria, G. Kastchiev and W. Kromp
5th International Conference on Nuclear Option in Countries with Small and Medium Electricity Grids Dubrovnik, Croatia, May 16-20, 2004
- Fundamentals in Natural Circulation Stability
F. D'Auria, A. Del Nevo and N. Muellner
Natural Circulation in Water-Cooled Nuclear Power Plants, International Centre for Theoretical Physics (ICTP), Trieste, June 28 to July 2, 2004
- Addressing the Scaling Issue by the Thermalhydraulic System Codes: Recent Results
F. D'Auria, M. Cherubini, G.M. Galassi and N. Muellner
Fifth Yugoslav Nuclear Society Conference YUNSC – 2004, Sept 27-30, 2004
- Investigation of a Possible Emergency Procedure for the VVER 440/213 NPP in Case of a Total Loss of Feedwater
N. Muellner, W. Giannotti and F. D'Auria
Workshop on "Severe Accident Management Guidelines for VVERs", Varna, Sept 12-17, 2004.
- "Analysis of measured and calculated counter part test data in PWR and VVER1000 simulators"*
D'Auria F., Cherubini M., Galassi G.M., Muellner N.
J. Nuclear Technology and Radiation Protection, Vol. XX, pages 3-15, 2005. YU ISSN 1451-3994
- Application of the Fast Fourier Transform Based Method (FFTBM) to Assist in the Qualification Process of for the PSB-VVER1000 Relap5*
Nikolaus Muellner, Emmerich Seidelberger, Alessandro Del Nevo, Francesco D'Auria
International Conference Nuclear Energy for New Europe 2005 Bled, Slovenia, September 5-8, 2005
- Relap5 Analysis of an Eop based on Mobile Pumps, at a Generic VVER-1000 NPP in case of a Total Loss of the Primary Heat Sink (for DBDA Conditions)
N. Muellner, W. Giannotti and F. D' Auria
11th International Topical Meeting on Nuclear Thermal-Hydraulics (NURETH-11), Popes' Palace

Conference Center, Avignon, France, October 2-6, 2005, Log Number: 151

Natural Circulation in water cooled nuclear power plants, Annex 8, Insights into natural circulation stability
D'Auria, A. Del Nevo, N. Muellner
IAEA-Tecdoc-1474, November 2005

Accident Management Technology in VVER-1000
Editor F.D'Auria, Authors: O.Melikhov, V.Melikhov, I.Elkin, A.Suslov, M.Bykov, A.Del Nevo, D.Araneo,
N.Muellner, M.Cherubini, W.Giannotti
EC TACIS-project 30303 Final Technical Report, July 2006

"Accident management in VVER-1000"
D'Auria F., Suslov A., Muellner N., Petrangeli G., Cherubini M.
15th Pacific Basin Nuclear Conference (PBNC), Sydney (Aus), Oct. 15-20, 2006, paper 191, ISBN
1877040-58-4

Implementation of the National Strategy for Scientific Research
F.D'Auria, D.Araneo, A.Bonaccorsi, A.Huber, M.Movsesyan, N. Muellner, G.Russo
EC PHARE-Project TwL BG-2004-IB-OT-01-UE, Final Technical Report, September 2006

A Procedure to Optimize the Timing of Operator Actions of Accident Management Procedures
Nikolaus Muellner, Marco Cherubini, Wolfgang Kromp, Francesco D'Auria, Gianni Petrangeli
Technical Meeting on Severe Accident and Accident Management, Toranomon Pastoral, Minato-ku
Tokyo, Japan, March 14-16, 2006, Proceeding of the Conference

Application of an Optimized AM Procedure following a SBO in a VVER1000
Marco Cherubini, Nikolaus Muellner, Francesco D'Auria, Gianni Petrangeli
Technical Meeting on Severe Accident and Accident Management, Toranomon Pastoral, Minato-ku
Tokyo, Japan, March 14-16, 2006, Proceeding of the Conference

The Nuclear Option, Climate Policy and Sustainability - An Assessment of UNFCCC COP 2006, Safety of Nuclear Power Plants
Oda Becker, Antony Froggatt, Helmut Hirsch, Georgui Kastchiev, Wolfgang Kromp, Helga Kromp-Kolb,
Roman Lahodynsky, Franz Meister, Nikolaus Müllner, Manfred Rotter, Steven Sholly, Geert Weimann,
Peter Weish
Austrian Nuclear Advisory Board, (Forum für Atomfragen)

A Procedure to Optimize the Timing of Operator Actions of Accident Management Procedures
Nikolaus Muellner, Marco Cherubini, Wolfgang Kromp, Francesco D'Auria, Gianni Petrangeli
Nuclear Engineering and Design, Volume 237, Issue 22, November 2007, Pages 2151-2156

Application of an Optimized AM Procedure following a SBO in a VVER1000
Nuclear Engineering and Design, Volume 238, Issue 1, January 2008, Pages 74-80
Marco Cherubini, Nikolaus Muellner, Francesco D'Auria, Gianni Petrangeli

"Safety of Nuclear Power Plants"
D'Auria F., Bousbia Salah A., Muellner N., Araneo D.
Invited at: Bulatom Conference 2007, Varna (Bg), June 6-8, 2007
"Relevance of Thermo-Fluid Dynamics for Establishing the Safety of Nuclear Power Plants"
D'Auria F., Cherubini M., Muellner N.
Invited at: 32nd IAHR Conference, Venice (I) July 4-7, 2007

"Developing the National Monitoring Institution and Certification Body for Refrigeration, Air-conditioning and Heat-pump Trade"
Zoltan Attila, Bibok Zsuzsanna, Kabay Krisztina, Toth Robert, Vince Annette, Araneo Dino, D'Auria
Francesco, Fantozzi Fabio, Galassi Cristina, Galassi Francesco, Huber Alexa, Melideo Daniele, Muellner
Nikolaus, Pelegrini Chiara, Russo Giovanna, Russo Antonella
Project Report University of Pisa, HRACA, MoEW Hungary, February 2008

"DEGB LBLOCA (2 X 100% Break in CL) in Atucha-2 NPP"
D'Auria F., Mazzantini O., Cherubini M., Giannotti W., Parisi C., Moretti F., Melideo D., Del Nevo A.,
Galassi G.M., Araneo D., Terzuoli F., Adorni M., Muellner N., Petrucci A., Lazzerini D., Santoro R.,
Bousbia-Salah A.

University of Pisa Report, DIMNP NT 628(08) - rev. 1, Pisa (I), March 2008

"Effect of SG Modelling on Primary Side Pressure and Temperature Trend During Long Term Station Black Out Conditions in VVER Using Relap5 and Cathare2 System Code"

Nikolaus Müllner, Dino Araneo, Marco Cherubini, Francesco D'Auria
Spring CAMP Meeting, May 28-29 2008, Grand Hotel Bonanno, Pisa

"Pressure Drop Characterization by means of a CFD Code"

Dino Araneo, Patricia Pla, Fabio Moretti, Francesco D'Auria, Nikolaus Müllner
Proceedings of the 7th International Conference on Nuclear Option in Countries with Small and Medium Electricity Grids, Dubrovnik, Croatia, 25-29 May 2008, Paper Ref. No. S-05.68

"Effect of SG Modelling on Primary Side Pressure and Temperature Trend during Long Term Station Black Out Conditions in VVER using Relap5 and Cathare2 System Codes"

Nikolaus Müllner, Dino Araneo, Marco Cherubini, Francesco D'Auria
Proceedings of the 7th International Conference on Nuclear Option in Countries with Small and Medium Electricity Grids, Dubrovnik, Croatia, 25-29 May 2008, Paper Ref. No. S-05.46

"Selected Aspects of the Licensing Process of the Argentine NPP Atucha2"

Martin Giersch, Regina Galetti, Claudio Camargo, Francesco D'Auria, Nikolaus Müllner, Oscar Mazzantini
Proceedings of the International Conference Nuclear Energy for New Europe, Portorož, Slovenia, Sept. 8-11, 2008

"Final Report - Bioenergie aus Gras"

Christan Gepp, Erika Kancsar, Gehard Linhard, Georg Wunderer, Helmut Schabschneider, Klaus Gufler, Maria Hufnagl, Maria Magdalena Picher, Markus Drapalik, Nikolaus Arnold, Nikolaus Müllner, Wolfgang Kromp, Emmerich Seidelberger, Walter Graf, Francesco D'Auria
Project Report University of Pisa – University of Vienna funded by "Schiedel Stiftung fuer Energietechnik", April 2009, Vienna, Austria

"Optimizing The Initial Pressure Of Accumulators For The Atucha2 NPP Using An Optimization Method"

Nikolaus Müllner, Alessandro Del Nevo, Marco Cherubini, Oscar Mazzantini, Francesco D'Auria,
Proceedings ICONE 17, 12-16 July 2009 , Brussels, Belgium

"Addressing Boron Dilution Scenario Through RELAP5/3.3 Analysis of PWR SB LOCA"

Patricia Pla, Regina Galetti, Francesco D'Auria, Carlo Parisi, Walter Giannotti, Alessandro Del Nevo, Nikolaus Müllner, Marco Cherubini, Giorgio Galassi, Francesco Reventos
Proceedings ICONE 17, 12-16 July 2009 , Brussels

"Analysis of condensation-induced water hammer in vertical geometry with RELAP5, WAHA and CODEX codes"

Oleg Melikhov, Vladimir Melikhov, Yuriy Parfenov, Mikhail V. Davydov, Iztok Tiselj, Francesco D'Auria, Nikolaus Müllner
Conference Proceedings "Nuclear Energy for New Europe 2009", Bled, Slovenia September 14-17

"The Best-Estimate Plus Uncertainty (BEPU) Challenge in the Licensing of Current Generation of Reactors"

F. D'Auria, O. Mazzantini, N. Müllner
AERB, Mumbai, India January 7-8, 2010-02-15

"Evaluation of the conservatism of NPP safety analysis dose calculations as typical for licensing purposes"

N. Arnold, N. Müllner, F. D'Auria, O. Mazzantini
Icone 18, May 17-21 2010, Xi'an, China

"THE BEPU (BEST ESTIMATE PLUS UNCERTAINTY) CHALLENGE IN CURRENT LICENSING OF NUCLEAR REACTORS"

F. D'Auria, O. Mazzantini, N. Müllner, A. Petrucci,
ASME 2010, 3rd Joint US-European Fluids Engineering Summer Meeting and 8th International Conference on Nanochannels, Microchannels and Minichannels, August 1-5 2010, Montreal, Canada